Zeitschrift: IABSE congress report = Rapport du congrès AIPC = IVBH Kongressbericht

Band: 8 (1968)

Rubrik: III. Tall multi-storey buildings

III

Bâtiments de grande hauteur
Hochhäuser
Tall Multi-Storey Buildings

IIIa

Calcul en plasticité
Plastizitätstheorie
Plastic Design

Leere Seite
Blank page
Page vide

DISCUSSION PRÉPARÉE / VORBEREITETE DISKUSSION / PREPARED DISCUSSION

The Plastic Design of Braced Multi-Storey Frames

Calcul plastique de portiques à plusieurs étages renforcés

Plastische Bemessung unverschieblicher Stockwerkrahmen

JACQUES HEYMAN
University of Cambridge

INTRODUCTION There are two essential steps in the design of a steel frame which is required to carry given loads. First, a set of structural forces must be determined which is in equilibrium with the applied loads; secondly, individual members must be proportioned to carry those equilibrium forces. These two steps cannot always be separated in the design process, as will be seen, but they are in fact logically distinct.

The first step has led to the proliferation of different methods of structural analysis, all of which "are nothing more than a ready way of finding a reasonable equilibrium solution that works in practice" [1]. This situation has been discussed elsewhere [2] with particular reference to the use of plastic theory for finding the basic equilibrium solution. (It may be noted here that the whole of the discussion in the present paper is confined to the case where deflexions are not the primary design criterion. That is, member sizes are determined on the basis of the strengths of the various portions of the structure, and it is assumed that any necessary deflexion checks will be made as a secondary matter).

The use of plastic theory as a design tool implies the use of load factors to give the required margin of safety to the actual structure. Thus the working values of the loads acting on a frame are hypothetically increased to certain factored values, and the frame is then designed to resist the action of those factored loads. The actual value of the factor used in the calculations depends on the type of structure and loading being considered, and is different in

different countries and at different dates. In England it is usual to apply a factor of 1·75 to both dead and superimposed loading in the design of simple factory buildings. However, a recent report [3] on the design of braced multi-story frames recommends the use of the factor 1·5, providing the design is carried out by the methods proposed in the report. This particular recommendation is examined in more detail below.

The function of the load factor is essentially two-fold. In the first place it provides a margin of safety against imperfections in the structure itself, which can be introduced at any stage in the processes of design, fabrication, and erection. Secondly, there is always some uncertainty in the actual values of the loads; that is, the real loading on a structure can only be assessed on a probabilistic basis. Thus the use of a load factor of 1·5, for example, implies that the probability of a 50% overload occurring is acceptably small.

However, a load factor need not be used only in conjunction with a plastic method of design. As an immediate example, the limit state of a column in a multi-storey frame may be governed by elastic instability; in this case, the designer would wish to check that the column remains stable under the factored loading. Again, this particular aspect is discussed more fully below.

THE DESIGN OF BRACED FRAMES There is some measure of agreement about the way in which braced multi-storey frames should be designed, even if considerable differences of detail are apparent between different proposals. Thus the report of a Joint Committee [3] referred to above outlines certain steps that will lead to a satisfactory design, and these steps are reflected, for example, in recent work in the US [4]. The two key moves in the Joint Committee's proposals are (a) the plastic design of the beams, and (b) the use of a limited substitute frame for the stability check of the columns.

Plastic design of beams is usually direct; that is, the determination of suitable equilibrium bending moment diagrams and the actual design of the beams proceed simultaneously. On relatively infrequent occasions it may be necessary to make iterative calculations, for example when a column section proves on later examination to be inadequate to carry the required full plastic moment of the beam. Leaving aside such anomalies, all the beams in a braced multi-storey frame may be designed virtually span by span just to carry the factored dead and superimposed loading.

By contrast all the methods so far developed for column design involve two distinct processes for (a) the determination of column bending moments and

(b) the actual proportioning of a particular column. The Joint Committee propose a limited substitute frame that should be considered for the design of each column length; in Fig.1, the column being investigated is regarded as connected to the adjacent members but there is no further "spread" into the structure as a whole. This substitute frame can be traced back to the work of the Steel Structures Research Committee [5], and the use of the frame greatly simplifies the work. The analysis must proceed by trial and error, since a column size has to be assumed in order to determine the elastic bending moments in the substitute frame. The stiffnesses of the members are calculated, and out-of-balance bending moments are then distributed either by the Hardy Cross method or by a one-step formula given by the Joint Committee.

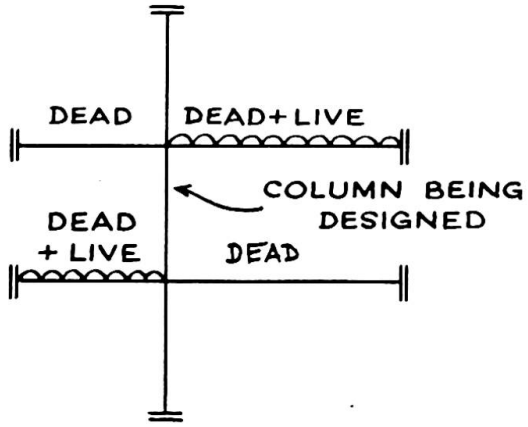

Fig. 1

The Joint Committee requires the calculations to be carried out using factored values of the loads; a typical beam loading pattern is shown in Fig.1, and the load factor 1·5 is supposed to be applied to both dead and live (superimposed) loading. Now, under full factored dead plus live loading, a beam will be on the point of collapse, and the state of the substitute frame of Fig. 1 will be as shown in Fig.2(a). The collapsing beams cannot absorb any further

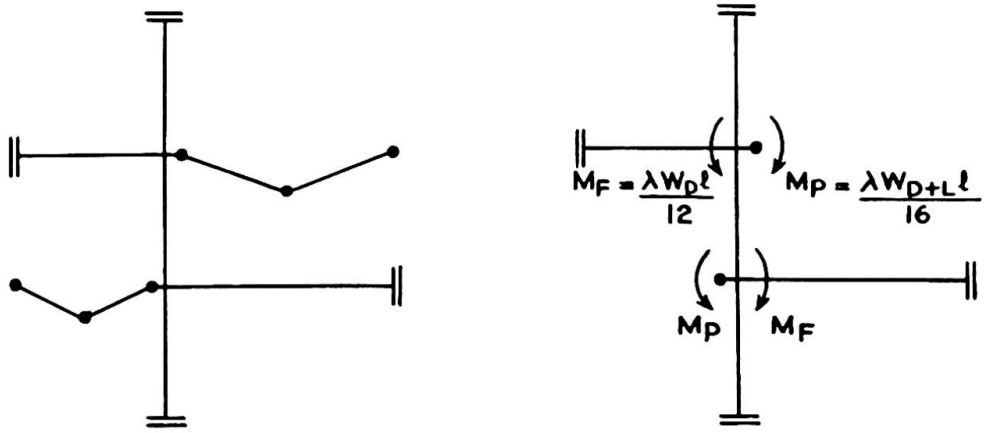

(a) (b)

Fig. 2

bending moment, and, in any moment distribution process, their stiffnesses must be assumed to be zero. The reduced substitute frame of Fig.2(b) is therefore used for checking the columns under these conditions; the collapsing beams have been replaced by "dead" moments of value M_p .

The out-of-balance bending moments in Fig.2(b) are distributed, and lead to values of terminal bending moments in the central column length; these values, together with that of the (factored) axial load, can then be used to check the suitability of the chosen column according to any required criterion (e.g. stability or the condition that the column shall just remain elastic).

There seem to be two anomalies in the method just outlined, the discussion of one of which is straightforward. In the first place, it is clear that more severe conditions would arise for the central column length in Fig.2(b) if the dead load moments (M_F), opposing the full plastic moments (M_p), were not factored. The use of an overall load factor (of value 1·5) on both dead and live loading allows the dead load to partially relieve the bending moments. In such cases, it might be appropriate to use a load factor of unity on the dead load, or of value 0·9 in accordance, for example, with current recommendations [6] on limit state design or with the French regulations for steelwork [7] . Thus the value of M_F in Fig.2(b) should be calculated with the factor λ set equal to unity or 0·9.

Retaining, however, the notion of an overall load factor of 1·5 to be applied to both dead and live loading, there is another sense in which the frames of Fig.2 may be criticized. Had the calculations of column moments been made under working values of the loads for the pattern shown in Fig.1, then there would have been no question of any of the beams collapsing. The fixed-end moments at the ends of the loaded beams would then have values $W_{D+L}\ell/12$, as shown in Fig.3, instead of the values $\lambda W_{D+L}\ell/16$ of Fig.3. In addition, the stiffnesses of all the beams should have their full values in the distribution process.

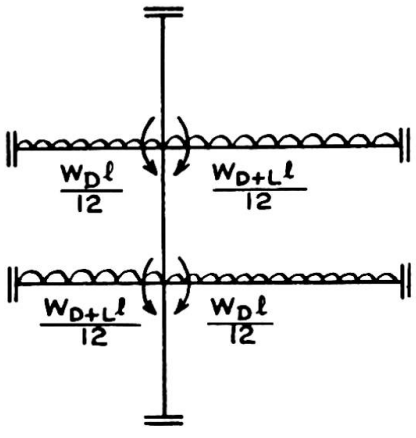

Fig. 3

A numerical example (below) confirms that the column moments resulting from Fig.3, when post-multiplied by the load factor, can exceed the moments resulting from Fig.2(b), in which the loading is pre-multiplied by the load factor. It becomes essential at this point to be clear about the nature of the check that

is made to confirm the suitability of the columns.

The column is a potentially unstable structural element, and, if the designer is to be completely assured of the safety of an entire structure, he must be satisfied that there is no danger of premature failure due to instability. Thus there must be an adequate margin of safety between the values of end moments and axial thrust computed for a particular column length and the corresponding values that would just cause failure of the column. If the calculations are made for the nominal working values of the loads, Fig.3, the column can be computed to have a certain margin of safety, and this margin may well be less than that given by the apparently more "real" configuration of Fig.2(b).

SAMPLE COLUMN CALCULATIONS The design of a large laboratory block has been reported [8], and some of the calculations afford a convenient basis for comparison. Fig.4 shows the three substitute frames for the calculations for a

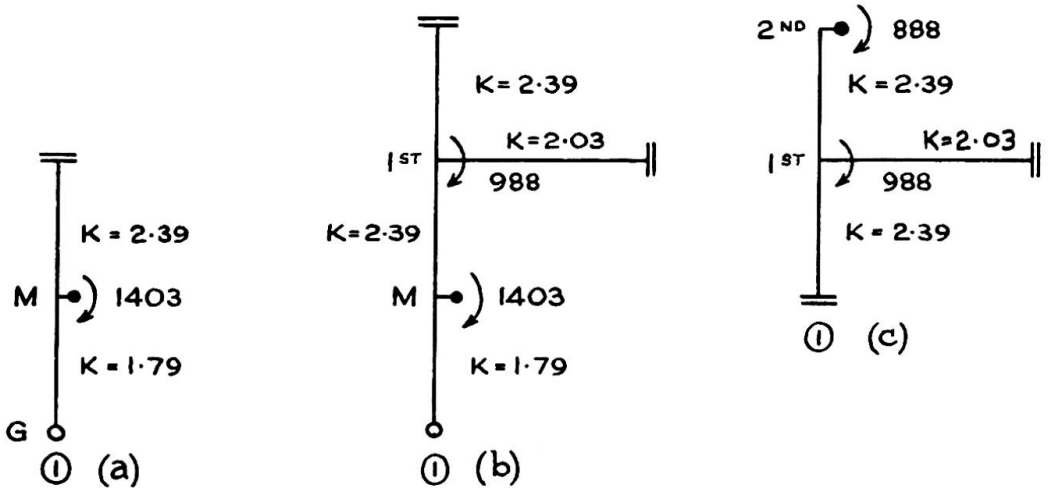

Fig. 4

typical external column; the column length under consideration is the lowest, centre and upper storey in Figs.4(a), (b) and (c) respectively. Note the introduction of the plastic hinges in accordance with Fig.2. The resulting bending moments in the individual column lengths are shown in Fig.5. A load factor of 1·5 has been used in these calculations, and the axial loads marked in Fig.5 are factored values.

The calculations made for unit load factor proceed using the substitute frames shown in Fig.6. The resulting bending moments are shown in Fig.7, to be compared with the values marked in Fig. 5. Comparing these two figures, it will

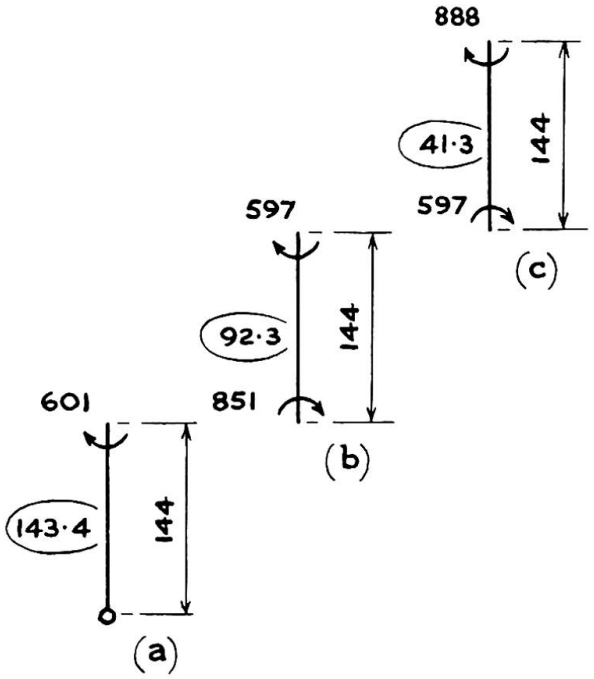

Fig. 5

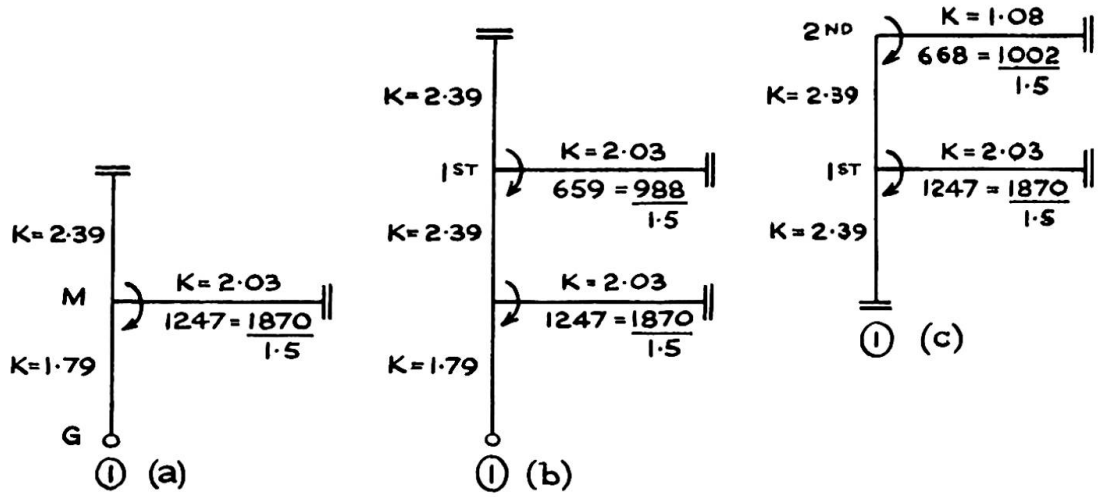

Fig. 6

be seen that for this case of an external column, the original design approach, using factored loads, leads to the more severe design condition. This result is typical for external columns, but the reverse is true for internal columns.

Fig.8 reproduces the design conditions for an internal column [8], and Figs. 8(b) and (c) show the factored design conditions for single and double curvature bending. The alternative calculations using working loads and a completely elastic frame, are displayed in Fig. 9. It will be seen that the resulting bending moments in the column when post-multiplied by the load factor

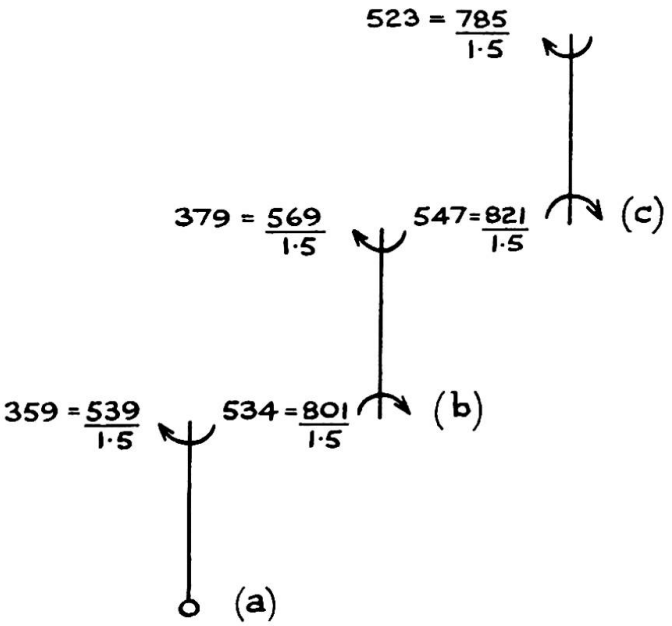

Fig. 7

1·5, are some 50% higher than the corresponding bending moments marked in Fig. 8. Thus the apparent margin of safety would be less if the calculations were performed according to the substitute frame of Fig. 9 rather than that of Fig. 8.

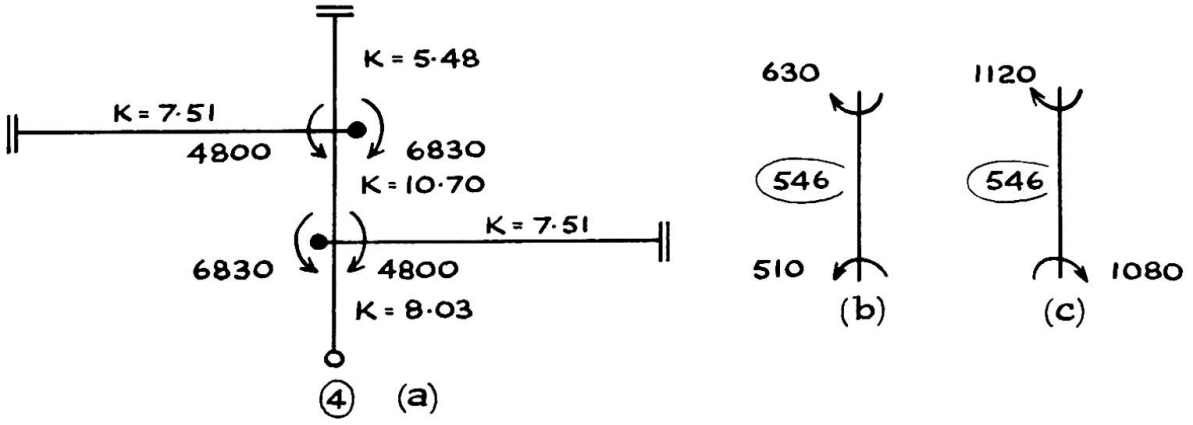

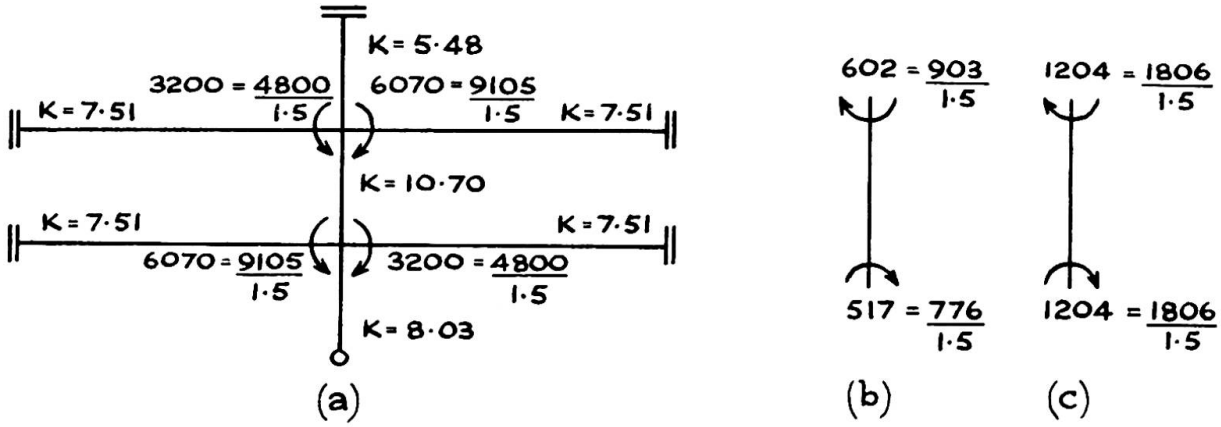

Fig. 9

DISCUSSION In a sense, this Paper is nothing more than an attempt to consider the concept of load factor which is so important in the design process. The idea of working loads gradually increased in proportion leads on the one hand to the idea of plastic collapse of a steel frame (which can be observed readily and accurately both in the laboratory and in the field), and on the other to the mathematical development of master theorems of structural design, concerned, for example, with the overall safety of a frame. The fact remains that the concept of a collapse load factor is reflected only in an insignificantly small probability of an actual overload of a real structure in practice. It is the nominal working loads that are of interest, and, in this sense, plastic theory is an easy and economical way of designing a frame under working loads.

There are no difficulties in the calculations by simple plastic theory of the beams in a multi-storey frame; The ratio collapse load to working load can be calculated uniquely for each beam. However, the determination of elastic bending moments in the columns is sensitive to the development of plastic hinges in the beams. Thus the apparent margin of safety of a column will depend on whether the calculations are made for the working values of the loads or for their fully-factored collapse values. If the second approach is adopted, and an attempt made to allow for the "real" behaviour of the frame by the insertion of plastic hinges in the beams, then less severe conditions may arise for the columns than if the frame were assumed to remain completely elastic.

REFERENCES

1. Arup, Ove and Jenkins R.S., The design of a reinforced - concrete factory at Brynmawr, South Wales. Proc. Instn. civ. Engrs., Part III, December 1953.
2. Baker, Sir John and Heyman J., Plastic design in Britain. Publications, International Association for Bridge and Structural Engineering, vol. 26, p.31, 1966.
3. Report of a Joint Committee: Fully rigid multi-storey welded steel frames. The Institution of Structural Engineers; The Institute of Welding, December 1964.
4. Tall S., Beedle L.S., Galambos T.V. et al, Structural steel design, New York, 1964.
5. Steel Structures Research Committee, First Report 1931, Second Report 1934, Final Report 1936, London, H.M.S.O.

6. British Standards Institution, Draft Code: New unified code for structural concrete (To be published).

7. Société de diffusion des techniques du bâtiment et des travaux publics, Règles de calcul des constructions en acier, Paris, December 1966.

8. Heyman J., Finlinson J.C.H., and Johnson R.P., Inglis A: A fully rigid multi-storey welded steel frame. The Structural Engineer, vol. 44, p.435, December 1966.

SUMMARY

A convenient way of making the design of a multi-storey braced frame is to allow a plastic method for the beams, and to ensure that the columns remain elastic and stable under all loading conditions. The plastic design of beams is straightforward, but the determination of the worst loading conditions for the columns is more difficult; a limited substitute frame can greatly shorten the work. The use of a load factor requires some care, or designs can result which are less safe than those intended by the designer.

RÉSUMÉ

Une façon pratique de projeter un portique à plusieurs étages renforcé consiste à dépasser la limite d'élasticité seulement pour les poutres, en garantissant que les colonnes restent élastiques et stables dans tous les cas de charge. Le calcul plastique des poutres est simple, mais la détermination du cas de charge déterminant pour les colonnes est plus difficile; un portique-modèle simplifié peut raccourcir le travail considérablement. Des précautions sont requises lors de l'utilisation d'un facteur de charge, sinon il pourrait résulter des constructions d'une moins grande sécurité que projetée.

ZUSAMMENFASSUNG

Ein gangbarer Weg, die Bemessung unverschieblicher Stockwerkrahmen vorzunehmen, besteht darin, für die Riegel plastische Rechnung zu erlauben, während für die Stützen angenommen wird, dass diese elastisch und für alle Lasten stabil bleiben. Einfach ist die plastische Bemessung für die Riegel, hingegen bereitet die Bestimmung der schlimmsten Laststellung für die Stützen Schwierigkeiten; ein begrenzter Ersatzrahmen kann die Rechnung erheblich kürzen. Die Verwendung der Lastfaktoren erfordert Sorgfalt, sonst kann die Bemessung unsicherer als diejenige des Verfassers sein.

Plastic Design

Calcul en plasticité

Plastische Bemessung

A. HRENNIKOFF, Sc.D.
Research Professor of Civil Engineering,
University of British Columbia,
Vancouver, Canada

It is appropriate to consider at the outset the basic principles underlying the theory of plastic design of steel structures and to compare this theory with its predecessor, the elastic theory. The elastic design is based on the working loads, a conservative but realistic set of loads that may be actually applied to the structure, and the allowable unit stresses, which must not be exceeded under the most unfavourable load combinations. The stress analysis is supposed to be conducted in conformity with the acceptable theory and the current engineering practice, and this of course implies a tacit acceptance of some degree of error. The allowable stress forms a certain fraction of the yield stress of structural steel of the particular grade used, and the reciprocal of this fraction is usually called the factor of safety. This factor is in effect the factor of ignorance covering a multitude of uncertainties and faults of all kinds associated with design, detailing, fabrication, construction, loads, materials, etc. It covers also, to some extent, mistakes which may be expected in design, as in all human activities.

Plastic design, on the other hand, restricted in its application to statically indeterminate flexural frames, is concerned not with the working but with the failure condition of the structure, which is defined as a state of a very large deformation. This condition is expected to be attained under a load whose intensity exceeds the working load by a quantity known as the load factor or, more correctly, the overload factor. This factor is the equivalent of the factor of ignorance of the elastic design. Nominally the overload factor provides for no uncertainties other than in loads; actually, of course it does provide for them in an indirect way, and in doing this it ceases to be a measure of overload in view of the variability of the other relevant factors involved. The load factor is thus another variety of the factor of safety-factor of ignorance, somewhat misnamed, and in no way better in principle than its conventional counterpart.

The implications involved in the existence of the two acceptable but different factors of safety were apparently not appreciated at the time of incorporation of plastic design into the American and Canadian specifications. As it stands now, a structure may be found as underdesigned by the elastic standards and overdesigned by the plastic. An elastic designer could justify the same structure on the basis of a higher allowable stress,

but the specifications would not permit this. Yet if he changes his approach to plastic the weak design becomes acceptable, —a situation hardly making any sense. A coexistence of two distinct and contradictary systems is no more rational in engineering practice than in any other realm of human endeavours.

The pioneers of plastic design claimed the advantages of their method over its elastic counterpart in the simplicity of calculation, requiring no recourse to indeterminate theory, and in the economy of the resultant structure. This, however, was before they fully realized that the mechanism theory, used in plastic design, while elegant in its simplicity, is insufficient for practical purposes, and that the examinations of instability of the structure and of the change in its geometry are all-important. (This is the field of the so-called non-rigid plastic theory). With instability occurring under partly elastic and partly inelastic conditions the plastic theory suddenly became a most complex assembly of numerous assumptions and hypotheses claimed to be justified by experimental evidence, which however strikes an independent observer as limited and questionable. The alleged economy of the theory also became doubtful in certain areas. Here are some other major uncertainties of plastic theory.

Flexural strength of a member is proportional to its yield strength, but this property of the material is highly indeterminate, varying by more than 50% from the average value for the same grade of structural steel.

Realistic treatment of live and other variable loads, comparable to the procedures used in the elastic design, is not available. There exist highly complicated plastic theories of incremental failure and alternating plasticity but the value of the load factor with which these theories must be associated is unknown apart from the fact that it should be smaller than the one used in the conventional plastic design, because failure under live load requires numerous applications of the load of limiting intensity, while a heavy steady load causes failure in a single application. To the writer's knowledge no attempts to correlate the two plastic load factors have ever been made.

There are no procedures or methods in existence of the non-rigid plastic analysis, as distinct from design; in other words there is no way to determine the load factor of a structure not conforming to the empirical formulae prescribed for prevention of different types of instability.

It is appropriate at this stage to make reference to the common criticism of the elastic theory advanced by the plasticians, that the allowable stress used in this theory is a fiction, because it excludes several participation stresses, (i.e. non-load-carrying stresses), like local stress concentrations, residual stresses etc. This criticism is invalid because the exclusion of the participation stresses is intentional. The non-load-carrying stresses must be excluded, because such

is the nature of the elastic theory and not because the theory is incomplete or inaccurate. A comprehensive review of the weaknesses of plastic theory may be found in the writer's papers (50), (51), (52).

The preceding discussion has been directed mostly at the plastic design of low frames. Tall or multi-storey frames, restrained from sidesway by rigid cores or diagonal bracing, are not too different in their action from the low frames.

In the design of tall frames with sidesway it is necessary to contemplate not only the instability of the individual members but also of the whole frame or its major parts. This compounds the difficulties and calls for more assumptions. The situation may be illustrated on the approach proposed by Professor Horne. He uses an empirical relation in which the true load factor is expressed through two others: the rigid plastic, which ignores instability, and the fully elastic. Since the latter is impossible to find, it is replaced by pseudo-elastic factor based on an imaginary rigid-plastic-rigid stress-strain relationship of the material. Apparently the proponent of the method expects designers to use it for all structures including the ones involving human occupancy. The writer can hardly share this view. His detailed appraisal of the method is found in his discussion of the Horne's paper (53).

The statement made earlier to the effect that the elastic and plastic factors of safety and overload are two different but equally legitimate in principle factors of ignorance, must be re-evaluated now. From all that has just been said, the writer feels that the difficulties encountered in the development of plastic theory have proved unsurmountable and the theory failed signally to live up to its claims.

There is however, something to say in favour of the plastic theory of low frames. Firstly, it assists in understanding structural behaviour of frames by giving an insight into their action at failure, and secondly, it points to desirability of using a variable allowable stress in the conventional elastic design and provides information for establishment of its numerical values. As an alternative to the elastic method of design the plastic theory is unnecessary. Its alleged rationality and economy are pure fictions, and its existence alongside the elastic design merely exposes a deficiency of logic in the specifications. Attempts to apply plastic design to multi-story buildings have no justification. Elastic design of a tall building, allowing for the deformation of the structure under load is complex enough even with the use of electronic computer and iteration procedure. The same problem under elasto-plastic conditions appears insoluble, and the attempts at its solution with the assistance of the proposed simplifying assumptions, seem unreliable.

The inclusion of plastic theory in the design specifications is mostly the work of the American plasticians, and their failure to meet and to counter, if possible, the closely defined objections of the opponents tends to cast further doubt on the validity and the applicability of their

theory. The continued research activity in the field of plastic design is no proof of its soundness, but is merely a testimonial to the tenacity of its proponents and to the availability of liberal funds.

The writer feels that the author's characterization of the method of plastic design as "by no means complete" is much too moderate.

---

(50) A. Hrennikoff. Weaknesses of the Theory of Plastic Design. The Engineering Journal (Engineering Institute of Canada, Montreal), November 1961 and July 1962.

(51) A. Hrennikoff. Plastic and Elastic Designs Compared. Preliminary Publication. Seventh Congress, Rio de Janeiro, 1964. International Association for Bridge and Structural Engineering.

(52) A. Hrennikoff. The Present Status of Plastic Design. The Engineering Journal (E.I. of Canada, Montreal), November 1965 and April 1966.

(53) A. Hrennikoff. Discussion. Generalized Approximate Method of Assessing the Effect of Deformation on Failure Loads by M.R. Horne. Seventh Congress, Rio de Janeiro, 1964. I.A.B.S.E.

SUMMARY

Although in principle the plastic design in steel is comparable to the conventional elastic design, in actuality it is inferior to it for several reasons, including the inability to analyze different types of buckling failure, the difficulty with the live load action and the wide variability of the plastic properties in the same grade of the material. The existence in the specifications of two distinct but equally acceptable methods of design the elastic and the plastic, leading to different solutions, is unsound.

RÉSUMÉ

En principe, l'analyse plastique et l'analyse élastique conventionnelle se valent dans la construction métallique. En fait, l'analyse plastique est inférieure à bien des égards: Par exemple par son incapacité d'analyser plusieurs types de ruine par voilement, la difficulté qu'on a avec l'action de la charge de service et les grandes divergences des propriétés plastiques dans une même qualité de matériau. Il n'est donc guère justifié de parler du calcul élastique et du calcul plastique comme de deux méthodes également valables, mais conduisant à des résultats différents.

ZUSAMMENFASSUNG

Obwohl die plastische Berechnungsmethode im Stahlbau im allgemeinen mit der konventionellen, elastischen Methode vergleichbar ist, so ist sie ihr doch aus verschiedenen Gründen unterlegen, inbegriffen die Unfähigkeit, verschiedene Bruchformen aus Beulen zu analysieren, sowie die Schwierigkeit der Verkehrslastbewegung und die weite Streuung der Plastizitätswerte desselben Materials. Es ist also nicht stichhaltig, von zwei gleich annehmbaren, ebenbürtigen Berechnungsmethoden zu reden, nämlich der elastischen und der plastischen, die zu verschiedenen Ergebnissen führen.

Leere Seite
Blank page
Page vide

Research on Plastic Design of Multi-Story Frames at Lehigh University

Recherche sur le calcul plastique des portiques multiétagés à l'Université de Lehigh

Forschung über das Traglastverfahren von Stahlhochbaurahmen an der Lehigh Universität

THEODORE V. GALAMBOS
Professor of
Civil Engineering
Washington University
St. Louis, Missouri

GEORGE C. DRISCOLL, Jr.
Professor of Civil Engineering
Lehigh University
Bethlehem, Pennsylvania

LE-WU LU
Associate Professor
of Civil Engineering
Lehigh University
Bethlehem, Pennsylvania

1) Introduction

The research team at the Fritz Engineering Laboratory of Lehigh University has extended a major effort since 1958 to the development of Plastic Design Methods for Planar Multi-Story Steel Frames. The principal motivation of this effort was the conviction that Plastic Design is both more rational and more economical than Allowable-Stress Design.

This research work can be subdivided into the following categories:

1) Research on Component behavior
2) Development of design and analysis methods
3) Experimental verification on frames

The summary of this research, as well as design methods and design examples for braced and unbraced multi-story frames, is given in Ref. 33 of the general report by Messrs. Steinhardt and Beer. The following brief comments are a review of the present status of this research and they are intended to provide additional information to that given in the General Report, especially emphasizing the Lehigh work.

2) Studies on Component and Subassemblage Behavior

A knowledge of the load-deformation behavior of the components of a structure is basic information required for a structural analysis. All the various components of a structure, such as wide-flange beams and beam-columns and many types of connections, were studied in several major research programs. In addition, the load-deformation behavior of subassemblages consisting of several members was thoroughly investigated. The purpose of this research has been the need to define the geometric and material limits which must be fulfilled for a successful application of Plastic Design procedures.

In the inelastic range the load-deformation relationship is highly non-linear, and it depends on yielding, strain-hardening, geometry changes, initial imperfections and on lateral-torsional and local buckling. A typical moment-rotation curve for a beam (Fig. 1) illustrates the initial elastic behavior (OA), the reduction in stiffness due to yielding in the presence of strain-hardening (AB), the point of instability due to combined local and lateral-torsional buckling (C) and the reduction of moment capacity in the unloading range (CD). The relationship is usually idealized in plastic design as a rigid-plastic (EF) or an elastic-plastic (OGF) relationship. However, some analysis methods utilize a bilinear curve (OGI) (Ref. 1) and in some applications the actual complete M-θ curve of beam-columns is utilized (Ref. 2, for example).

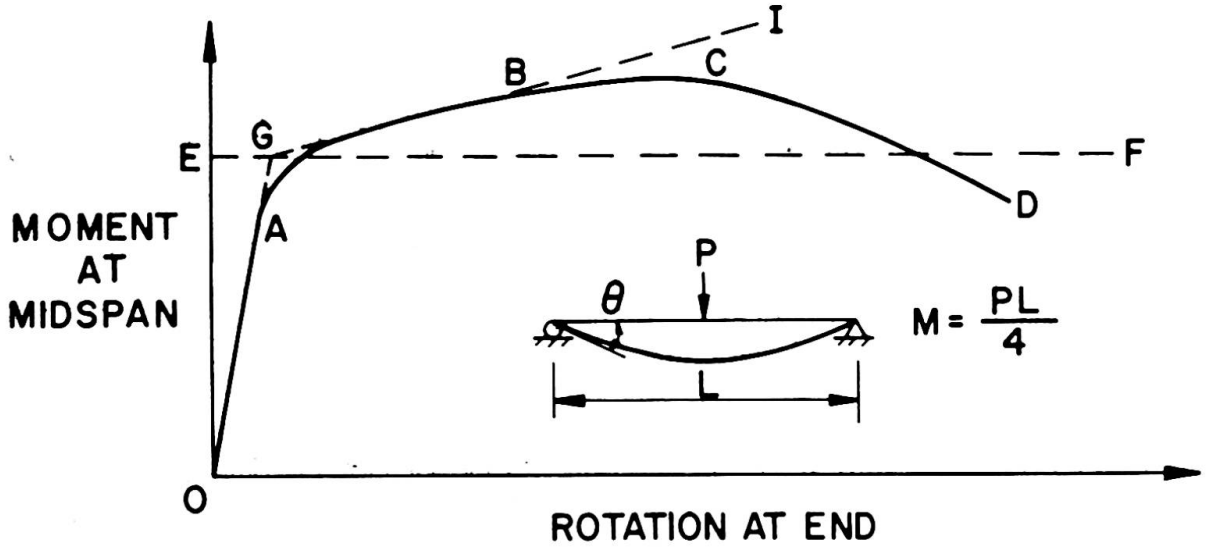

Fig. 1 Moment-Rotation Relationship of Beam

The research on components has concentrated on developing theoretical models whereby the whole M-θ curve, or significant portions of it, can be predicted. Many experiments were also performed to substantiate or complement these theoretical predictions.

Research on Beams

Numerous experiments were performed on wide-flange beams under uniform moment (Ref. 3) and moment gradient (Ref. 4), with various types of lateral bracing (Ref. 5), and on beams of high strength steel (Ref. 6), to study the post-yield behavior. Theoretical models, based on the concept that failure results when local and lateral-torsional buckling occur simultaneously, permitted a prediction of the limits of inelastic rotation capacity, and a definition of the required maximum flange and web width-thickness ratios and maximum bracing spacing (Refs. 7 through 12). For example, the maximum flange width-thickness ratios for steels with yield points of 36 and 50 ksi, respectively, were found to be 18 and 14. The corresponding maximum unbraced lengths for beams under uniform moment were determined to be, respectively, $38r_y$ and $28r_y$, where r_y is the weak axis radius of gyration.

Research on Beam-Columns

This work concentrated on the theoretical determination of the in-plane end moment-versus-end rotation curves of beam-columns, extending the work of Chwalla (Ref. 12.28 of the general report) to wide-flange members containing residual stress (Refs. 13 and 14; a summary of this work is given in Chap. 9 of Ref. 33 of the general report). The solution of the problem was achieved by numerical integration procedures, and non-dimensional curves for use in design are presented in Ref. 15. Experiments have given excellent verification of the theoretically obtained curves over a wide-range of the relevant parameters (Refs. 16 and 17). Theoretical studies on inelastic lateral-torsional buckling of unbraced beam-columns bent about their major axis have also shown good agreement with experiments (Refs. 18 and 19). Design procedures, based on this research, have been developed. These are summarized in Chap. 4 of Ref. 33 cited in the general report.

Research on Connections

Extensive experimental programs were performed on various types of rigid corner connections and rigid beam-to-column connections (for a review of this work see Chap. 8 of Ref. 12.27 of the general report). Design procedures, based on this work, were developed to assure that connections have adequate rotation capacity and a greater moment capacity than the members to be joined. These procedures are summarized in Chap. 5 of Ref. 33 given in the general report.

Research on Subassemblages

The basic design element for multi-story frames was found to be a "subassembly" consisting of one beam-column with a restraining beam framing into it at its upper and lower end. The load-deformation behavior of such a subassembly can be determined, using equilibrium, compatibility, and the moment-rotation relationships of its three elements (Chaps. 9, 10 and 17 in Ref. 33 of the general report and Refs. 2 and 20). Excellent correlation was noted between theoretically predicted and experimentally measured behavior (Ref. 17). These tests also provided experimental confirmation of individual beam, beam-column and connection behavior.

3) Frame Design Procedures

Following a phase of planning and layout, the design and analysis procedure can be divided roughly into three phases. These are (1) preliminary analysis, (2) selection of members, and (3) evaluation and revision of the preliminary design. The challenge in the preliminary analysis is to determine sets of forces on each member resulting from the expected loading which will permit selection of members in a straightforward fashion while using the knowledge which has been gained about component behavior. Frequently, the preliminary forces must be determined based on very limited information about the actual member sizes of the structure. It is also highly desirable that the preliminary force information be obtained in a form which permits selection of member sizes with a minimum of additional computation. Member selection should be followed by procedures for evaluation of the design or at least give a conservative measure of the relative performance of the structure. Evaluation procedures which will do an accurate job for a localized portion of the structure are especially

valuable. They permit revision of an unsuitable design before proceding to additional parts of the structure.

4) Design of Braced Frames

The development of preliminaru analysis and design procedures for braced frames resulted in methods which were exactly what would have been expected on the basis of earlier methods for low buildings. Beams were designed to develop three-hinge mechanisms in the clear span between column flange faces under full factored gravity load. The end moments of the beams were distributed arbitrarily to the columns above and below each joint, but can be justified by some other distribution. Though this practice might seem questionable to some, the lower bound theorem may be interpreted as supporting it. If only one distribution of internal forces could support the applied loads without violating the plasticity conditions, it would have to be the correct distribution of forces.

Design procedures for x-type diagonal bracing were formulated on the assumption that slender members would be used which could only carry tension and would buckle in the elastic range under compression. The bracing members were assumed to carry all lateral shears and to resist all shears due to the PΔ effect in simple truss action without assistance from the frame. Evaluation of the probable actual behavior of such a structural system would reveal that the frame must accept part of the lateral shear in order to deform sufficiently to allow the bracing members to deform enough to accept the lateral force. The usual design practice imposing a smaller load factor for gravity loads in combination with wind or earthquake loads allows the frame designed for gravity loads to retain some capacity for resisting lateral loads in combination with the diagonal bracing. Of course some revisions may be necessary in beams and columns adjacent to the diagonal bracing in order to resist axial force components imposed by the diagonal members.

Summaries of the design methods for braced frames are given in Refs. 21, 22 and 23.

5) Tests of Braced Frames

Tests of four frames which approximate the concepts of Steinhardt and Beer's Fig. 4a and 5a have been made.(Refs. 24, 25 and 26) All four frames had three 10 ft. stories and two 15 ft. bays but they were subjected to different combinations of loading. Twelve inch deep beams and 6W columns were used in all frames. Fig. 2 shows a load-deflection curve of one of the tests and a comparison typical of all the tests with a theoretical prediction ignoring the PΔ effect. The photograph in Fig. 2 shows the loading frame used to support the specimen laterally so a single plane frame could be tested alone. Also shown is the system of gravity load simulator devices which allow the application of truly vertical loads even though the frame sways laterally in its plane. The details of the experimental techniques are given in Ref. 27.

Conclusions of the test series were that lateral loading had no significant effect on the ability of the frames to reach the vertical load predicted on the basis of first order theory. Diagonal bracing carried most of the lateral load and the rigid frame was required to resist only 14 to 26 percent of the total lateral load. Very slender brac-

ing performed best when it was tightened during erection so that sag and slack were removed and diagonals subject to compression would remain in tension until the maximum expected lateral load was applied to the frame.

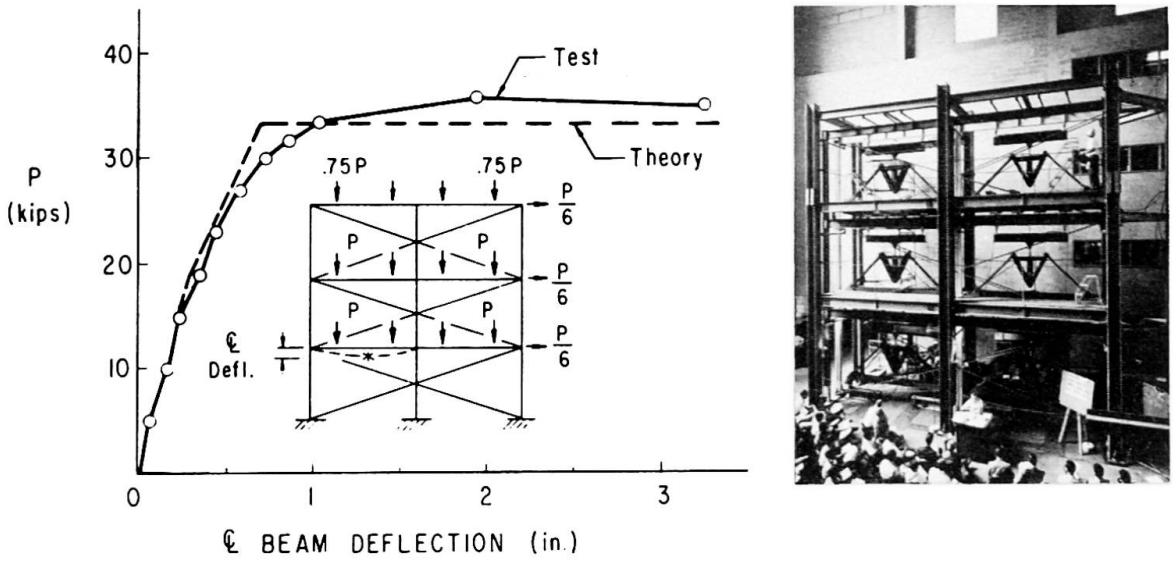

Fig. 2 Results of Braced Frame Test

6) Design and Analysis Procedures for Unbraced Frames

Three key quantities based on elementary statics form the basis of preliminary design procedures for unbraced frames subjected to combined gravity and wind or earthquake loading. A sum of column end moments in a story can be based on the total shear in the story caused by lateral loads and the PΔ effect initially estimated from an assumed story sway. The sum of girder end moments within one floor level can be based on an arbitrary reasonable assignment (such as one-half) of the sums of column end moments in the stories immediately above and below the floor. The third key quantity is the limiting end moment of a framed girder subjected to transverse loads in combination with the anti-symmetric moment pattern resulting from lateral loads. Many current design proposals avoid this issue by placing all loads at the joints, but this does not reflect the actual capacity of the members. For most loadings there will be a substantial beam moment at the lee column due to gravity load alone. Addition of the lateral loading causes this moment to increase to the plastic hinge value rapidly, thus revising the strength and stiffness characteristics of the beam for the duration of loading. Design charts giving important ordinates of the moment diagrams for usual loadings are available (Ref. 33 of the general report and Ref. 28).

The final operation of the analysis made for preliminary design purposes is a process called moment balancing. This process is primarily a "bookkeeping" method for assigning the general sums of column and girder end moments determined from prior steps to discrete locations within the story so that beams and columns may be selected each for their own separate force system.

Progress is being made in developing computer programs to parallel the manual computation procedures for preliminary design of unbraced frames. A program has been developed to handle the routine effort of tabulating forces on each member from tributary areas of floors, calcu-

lating story moments and shears, and performing the moment balance to determine all beam and column moments (Ref. 29). The designer then needs to select beams from standard economy tables for plastic design and columns from design charts of reduced plastic moments.

The trial design resulting from the preliminary procedure reflects a complete disregard of compatibility and an assumed story sway which is at best a guess. The subassemblage method of analysis has been developed to give an insight into the probable behavior of the structure selected (Refs. 30 and 31). This method uses the properties of the actual members to determine both the load vs. lateral deflection behavior of individual subassemblages and the behavior of a larger assemblage consisting of a whole story. It is necessary to construct load-deflection curves for each column in a story from design charts and then combine the curves for a whole story in order to use the subassemblage method manually. The complexity of this process is currently the largest barrier to practical application of plastic design of unbraced multi-story frames. Fortunately a computer program in the FORTRAN Language has been developed to compute the complete load-deflection curve for a story having known member sizes (Ref. 28).

Another computer program gives the elastic-plastic second order load-deflection curve of a complete unbraced multi-story frame up to maximum load (Ref. 32). It uses an iterative process for solution and requires surprisingly little computer capacity to handle frames up to thirty stories high and five bays wide. The disadvantage of such a program is that it ceases to function when it reaches the maximum load of the frame. Information as to the true relative suitability of less heavily loaded portions of the structure is lacking. This points up the main advantage of the other computer program based on the subassemblage method which discloses maximum strength of each story as well as deflections in the elastic range.

7) Tests of Unbraced Frames

Two series of unbraced frame tests were conducted. One series resulted from a frame stability investigation (Ref. 33). Two three-story frames 10 ft. wide were tested. Beams were 6 in. deep members and columns were 4 inch wide-flange members with strong axis slenderness ratios of 40 or 45. A typical test result is shown in Fig. 3.

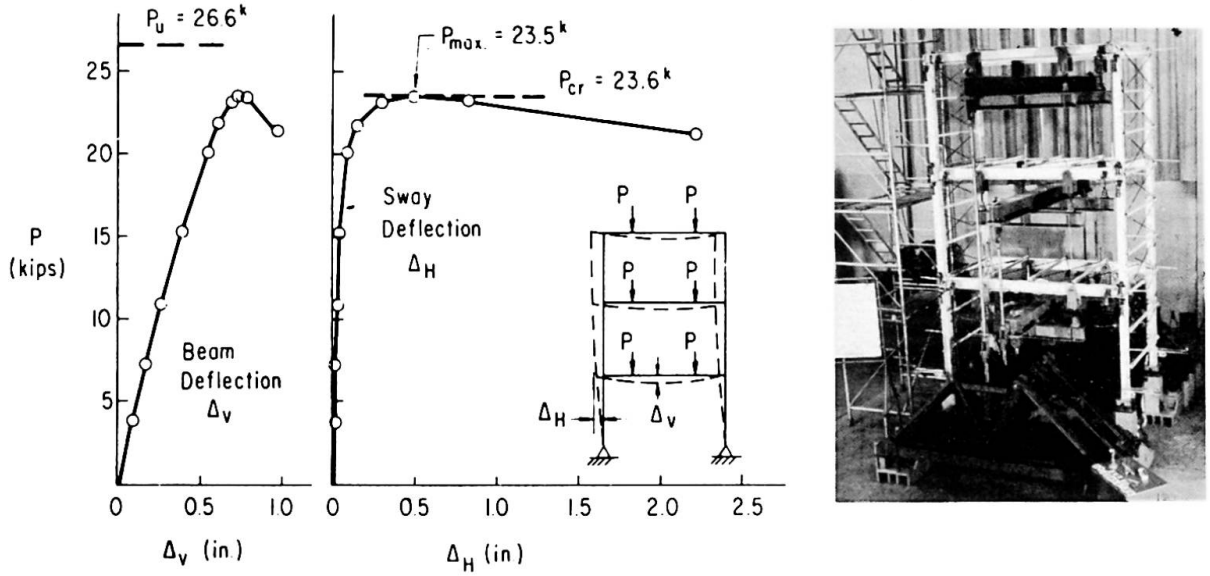

Fig. 3 Results of Frame Buckling Test

Results show that the reduction of the frame buckling load below the load to form a mechanism was predictable. The best method of prediction was a small lateral load method which used a load-deflection solution for the vertically loaded frame subjected to a simultaneous lateral load of one percent of vertical load or less. Both buckling test results exceeded the prediction based on an accidental lateral load equal to one-half percent of the vertical load.

The second series of unbraced frame tests was conducted on two three-story one-bay frames and one three-story two-bay frame subjected to combined vertical and horizontal loads in the plane of the frames (Ref. 34). All stories were 10 ft. high and all bays were 15 ft. wide. Various combinations of 8, 10 and 12 inch deep beams were used with 5 and 6 inch deep columns. A typical test result is shown in Fig. 4. The inadequacy of the first-order theory for prediction of behavior was de-

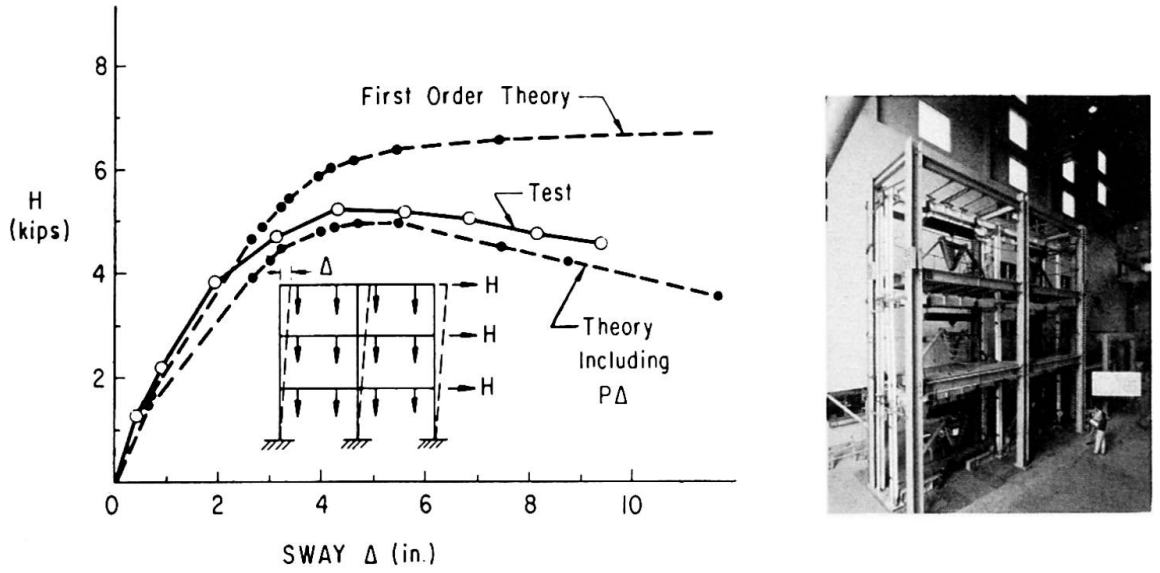

Fig. 4 Results of Unbraced Frame Tests

monstrated. Adequate predictions were obtained by using a linearized elastic-plastic second-order analysis which considered the PΔ a small number of cycles of reversed static loading providing data to assist in future earthquake resistant design studies.

8. Summary

The brief review of the research on component behavior shows the importance which was attached to the attainment of an understanding of the limiting capacity of beams, beam-columns and connections. Without such an understanding, Plastic Design would be impossible. Fortunately, the limits imposed by the component capacities can be achieved in practical design without offsetting the advantages of economy gained by Plastic Design of the total structure.

The understanding of component behavior is by no means complete. Many problems remain to be solved. Among these the following are currently under study: biaxial bending of beam columns, subassemblies with unbraced beam-columns, the post-yield material properties of new types

of high-strength steel, web local buckling, and behavior of components under repetitive reversed loading into the plastic range. Furthermore, the behavior of connections and of beams under moment gradient is under renewed study.

The outlook for adoption of a plastic design method for braced multi-story frames is promising. The 1968 revision of the American Institute of Steel Construction Specification will extend plastic design coverage to braced multi-story steel frames will soon be published and distributed (Ref. 23). It is significant to note that the plastic design method has already been applied successfully to the design of a braced eleven-story apartment building (Ref. 35).

The continuing efforts to produce practical methods for unbraced frames should bear fruit in the not-so-distant future. Experience with and refinement of these new methods can be expected to eventually lead to the economic limit of ordinary beam and columns skeleton type framing. There is no need to apologize when these limits are reached. The knowledge gained about component behavior and new procedures will help when new and better framing systems are developed.

REFERENCES

1. M. G. Lay
"A New Approach to Inelastic Structural Design"
Proc. Instn. of Civil Engineers, Vol. 34, May 1966.

2. V. Levi, G. C. Driscoll, Jr., L. W. Lu
"Structural Subassemblages Prevented from Sway"
ASCE Proceedings, Vol. 91, ST5, Oct. 1965.

3. G. C. Lee, T. V. Galambos
"Post-Buckling Strength of Wide-Flange Beams"
ASCE Proceedings, Vol. 88, EM1, Feb. 1962.

4. H. A. Sawyer
"Post-Elastic Behavior of Wide-Flange Steel Beams"
ASCE Proceedings, Vol. 87, ST8, Dec. 1961.

5. G. C. Lee, A. T. Ferrara, T. V. Galambos
"Experiments on Wide-Flange Steel Beams"
WRC Bulletin No. 99, Sept. 1964.

6. P. F. Adams, M. G. Lay, T. V. Galambos
"Experiments on High-Strength Steel Members"
WRC Bulletin No. 110, Nov. 1965.

7. M. G. Lay
"Yielding of Uniformly Loaded Steel Members"
ASCE Proceedings, Vol. 91, ST6, Dec. 1965.

8. M. G. Lay, T. V. Galambos
"Inelastic Steel Beams under Uniform Moment"
ASCE Proceedings, Vol. 91, ST6, Dec. 1965.

9. M. G. Lay
"Flange Local Buckling in Wide-Flange Shapes"
ASCE Proceedings, Vol. 91, ST6, Dec. 1965.

10. G. Haaijer
"Plate Buckling in the Strain-Hardening Range"
ASCE Proceedings, Vol. 83, EM2, April 1957.

11. M. G. Lay, T. V. Galambos
"Bracing Requirements for Inelastic Steel Beams"
ASCE Proceedings, Vol. 92, ST2, April 1966.

12. M. G. Lay, T. V. Galambos
"Inelastic Beam under Moment Gradient"
ASCE Proceedings, Vol. 93, ST1, Feb. 1967.

13. M. Ojalvo
"Restrained Columns"
ASCE Proceedings, Vol. 86, EM5, Oct. 1960

14. M. Ojalvo and Y. Fukumoto
"Nomographs for the Solution of Beam-Column Problems"
WRC Bulletin No. 78, 1962.

15. B. P. Parikh, J. H. Daniels, L. W. Lu
"Plastic Design of Multi-Story Frames - Design Aids"
Fritz Engineering Laboratory Report No. 273.24, Lehigh University, 1965.

16. R. C. Van Kuren, T. V. Galambos
"Beam-Column Experiments"
ASCE Proceedings, Vol. 90 ST2, April 1964.

17. M. G. Lay, T. V. Galambos
"Experimental Behavior of Restrained Columns"
WRC Bulletin No. 110, Nov. 1965.

18. Y. Fukumoto, T. V. Galambos
"Inelastic Lateral-Torsional Buckling of Beam-Columns"
ASCE Proceedings, Vol. 92, ST2, April 1966.

19. T. V. Galambos, P. F. Adams, Y. Fukumoto
"Further Studies on the Lateral-Torsional Buckling of Steel Beam-Columns
WRC Bulletin No. 115, July 1966.

20. V. Levi
"Plastic Design of Braced Multi-Story Frames"
Ph.D. Dissertation, Lehigh University, 1962, University Microfilms Inc., Ann Arbor, Michigan

21. L. W. Lu
"Design of Braced Multi-Story Frames by the Plastic Method"
Engineering Journal, AISC, Vol. 4, No. 1, January, 1967

22. L. W. Lu, J. O. Armacost, III and G. C. Driscoll, Jr.
"Plastic Design of Multi-Story Frames-Braced Frames"
Fritz Engineering Laboratory Report No. 273.55, Lehigh University
January, 1968

23. "Plastic Design of Braced Multi-Story Steel Frames"
American Iron and Steel Institute, New York, 1968.

24. J. A. Yura
"The Strength of Braced Multi-Story Steel Frames"
Ph.D. Dissertation, Lehigh University, 1965, University Microfilm Inc., Ann Arbor, Michigan.

25. G. C. Driscoll, Jr.
"Lehigh Conference on Plastic Design of Multi-Story Frames - A Summary"
Engineering Journal, AISC, Vol. 3, No. 2, April, 1966.

26. J. A. Yura and L. W. Lu
"Ultimate Load Tests on Braced Multi-Story Frames"
Fritz Engineering Laboratory No. 273.60, May 1968.

27. E. Yarimci, J. A. Yura, and L. W. Lu
"Techniques for Testing Structures Permitted to Sway"
Experimental Mechanics, SESA, Vol. 7, No. 8, August, 1967.

28. J. O. Armacost, Jr.
"The Computer Analysis of Unbraced Multi-Story Frames"
Fritz Engineering Laboratory Report No. 345.5, May, 1968

29. W. C. Hansell
"Preliminary Design of Unbraced Multi-Story Frames"
Ph.D. Dissertation, Lehigh University, 1966, University Microfilm Inc., Ann Arbor, Michigan.

30. J. H. Daniels
"A Plastic Method for Unbraced Frame Design"
Engineering Journal, AISC, Vol. 3 No. 4, October, 1966.

31. J. H. Daniels
"Combined Load Analysis of Unbraced Frames"
Ph.D. Dissertation, Lehigh University, 1967, University Microfilm Inc., Ann Arbor, Michigan.

32. B. P. Parikh
"Elastic-Plastic Analysis and Design of Unbraced Multi-Story Steel Frames"
Ph.D. Dissertation, Lehigh University, 1966, University Microfilm Inc., Ann Arbor Michigan.

33. B. M. McNamee
"The General Behavior and Strength of Unbraced Multi-Story Frames under Gravity Loading"
Ph.D. Dissertation, Lehigh University, 1967, University Microfilms Inc., Ann Arbor, Michigan.

34. E. Yarimci
"Incremental Inelastic Analysis of Framed Structures and Some Experimental Verifications"
Ph.D. Dissertation, Lehigh University, 1966, University Microfilm Inc., Ann Arbor, Michigan.

35. Anon.
"Plastic Design Cuts Cost on Prototype Highrise"
Engineering News-Record, Vol. 73, No. 3, July 1967.

SUMMARY

The research team at the Fritz Engineering Laboratory of Lehigh University has extended a major effort since 1958 to the development of Plastic Design Methods for Planar Multi-Story Steel Frames. The highlights of this work are presented in this discussion. The following topics are described: 1) component behavior, 2) development of design and analysis methods, and 3) experimental verification on frames.

RÉSUMÉ

L' équipe de recherche du Fritz Engineering Laboratory de l' université de Lehigh a porté, depuis 1958, son principal effort dans le domaine des méthodes de calcul plastique pour des structures multiétagées planes en acier. Les résultats de ces recherches avancées sont présentés dans cet exposé. Les sujets suivants sont décrits: 1) facteurs impliqués dans le comportement des structures, 2) exposé du calcul et des méthodes d'analyses, et 3) vérification expérimentale sur portiques.

ZUSAMMENFASSUNG

Die Forschungsgruppe des Fritz Engineering Laboratory an der Lehigh Universität hat seit 1958 einen erheblichen Aufwand gemacht an der Entwicklung des Traglastverfahrens fur ebene Stahlochbaurahmen. Die wichtigsten Erfolge dieser Forschung sind hier zusammengefasst. Die folgende Themen werden beschrieben: 1) das Verhalten von Fachwerkskomponenten, 2) die Entwicklung von Methoden für Dimensionierung und für Berechnung der Traglast, und 3) experimentelle Prüfung an Rahmen.

Leere Seite
Blank page
Page vide

Tests on a Full-Scale Rigid Jointed Multi-Storey Steel Frame

Tests à échelle réelle d'un câdre en acier de plusieurs étages

Prüfung eines maßstäblichen, steifknotigen Stockwerkrahmens

F.H. NEEDHAM
Great Britain

Introduction

The use of rigid jointed multi-storey steel frames, and the achievement of the economies which undoubtedly would accrue, has been inhibited for two reasons. Firstly, the difficulty of achieving in practice the necessary degree of continuity at the joints and secondly the complexity of design. With the development of site welding and its feasibility for effecting truly rigid joints (together with the development of the High Strength Friction Grip bolt) the former problem has been largely overcome. The latter problem, the evolution of a practical design method, has been the subject of study by a committee, set up jointly by the Institute of Welding and the Institution of Structural Engineers in 1957. Their first Report was published in December 1964. Rigorous analysis, taking into account full continuity and all possible loading combinations, remains intractable. However, by making certain simplifying assumptions, and by presenting in tabular form the results of a computer programme, this Report presents a logical and practical method of design for such frames. This contribution describes briefly a series of tests on a full scale frame carried out to verify the method and to determine the degree of error inherent in the simplifying assumptions.

Summary of Design Principles

The basic principle of the Report method is that of ultimate load design and being more accurate than simple design hitherto common it proposes that an overall load factor of 1.5 can safely be adopted, (instead of the usual 1.75).

The fundamental assumptions are as follows:-

(a) Steel is mild steel to British Standard 15, with a yield stress of 16.0 ton f/in^2 (25.2 kgf/mm^2).

(b) Connections between beams and columns have the full rigidity that can be made possible by welding. (The Report applies also to frames in which full rigidity of connections can be provided by HSFG bolts).

(c) The beams receive no assistance from composite action with the floors they support, and the columns no assistance from encasement.

(d) Lateral forces are resisted separately by walls or bracing, the steel frame being thus relieved of sway.

Individual beams and columns are designed on the following principles:-

(i) Major-Axis beams, i.e. beams which at both ends bend or restrain the columns about their major axes, are designed in accordance with the plastic theory. In general, a major-axis beam is designed on the assumption that the beam is "fixed-ended", developing under factored loading three plastic hinges, one at each end and one in the middle. The assumption of "fixed ends" is justified provided that at each end of the beam the sustaining moment supplied by the adjoining beam and columns is at least equal to the hinge moment at that end. Where this condition is not satisfied, the magnitude of the moment at the end of the beam reduces to that of the sustaining moment.

(ii) Minor-Axis beams, i.e. those other than major-axis beams, are designed elastically for factored loading to a limiting extreme fibre stress of 16.0 tonf/in^2, in order to provide elastic restraint to the columns about their minor axes. Here the stress in the beam is dependent on the loading and stiffness of all other members of the frame, and hence exact assessment is most complex. To overcome this difficulty the report introduces the "limited-frame" concept. This assumes that it is sufficiently accurate to consider only that limited part of the frame to which the member is connected (in the plane of bending). Further, that the remote ends of this limited frame can be considered as fixed. (See Fig. 1)

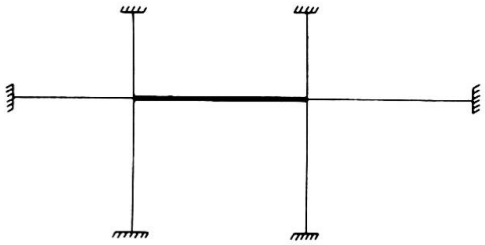

FIG 1 THE LIMITED FRAME FOR BEAM DESIGN

Having established the critical combination of dead and live loading applied to the limited frame, the support moments at the ends of the beam are found by a moment distribution procedure.

(iii) Columns

Evaluation of bending moments entails the use of the limited-frame concept in a manner similar to that employed in the design of minor-axis beams, except that in this case two limited-frames need to be considered, one in the plane of the major-axis and one in the plane of the minor-axis (see Fig. 2). Axial and bending stresses can then be found.

To these stresses are added firstly those due to axial load acting on the initially curved columns, and secondly those extra stresses arising from the axial load operating on the column as bent by the beams.

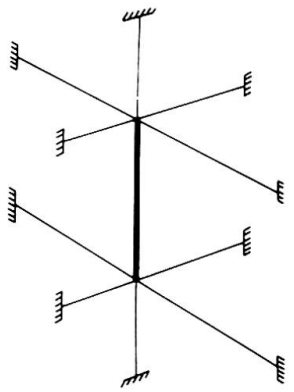

FIG. 2 THE LIMITED FRAME FOR COLUMN DESIGN

These incremental stresses have been evaluated on a computer for a wide range of values of axial stress, joint stiffness ratios, type of curvature and slenderness ratio. The results are presented in the Report in the form of design tables of reduced permissible column stresses (i.e. yield stress less the incremental stresses).

The design criterion adopted is that of attainment of yield stress at the extreme fibres in single curvature bending under factored load. This recognises that some plasticity will occur at the ends of a column under double curvature bending but can be safely accommodated.

Experimental Procedure

The experimental work was carried out through a collaborative agreement between the British Iron & Steel Research Association and the Government Building Research Station, whereby BISRA designed and secured a frame and BRS provided laboratory accommodation and services. Testing to a jointly agreed programme was carried out by personnel from both organisations.

Details of Test Frame

In order fully to verify the Report a 5-storey 5 x 5 bay frame would be needed. Consideration was given to testing a model but was rejected on various grounds.

Having regard to the available laboratory space, a 3 storey 2 x 1 bay frame was designed having the form shown in Fig. 3. The frame was designed to sustain at failure the following loadings:-

	Roof Level	2nd Floor Level	1st Floor Level
Dead Load	50 lb/Ft^2 (244 kg/m^2)	75 lb/Ft^2 (366 kg/m^2)	75 lb/Ft^2 (366 kg/m^2)
Live Load	80 lb/Ft^2 (391 kg/m^2)	90 lb/Ft^2 (439 kg/m^2)	90 lb/Ft^2 (439 kg/m^2)

It was assumed that one way spanning floor slabs, with intermediate beams, would be carried as uniformly distributed load for minor-axis beams and centre point loads for major-axis beams. For the test, point loads at quarter-points represented U.D.L. The range of available sections is such that many members were over-designed.

Sway was prevented by tying the frame to the laboratory balconies. Rigid joints were effected with High Strength Friction Grip bolts. Intermediate beams were made heavy so as to exclude premature yielding in them.

The average yield stress of the steel was found to be 19 tonf/in^2 (30 kgf/mm^2). This was not taken into account in design.

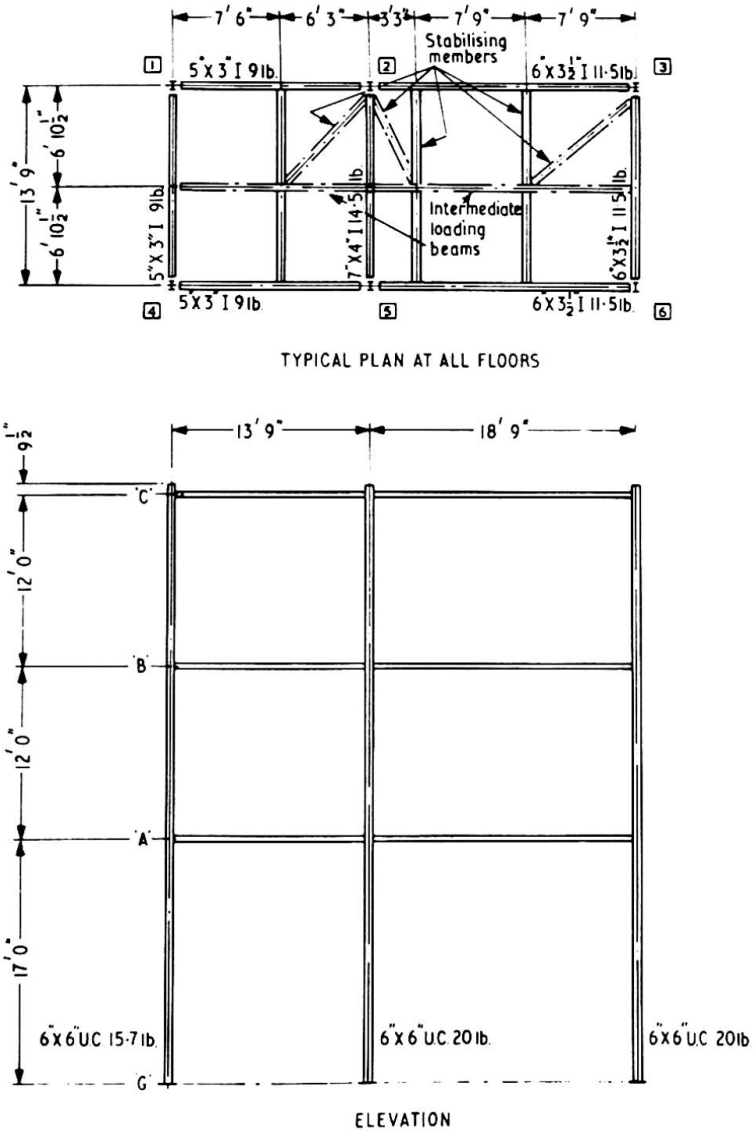

FIG. 3 OVERALL FRAME DIMENSIONS

Loading and Instrumentation

Loading was applied to beams and columns by means of spreader beams acted upon by cables passing through the laboratory strong floor. These were tensioned by hydraulic jacks reacting against the underside of the floor. A total of 396 electrical resistance strain gauges were fixed to the structure in groups of four, at the beams and columns at the joints, and at the mid-span of the beams. Transducers measured deflections of beams at mid-span and of columns at five points about both axes. Load cells measured cable forces.

Test Programme

In an ideal test frame, at the factored working load major-axis beams should have developed three plastic hinges, and minor-axis beams and columns should have attained yield at the extreme fibres To achieve this the following conditions should obtain:-

(i) A wholly accurate design method.

(ii) The ability to provide sections with exactly the right properties.

(iii) An accurate knowledge of the yield stress.

These conditions cannot be achieved in practice and it was item (i) which was being investigated in this case.

Testing was therefore carried out in the following stages:

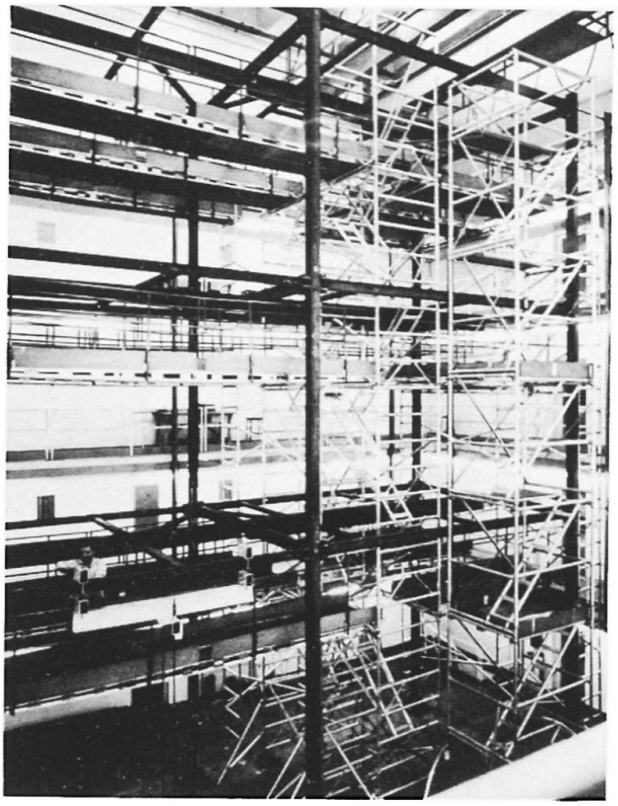

Fig. 4 - Overall View of Test Frame

Stage 1

Stanchions and beams were loaded in turn to their design loads (i.e. working load x 1.5).

Stage 2

Stanchions and beams were loaded up to their limiting values, as calculated by the Report method, taking discrepancies due to (ii) and (iii) above into account.

Stage 3

Test loads were successively increased until strain and deflection measurements confirmed that limiting conditions, as defined by the Report, had been attained. (Thus the difference between Stage 2 and Stage 3 would indicate the degree of conservatism in the design method).

Stage 4

Loading was continued to outright collapse of columns, by imposing additional axial load (major-axis beams having already attained full plasticity.)

Summary of Results

Stage 1

As was to be expected all frame members remained elastic throughout.

Stage 2

Major-axis beams achieved central plastic hinges, but although some plasticity was achieved at the supports, full plastic hinges were not developed there.

Adjacent to the centre columns, minor-axis beams reached yield stress.

Peak stresses in the columns were in all cases less than the yield stress.

Stage 3

Major-axis beams reached full plasticity at three points.

Minor-axis beams yielded.

Columns were loaded so as to produce the maximum single curvature bending condition and axial load was applied to produce yielding.

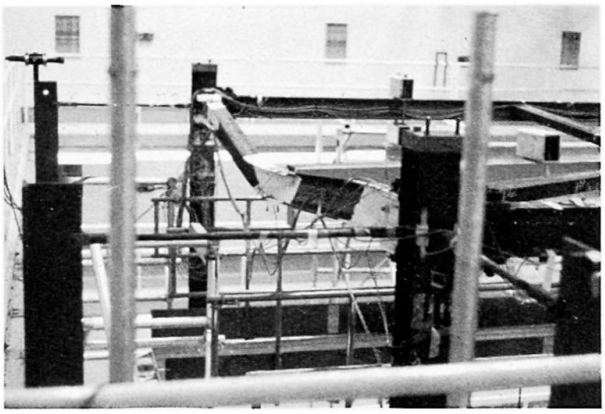

Fig. 5 - Major-Axis Beam at Collapse

In general the loads applied to a group of members under test were increased until one or other of these members reached its limiting condition. When that occurred the load on that member was maintained whilst the loads on the remaining members were increased until the next failure, and so on. Thus at this stage loading departed from a hypothetical floor loading.

Stage 4

Three column lengths were loaded to collapse, one at each floor level. They were first subjected to the same beam end moments as in Stage 3 and then direct axial load was applied until collapse.

Conclusions

Having in Stage 2 applied loads which compensate for the chosen sections and for a yield stress of 19 tonf/in^2 (30 kg f/mm^2), it can be asserted that the design method is safe.

From the results of Stage 3 loading the following broad conclusions can be drawn:-

(i) Major-axis beam design was slightly conservative, the ultimate loads being underestimated.

(ii) The minor-axis beams were slightly underdesigned in that the limited frame concept gave slightly smaller design moments than an accurate elastic analysis.

(iii) The measured column stresses were consistently slightly less than the stresses predicted by the Report. It was clear from Stage 4 loading that a considerable margin for the addition of axial load exists beyond the limiting condition as defined by the Report, i.e. the attainment of yield in the extreme fibres under single curvature bending. These results show that the criterion of column design could be considerably improved by subsequent research leading to an accurate criterion for collapse with increased plasticity.

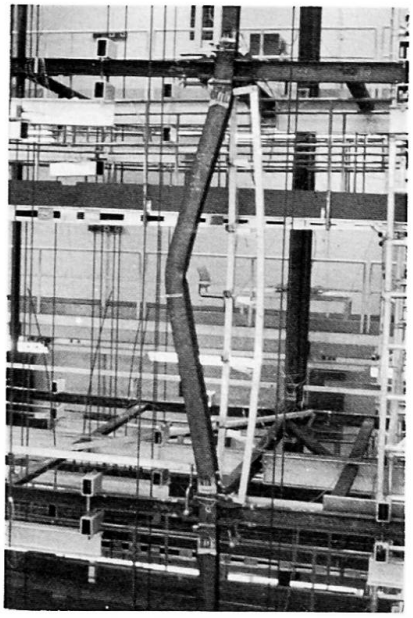

Fig. 6 - Column at Collapse

In short, the Joint Committee Report presents a logical design method for rigid jointed frames, which is reasonably accurate and which can be applied with confidence.

Future Work

Following the publication of the first Report, the Joint Committee has been reconvened to extend the method to include such things as the use of High Tensile Steel, composite action of beams, concrete encased columns, plastic design of minor-axis beams, etc.

At the time of writing it is hoped that a second frame will be tested by the same procedure. It will be of larger dimensions, incorporating an internal column, and will be of High Tensile Steel to BS.968.

Acknowledgements

This work is more fully reported in a paper presented to the Institution of Structural Engineers in April, 1968 by R.H. Wood, R.F. Smith and the present author, who would like here to pay tribute to his colleague's work.

This project formed part of the respective programmes of the Building Research Station and BISRA and is published by permission of the Directors.

SUMMARY

This contribution briefly describes a new design method, based on certain simplifying assumptions, for treating rigid-jointed multi-storey frames, and which was published in 1964. By a collaborative arrangement a 2 bay x 1 bay frame, 3 stories high was designed by BISRA to this method and tested at the Building Research Station Laboratory. A series of tests were carried out at working load and to failure, to verify the design method and to establish actual load factors.

RÉSUMÉ

Ceci est la brève description d'une nouvelle méthode d'études, basée sur certaines hypothèses simplificatrices, du traitement des câdres à plusieurs étages, publiée en 1964.

Un câdre de trois étages, consistant en un arrangement de 2 x 1 câdre fut conçue selon cette méthode par BISRA et testée au Building Research Laboratory. Une série de tests fut menée dans les conditions de travail et jusqu'au point de rupture, pour vérifier la méthode d'étude et pour établir les facteurs de charge réelle.

ZUSAMMENFASSUNG

Dieser Beitrag beschreibt in knappen Worten eine neue Bemessungsregel für steifknotige Stockwerkrahmen, die auf einigen vereinfachenden Annahmen beruht und 1964 veröffentlicht worden war. Ein 2mal eine Abteilung umfassender, dreistöckiger Rahmen ist von der BISRA entworfen und beim Building Research Station Laboratory geprüft worden. Eine Versuchsreihe ist für Arbeits- und Traglast durchgeführt worden, um die plastische Bemessung zu erhärten und Nutzlastwerte zu finden.

Die Traglast von eingespannten Geschoß-Stützen mit I-Querschnitt bei Biegung um beide Hauptachsen

Ultimate Strength of I-shaped Restrained Columns in Biaxial Bending

Charge de rupture de colonnes en I encastrées soumises à des moments de flexion autour des deux axes principaux

UDO VOGEL
Privatdozent, Dr.-Ing., Universität Stuttgart (TH)

1. Einleitung

Für die Berechnung der Grenzlasten von e b e n e n Rahmentragwerken aus Stahl stehen Verfahren der Plastizitätstheorie zur Verfügung, die mit ausreichender Genauigkeit die stabilen, indifferenten und labilen Gleichgewichtszustände im unelastischen Bereich beschreiben (z.B. [1], [2], [3]). Bei Hochhäusern ist das Verhalten der Stützen von ausschlaggebender Bedeutung für die Stabilität des ganzen Gebäudes. Sind die Stützen Teile eines ebenen, rahmenartigen Skeletts, so können sie nach einem der bekannten Verfahren dimensioniert werden. Häufig werden diese Stützen jedoch durch rechtwinklig zu den Hauptrahmen verlaufende "Sekundär-Rahmen", biegesteif angeschlossene Quer-Unterzüge oder durchlaufende Decken auch rechtwinklig zur Hauptrahmenebene auf Biegung beansprucht. Die genaue Traglastberechnung solcher zweiachsig aussermittig gedrückter Stützen ist - schon bei statisch bestimmter Lagerung - sehr schwierig und kompliziert, wie die wenigen bisher bekannten Veröffentlichungen auf diesem Gebiet zeigen ([4], [5], [10]).

Im Folgenden wird ein Verfahren entwickelt, mit dessen Hilfe die Traglasten von eingespannten - seitlich unverschieblichen - Geschosstützen mit I-Querschnitt bei Biegung um beide Hauptachsen näherungsweise mit geringem Rechenaufwand ermittelt werden können. Dies ist die Erweiterung einer früher veröffentlichten Untersuchung ([3], [6]), in der die Traglast von Geschosstützen bei Biegung in einer Ebene behandelt wurde.

Mehrere Traglastversuche an Stützen natürlicher Grösse dienen der Verbesserung und Bestätigung der theoretischen Ergebnisse.

2. Theoretische Traglast-Ermittlung

2.1. Vorbemerkung

Bei eingespannten Stützen werden die Biegemomente durch die Auflagerverdrehungen der angeschlossenen Riegel, Unterzüge oder Decken erzeugt. Diese Biegemomente sind abhängig von der Steifigkeit der Stützen, d.h. von den vorhandenen Axiallasten und vom Grad der Plastifizierung. Es ist daher sinnvoll, neben den Axiallasten nicht die Biegemomente sondern direkt die Kopf- und Fuss-Drehwinkel φ_x (um die x-Achse) und φ_y (um die y-Achse) als weiters Beanspruchungsmass für die Stützen einzuführen. Diese Winkel können wegen der im Verhältnis zur Stützen-

steifigkeit grossen Steifigkeit der Deckenkonstruktion und wegen der geringen Grösse der aufnehmbaren Stützenendmomente im Versagenszustand als Auflagerdrehwinkel der an den Stützen frei drehbar gelagert gedachten Decken bzw. Unterzüge ermittelt werden. Damit können auch die Einflüsse von zusätzlichen Kriech-Durchbiegungen bei Stahlbeton oder Verbundträgerdecken leicht erfasst werden.

2.2 Voraussetzungen der Näherungstheorie

a) Es gilt das bekannte idealelastisch- idealplastische Spannungs-Dehnungs-Gesetz für Baustahl mit der Fliessgrenze σ_F.

b) Die Traglast der Stütze ist erreicht, wenn durch Bildung einer genügenden Anzahl von Fliessgelenken (mindestens 3) eine kinematische Kette entstanden ist.

c) Die Ausbreitung teilplastischer Zonen neben den Fliessgelenken wird vernachlässigt.

d) Werden sowohl der Stützenkopf als auch der Stützenfuss verdreht, so sei das Verhältnis φ_y/φ_x an Kopf und Fuss gleich gross.

e) Die verformte Achse der Stütze liegt im Traglastzustand in einer durch die Lage der Fliessgelenke definierten E b e n e . Torsionsmomente infolge der tatsächlich räumlich gekrümmten Stabachse werden vernachlässigt (s.a. [4]).

f) Der Einfluss der Verformungen auf das Kräfte-Gleichgewicht wird berücksichtigt.

g) Der Einfluss der Axiallast auf die Stützensteifigkeit und auf das aufnehmbare vollplastische Moment wird ebenfalls berücksichtigt.

Es sei darauf hingewiesen, dass die Voraussetzungen f) und g) notwendig sind, um das Traglastproblem richtig als Stabilitätsproblem ohne Gleichgewichtsverzweigung zu behandeln. Die Voraussetzungen b) und c) hingegen führen gegenüber der genaueren Untersuchung (z.B. [4], [5], [10]) zu einer wesentlichen Vereinfachung der Rechnung.

2.3 Die Komponenten des aufnehmbaren vollplastischen Moments des dünnwandigen doppeltsymmetrischen I-Querschnitts bei schiefer Biegung mit Normalkraft

Für die Herleitung der den Einfluss von Normalkraft und schiefer Biegung erfassenden Reduktionsfaktoren ψ_x und ψ_y für die vollplastischen Momente um die x- und um die y-Achse können die Momentenanteile der Spannungen in den Stegflächen vernachlässigt werden. Es wird also das I-Profil mit unendlich dünnem, jedoch schubsteifem Steg untersucht.

Bei schiefer Biegung und Normalkraft sind im Zustand der vollständigen Durchplastifizierung zwei Fälle für die Lage der Spannungsnullinie möglich:

a) Die Nullinie verläuft durch beide Flansche (Bild 2.1.a).
b) Die Nullinie verläuft nur durch einen Flansch (Bild 2.1.b).

Im Fall a) ergibt sich mit Bild 2.1.a und den folgenden Bezeichnungen

$M^*_{plx} = bt(h - t)\sigma_F$ (Vollplast. Moment bei Biegung um x-Achse allein)

$M^*_{ply} = \frac{tb^2}{2}\sigma_F$ (Vollplast. Moment bei Biegung um y-Achse allein)

$N_{pl} = F\sigma_F = 2\,bt\sigma_F$ (Vollplast. Normalkraft bei Druck allein)

aus den Gleichgewichtsbedingungen im Querschnitt $\Sigma N=0$, $\Sigma M_x=0$ und $\Sigma M_y=0$:

$$M_{plx,N} = \varrho \cdot M^*_{plx} \qquad (2.1.a)$$

$$M_{ply,N} = (1 - \varrho^2 - \varkappa^2) M_{ply} \tag{2.2.a}$$

Hierin bedeuten:

$$\varrho = \frac{\operatorname{ctg}\beta}{b/(h-t)} \tag{2.3}$$

$$\varkappa = \frac{N}{N_{pl}} = \frac{N}{F\sigma_F} \tag{2.4}$$

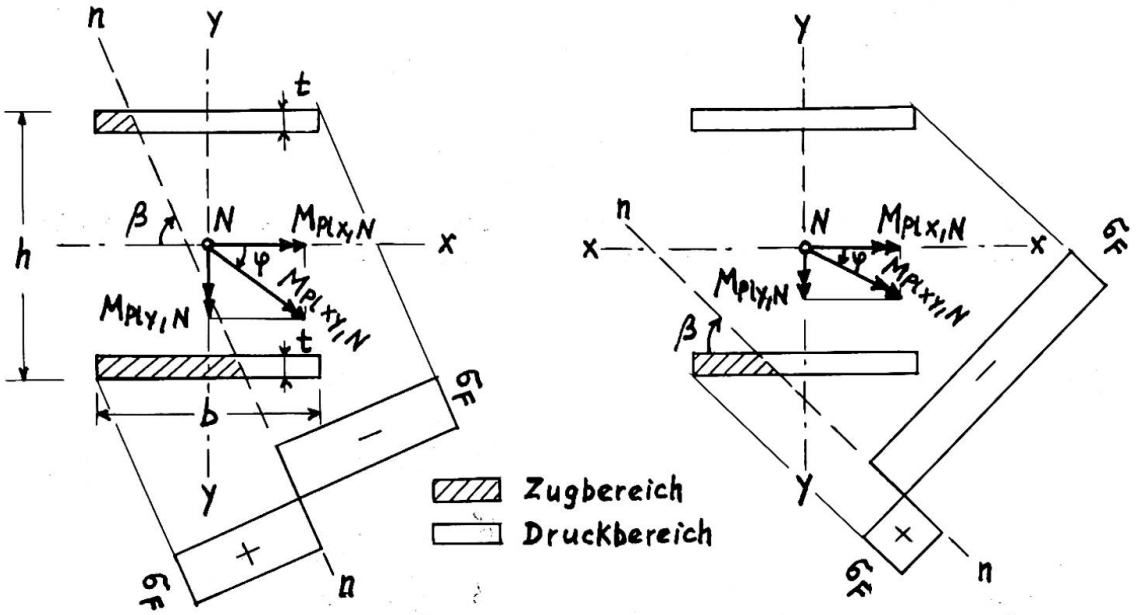

a) Nullinie in beiden Flanschen b) Nullinie in einem Flansch

Bild 2.1: Vollplastizierter I-Querschnitt bei schiefer Biegung und Normalkraft

Der Faktor ϱ lässt sich auch als Funktion des häufig aus anderen Bedingungen bekannten Neigungswinkels φ des resultierenden Biegemomenten-Vektors zur x-Achse ausdrücken:

$$\operatorname{tg}\varphi = \frac{M_{ply,N}}{M_{plx,N}} = \frac{1 - \varrho^2 - \varkappa^2}{\varrho} \cdot \frac{\frac{1}{2}tb^2\sigma_F}{bt(h-t)\sigma_F} = \frac{1 - \varrho^2 - \varkappa^2}{2\varrho} \cdot \frac{b}{(h-t)} \tag{2.5.a}$$

Mit dem Hilfswert

$$\gamma = \frac{\operatorname{tg}\varphi}{b/(h-t)} \tag{2.6.a}$$

erhält man aus der quadratischen Gleichung (2.5.a)

$$\varrho = -\gamma \overset{+}{(-)} \sqrt{\gamma^2 + (1-\varkappa^2)} \tag{2.7}$$

Im Fall b) ergibt sich analog aus den Gleichgewichtsbedingungen:

$$M_{plx,N} = (1 - \varkappa) M^*_{plx} \tag{2.1.b}$$

$$M_{ply,N} = 2\varkappa(1 - \varkappa)\, M^*_{ply} \tag{2.2.b}$$

Der Wert für $M_{plx,N}$ nach Formel (2.1.b) kann bei schiefer Biegung nicht überschritten werden, da er bereits gleich dem Wert des vollplastischen Moments bei einachsiger Biegung um die x-Achse und gleichzeitig wirkender Normalkraft ist (vgl.[3], S.23, Gl.(3.6)).

Hier erhält man für $tg\varphi$ die Beziehung:

$$tg\varphi = \varkappa \cdot \frac{b}{h-t} , \qquad (2.5.b)$$

und damit für den Hilfswert γ den Grenzwert

$$\gamma_{gr} = \frac{tg\varphi}{b/(h-t)} = \varkappa , \qquad (2.6.b)$$

der zu dem möglichen Maximalwert von $M_{ply,N}$ führt.

Für $\gamma \geq \varkappa$ gelten die Formeln (2.1.a) und (2.2.a),
für $\gamma \leq \varkappa$ gelten die Formeln (2.1.b) und (2.2.b).

Zur Erleichterung der praktischen Berechnung sind diese Beziehungen graphisch in zwei Interaktions-Diagrammen in Bild 2.2 dargestellt.

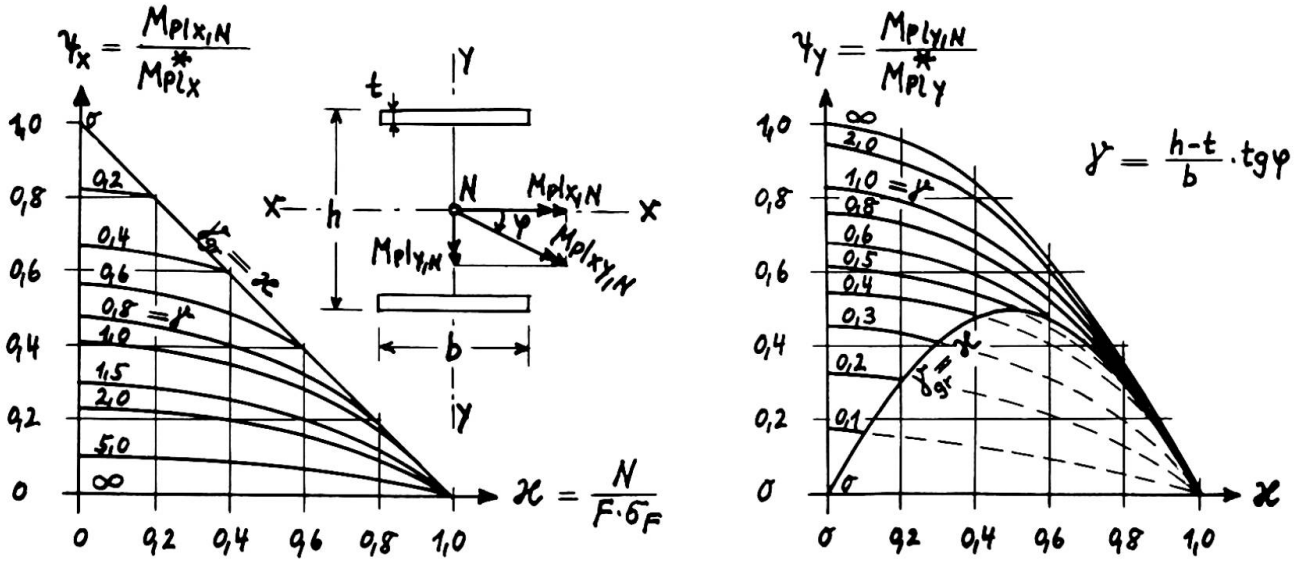

Bild 2.2 : Abminderungsfaktoren für die Komponenten des vollplastischen Moments bei schiefer Biegung und Normalkraft

2.4 Traglast von Geschosstützen bei entgegengesetzt gleich grossen Kopf- und Fussdrehwinkeln um x- und y-Achse

Dieser Beanspruchungsfall ist in Bezug auf die Traglast in der Regel der ungünstigste, da ein einsinniger Krümmungsbauch der Stütze entsteht (s. Bild 2.3, Stütze I).

Die Traglast einer Stütze vom Typ I ist erreicht, wenn drei Fliessgelenke entstanden sind. In [3] , S. 35, wurde für einachsige Biegung gezeigt, dass das erste Fliessgelenk in Stabmitte und die beiden letzten gleichzeitig an Kopf und Fuss entstehen. Dies gilt auch bei zweiachsiger Biegung.

Die Traglast kann aus den Gleichgewichts- und Verformungsbedingungen der deformierten Stütze im Zustand des beginnenden Versagens ermittelt werden. In diesem Zustand hat noch keine Verdrehung in den sich zuletzt bildenden Fliessgelenken stattgefunden.

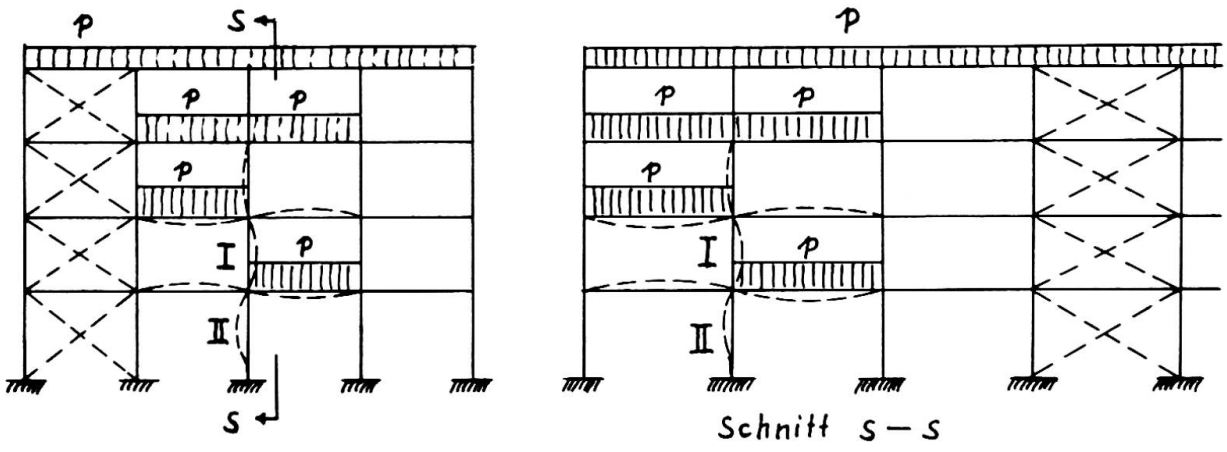

Bild 2.3 : Schachbrettbelastung im Bereich der untersuchten Stützen

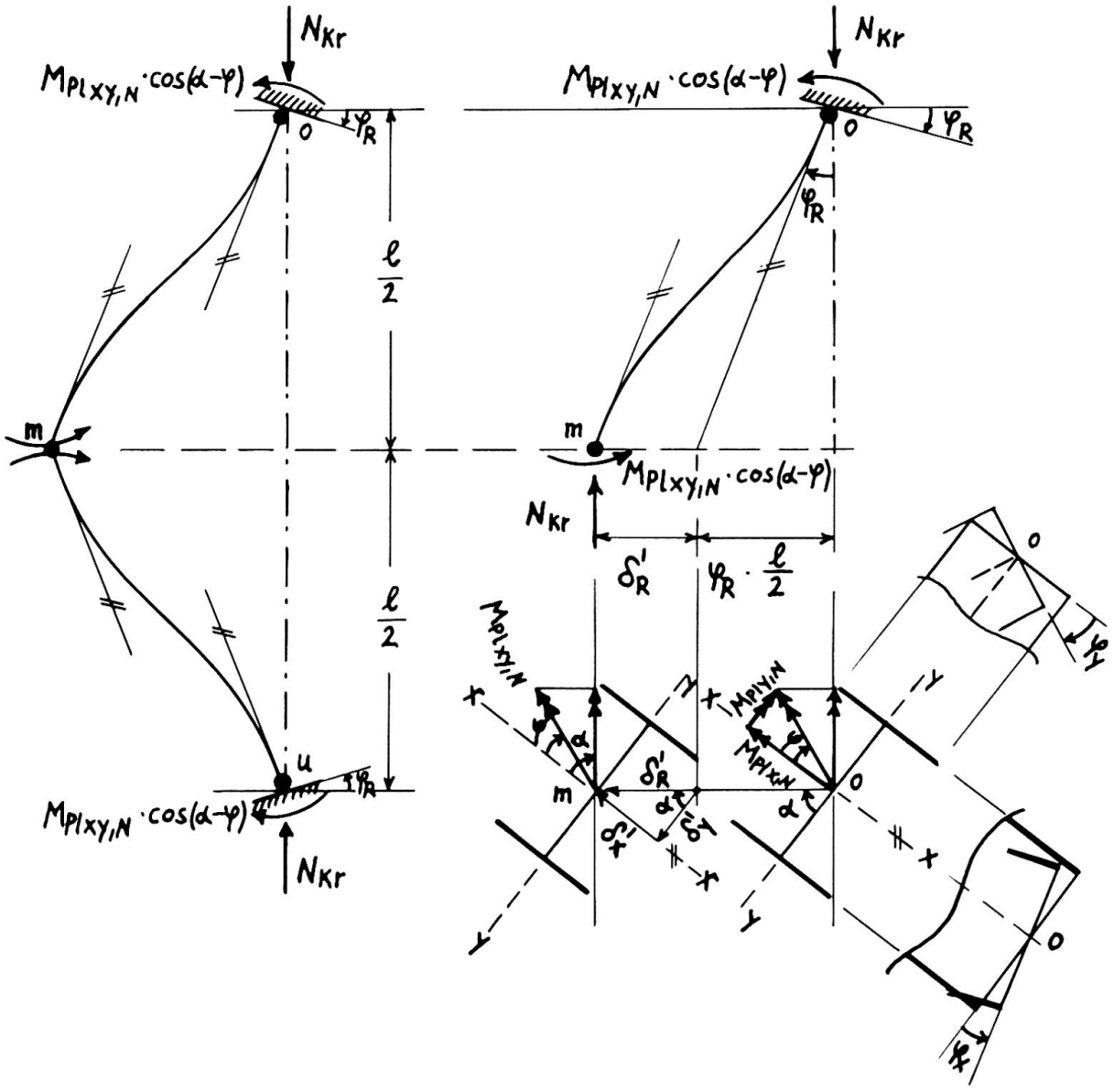

Bild 2.4 : Kräftespiel und Verformungen beim Erreichen der Traglast (Kopf- und Fussdrehwinkel gleich gross)

Die Bedingung für das Momentengleichgewicht in der Verformungs-Ebene der oberen Stabhälfte lautet mit den Bezeichnungen von Bild 2.4

$$N_{kr} \cdot (\delta'_R + \varphi_R \cdot \tfrac{l}{2}) = 2\, M_{plxy,N} \cdot \cos(\alpha - \varphi) \qquad (2.8)$$

Mit der Voraussetzung e) des Abschnittes 2.2 lassen sich die Verformungen in x- und y- Richtung getrennt ermitteln. Man erhält somit nach Theorie II. Ordng.:

$$\delta'_R = \frac{\delta'_y}{\cos\alpha} = \frac{1}{\cos\alpha} \cdot \frac{(l/2)^2}{EI_x} \cdot \psi_x \cdot M^*_{plx} \,(\alpha'_x - \beta'_x) \qquad (2.9.a)$$

mit den Hilfswerten α'_x und β'_x, die als Funktionen der Stabkennzahl

$$\varepsilon_{x\,(y)} = \frac{l}{2} \sqrt{\frac{N_{kr}}{EI_{x\,(y)}}} = \sqrt{\pi} \cdot \lambda_{x\,(y)} \sqrt{\frac{\sigma_F}{E}} \qquad (2.9.b)$$

aus [8] entnommen werden können. Für praktische Berechnungen ist die Differenz $(\alpha' - \beta')$ als Funktion von ε in Bild 2.5 graphisch dargestellt.

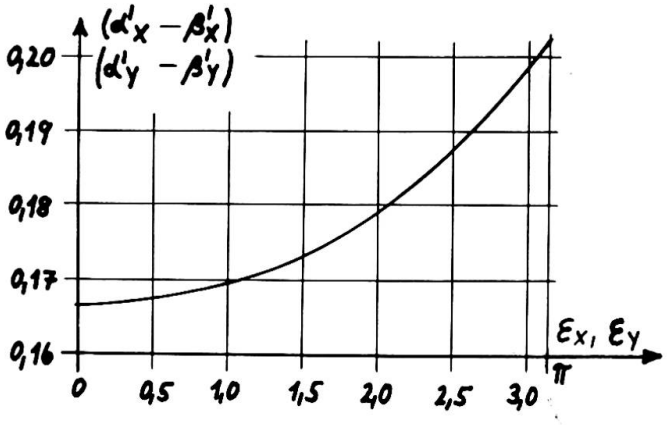

Bild 2.5 : Hilfswerte $(\alpha' - \beta') = f_{(\varepsilon)}$

Für den resultierenden Kopf- bzw. Fussdrehwinkel gilt:

$$\varphi_R = \varphi_x \cdot \cos\alpha + \varphi_y \cdot \sin\alpha = \varphi_x \left(\cos\alpha + \frac{\varphi_y}{\varphi_x} \cdot \sin\alpha\right) \qquad (2.10)$$

Und für den Neigungswinkel α der Verformungsebene gegen die Ebene durch die y-Achse des Querschnitts erhält man entsprechend (2.9.a):

$$\operatorname{tg}\alpha = \frac{\delta'_x}{\delta'_y} = \frac{I_x \cdot \psi_y \cdot M^*_{ply}\,(\alpha'_y - \beta'_y)}{I_y \cdot \psi_x \cdot M^*_{plx}\,(\alpha'_x - \beta'_x)}$$

Setzt man $M^*_{plx} = \alpha_x \cdot W_x \cdot \sigma_F$, $M^*_{ply} = \alpha_y \cdot W_y \cdot \sigma_F$ und beachtet, dass $\frac{I_x \cdot W_y}{I_y \cdot W_x} = \frac{h}{b}$ ist, so wird daraus

$$\operatorname{tg}\alpha = \frac{\psi_y}{\psi_x} \cdot \frac{\alpha_y}{\alpha_x} \cdot \frac{h}{b} \cdot \frac{\alpha'_y - \beta'_y}{\alpha'_x - \beta'_x} \,, \qquad (2.11)$$

worin α_x und α_y die "Formfaktoren" für plastische Biegung um x-, bzw. y-Achse des I-Querschnitts bedeuten.

Der Wert $\operatorname{tg}\varphi$ ist durch (2.5.a) definiert. Mit der Annahme, dass das V e r h ä l t n i s der vollplastischen Momente um y-Achse und x-Achse zueinander gleich dem V e r h ä l t n i s der Biegemomente nach Theorie I. Ordnung ist,

ergibt sich die - gegenüber (2.5.a) unabhängige - Beziehung :

$$\operatorname{tg}\varphi = \frac{M_{y,Th.I.O.}}{M_{x,Th.I.O.}} = \frac{I_y \cdot \varphi_y}{I_x \cdot \varphi_x}, \qquad (\gamma \geq \varkappa) \tag{2.12}$$

die nur im Bereich $(\gamma \geq \varkappa)$ gültig ist. Ergibt sich mit (2.12) der Wert $\gamma < \varkappa$, so ist $\gamma = \varkappa$ zu setzen und für $\operatorname{tg}\varphi$ Gleichung (2.5.b) zu verwenden.

Setzt man nun (2.9.a) und(2.10) in Gleichung (2.8) ein, so erhält man nach Umformung die gesuchte Traglastbedingung zu:

$$\varkappa = \frac{N_{kr}}{F\sigma_F} = \frac{2 \cdot \psi_x \cdot \alpha_x \cdot (1 + \operatorname{tg}\alpha \cdot \operatorname{tg}\varphi)}{(\alpha'_x - \beta'_x)\frac{\psi_x \alpha_x}{\cos^2\alpha}\left(\lambda_x \sqrt{\frac{\sigma_F}{E}}\right)^2 + (\lambda_x \cdot \varphi_x) \cdot \frac{h}{2i_x} \cdot \left(1 + \frac{\varphi_y}{\varphi_x} \cdot \operatorname{tg}\alpha\right)} \tag{2.13}$$

Diese Gleichung muss - zusammen mit (2.11) und (2.12) - durch Probieren gelöst werden, da auch auf der rechten Seite der gesuchte Wert $\varkappa$ in den Funktionen für $\psi_x, \alpha'_x, \beta'_x$, $\operatorname{tg}\alpha$ und gegebenenfalls auch $\operatorname{tg}\varphi$ enthalten ist.

Bild 2.6 gibt die graphische Parameter-Darstellung der numerischen Auswertung von (2.13) mit $\varphi_y/\varphi_x = 1$ und $\varphi_y/\varphi_x = o$ (einachsige Biegung) für die Stützenprofile IPB loo ÷ 3oo nach DIN 1025 wieder, wobei für die Verhältnisse der Querschnittswerte folgende Mittelwerte eingesetzt wurden:

$h/i_x = 2{,}34$, $I_y/I_x = o{,}353$, $b/(h-t) = 1{,}o8$, $h/b = 1$, $\alpha_x = 1{,}13$, $\alpha_y = 1{,}5$.

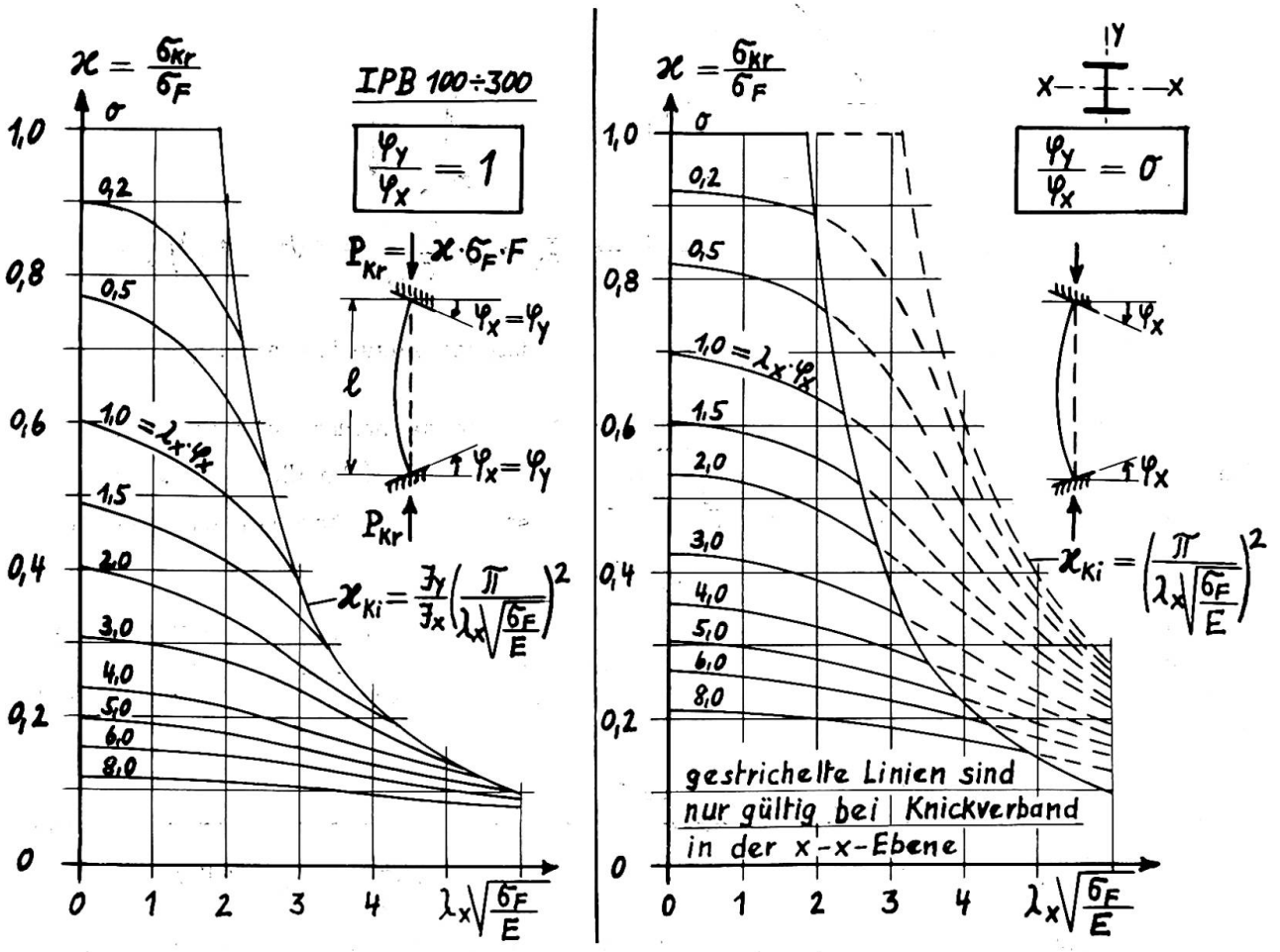

a) zweiachsige Biegung b) einachsige Biegung

Bild 2.6 : Traglasten eingespannter Stützen mit Kopf- und Fussverdrehung

Die Traglasten für Werte von $1 > \varphi_y/\varphi_x > 0$ können mit ausreichender Genauigkeit durch lineare Interpolation zwischen den Bildern 2.6.a und 2.6.b ermittelt werden. Der Wert $\varphi_y/\varphi_x > 1$ wird i.a. nicht auftreten, dann man dann das Stützenprofil um 90° drehen wird.

2.5 Traglasten von Geschosstützen mit starrer Fusseinspannung und Verdrehung des Kopfes um x- und y-Achse

Dieser Beanspruchungsfall entspricht der Stütze II in Bild 2.3. Die Traglast ist auch hier erreicht, wenn drei Fliessgelenke entstanden sind. In [3], S. 38/39, wurde für einachsige Biegung gezeigt, dass im Bereich der Stabkennzahl $\bar{\varepsilon} \leq 0{,}745 \cdot \pi$ die Traglast durch Vollplastizierung infolge der Normalkraft P allein bestimmt ist, da hier keine drei Fliessgelenke entstehen können. Im Bereich $0{,}745 \cdot \pi < \bar{\varepsilon} \leq 2 \cdot \pi$ bilden sich jedoch drei Fliessgelenke in folgender Reihenfolge aus: Das erste Fliessgelenk an der Stelle x_o zwischen Stützenkopf und Stützenmitte, das zweite am Stützenfuss und das letzte am Stützenkopf. Dies gilt auch bei zweiachsiger Biegung. Die Lage des ersten Fliessgelenks ist von der Stabkennzahl $\bar{\varepsilon}$ abhängig und kann in dem aus [3] entnommenen Diagramm des Bildes 2.7 abgelesen werden.

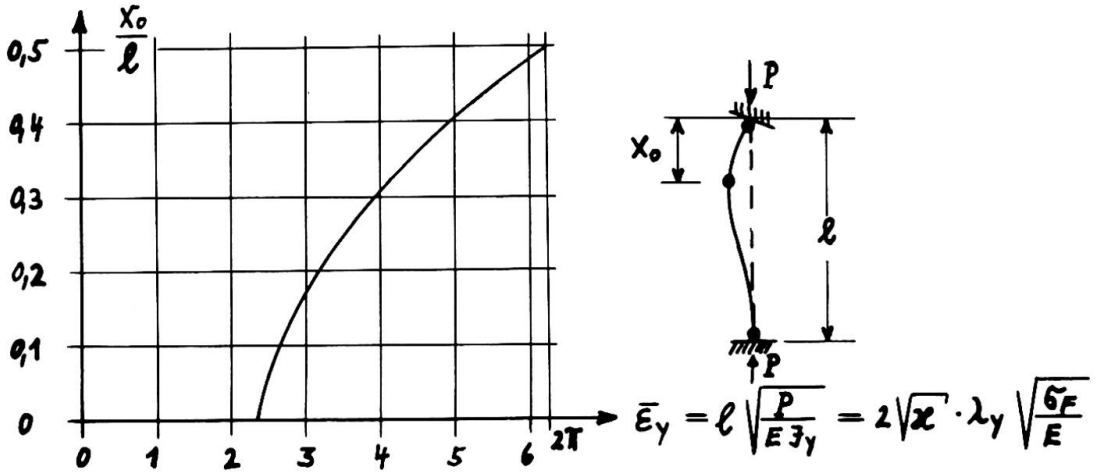

Bild 2.7 : Lage des 1. Fliessgelenks bei starrer Fusseinspannung

Dabei wird die ~~die~~ etwas zu ungünstige Näherungsannahme getroffen, dass x_o bei schiefer Biegung durch $\bar{\varepsilon}_y = l \sqrt{P/EI_y}$ bestimmt ist. (Tatsächlich wird x_o zwischen den durch die Kennzahlen $\bar{\varepsilon}_x$ und $\bar{\varepsilon}_y$ bestimmten Werten für die Stellen der Momenten-Maxima $M_{x,max}$ und $M_{y,max}$ liegen.)

Die Traglastermittlung kann analog Abschnitt 2.4 erfolgen. Der Vergleich der Bilder 2.4 und 2.7 zeigt, dass die Traglastbedingung unmittelbar angeschrieben werden kann, indem in Gleichung (2.13) der Wert 1/2 durch x_o ersetzt wird:

$$\varkappa = \frac{N_{kr}}{F\sigma_F} = \frac{2 \cdot \psi_x \cdot \alpha_x \cdot (1 + \operatorname{tg}\alpha \cdot \operatorname{tg}\varphi)}{(\alpha'_x - \beta'_x)\frac{\psi_x \alpha_x}{\cos^2 \alpha} \left(\frac{x_o}{1/2} \cdot \lambda_x \sqrt{\frac{\sigma_F}{E}}\right)^2 + \left(\frac{x_o}{1/2} \cdot \lambda_x \cdot \varphi_x\right) \frac{h}{2i_x}\left(1 + \frac{\varphi_y}{\varphi_x} \operatorname{tg}\alpha\right)} \qquad (2.14)$$

Für $\operatorname{tg}\alpha$ und $\operatorname{tg}\varphi$ gelten wieder die Beziehungen (2.11) und (2.12), für x_o Bild 2.7. Die Differenzen $(\alpha'_x - \beta'_x)$ und $(\alpha'_y - \beta'_y)$ sind als Funktion von

$$\underset{(y)}{\bar{\bar{\varepsilon}}_x} = \sqrt{\varkappa} \cdot \frac{x_o}{1/2} \cdot \underset{(y)}{\lambda_x} \sqrt{\frac{\sigma_F}{E}} \qquad (2.15)$$

aus Bild 2.5 zu entnehmen.

Wie (2.13) so kann auch (2.14) nur durch Probieren gelöst werden. Die Bilder 2.8.a und 2.8.b geben die numerische Auswertung von Gl. (2.14) für $\varphi_y/\varphi_x = 1$ und $\varphi_y/\varphi_x = o$ für die Stützenprofile IPB 1oo ÷ 3oo wieder. Auch hier kann man für Zwischenwerte von φ_y/φ_x linear interpolieren.

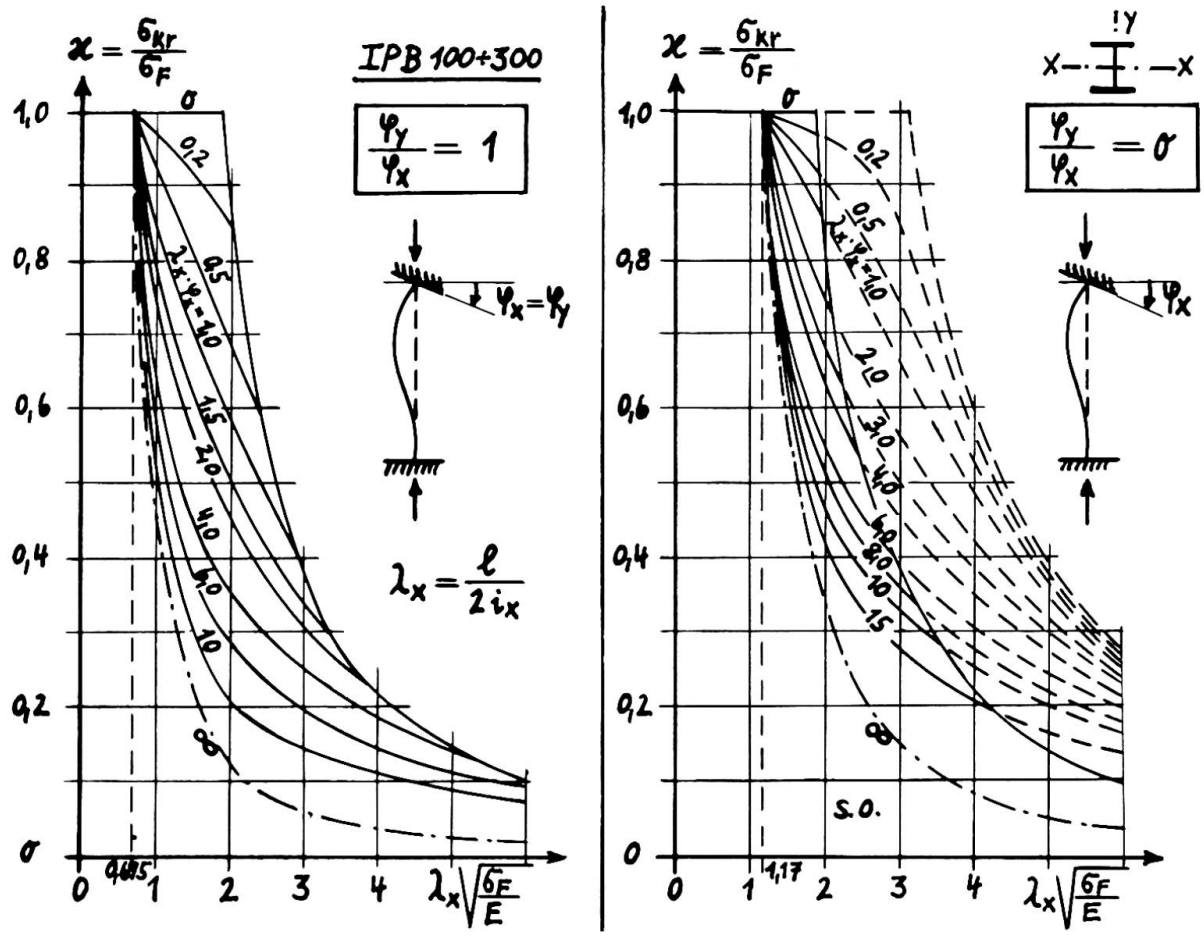

a) zweiachsige Biegung b) einachsige Biegung

Bild 2.8 : Traglasten eingespannter Stützen bei starrer Fusseinspannung

3. Experimentelle Traglast-Ermittlung

3.1. Vorbemerkung

Zur Überprüfung und Ergänzung der in Abschnitt 2 entwickelten Näherungstheorie wurden im "Otto-Graf-Institut" der Universität Stuttgart (TH) vier Traglastversuche durchgeführt. Eine ausführliche Beschreibung dieser Versuche einschliesslich der Auswertung der Messergebnisse wird in [9] gegeben. Es werden daher hier nur die wichtigsten Ergebnisse zusammengestellt.

Die Versuchsstützen erhielten angeschweisste Kopf- und Fussplatten. Beim Traglastversuch wurden Keilplatten mit Neigungen in x- und y-Richtung zwischen

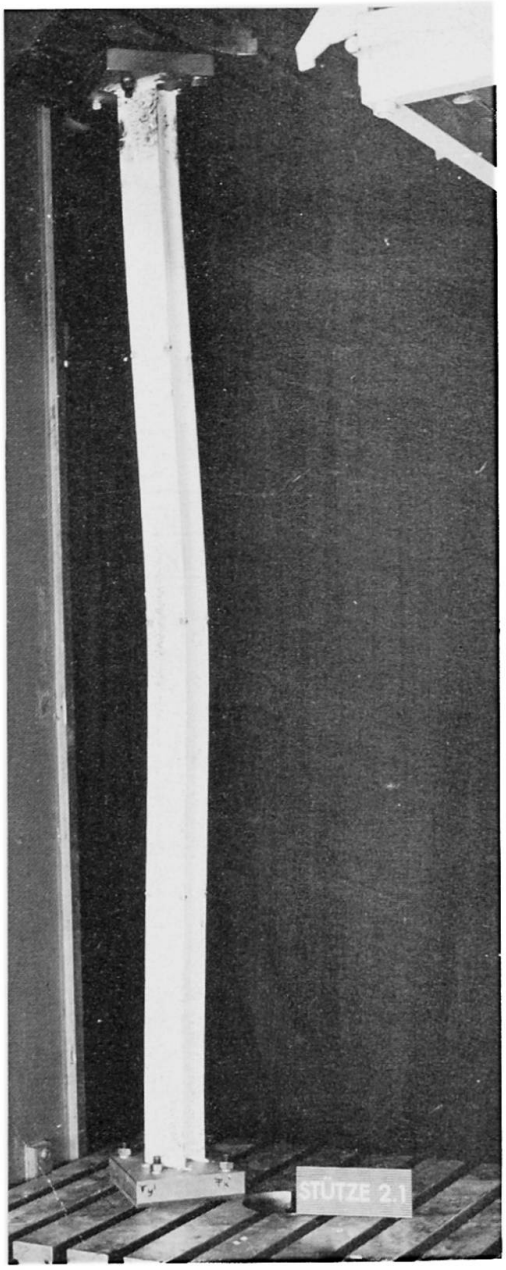

Bild 3.1 : Stütze 2.1 nach dem Traglastversuch

die Kopf- bzw. Fussplatten und die parallel zur Stützenachse geführten Pressen-Querhäupter der Versuchsmaschine gelegt. Durch das Vorspannen von HV-Schrauben, welche die Fuss- und Kopfplatten mit den Pressen-Querhäuptern verbinden, wurden die den Keilplatten entsprechenden Neigungen als Enddrehwinkel in die Stützen eingetragen (Bild 3.1). Anschliessend wurde die Axiallast über die Pressen-Querhäupter bis zur Traglast gesteigert.

3.2 Einführung von baupraktisch unvermeidbaren Imperfektionen

Es zeigte sich, dass trotz sorgfältiger Werkarbeit die vorgesehenen Stabendverdrehungen nicht genau eingehalten werden konnten. Diese Ungenauigkeiten lagen insbesondere in den Abweichungen vom Rechten Winkel zwischen den angeschweissten Kopf- bzw. Fussplatten und den Stabachsen und sind daher auch bei praktischer Bauausführung zu erwarten. Da ausserdem die Stützen auch gewisse Vorverformungen aufweisen und sicher auch Eigenspannungen aus den Walzvorgängen vorhanden sind, wird vorgeschlagen, bei der Bemessung einen zusätzlichen Enddrehwinkel stellvertretend für den Einfluss aller möglichen Imperfektionen anzunehmen. Gleichzeitig können damit auch die praktisch auftretenden Abweichungen von den Voraussetzungen a) und c) des Abschnittes 2.2 zumindest qualitativ etwas ausgeglichen werden.

In Anlehnung an DIN 4114, Ri. 7.22 wird eine parabelförmige Verkrümmung der Stabachse mit dem Biegepfeil

$$u = \frac{i}{20} + \frac{l}{500}$$

in Stabmitte in x- und y-Richtung angesetzt. Die Enddrehwinkel betragen dann:

$$\Delta\varphi = \frac{4u}{l} = 0{,}1 \cdot \frac{2i}{l} + \frac{1}{125}$$

Mit $\lambda = l/2i$ für die eingespannte Stütze wird daraus:

$$\Delta\varphi_{\substack{x \\ (y)}} = \frac{0{,}1}{\lambda_{(\substack{x \\ y})}} + 0{,}008 \qquad (3.1)$$

Der erste Anteil kann dabei die Einflüsse von Eigenspannungen und von der Ausbreitung teilplastischer Zonen neben den Fliessgelenken berücksichtigen, die beide tatsächlich mit wachsender Schlankheit abnehmen. Der zweite Anteil ist jedoch konstant und berücksichtigt die Bau-Ungenauigkeiten, die mit einem $\Delta\varphi_2 = 0{,}008$, d.h. $\Delta\varphi_2 = 0^{\circ}\ 27'$ sicher nicht zu gross angesetzt sind.

3.3 Zusammenstellung der Versuchsergebnisse und Vergleich mit der Theorie

In der Tabelle 3.1 sind die Versuchsergebnisse den nach Abschnitt 2 ermittelten theoretischen Werten für die Traglast bei berücksichtigung der tatsäch-

lich gemessenen Enddrehwinkel gegenübergestellt. Die Versuchsergebnisse liegen i.M. um 7,4 % unter den theoretischen Ergebnissen , d.h. auf der "unsicheren Seite".

Versuch	System	Profil σ_F(Mp/cm²)	l (m)	Soll $\varphi_x = \varphi_y$	vorhanden φ_x	vorhanden φ_y	$P_{kr}^{theor.}$ ($\varphi_{vorh.}$)	$P_{Exp.}$ (Mp)	$\frac{P_{Exp.}}{P_{kr}^{theor.}}$
1.1		IPB 120	3,o	o,oo71	o,oo67	o,oo82	76,5	69,2	0,9o4
1.2		2,43	6,o	o,oo71	o,oo97	o,o124	5o,4	44,4	o,88o
2.1		IPB 12o	3,o	o,o142	o,o169	o,o126	61,8	62,2	1,o5o
2.2		2,48	6,o	o,o142	o,o236	o,o16o	36,9	33,7	o,915

Tabelle 3.1 : Vergleich der Traglasten nach Theorie (mit $\varphi_{vorh.}$) und Experiment

Führt man jedoch den Winkel $\Delta\varphi$ nach Gleichung (3.1) ein, so erhält man die Werte nach Tabelle 3.2. Die theoretischen Ergebnisse liegen nun i.M. um 8 % über den Versuchsergebnissen.

Versuch	$\Delta\varphi_x$	$\Delta\varphi_y$	$P_{kr}^{theor.}$ (Mp)	$P_{Exp.}$ (Mp)	$\frac{P_{EXp.}}{P_{kr}^{theor.}}$	P_F (Mp)
1.1	o,o114	o,oloo	64,o	69,2	1,o81	o
1.2	o,oo97	o,oo9o	43,5	44,4	1,o21	21,o
2.1	o,o114	o,oloo	51,o	62,2	1,219	o
2.2	o,oo97	o,oo9o	33,7	33,7	1,ooo	24,5

Tabelle 3.2 : Vergleich der Traglasten nach Theorie (mit $\varphi_{soll} + \Delta\varphi$) und Experiment

Es sei noch auf die letzte Spalte von Tabelle 3.2 hingewiesen, in welcher diejenigen Werte von P eingetragen sind, die bei Vorhandensein der gemessenen Enddrehwinkel den Fliessbeginn in den am ungünstigsten beanspruchten Querschnitten erzeugen. Man erkennt, dass z.B. nach einer "elastischen Berechnung" die Stützen 1.1 und 2.1 überhaupt nicht mehr belastet werden dürften, obwohl gerade sie wegen ihrer geringen Schlankheit die grössten Traglasten aufweisen!

L . T E R A T U R

[1] "Plastic Design of Multi-Story Frames", Lecture Notes, Vol. 1 u. 2, Lehigh University, Bethlehem, Pa., 1965

[2] H o r n e , M.R. und M a j i d , K.I.:
"The Design of Sway Frames in Britain", Guest Lectures of the 1965 Summer Conference on Plastic Design of Multi-Story-Frames, Lehigh University, Bethlehem, Pa., 1965

[3] V o g e l , U.:
"Die Traglastberechnung stählerner Rahmentragwerke nach der Plastizitätstheorie II.Ordnung", Forschungshefte aus dem Gebiet des Stahlbaues, Heft 15, Köln 1965

[4] K l ö p p e l , K. und W i n k e l m a n n , E.:
"Experimentelle und theoretische Untersuchungen über die Traglast von zweiachsig aussermittig gedrückten Stahlstäben", Der Stahlbau 31 (1962), S.33 ff.

[5] B i r n s t i e l , Ch. and M i c h a l o s , J.:
"Ultimate Load of H-Columns under Biaxial Bending" Proc.ASCE, Journal of the Struct.Div., Vol.89, No.ST 2, Apr.1963, p.161-197

[6] P e l i k a n , W. und V o g e l , U.:
"Die Tragfähigkeit von Stahlstützen in Geschossbauten mit Betondecken", Der Stahlbau 33(1964), S.161-167

[7] V o g e l , U.:
"The Influence of Deformations on the Ultimate Load of Rigid Steel Frames", Guest Lectures of the 1965 Summer Conference on Plastic Design of Multi-Story-Frames, Lehigh University, Bethlehem, Pa., 1965

[8] "Hilfstafeln zur Berechnung von Spannungsproblemen der Theorie II. Ordnung und von Knickproblemen", Stahlbau-Verlag GmbH Köln 1959

[9] V o g e l , U. und Z i m m e r m a n n , W.:
"Traglastversuche an eingespannten Geschoss-Stützen mit I-Querschnitt bei Biegung um beide Hauptachsen", IVBH-Abhandlungen, Vol.28 (1968)

[10] H a r s t e a d , G.A.:
"Elasto-Plastic Behavior of Columns subjected to Biaxial Bending", Ph.D.-thesis, New York University at Bronx, N.Y., 1966

ZUSAMMENFASSUNG

Im vorliegenden Aufsatz wird eine Näherungslösung nach der Plastizitätstheorie zur Ermittlung der Traglasten von eingespannten Geschosstützen bei zweiachsiger Biegung entwickelt. Für einige praktisch auftretende Randbedingungen werden die Ergebnisse in Kurventafeln dargestellt. Traglastversuche haben gezeigt, dass die entwickelten Traglastformeln bei Berücksichtigung einer zusätzlichen Annahme für mögliche Imperfektionen nach Gleichung (3.1) zu für die Praxis ausreichend genauen und "sicheren" Ergebnissen führen.

SUMMARY

In this paper an approximate solution by plastic design method for the calculation of the ultimate strength of biaxially loaded restrained columns is developed. For some practical boundary conditions the results are given in interaction-diagrams. Ultimate load tests have shown, that the developed ultimate strength formulas lead to a design which is sufficient and conservative for practical purposes, if additional possible imperfections (equation 3.1) are taken into account.

RÉSUMÉ

L'exposé développe une solution approximative selon la théorie de plasticité pour la détermination de la charge de rupture de colonnes encastrées soumises à des flexions biaxiales. Les résultats sont présentés sous forme de graphiques pour quelques conditions limites qu'on trouve dans la pratique. On a démontré par des essais de rupture que les formules développées conduisent à des résultats suffisamment exacts et sûrs, à condition de respecter une supposition supplémentaire pour de possibles imperfections selon l'équation (3.1).

Leere Seite
Blank page
Page vide

Tests on Hinged Connections for Non-Sway Continuous Frames

Essai de noeuds articulés pour ossatures contreventées

Versuche an gelenkigen Knoten für verstrebte Skelette

CH. MASSONNET Professor
R. ANSLIJN Instructor
University of Liège

S. BAAR Engineer
J. DELIÈGE Engineer
SERCOM (Station d'Essais et de Recherches de la Construction Métallique)

1. INTRODUCTION.

Most of multi-story frames built at present have either a rigid central concrete core, or a diagonal bracing to resist wind forces, so that these structures may be designed as non-sway structures. They usually have rigid connections between beams and columns.

Research conducted in the United States, in Great Britain, and elsewhere have made possible the plastic analysis of such structures on a practical basis. In particular, the Lehigh team has developed a method solving the problem of verifying the rotational capacity of joints, and analysing the buckling of columns, by means of "column deflection curves", obtained theoretically for current shapes.

A simplification of this type of structure can be obtained by hinging continuous beams on continuous columns. The work of the designer is greatly reduced: beams are treated as continuous beams, either in plastic or elastic design; and columns become axially loaded, without bending. Such structures are also interesting from an economical point of view as substantial savings can be made on the columns, relatively to rigid-joint design. Of course, this advantage is partly compensated by an increase of the size of the beams. Two students working on different structures at Liege University have shown that the point of equilibrium between the two conceptions lies around 7 stories; the hinged solution shows better under this figure. When the number of stories increases, the bending effect in columns of rigid-joint structures become less and less significant against axial loading and this last effect governs the design, as in the hinged solution, so that the savings made on beams make the rigid solution more economical.

Of course, a prior requirement for the hinged-joints design is that these hinges may be effectively fabricated. Another requirement is that their cost must not off-set the savings made on the columns.

2. DESCRIPTION OF THE CONNECTIONS.

In order to check these two points, a research sponsored by the CECA (Commission Européenne du Charbon et de l'Acier) was undertaken by SERCoM (Station d'Essais et de Recherches de la Construction Métallique) in the laboratories of Liege University. Four types of joints were designed (Fig. 1 - 2 - 3 - 4) and one sample of each tested.

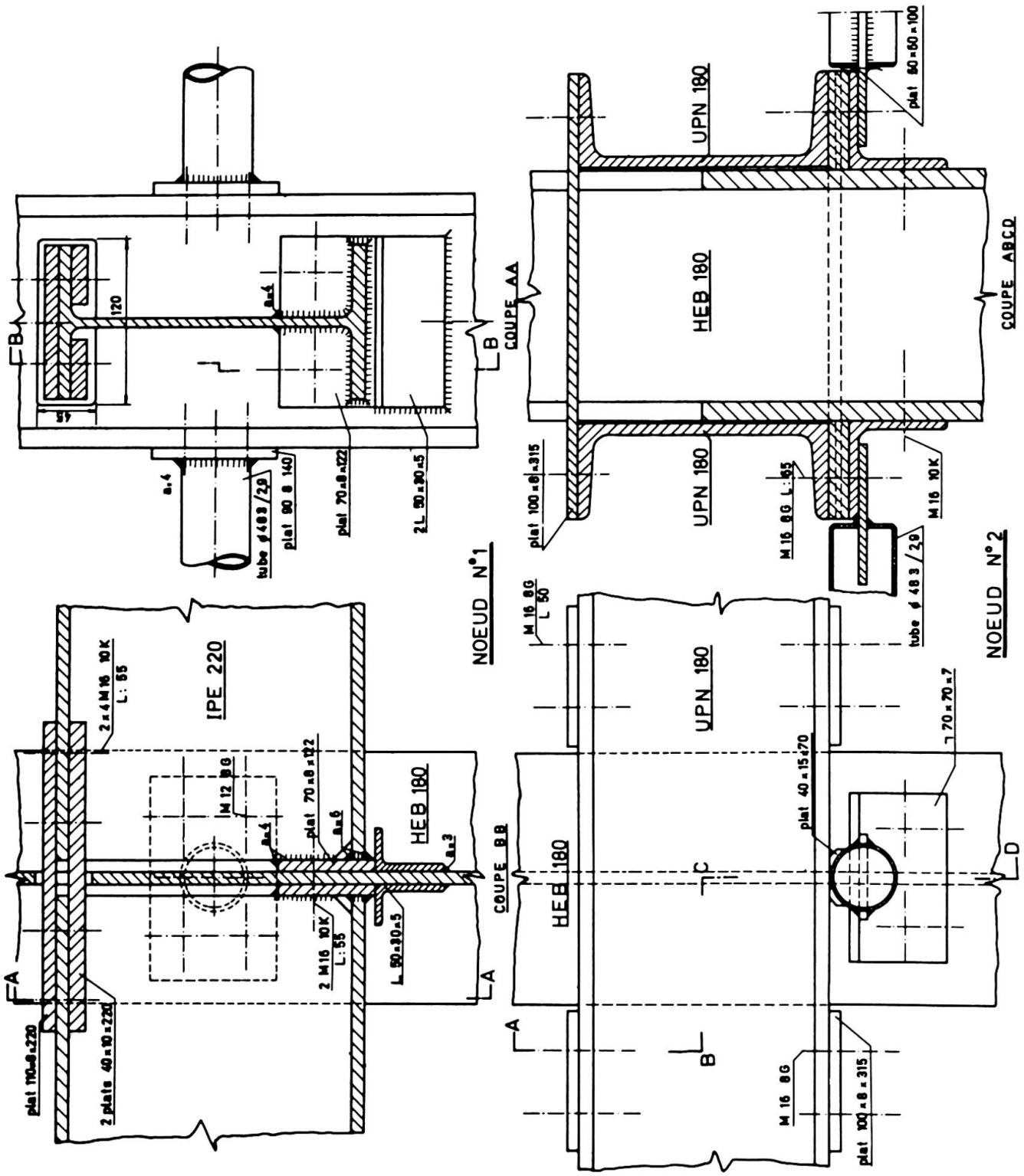
NOEUD N°1
IPE 220
HEB 180
2 x 4 M16 10K L: 55
M 12 8G
plat 70 x 8 x 122
2 M16 10K L: 55
L 50 x 30 x 5
plat 110 x 8 x 220
2 plats 40 x 10 x 220
COUPE BB
NOEUD N°2
UPN 180
HEB 180
plat 80 x 60 x 100
COUPE AA
COUPE ABCD
plat 100 x 8 x 315
M 16 8G L: 65
M 16 10K
tube ϕ 48 3 / 29
M 16 8G L 50
plat 40 x 15 x 70
70 x 70 x 7
M 16 8G
plat 100 x 8 x 315

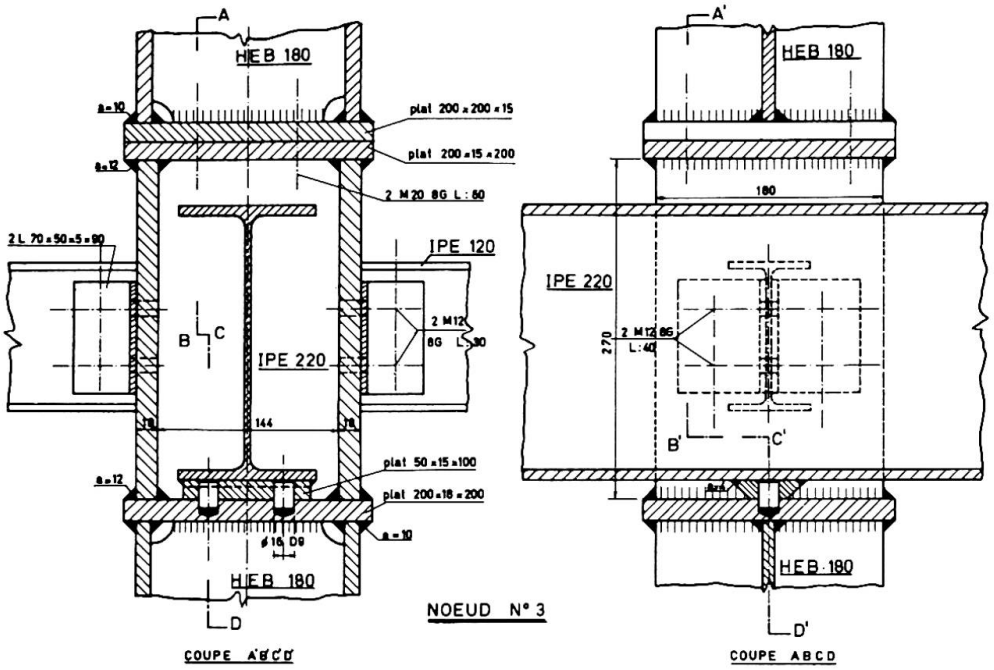
A
HEB 180
a=10
plat 200 x 200 x 15
plat 200 x 15 x 200
a=12
2 M20 8G L:60
2 L 70 x 50 x 5 x 90
IPE 120
B
C
IPE 220
2 M12
8G L:30
144
plat 50 x 15 x 100
plat 200 x 18 x 200
a=12
a=10
HEB 180
D
COUPE A'B'C'D'
A'
HEB 180
180
IPE 220
270
2 M12 8G
L:40
B'
C'
HEB 180
D'
COUPE ABCD
NOEUD N° 3

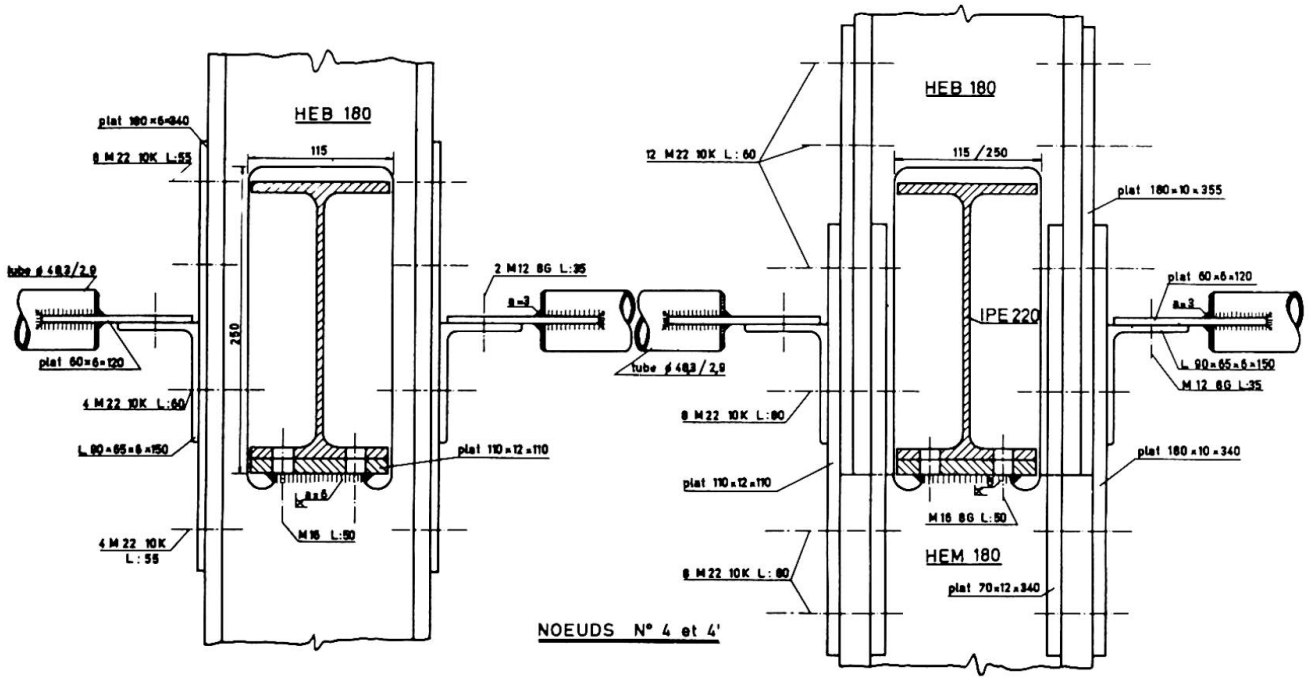
HEB 180
plat 180 x 6 x 340
8 M22 10K L:55
115
tube ø 48,3 / 2,9
plat 60 x 6 x 120
4 M22 10K L:60
L 90 x 65 x 6 x 150
4 M22 10K
L:55
230
2 M12 8G L:35
a=3
plat 110 x 12 x 110
a=6
M16 L:50
HEB 180
12 M22 10K L:60
115 / 250
plat 180 x 10 x 355
IPE 220
plat 60 x 6 x 120
a=3
L 90 x 65 x 6 x 150
M12 8G L:35
tube ø 48,3 / 2,9
8 M22 10K L:80
plat 110 x 12 x 110
plat 180 x 10 x 340
M16 8G L:50
HEM 180
8 M22 10K L:80
plat 70 x 12 x 340
NOEUDS N° 4 et 4'

N° 1 was developed from a scheme suggested by Romanian searchers working at Liège. The beam is cut at the joint and the two parts are placed on both sides of the web of the column, resting on small shoes. These are welded or bolted on the web of the column, and theoretically, they serve only during the assembly phase, for positioning the beams. On each half-beam, a small steel plate is welded on the lower flange and the bottom part of the web. They are joined together through the column by two high-strength bolts which insure transmission of the shear forces to the column.
Compression efforts in the lower flange are transmitted directly by contact, while tensile forces in the upper flanges are transmitted through coverplates going through a hole purposely made in the web of the column.
It is important to note that the plates on the webs of the beams must be as small as possible in height and the bolts as near as possible to the lower flange, in order to obtain a good rotational capacity of the beam. The design may be completed by shear stiffeners if needed, but they were not necessary in the tested model.

In N° 2 design, the beams are made of two U shaped profiles which pass on each side of the column. Each is supported by a small console, bolted to the flanges of the column. A small rocking skid is welded under the lower flange, to provide hinging. A bolt avoids translations. This system is quite simple, but the double-U beams are generally heavier than an equivalent I-beam, and they must be braced together against torsional effects proper to U-sections.

In type 3 design, the column is interrupted at joint level and provided with a hollow box, the walls of which must be able to resist the vertical forces coming from above. The beam goes uninterrupted through the box, hinged on a rocking skid and secured against translation by pins. The box is welded on top of the column section below, and the bottom of the above column section is bolted on top of the box. Of course, columns must not have a joint at each level, and they might come from workshop in lengths involving three or four boxes, in all-welded execution. It can be noticed here that, as the column buckles centrically, the orientation of the column does not matter, so it can be placed with its weak axis of inertia in the plane of the frame. In this way, the walls of the box are in the same plane as the flanges of the column, and the horizontal plates of the box may be relatively thin. If the column were placed with its strong axis in the plane of the frame, the walls and flanges would be orthogonal to each other and the horizontal plates would have to be very thick to provide a good transmission of forces. Anyway, troubles would occur at the corners of the flanges.
This design, though quite simple in its principle, involves some disagreements which grow with the size of the column: milling of thick plates, much welding, etc... and the erection of a large structure with these joints could lead to some difficulties because of the necessity of running the beams through the boxes.

Type 4 is in some way a digest of types 1 and 3: a large hole is cut in the web of the column and the beam passes through it.
The flanges are reinforced by cover plates to compensate for the hole. The beam rests directly on the edge of the web which is locally reinforced.
The small tongue of web so formed constitutes the hinge. As in type 3, the beam-column connection can easily be combined with a joint in the column.

Each of the above connections is completed by connections between the column and the secondary beams. This does not lead to any difficulty.

3. TESTING LAYOUT.

The testing layout was arranged according to the scheme described at fig. 5 : (Specimen is turned upside down from normal position):

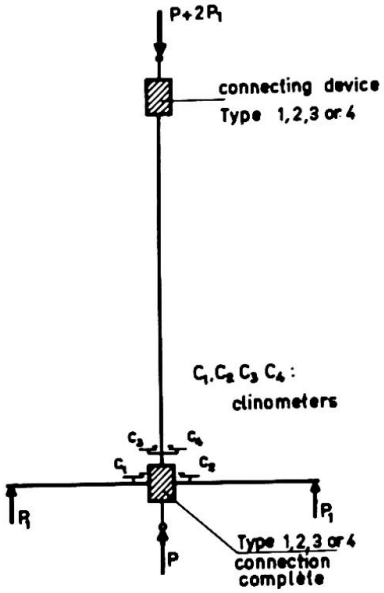

a column section supports two connections; the one at the bottom is complete, with main and secondary beam; the one at the top has only the connecting device and the beams are omitted.
The loading is composed of :

a) vertical loading on the column, to simulate the effect of the higher stories ;

b) vertical loading on the end of the main beam, to produce a negative moment in the beam at the right of the connection.

The column section is hinged at its two ends, with hinges placed as near as possible to the connection levels, in order to respect the buckling length.

The maximum load that could be applied with the testing equipment was 160 tons (metric), so it was decided to make the tests at a 6/10 scale.
The profile of the column was HEB 180, and for the beam: IPE 220 (and UPN180 for type 2). The distance between two levels was 2,10 m. The specimen so obtained represents a current column in a building of 8 x 4 m module, supporting loads of 750 kg/m^2.

There is little to say about the testing apparatus :
The specimens are place in a frame structure bolted to the concrete slab equipping the laboratory, and loads are applied by means of hydraulic jacks, placed under the column for the column load, and under the ends of the beam. Loads are controlled by strain-gages load cells. The apparatus is shown at fig. 6.

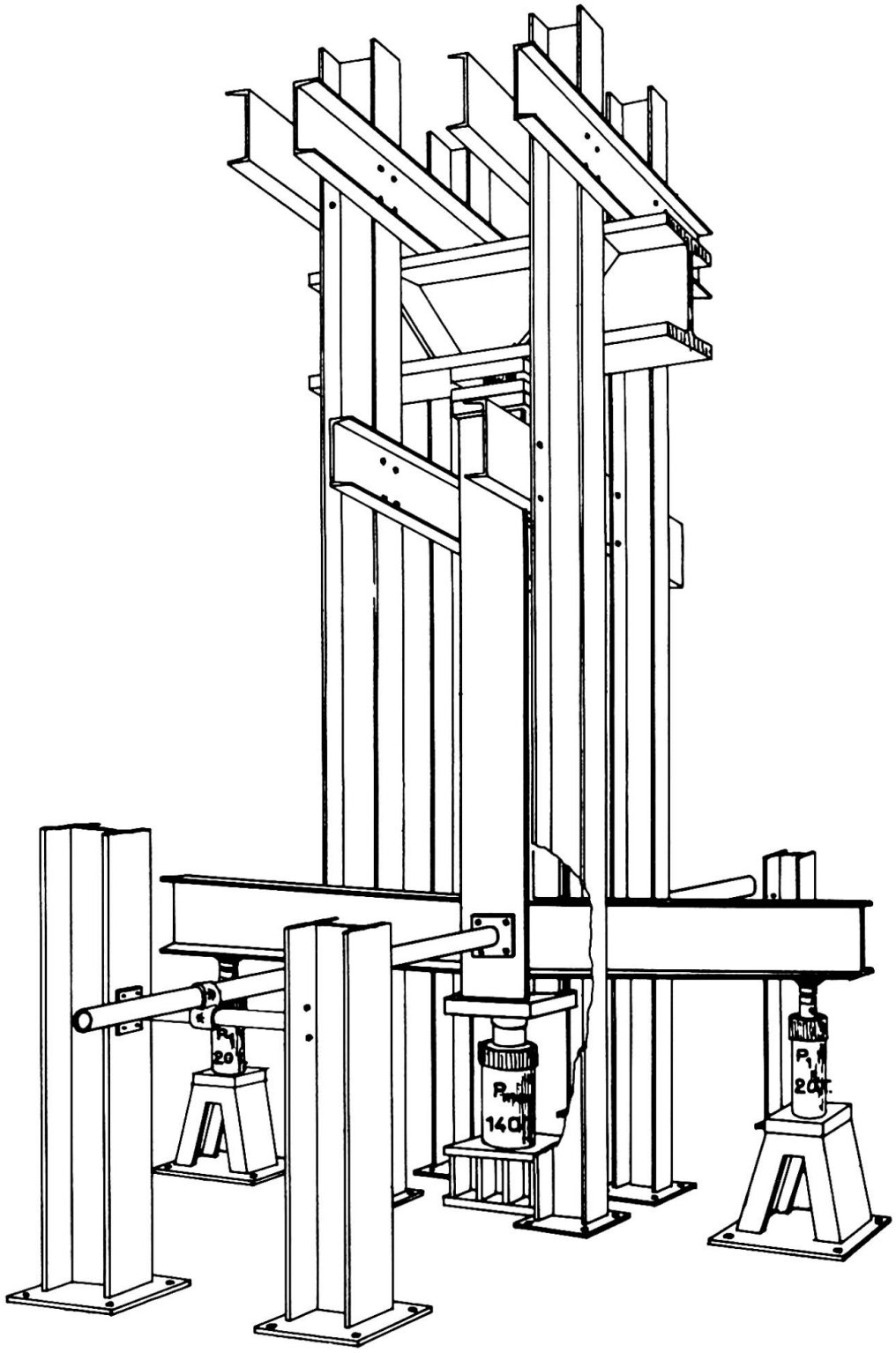
20
140
20

Testing for each specimen was conducted in three phases :

a) In phase 1, a small load is applied to the column and two equal forces are applied to the beam at different distances from the column. In this way, the rotational capacity of the "hinge" can be tested.
b) In phase 2, the loads on the beam, acting symetrically, are increased until the full plastic moment is developed in the beam. A small load is applied on the column.
c) In phase 3, the column loading is increased up to the collapse of the column or the maximum loading, whichever occurs.

During phase 1, measurement is made of the rotations of the beam and the column sections near the connection, by means of clinometers (see fig. 5).

During phases 2 and 3, only loads and the plastic rotation in the beam are measured.

4. EXPERIMENTAL RESULTS.

4.1. Phase 1 - Control of hinging action.

The table below gives the mean value of the rotations of the beam and the column during the phase 1 tests on the four types of connections.

The rotation was obtained by placing the beam jacks at 0.7 and 1.0 meter apart from the center of the joint.

For reasons of clarity, the values of the angular rotations ϕ_c and ϕ_b of the column and the beam, respectively, are given in decimal division of the degree .

The reference value is obtained by applying some load on the column (usually one ton) to get rid of errors due to the initial self-positioning of the different devices.

		Type 1		Type 2		Type 3		Type 4	
F_c Tons	F_b Tons	ϕ_b	ϕ_c	ϕ_b	ϕ_c	ϕ_b	ϕ_c	ϕ_b	ϕ_c
1.0	0			0	0	0		0	0
15.0	0	0	0	0.033	0.036	0.028	less	0.06	0.06
15.0	0.5	0.13	0.015	0.46	0.038	1.79	than	0.54	0.06
15.0	1.0	0.36	0.018	0.98	0.051	3.00	0.01	2.50	0.02
15.0	2.0	0.62	0.056	2.26	0.085	***		▼	
15.0	3.0	0.89	0.086						
15.0	4.0	1.45	0.120						
15.0	5.0	* 2.60	0.206						
15.0	0	1.45 **	0.016	0.28	0.037				

* When this value was reached, web of beam was abuting against web of column.
** Actually, F_c for this tests was not maintained constant, but gradually increased from 15 tons ($F_b = 0$) to 22 Tons ($F_b = 5$) and back to 15 tons.

*** The freedom of rotation was such that no state of equilibrium could be obtained beyond 0.5 T. The 3.00 deg. value was reached before 1.0 T was acting as F_b.

▼ Test was stopped at this point because farthest jack was out of stroke.

As can be seen from above results, all four types of connections behave satisfactorily, and have a good rotational ability. As could be predicted, type one is the stiffest of the four.
The rotation of the beam occurs without inducing significant rotation in the column, excepted for the "stiff" type one. But even for the latter, the rotation of the column does not exceed ten percent of that of the beam. Furthermore, some part of the column's rotation may be a result of the increasing of the load on the column, as the whole specimen is hinged at its two ends.
The lower hinge is constituted by the jacks themselves, and for kinematical reasons its center of rotation is the center of the lower face of the corresponding bearing plate.

So, it may be concluded that the four proposed types can be considered as real "hinged" connections. The relative rotation of more than 2 degrees between beam and column is far beyond service values.

4.2. Testing of resistance.

4.2.1. Phase 2 - Moment transmission capacity.

The steel of the IPE 220 beams, theoretically of A 37 grade, has its yield-point at 28 kg/mm^2, which leads to a theoretical plastic moment of 8.400 kgm. For the UPN 180, these values were 30 kg/mm^2 and 5.125 kgm, respectively, giving 10.250 kgm for the tested double beam.

The beams were submitted to the moment distribution of fig. 7, obtained by placing the two jacks at one meter from the column.

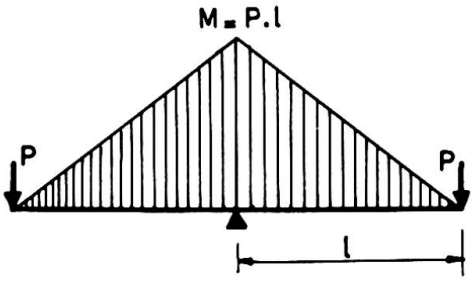

This distance was chosen in order to respect the shear-moment relationship existing at the support of a uniformly loaded continuous beam. A 15 T load acted on the column.

Lateral buckling of the beam was prevented by appropriate guiding devices or local reinforcement of the tips.

The whole specimens were coated with whitewash to allow visualization of the development of plastic yielding.

The behaviour of the four specimens was as follows :

Type 1 : At 9 Tm, a gliding in the joint of the flanges, and yielding of both upper flanges occured, thus forming a plastic hinge.
The relative rotation between the two halves of the beam was 4.3 deg.

Type 2 : At 9 tm, some yielding appeared in the webs, near the support, combined with some bending of the consoles.
Yielding developed regularly when load was increased, until it appeared on the flanges at 11 Tm. The formation of the plastic hinges continued until the test was stopped at 12.0 Tm. The relative rotation of the two halves was 5.7 deg.

Type 3 : Plastic hinge began to form at 9 Tm and processed while loads was increased up to 11 Tm, where the beam collapsed by buckling of the compressed flange. Rotation was 7.8 deg.

Type 4 : At 9.0 Tm, 45° shear yield-lines appeared in the web of the beam, at the support.
At 9.45 Tm, some yielding began in the web of the column under the beam.
At 10.9 Tm, the stretched flange of the beam began to yield while the compressed flange collapsed by local buckling on both sides of support.
Total relative rotation was 6.6 deg.

It is clear from above results that the four connections are perfectly able to perform the transmission of the full plastic moment of the beam. None showed premature failure or instability in the beam, the column or the binding parts before reaching the plastic moment.

4.2.2. Phase 3 - Vertical load transmission capacity.

For this test, the load acting on the column was increased as high as possible, while a load of 10 Tons was maintained in the two beam-jacks.

The four specimens behave as follows :

Type 1 : The column buckled in the weak plane under a load of 130 T.
No special phenomenon occured in the hole in the web.

Type 2 : The column buckled in the weak plane under a load of 158 T.
Fig. 8 gives a general view of the testing apparatus, with buckling column of type 2 specimen.

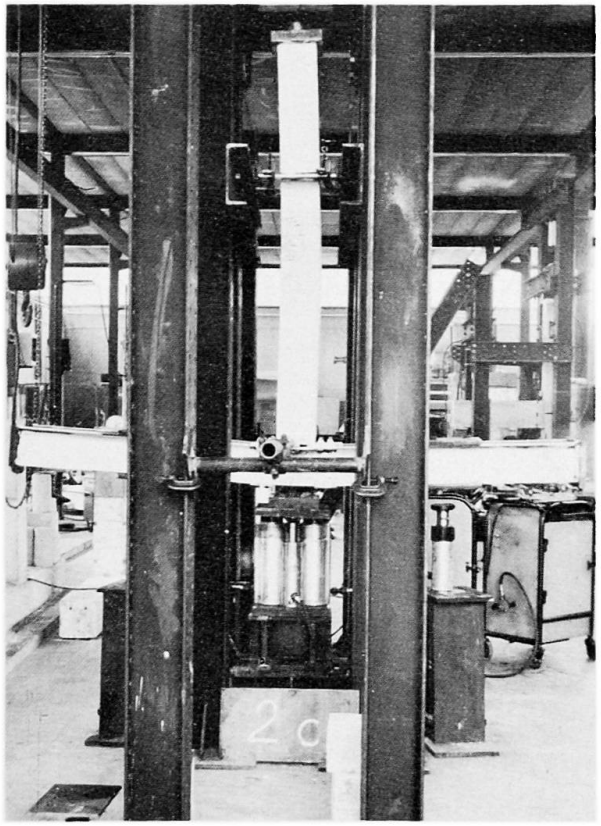

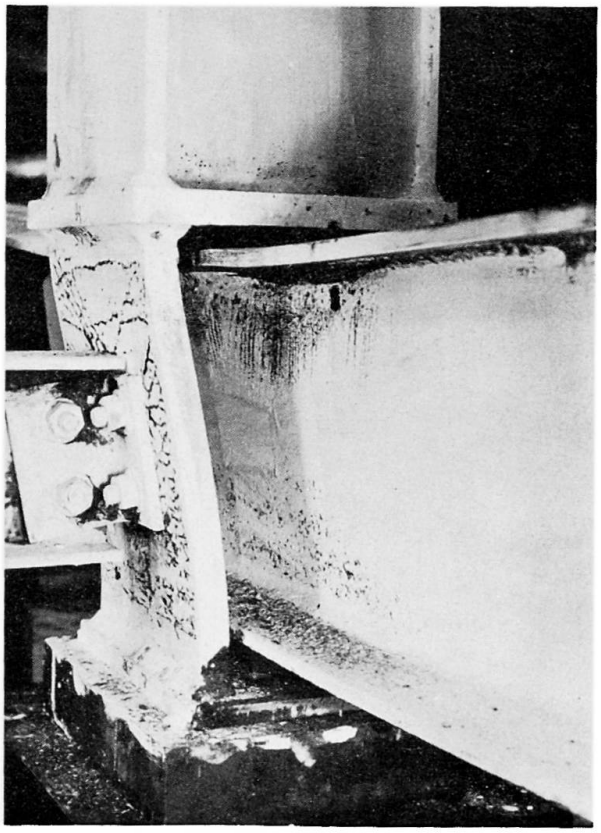

Type 3 : The upper box, with no primary nor secondary beam, began to show signs of yielding in the walls at 95 T.
The upper box collapsed by buckling of the walls at 117 T.
That box was then removed and the load increased again. The test was interrupted at 156 T, when the lower box, in turn, collapsed by local buckling (see fig. 9). That difference in the resistance of the two boxes is due to the fact that the lower box is reinforced locally by the connecting parts for the secondary beams, and braced by those beams, while the upper box is not.

Type 4 : Load was increased up to 160 T without exhausting the resistance of the specimen.

We do not intend here to make a complete discussion of the buckling of the column, as this was only a secondary aspect of the research. It will suffice to observe that, excepted for type 3, the collapse of the column, when achieved, obviously proceeded from the overall conditions of testing and not from local weakenings due to the connections. In case of type 3, it can be seen that the boxes are weak points of the structure. The walls of the box should be reinforced in order to prevent buckling, either by thickening the walls or by welding stiffeners thereon.

5. CONCLUSIONS.

From the above results, we may conclude that at least three of the four types of tested connections completely fulfill the required strength conditions : they are able to transmit the full plastic moment, they have a sufficient hinging action and they do not involve early local failure or collapse.
The fourth (type 3), though satisfactory as far as hinging and bending behaviour are concerned, should be improved with respect to its behaviour under vertical loading. One improvement could be the use of T-shaped walls, instead of plates, the webs being placed vertically and outside, thus serving accessorily as binding part with the secondary beam.

Up to now, we do not have enough information to make a numerical estimation of the cost of a plastically designed "hinged" structure, and compare it with the cost of the same structure with rigid connections. Such a study would be rather intricated as, to be complete, it should include not only the cost of steel and labour to manufacture the connections, but also a comparison of the ease or difficulty of assembly (local and global) in each conception and a prevision of the troubles that could appear in one and not in the other.

However, if as a first approximation, we limit the comparison to the connections themselves, it can be expected that the hinged connections will not be more expensive than rigid ones, excepted for type 3 (which had also the less interesting behaviour).
Type 2 and 4 which are quite simple, could even reveal cheaper.
There is thus reasonable matter to hope that the "hinged" solution could lead to actual savings.

The prior requirement for the application of this solution, that is feasibility is then certainly met, and it can be expected that the second, that is economy, will be, too.

ACKNOWLEDGMENTS.

The authors thank the personal of the Laboratory of Strength of Materials and especially Mr. J. HAINAUT, Engineer-technician, for the considerable help they gave in performing the tests.

RÉSUMÉ

Cet article présente quelques essais effectués à l'Université de Liège sur des noeuds articulés destinés à des ossatures, du type "à noeuds fixés", conçues avec poutres et colonnes continues articulées entre elles à leurs points de jonction.

Quatre types de noeuds sont décrits, ainsi que les résultats d'essais sur la capacité de rotation des articulations, la résistance à la flexion, et la résistance aux charges verticales.

La discussion des résultats montre que le comportement des noeuds est très satisfaisant et l'article se termine par quelques considérations d'ordre économique.

SUMMARY

This paper presents some tests made at Liege University on hinged connections between continuous beams and columns of accordingly designed non-sway frames.

Four types of connections are described, so as the results of tests made on them, investigating rotational ability, bending moment transmission, and vertical load transmission.

A discussion of the results shows that the connections behave satisfactorily, and paper ends with some economical considerations.

ZUSAMMENFASSUNG

Dieser Beitrag beschreibt einige Versuche der Universität Lüttich über gelenkige, unverschiebliche Balken und Stützen, die gelenkig verbunden sind. Vier Knoten werden beschrieben, ebenso die Versuchsergebnisse über die Drehfähigkeit der Gelenke, die Biegefestigkeit sowie die Tragfähigkeit gegen lotrechte Lasten. Die Ergebnisse über das Verhalten der Knoten sind sehr zufriedenstellend. Betrachtungen über die Wirtschaftlichkeit beschliessen den Bericht.

Inelastic Behaviour of Reinforced Concrete Shear Wall-Frame

Comportement inélastique de structures en béton armé composées de murs et de portiques

Unelastisches Verhalten der Stahlbeton-Scheibenrahmen

W.J. CLARK
Graduate Student

J.G. MacGREGOR
Professor

P.F. ADAMS
Associate Professor
University of Alberta, Edmonton, Canada

INTRODUCTION

This paper presents some results of a computer study of the behavioural characteristics of a plane reinforced concrete frame braced laterally by a shear wall. The method of analysis employed traces the load-deflection behaviour of the structure until failure occurs either by instability or by a collapse mechanism. The members are assumed to be elastic-perfectly plastic.

The behaviour of a twenty storey two bay reinforced concrete structure is taken as the basis for the discussion. The properties of the structure were adjusted to study the effects of variations in the wall stiffness, axial shortening of the wall and columns, and the secondary or P-Δ moments due to lateral deflections.

METHOD OF ANALYSIS

Many first order elastic solutions exist for the case of a frame coupled with a shear wall subjected only to lateral loads. In addition, a number of elastic-plastic solutions for unbraced metal frames have been described in the literature. To date, however, the inelastic action of coupled shear wall-frame structures has not been studied extensively.

The analysis on which these results are based provides a second order elastic-plastic solution to the coupled shear wall-frame system [1]. An iterative procedure is used to solve slope-deflection equations modified to consider axial load effects and the finite shear wall width. As the loads are incremented and plastic hinges are detected in the structure, adjustments are made to the appropriate slope-deflection equations. Axial shortening of the columns and walls is considered although creep deflections have been ignored. Failure may be due to instability or the formation of a collapse mechanism. The structure is assumed to be braced against local and out-of-plane buckling. It is possible to consider any rectangular configuration of beams, columns and walls in a single plane.

For reinforced concrete members an elastic-perfectly plastic moment-curvature relationship has been derived for the girder, column and wall sections. This relationship considers the section geometry, material properties and the effects of axial loads. Deformations due to shear or inclined cracking have not been considered.

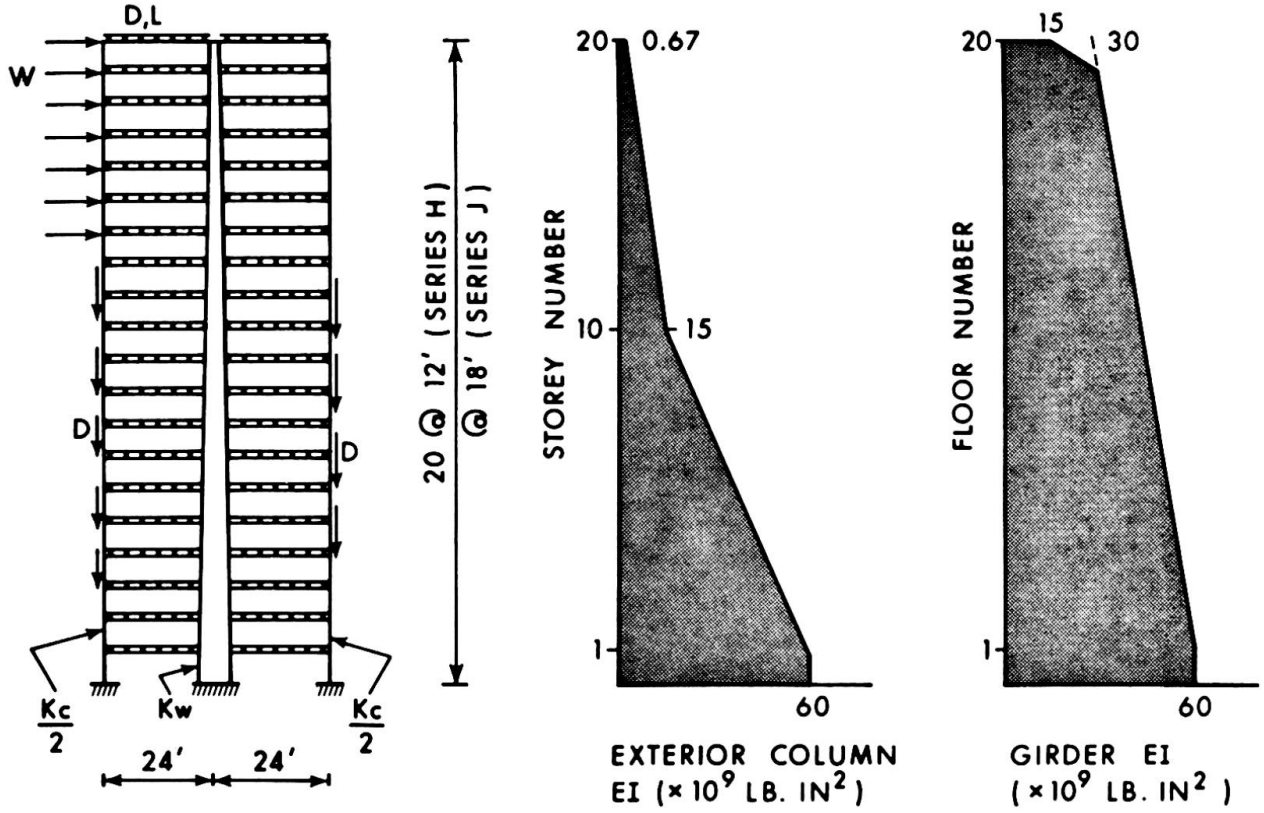

(a) Elevation of Frame (b) Distribution of Member Stiffnesses

Figure 1. DETAILS OF FRAMES

STRUCTURE AND LOADING

The behaviour of two series of reinforced concrete frames will be discussed in this paper. The frames will be referred to by means of a letter denoting the frame series and a number denoting the ratio, K_w/K_c, of the EI of the shear wall to the sum of the EI values of the columns in each storey. Details of the frame geometry and the distribution of member stiffnesses are shown in Fig. 1.

The series H and J frames had a 12 foot and an 18 foot storey to storey height, respectively. In each case they consisted of square, symmetrically reinforced tied columns with a total longitudinal reinforcement ratio of 0.04 and rectangular beams reinforced in tension only with $pf_y/f'_c = 0.18$. In all cases the yield strength of the reinforcement was taken as 60,000 psi and the concrete strength was assumed to be 4,000 psi.

To facilitate studies of the effects of variables, all the frames discussed in this paper had the same columns and beams. The structure H1 was designed by the ultimate strength procedures in the ACI Building Code assuming material understrength factors, $\emptyset$, equal to 1.0 for all members. The resulting member stiffnesses are plotted in Figures 1(b) and 1(c). The series J frames had the same member sizes as the series H frames.

The columns varied in size from 8.5 inches square in the top storey to 22 inches square in the bottom storey. The girders varied from 10 inches wide by 22 inches deep at the roof to 14 by 30 inches at the first floor.

In frames H1 and J1, designed as unbraced frames, the "shear walls" were solid tied column sections with 4 percent longitudinal reinforcement. These walls varied from 9.5 inches square in the top storey to 26 inches square in the bottom storey. To augment the shear wall stiffness in the other frames the moment of inertia and plastic moment capacity of the wall were increased by the appropriate value of K_w/K_c. The width of the wall in the plane of the frame was kept constant to eliminate the effects of wall-width from the basic study. Similarly, to minimize the effects on hinge formation of the relative axial shortening of the wall and columns, the wall area was held constant as K_w/K_c was varied.

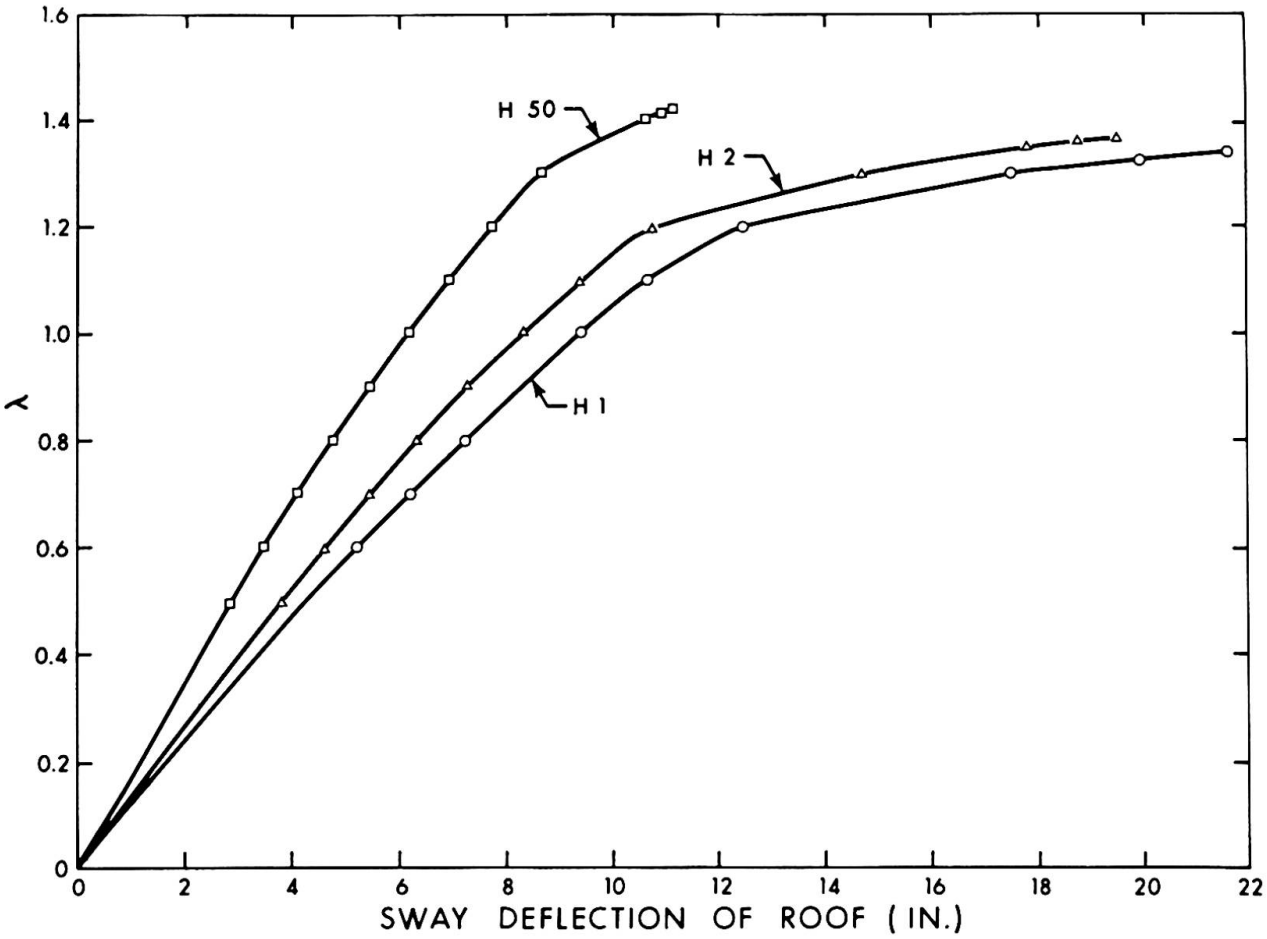

Figure 2. EFFECT OF WALL STIFFNESS ON SWAY DEFLECTION OF TOP OF FRAME

In all cases the loading was applied statically and was proportionally increased until failure occurred. In this paper results will be given in terms of the load factor λ in the expression $\lambda(D + L + W)$ where D, L and W represent reasonable working load values of the dead, live and wind loads for structures of the type considered.

EFFECTS OF VARIATION OF WALL STIFFNESS ON LOAD DEFLECTION BEHAVIOUR

Second order elastic-plastic analyses were carried out on Series H and J frames with relative wall stiffness values, K_w/K_c, of 1, 2, 6, 12, 20, and 50. Typical load-deformation plots from these analyses appear in Figure 2. Figure 3 shows bending moment diagrams for the walls in frames H1 and H50 at $\lambda = 1.00$, prior to the formation of any plastic hinges in the structure.

It is apparent that, although the wall and columns of Frame H56 posess a total lateral stiffness of 25.5 times that in H1, the overall frame stiffness does not increase in this proportion. This can be explained by the difference in behaviour between a portal frame and a cantilever wall. Inspection of the wall bending moment diagrams in Figure 3 indicates that the stiffening function of the wall is diminished as the structural action reverts to cantilever behaviour at the base of the wall, as indicated by a gradual shift of the initial point of contraflexure up the wall as the wall stiffness increases. Similar behaviour was noted in the Series J frames.

In considering the effect of wall stiffness on the portion of the total lateral load carried by the wall it was also evident that the loads carried by the wall did not increase in direct proportion to the increase in the relative stiffness of the wall.

The implication of this is that, except for structures with extremely stiff walls, the frame members may be underdesigned if the wall is assumed to carry the entire lateral load.

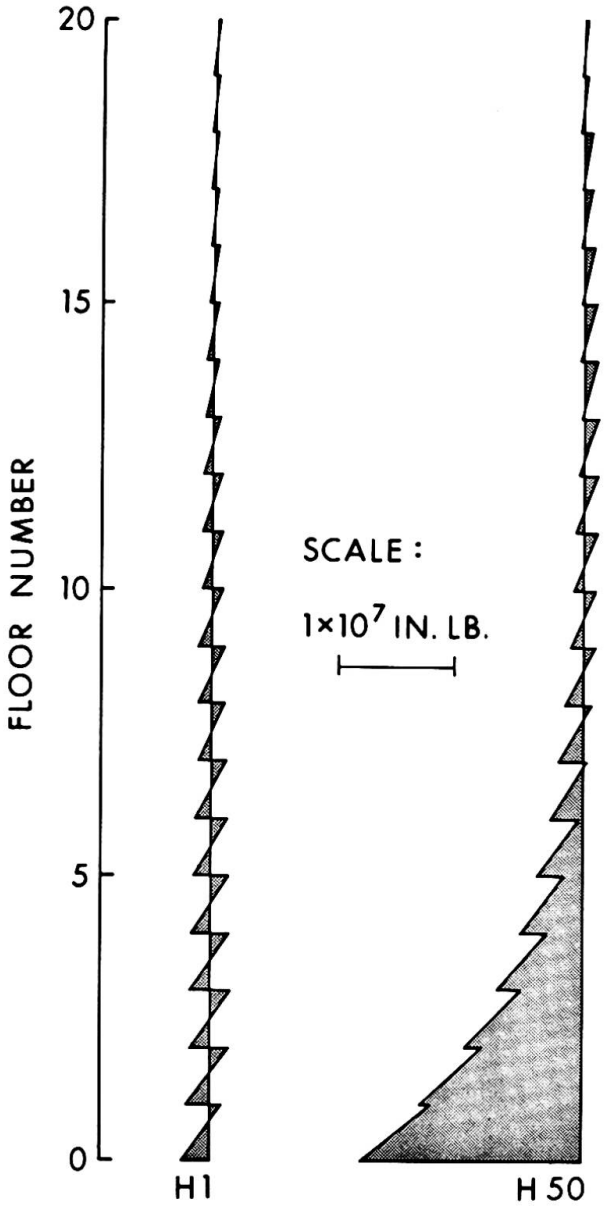

Figure 3. BENDING MOMENTS IN THE WALLS IN FRAMES H1 AND H50 AT WORKING LOADS

EFFECTS OF COLUMN AXIAL SHORTENING

Frame H1 was used as the basis for a study of the effects of relative axial shortening of the columns and wall in a frame. The load-deflection plots from three analyses of this frame are shown in Figure 4.

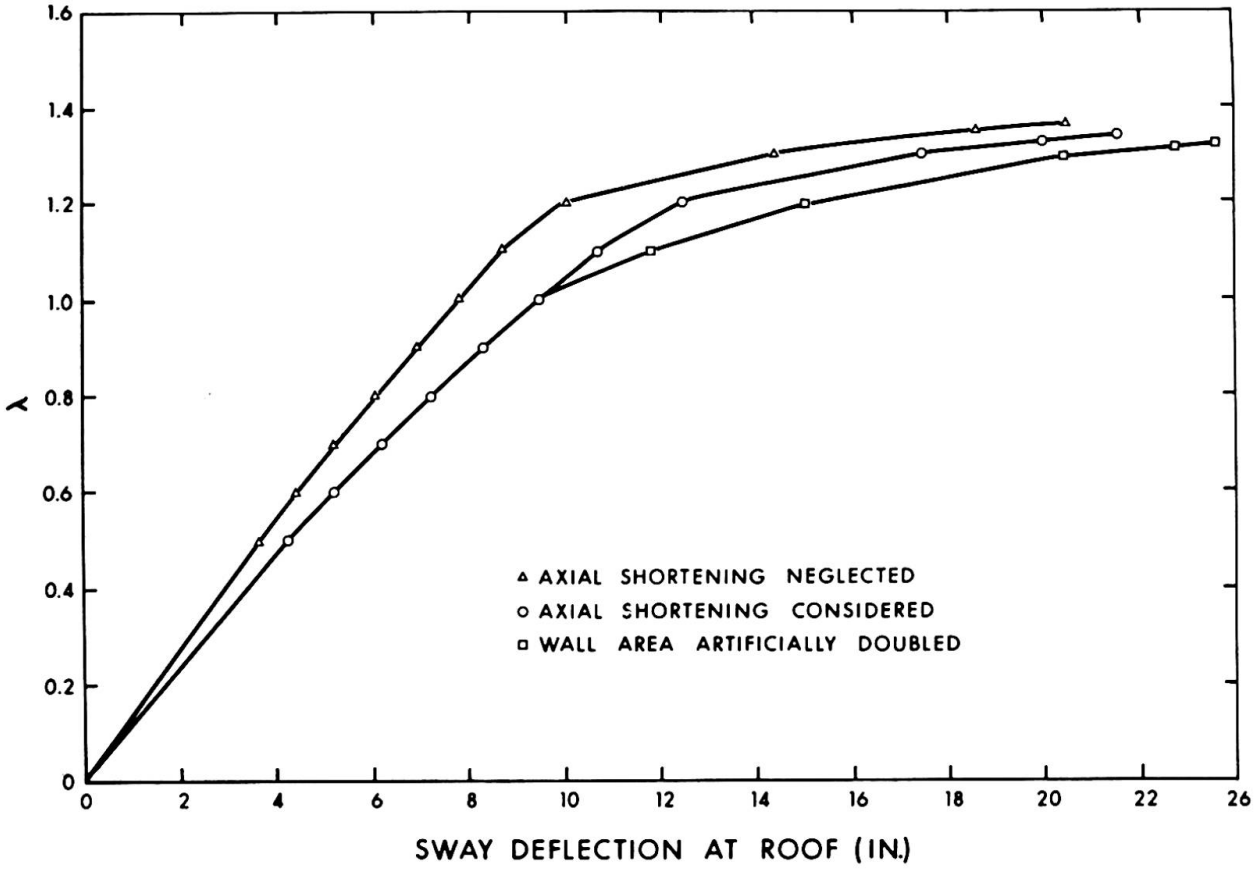

Figure 4. EFFECTS OF AXIAL SHORTENING IN FRAME H1

In this particular case the lateral deflection of the top storey at working loads was underestimated by 18 percent and the failure load was overestimated by 2 percent when the axial shortening of the members was neglected.

When the wall area was doubled without changing its EI or plastic moment capacity there was no change in the stiffness of the structure at low loads. However, the reduction in the axial shortening of the wall resulted in greater relative column to wall deflections and caused premature hinges in the girders near the top of the structure. This reduced the stiffness of the structure and let to earlier instability.

This effect was more pronounced when the ratio of shear wall stiffness to column stiffness qas greater, especially if the shear wall section remained constant over the height of the building. These results have not been included here since in most practical designs the thickness of the core walls would be varied in accordance with the axial loads in the core. However, in the case of buildings with prismatic core walls as might be the case if the core was slipformed, for example, the relative axial shortening of the walls and columns should be considered.

TRANSITION FROM SWAY INSTABILITY TO BRACED FRAME INSTABILITY

In conjunction with the second order elastic-plastic analyses, first order elastic analyses were performed on the Series H and J frames. The resulting bending moment values were compared to observe the significance of the secondary (P-△) moments in the various frames. This effect was expressed in terms of a moment magnifier, F , equal to the second order analysis moment at any point divided by the corresponding moment from the first order analysis.

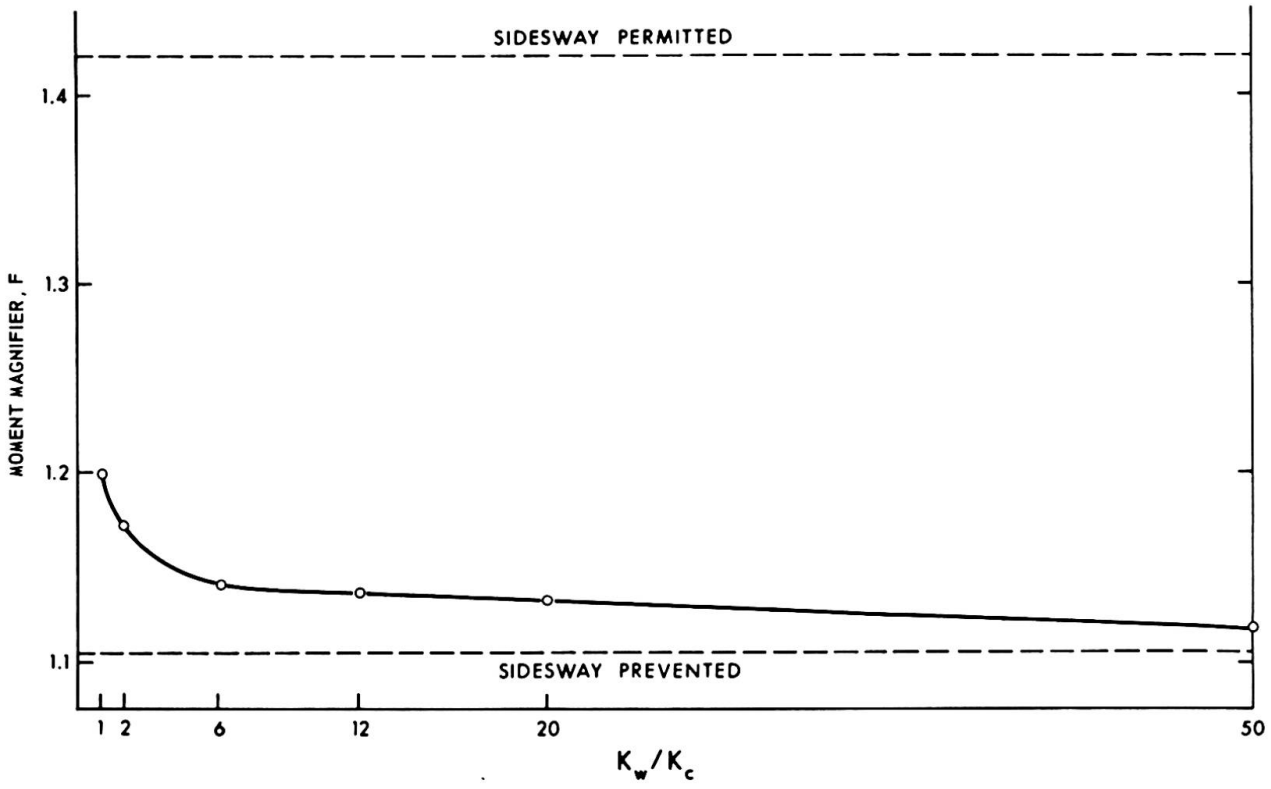

Figure 5. EFFECT OF RELATIVE WALL STIFFNESS ON MOMENT MAGNIFIER

The values of the moment magnifier, F , at working loads (λ = 1.00) in the leeward column of the ninth storey of Series J frames are plotted as a function of K_w/K_c in Figure 5. It should be noted that at λ = 1.00 , no hinges had formed in any of the structures considered. The two horizontal dashed lines appearing on this graph represent the values of F derived using the traditional moment magnifier relationship [2] given by Equation 1. The critical load, P_e , is based on a nomographic evaluation of effective length [2, 3].

$$F = \frac{1}{1 - \frac{P}{P_e}} \qquad \ldots\ldots\ldots\ldots\ldots \quad (1)$$

The F values derived from this analysis never approached the values computed using Equation 1 assuming the frames are free to sway. Part of this discrepancy is caused by the fact that the values of the effective lengths used were derived assuming a typical interior column in an infinitely large, rectangular structure. In addition, the effective lengths were derived assuming only axial loads in the columns, while the frames considered here had both wind and uniformly distributed gravity loads.

On the other hand, however, for values of K_w/K_c greater than about 6 , the moment magnifier values computed in this study did approach the F values computed using Equation 1 assuming a frame braced against sidesway. Similar effects were noted for the columns in other stories of the H and J frames.

The values of the moment magnifiers presented in Figure 5 suggest that a safe approximate design procedure for multi-storey frames would be:

(1) Analyze forces and moments using a conventional first order elastic analysis.

(2) Amplify the column moments, and where necessary the girder moments, using a moment magnifier given by Equation 1. The effective length for braced columns could be used in computing P_e if K_w/K_c is greater than 6 , and that for unbraced columns if K_w/K_c is less than 6 .

(3) Design all sections to have a plastic moment capacity equal to or greater than the moments computed in Step 2.

NOTATION

F = Moment Magnifier

f'_c = Compressive strength of the concrete

f_y = Yield strength of the reinforcement

K_c = Sum of EI/h values for all columns in any storey

K_w = EI/h of shear wall in any storey

P = Axial load on column

P_e = Euler column buckling load

REFERENCES

1. W. J. Clark, "Behaviour of Reinforced Concrete Shear Wall-Frame Structures," Ph. D. Thesis, Department of Civil Engineering, University of Alberta, 1968.

2. "Guide to Design Criteria for Metal Compression Members," Column Research Council of Engineering Foundation, 1960.

3. "Manual of Steel Construction", Sixth Edition, American Institute of Steel Construction, New York, 1963.

SUMMARY

An elastic-plastic analysis for reinforced concrete structures consisting of a coupled frame and shear wall has been derived and applied to several examples. The results of this analysis suggest that relative axial shortening of walls and columns may lead to a premature instability failure of the structure. In addition, the studies suggest that a relatively low shear wall stiffness is required to change the behaviour from that of an unbraced frame to that of a braced frame with respect to instability.

RÉSUMÉ

L'analyse plastique-élastique pour des structures de béton armé composées d'un câdre et d'un mur accouplés a été dérivée et a été appliquée a plusieurs exemples. Les résultats de cette analyse suugèrent que le raccourcissement axial relatif des murs et des colonnes peut conduire à un affaisement de la structure dû à une instabilité prématurée. En addition, les études montrent qu'un mur d'assez petite rigidité suffit pour changer les propriétés de stabilité d'un portique seul en celles d'un portique renforcé d'un mur bien rigide.

ZUSAMMENFASSUNG

Eine elasto-plastische Analyse für Stahlbetonhochhäuser bestehend aus einer Zusammenfassung von Rahmen und Schubwand ist präsentiert durch verschiedene Beispiele. Die Resultate dieser Analyse regen an, dass eine verhältnismässige Verkürzung der Wände und Stützen zu einem vorzeitigen Zusammenbruch des Bauwerks führen mögen. Des weiteren schlagen die Studien vor, dass eine verhältnismässig niedrige Schubwand-Steifigkeit erforderlich ist, um eine Veränderung des Verhaltens, mit Hinsicht auf die Unstabilität, zwischen einem unverankerten und verankerten Rahmen zu erzielen.

Approximate Inelastic Analysis of Shear Wall-Frame Structures

Analyse inélastique approximée pour des structures composées de portiques et de murs

Angenäherte unelastische Berechnung von Scheiben-Rahmentragwerken

S.N. GUHA MAJUMDAR
R.P. NIKHED
Research Assistants, Department of Civil Engineering

J.G. MacGREGOR
Professor of
Civil Engineering

P.F. ADAMS
Associate Professor
of Civil Engineering

University of Alberta, Edmonton, Canada

INTRODUCTION

Plastic design methods are available for structures in which sway displacements are completely prevented and for those which consist entirely of moment resisting frames [1]. Both methods are based on assumptions which make the design of tall structures feasible even using manual computation procedures.

Commonly, however, multi-story structures are neither completely braced nor unbraced but consist of frames coupled to flexural shear walls [2]. The shear walls have greater stiffnesses than do the frames and thus tend to dominate the behavior of the structure.

Under lateral loads the deflected shapes of the free frame and shear wall are shown in FIGS. 1 (a) and (b). Since the deformations of the two elements must be compatible, the final deflected shape of the structure will be that shown in FIG. 1 (c). In the top stories the shear wall exerts large shears on the frame. These shears are accounted for in present elastic design procedures which consider the interaction between the frame and shear wall [3].

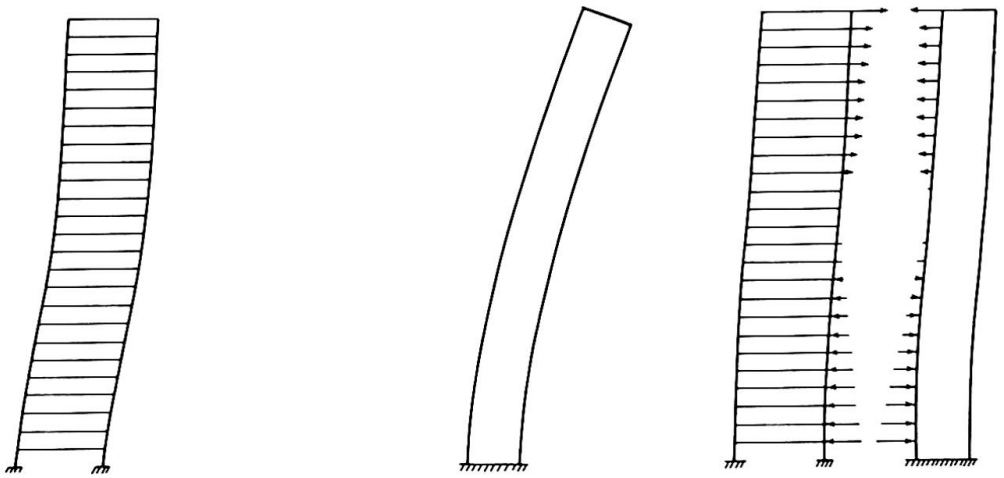

(a) (b) (c)

FIG. 1. DEFLECTED SHAPES

In the inelastic range, the frame-shear wall interaction may force plastic hinges to form in the frame early in the loading history, thus reducing the stiffness for additional load increments. The vertical loads on the structure acting through the lateral displacements produce "secondary moments" known as P-△ moments. The P-△ effect combined with the inelastic action of the structure may cause significant reductions in load-carrying capacity.

METHOD OF ANALYSIS

To reduce the analysis of the structure to manageable terms the actual structure is replaced by the model shown in FIG. 2. The shear walls and frames of the actual structure have been replaced by the systems shown. These are designed to have equivalent lateral stiffnesses and strengths [4].

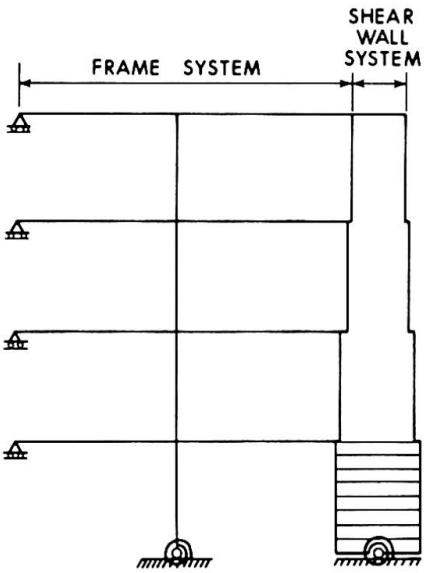

FIG. 2. ANALYTICAL MODEL

This procedure implies that the structures considered are reasonably symmetrical and do not exhibit significant torsional deformations. The lumping procedures used to form the analytical model are similar to those used for the elastic analysis of frame-shear wall structures [3]

To analyze the model for a given set of lateral loads, the loads are first applied to the shear wall and its free deflection is computed. The frame is then forced into a compatible set of deformations and the shears developed by the frame are computed. These are applied to the wall as corrective forces and a new deflected shape computed. The process is continued until the total shears developed are in equilibrium with the applied lateral loads [3]. To obtain the complete load-deformation relationship for the structure the lateral loads are increased and the above process is repeated.

At each step in the process the inelastic action of the frame and the shear wall is accounted for by using the inelastic moment-curvature (M-ϕ) relationships in the computation of deflections and the resulting forces [4]. An elastic perfectly plastic M-ϕ relationship is used for the frame members with the plastic moment capacity of the columns reduced to account for axial loads. For the shear wall a bilinear M-ϕ relationship is assumed.

The P-Δ effect is also included at each stage of the process. The secondary moments in each story are computed from a knowledge of the deflected shape and vertical loads. The corresponding shears are then added at each floor level and the additional deflections computed. The process is continued until the deflected shapes converge.

FOURTEEN-STORY BUILDING

The first structure considered is a fourteen-story building, rectangular in plan, with nineteen bays of 11 feet 6 inches in the long direction and three bays of 20 feet 0 inches in the short direction. The building had been analyzed previously for a load of 20 psf. applied perpendicular to the long side of the building [3]. The results are presented only to check the validity of the analytical model shown in FIG. 2.

The properties of the original structure are given in REF. 3. The analytical model is shown in FIG. 3, the members have been lumped to form the

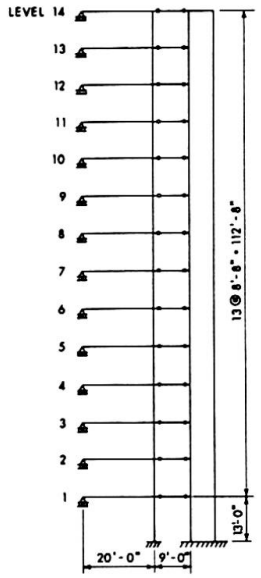

FIG. 3. FOURTEEN-STORY BUILDING

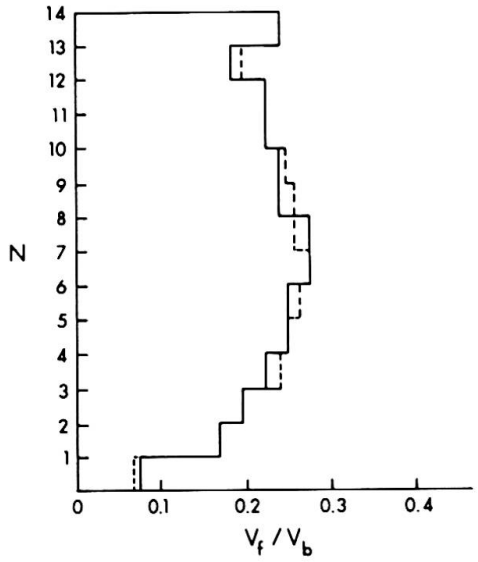

FIG. 4. SHEAR DISTRIBUTION

equivalent systems [4]. In FIG. 4 the story number, N , is plotted versus the proportion of the total base shear carried by the frame, V_f/V_b . The solid lines indicate the shears obtained using the model shown in FIG. 2, the dashed lines represent the results obtained previously [3]. The agreement is satisfactory. At this stage of loading the structure is elastic and the P-Δ effect has little influence [4].

In FIG. 4, the frame shear, V_f , is relatively constant in the top portion of the structure. The applied shear, however, increases linearly (approximately) from the top of the structure. Thus the top stories of the frame must carry shears in excess of those applied on the story due to the pull exerted by the shear wall. To study the influence of the wall stiffness on the shear distribution several additional analyses were performed. The structure was changed for each analysis by reducing the stiffness of the shear wall

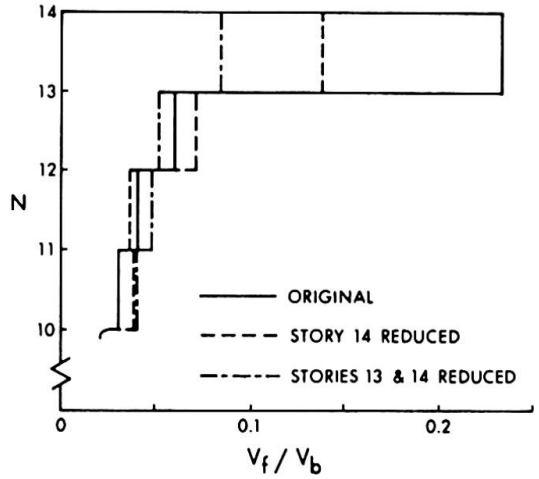

FIG. 5. VARIATION IN SHEAR DISTRIBUTION

to one-hundredth of the original value in the top stories. The results are summarized in FIG. 5 which plots N versus V_f/V_b. The results of the analysis of the original structure are shown as the solid lines. The dashed lines represent the values obtained when the top story stiffness is reduced to one-hundredth of the original value and the broken lines represent the results when the stiffnesses of the top two stories are reduced. As the stiffness of the wall is reduced the shears carried by the more flexible stories are also reduced, however, the shears carried by the other stories may be increased. The action of the lower portion of the structure is unchanged.

TWENTY-FOUR STORY BUILDING

The second example considered is a twenty-four story, three bay steel frame. The frame had been designed using both the allowable stress and plastic strength

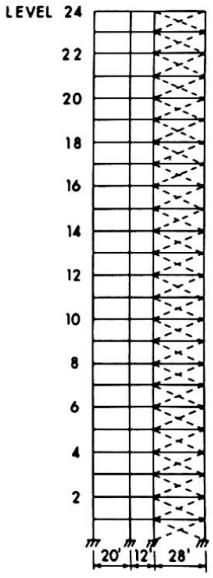

FIG. 6. TWENTY-FOUR STORY STRUCTURE

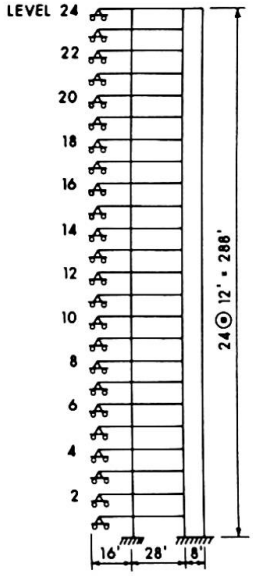

FIG. 7. LUMPED STRUCTURE

techniques, under the assumption that it was completely braced [1]. The original frame is shown in FIG. 6 and the analytical model in FIG. 7. The member properties and the vertical loads acting at each floor level are given in REF. 1; the structure was lumped according to methods used in REFS. 3 and 4 and the properties of the analytical model are given in REF. 4. No attempt was made to obtain a flexural shear wall corresponding to the truss shown in FIG. 6, instead several analyses were performed with varying shear wall stiffnesses. The ratio of the wall stiffness to the column stiffness, K_w/K_c, was held constant in each story. The plastic strength of the wall was chosen to bear a reasonable relationship to the stiffness; this strength/stiffness ratio was

maintained for each story. The shear wall was assumed to have a constant width of 8 feet 0 inches.

The model was subjected to vertical loads at each floor level and to concentrated lateral loads. The vertical loads were held constant for the analysis while the lateral loads increased monotonically. The lateral load at the roof level was one-half those at the other levels.

FIG. 8 shows graphs of the lateral force at the top of the frame, H , versus the top level column rotation, ρ . The frame has a ratio of wall stiffness to column stiffness of 50 . The upper curve has been obtained from an analysis which neglects the P-Δ effect. The first hinge in the frame is detected at point 'a' . The shear wall yields first at the base as shown by point 'b' on the graph. The structure is essentially, a

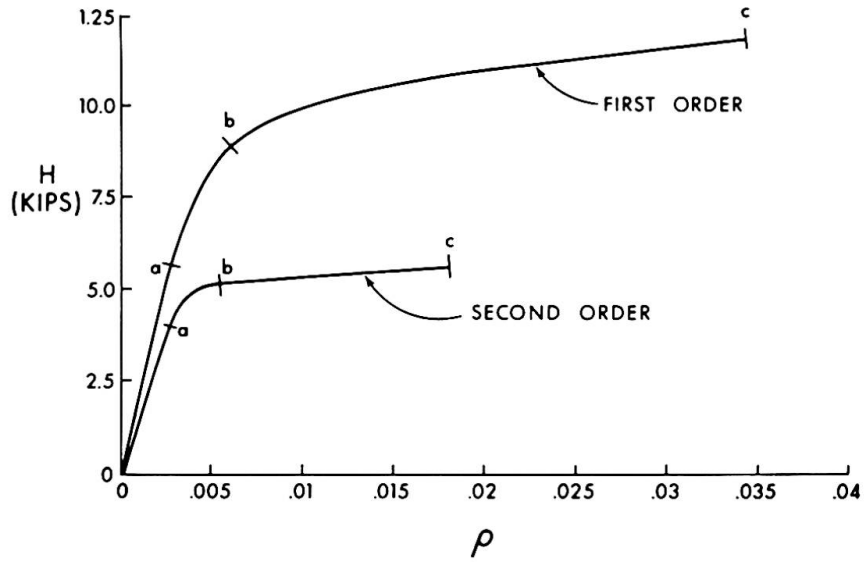

FIG. 8. LOAD-DEFLECTION CURVE

'weak beam-strong column' type and at point 'c' hinges have formed at the ends of all the beams. The only column hinge detected between points 'b' and 'c' occurs at the top of the column in the 24th story. Since a bilinear moment-curvature relationship has been assumed for the wall it will continue to accept increasing load. To demonstrate the P-Δ effect, an analysis represented by the lower curve in FIG. 8 was performed. In this case, the structure was analyzed with reduced plastic moment capacities for the c columns. The reduced capacities did not influence the results as the structure failed due to instability without hinges forming in the columns. At point 'a' on the lower curve, the first hinge in the structure was

detected. Up to point 'b' the rate of decrease of stiffness is moderate. Beyond point 'b' the deflection of the structure increases rapidly up to point 'c' . At this load level, the wall becomes inelastic. For the next increment of lateral load, the deformations become so large that the system does not converge. The load corresponding to 'c' has been taken as the ultimate load carrying capacity of the structure. In FIG. 8 the difference in load carrying capacity predicted by the two analyses is primarily due to the P-Δ effect, since only one hinge forms in the columns.

FIG. 9 consists of several plots showing the deflected shape of the structure as the lateral load is incremented. The curves are obtained from the second order analysis corresponding to the lower curve. In FIG. 9 the

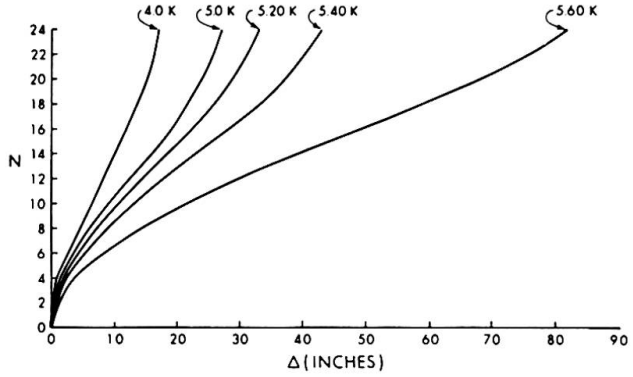

FIG. 9. DEFLECTED SHAPES

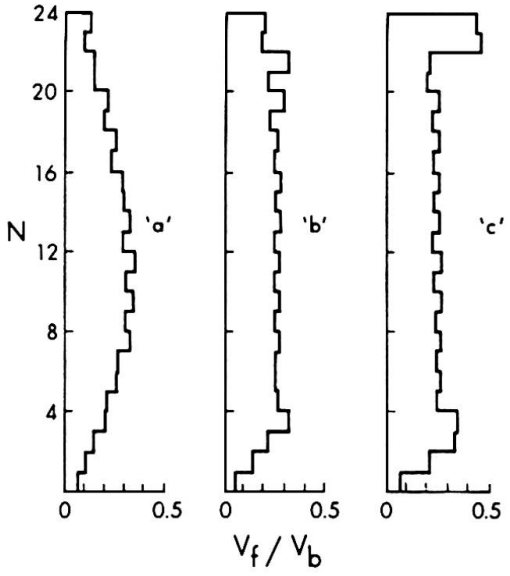

FIG. 10. SHEAR DISTRIBUTION

deflected shapes for lateral loads of 5.20 and 5.60 kips correspond to points 'b' and 'c' on FIG. 8. These two curves emphasize the rapid increase in deflection which occurs as the wall enters the inelastic range.

The shear distribution between the wall and the frame is of interest in this study.. FIG. 10 plots the story, N , versus the ratio V_f/V_b for three stages in the loading history. The stages correspond to points 'a' , 'b' and 'c' of FIG. 8. The base shear at each stage includes the appropriate component of the P-Δ effect. At the elastic limit (stage 'a') large shears act near mid-height of the frame. As the frame yields (between 'a' and 'b') the shears are redistributed and near the ultimate load (stage 'c') are largest near the top and bottom. Relative to the applied story shear,

large shears occur in the top stories at all stages and are accentuated by yielding in the frame.

The effect of varying the wall stiffness was also studied. FIG. 11 is a plot of the top level lateral force, H, versus the top level lateral deflection, Δ. In all cases, the P-Δ effect was considered and the reduced plastic moment capacities used for the columns. The curves are

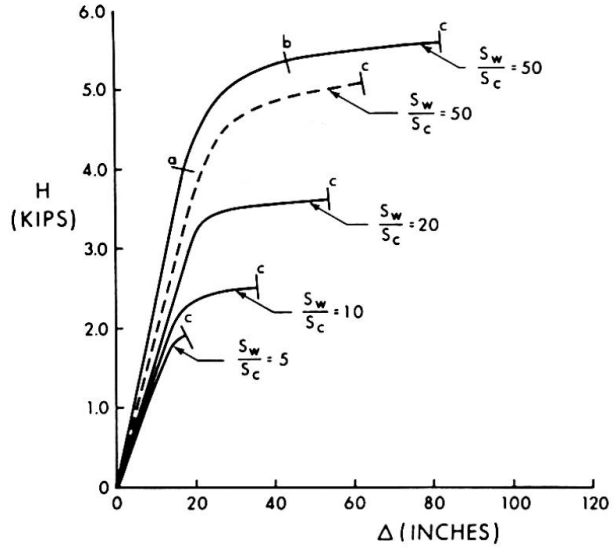

FIG. 11. LOAD-DEFLECTION CURVES

plotted for ratios of K_w/K_c varying from 5 to 50. The load carrying capacity of the structure decreases with a reduction in the shear wall stiffness. This is primarily due to the increased severity of the P-Δ effect.

The structure having $K_w/K_c = 50$ was reanalyzed assuming zero wall width. The result is shown as the dashed curve. In this case, the analysis (assuming zero wall width) yields conservative results, apparently since it neglects the extra restraining moment on the wall. This moment is the result of the shear at the wall end of the beam acting through half the wall width.

It can be observed from FIG. 11 that the difference in behavior due to the variation in wall to column stiffness is considerable. In all cases, the analysis did not converge beyond point 'c'. The loads corresponding to points 'c' have been taken as the ultimate load carrying capacities of the structures. Due to the procedure used in the analysis, the unloading branch of the load-deflection curve can not be obtained.

REFERENCES

1. "Lecture Notes, Plastic Design of Multi-Story Frames," Fritz Engineering Laboratory Report No. 273.20, Lehigh University, 1965.

2. Coull, A. and Smith, B. S., "Tall Buildings", Proceedings of Symposium on Tall Buildings, University ofSouthampton, Pergamon Press, 1967.

3. Khan, Fazlur, R. and Sbarounis, John A., "Interaction of Shear Walls with Frames in Concrete Structures Under Lateral Loads", Proc. ASCE, Vol. 90, ST3, June 1964.

4. Majumdar, S. N. G., Nikhed, R. P., MacGregor, J. G. and Adams, P. F., "Approximate Analysis of Frame-Shear Wall Structures", Structural Engineering Report No. 14, University of Alberta, Edmonton, Canada, May 1968.

SUMMARY

A method has been presented for the approximate inelastic analysis of frame-shear wall structures. The method accounts for the wall-frame interaction and the P-Δ effect. The results presented illustrate the shear distributions obtained and the reduction in load-carrying capacity due to the secondary effects.

RÉSUMÉ

Une méthode a été présentée pour l'analyse inélastique approximée d'une forme de structures composées de murs et de câdres. La méthode tient compte de l'action réciproque du mur et du câdre, et de l'effet du P-Δ . Les résultats présentés servent à démontrer les distributions de forces et les rapetissements de la charge limite qui résulte des effets secondaires.

ZUSAMMENFASSUNG

Für die angenäherte unelastische Berechnung von Scheiben-Rahmentragwerken wird ein Verfahren vorgestellt. Diese Methode zieht das Zusammenwirken der Scheibenrahmen und des P-Δ-Effekts in Betracht. Die Ergebnisse zeigen die Schubverteilung sowie die Traglastverminderung aus sekundärem Einfluss.

Leere Seite
Blank page
Page vide

Non Linear Plastic Analysis of High Strength Steel Plane and Space Frameworks

Analyse plastique non-linéaire de système de portiques dans le plan et dans l'espace en aciers de haute résistance

Nichtlineare, plastische Analyse ebener und räumlicher Stahl-Rahmentragwerke hoher Festigkeit

BULENT OVUNC
University of Southwestern Louisiana
USA

1_Introduction.

The plastic analysis of framed structures requires the determination of the collapse mechanism under the action of proportional loads. Although the collapse mechanism is simple in concept, it depends on too many factors. In rigid plastic theory the collapse mechanism can be obtained by static and kinematic theorems[1] or following the successive formation of plastic hinges until the failure of the structure. Whenever a plastic moment is attained at any cross section, a plastic hinge forms at this section, and it can undergo rotation of any magnitude as long as the bending moment stays constant at the fully plastic value. However there are some discrepancies between the assumptions of rigid plastic theory and the actual behavior of the structure. The plastic hinges develop along a plastified zone, and the strain hardening assures that the plastic hinges will extend over increasing lengths of the member even before the extensive ductility is exceeded[2]. The structure being loaded beyond the elastic limit of its material, the moment curvature diagrams are not linear and the deformations and also the effect of the deformations upon the equilibrium equations are more accentuated than the linear elastic analysis. The fully plastic moment is subject to variation by the slenderness ratio of the member[2][3] by the rotational angle change[3] and also by the member axial and shear forces[1].

Computer programs have been developed for plastic analysis. The program proposed by Wang[4] will trace definitely the location and the sequence of formation of all plastic hinges until collapse, yields the cumulative load factor and the deflections and moments at all nodal points at the time of formation of each plastic hinge.

Wang's program has been modified by Harrison[5] in order to include the finite deformation effects. Rubinstein and Karagozyan[6] have given a solution for minimum weight design.

Intensive experiments have been evolved to show the agreement between the theory and the actual behavior, primarily in two centers: the Cambridge University[7], England, and Lehigh University[8], U.S.A.

In the present paper an attempt has been made to solve the space or plane framework structure accounting for the finite deformation effects, the reduction of plastic moments due to axial member forces, the change in flexural stiffness caused by member axial forces and the influence of shear forces to the deflections[9]. But the effect of strain hardening[10] and the reduction of plastic moment due to member shear forces are neglected. Also the spread of plastic zone and the residual stresses due to live loads[11] are ignored.

The computer program gives as results the collapse mode, that is, whether the collapse occurred by a plastic collapse mechanism or by the instability of whole structure or by a member instability. With an out-of-core Cholesky routine a big structure with more than 2000 unknowns may be handled without any increase in the capacity of the computer. The required computer time is much higher than the non-linear analysis of the same structure, since a non-linear analysis is performed at the formation of each new hinge.

Numerical examples have been given in order to compare the results obtained with those already worked out experimentally or theoretically and one more to illustrate the behavior of the space structures.

2_Non_Linear Analysis of Framed Space Structure.

An iteration procedure[12] is applied to framed space or plane structure to determine its deformed configuration. The basic idea in this procedure is to perform a standard linear analysis under the action of a given set of external loads and then calculate the member end forces using the deformed geometry. If the member end forces at a joint are not in equilibrium with the given external loads, the out-of-balance forces are applied on to the deformed geometry to yield another set of deformations and forces. If the new forces do not satisfy the joint equilibrium, the linear analysis continues with the latest geometry and with the latest out-of-balance forces. This procedure is repeated until equilibrium is reached at every joint.

The stiffness method has been used as a standard linear analysis procedure. The member center line is chosen as the y-axis while the two principal inertia axes of the section constitute the x and z axes of a cartesian co-ordinate system. These axes are called the "member axes" and are referred to a general stationary XYZ cartesian co-ordinate system (Figure 1). The joint deformations obtained from the linear analysis are relative to the generalized XYZ co-ordinate axes. In evaluating the member end forces, it is extremely convenient to work with the member end

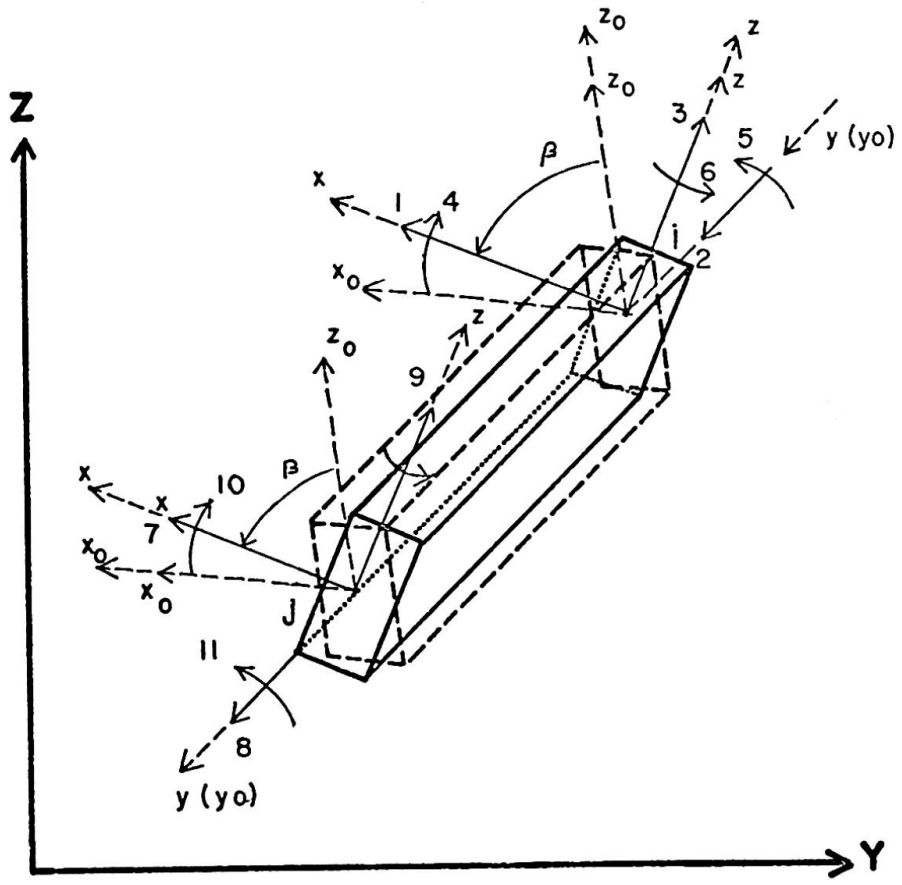

Figure 1. Co-ordinate Axes.

deformations relative to the deformed member axes which are obtained from

$$\{\delta\}_{xyz} = [T]\{\delta\}_{XYZ}$$

where,

$\{\delta\}_{xyz}$ = the column vector of member end deformations relative to the deformed member axes,

$\{\delta\}_{XYZ}$ = the column vector of generalized XYZ co-ordinates

$[T]$ = the orthogonal transformation matrix involving the direction cosines of the deformed member axes

The member forces relative to the deformed member axes, (Figure 2) may be written as follows

$$F_2 = -F_8 = (L_0 - L')AE/L_0$$

$$F_4 = (4EI_x/L'(1+\phi_x))\theta'_4 S_{1x} + (2EI_x/L'(1+\phi_x))\theta'_{10} S_{2x}$$

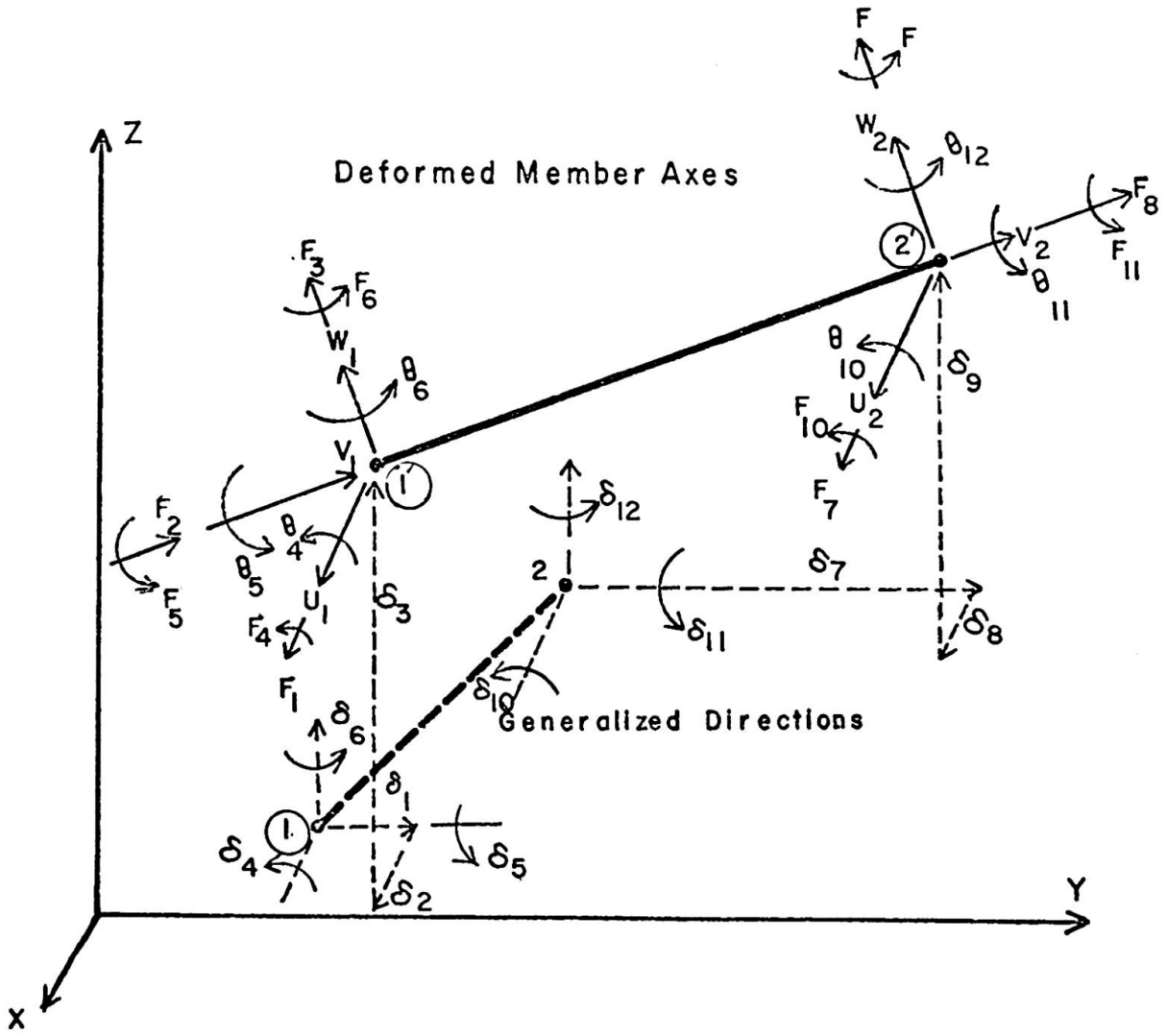

Figure 2. A Beam-Column Member in Space

$$F_{10} = (4EI_x/L'(1+\phi_x))\theta'_{10}S_{1x} + (2EI_x/L'(1+\phi'_x))\theta'_4S_{2x}$$

$$F_6 = (4EI_z/L'(1+\phi_z))\theta'_6S_{1z} + (2EI_z/L'(1+\phi_z))\theta'_{12}S_{2z}$$

$$F_{12} = (4EI_z/L'(1+\phi_z))\theta'_{12}S_{1z} + (2EI_z/L'(1+\phi_z))\theta'_6S_{2z}$$

$$F_5 = -F_{11} = (GJ/L')(\theta_5 - \theta_{11})$$

$$F_7 = -F_1 = (F_6+F_{12})/L'$$

$$F_3 = -F_9 = (F_4+F_{10})/L'$$

where

$$L_0 = \left[(X_2-X_1)^2 + (Y_2-Y_1)^2 + (Z_2-Z_1)^2\right]^{\frac{1}{2}}$$

$$L' = \left[(X'_2-X'_1)^2 + (Y'_2-Y'_1) + (Z'_2-Z'_1)^2\right]^{\frac{1}{2}}$$

$$\theta'_4 = \theta_4+\theta_w \quad : \quad \theta'_{10} = \theta_{10}+\theta_w$$

$$\theta'_6 = \theta_6+\theta_u \quad : \quad \theta'_{12} = \theta_{12}+\theta'_u$$

$$\theta_u = \text{Arcsin}\left(\frac{u_2-u_1}{L_0}\right)$$

$$\theta_w = \text{Arcsin}\left(\frac{w_1-w_2}{L_0}\right)$$

In the above expressions, u_1, u_2, w_1 and w_2 are the translations and θ_4, θ_{10}, θ_6, θ_{12}, θ_5 and θ_{11} are the rotations of the member ends relative to the deformed member axes as obtained from the linear analysis. S_{1x}, S_{2x}, S_{1z}, S_{2z}, are the correction factors to include the influence of the axial force on the member flexural stiffness coefficient and ϕ_x, ϕz are the correction factors to include the influence of member shear forces on to the displacements.

3. Plastic Analysis of Framed Structures.

To determine the collapse mechanism, a non-linear analysis as mentioned above is performed after each succesive hinge formation. The rotation of all previously formed hinges is checked, and if the rotation of one of the previous hinges decreases, this hinge is locked again. The collapse may occur with the formation of a new hinge or within the non-linear cycles. In the former case, the collapse is caused by a plastic mechanism, and in the latter case it is caused either by a member instability or by the instability of the whole structure.

The member instability and the effect of the member shear forces are taken into account by introducing proper factors in the member flexural stiffness coefficients. At every step the value of the member plastic moment is modified, depending on the member axial force. For I beams both cases[1] are considered separately, that is, whether the neutral axis lies in the web or in the flange.

No allowance for strain-hardening is made. Also the spread of plastic zone, reduction of plastic moment due to member shear forces

and the residual stresses due to live loads are ignored.

Structures having members with variable moments of inertia can also be solved.

4_ Computer Programming.[13]

The data values fed in computer are respectively the characteristic of the structure such as: the Young modulus E, the Poisson ratio μ, the co-ordinates of the joints referred to XYZ generalized co-ordinate axes, the two end joints of each member, moments of inertia in two principal inertia axes, polar moment of inertia, area of the section, the web area and depth if it is an I section, plastic moments in two principal inertia axes, redundant joints information, joint and member loads if any. All the other operations are performed automatically in computer.

The computer gives as output the displacements and rotations at every joint and the member end reactions of all the members for first linear analysis, then the same information for non-linear analysis. This pattern is repeated after formation of each new hinge until the collapse of the structure. The collapse occurs either by the singularity of structure stiffness matrix or by the large joint deformations. The load factors for each step and the cumulative load factor are also pointed out.

5_ Examples of Analysis

The dimensions and member characteristics of the first two examples are selected from previous studies in order to compare the results. An example of space frame is also given. The parameters NL and NC show respectively whether the reduction of plastic moment due to member axial forces and the stability correction factors are taken into account or not. These parameters may have the value equal either to zero or one which means respectively that the corresponding correction factors are included or not in the analysis. QP is the cumulative load factor.

5_1. Portal Frame.

The dimensions and member characteristics are given in Figure 3. The successive hinge formation and their location, cumulative load factors, the horizontal displacement at joint B, (Δ_1), and H, (Δ_3), and the vertical displacement at joint E, (Δ_2), are also given in the tables for linear and non-linear analysis.

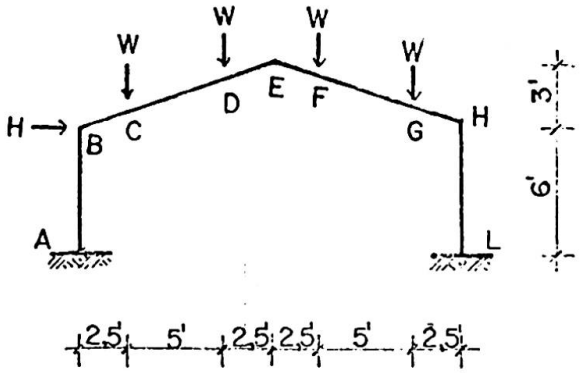

A S B 104, 5" x 2,5" I
I_x = 10,91(in^4) A = 2,65(in^2)
M_p = 16,66(k-ft)

Figure 3

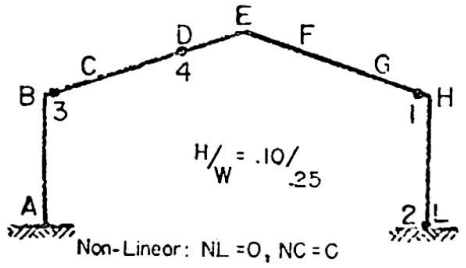

Figure 4

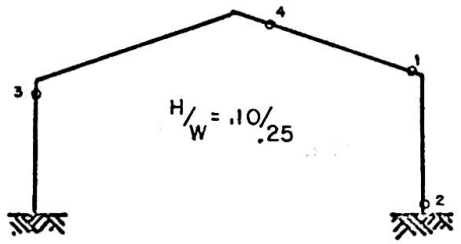

Linear :

Non-Linear NL=1 , NC=0

NL =1 , NC=1

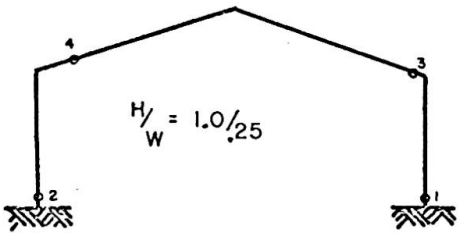

Linear

No-Linear NL = 0 , NC= 0

NL= 1 , NC= 0

NL = 1 , NC = 0

Figure 5

Figure 6

Table I H/W = .10/.25

		LINEAR ANALYSIS	NON—LINEAR ANALYSIS		
			NL=0 NC=0	NL = 1 NC = 0	NL = 1 NC = 1
PLASTIC HINGE ORDER	1	14.051	13. 85	13.428	13.40
	2	14.555	14. 38	13. 937	13.89
	3	16.161	15. 90	15.717	15. 66
	4	18.330	18.02	17.703	17.69
DEFORMATION (in)	Δ_1	0.172	0.178	0.220	0. 220
	Δ_2	3.253	3.272	3.264	3. 324
	Δ_3	2.097	1.996	2.034	2.065

Table II H/W = 1./.25

		LINEAR ANALYSIS	NON–LINEAR ANALYSIS NL=0 NC=0	NL=1 NC=0	NL=1 NC=1
PLASTIC HINGE ORDER	1	6.627	6.559	6.386	6.367
	2	8.666	8.562	8.474	8.463
	3	9.008	8.911	8.724	8.729
	4	10.286	10.077	9.920	9.922
DEFORMATION (in)	Δ_1	4.127	4.141	4.162	4.224
	Δ_2	2.363	2.555	2.579	2.617
	Δ_3	5.521	5.461	5.507	5.586

5_2, Four Storey Frame.

The dimensions and member characteristics are given in Figure 7. The successive hinge formations and their location, cumulative load factors, the horizontal displacement at joint C(Δ_1), N(Δ_3), R(Δ_5), the vertical displacement at joint D(Δ_2) and P(Δ_4) are also given in the tables for linear and non-linear analysis.

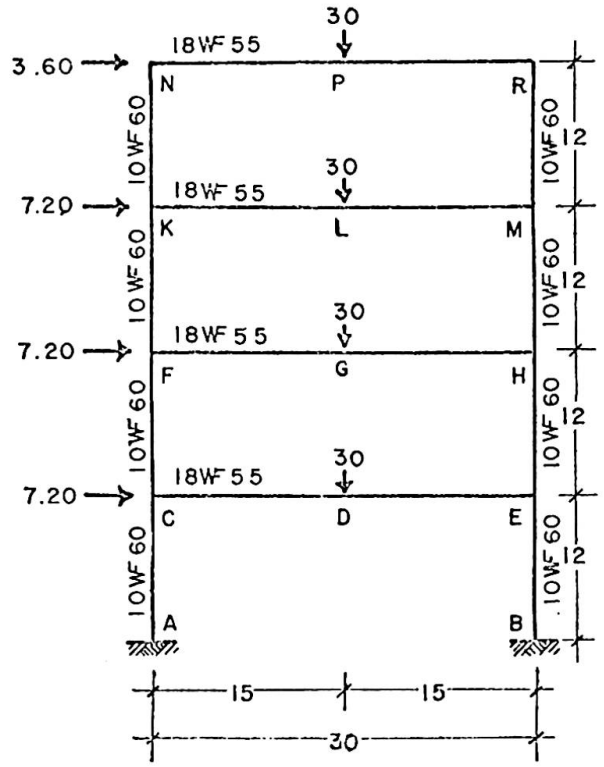

Figure 7

	I_x (in)^4	I_z (in)^4	J(in)^4
10WF60	343.0	116.5	2.15
18WF55	888.9	42.0	2.65
18WF60	984.0	47.1	2.94

	A(in^2)	Mpx(k.ft)	Mpz(k.ft)
10WF60	17.60	213.73	99.68
18WF55	16.19	317.69	54.52
18WF60	17.64	349.10	60.94

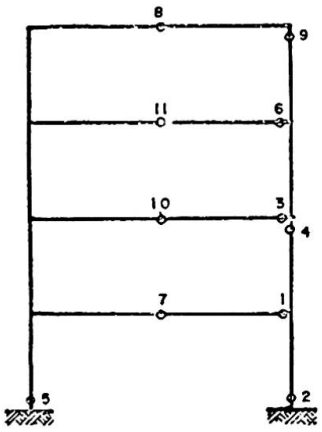

Linear.

Figure 8

PLASTIC HINGE ORDER	LINEAR ANALYSIS	NON-LINEAR ANALYSIS		
		NL=1 NC=0	NL=0 NC=0	NL=1 NC=1
1	1.739	1.739	1.739	1.739
2	1.903	1.759	1.906	1.769
3	1.916	1.851	1.914	1.812
4	1.991	1.941	1.996	1.891
5	2.147	2.059	2.139	1.975
6	2.148	2.123	2.146	2.038
7	2.158	2.135	2.151	2.127
8	2.162	2.141	2.154	2.133
9	2.189	2.158	2.177	2.138
10	2.210	2.160	2.190	2.148
11	2.230	2.161		2.143
12		2.186		

Table III

PLASTIC HINGE ORDER	NON-LINEAR ANALYSIS (NL=0, NC=0)				
	Δ_1	Δ_2	Δ_3	Δ_4	Δ_5
1	0.899	0.731	2.889	1.023	2.867
2	1.088	0.922	3.396	1.113	3.371
3	1.103	0.939	3.427	1.107	3.402
4	1.249	1.047	3.889	1.042	3.862
5	1.522	1.273	4.721	1.228	4.685
6	1.557	1.287	4.781	1.229	4.762
7	1.588	1.300	4.862	1.229	4.832
8	1.604	1.306	4.899	1.234	4.869
9	2.608	2.595	6.824	1.546	6.793
10	3.136	3.271	8.001	1.691	7.964

Table IV

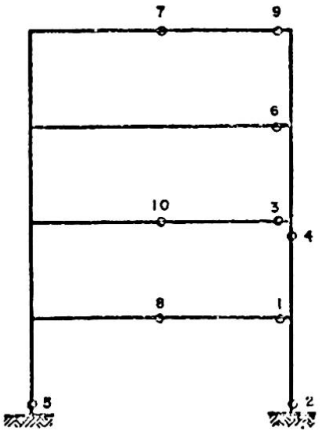

Non-Linear: NL=0, NC=0.

Figure 9

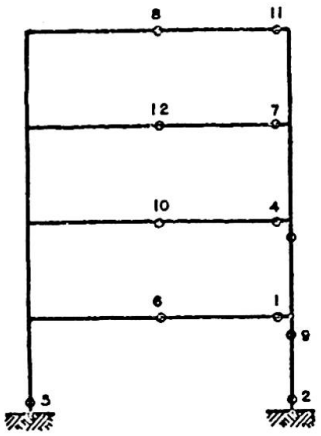

Non-Linear NL=1, NC=0

Figure 10

PLASTIC HINGE ORDER	LINEAR ANALYSIS				
	Δ_1	Δ_2	Δ_3	Δ_4	Δ_5
1	0.898	0.730	2.885	1.017	2.868
2	1.083	0.921	3.383	1.114	3.364
3	1.103	0.938	3.429	1.121	3.410
4	1.253	1.063	3.890	1.169	3.880
5	1.524	1.288	4.735	1.254	4.713
6	1.530	1.291	4.746	1.255	4.724
7	1.582	1.312	4.867	1.261	4.846
8	1.681	1.448	5.065	1.264	5.044
9	2.311	2.314	6.328	1.360	6.306
10	2.806	2.992	7.563	1.803	7.541
11	4.150	4.731	11.344	2.720	11.322

Table V

5-3. Space Frame.

The dimensions and member characteristics are given in Figure 10. The successive hinge formation and their location, cumulative load factors, the horizontal displacement at joints E(Δ_1), G(Δ_3) and vertical displacement at joint F(Δ_2) are also given in the tables for non-linear analysis.

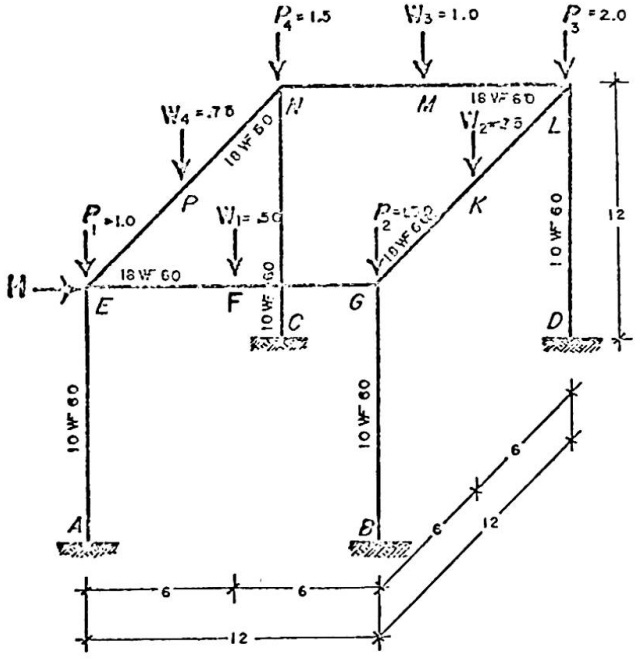

Same steel section characteristics as Four Storey Frame

Figure 11

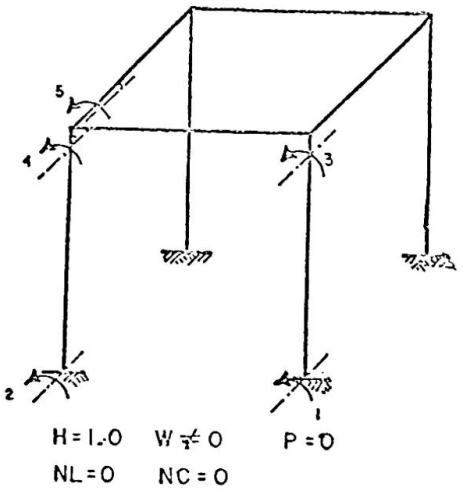

Figure 12

		NL = 0		NC = 0		NL = 1		NC = 0	
		QP	Δ_1	Δ_2	Δ_3	QP	Δ_1	Δ_2	Δ_3
PLASTIC HINGE ORDER	1	67.8013	- 0.0051	0.9448	- 0.0639	67.8184	- 0.0051	0.9450	- 0.0639
	2	71.9553	- 0.0071	1.0379	- 0.0682	70.1642	- 0.0062	0.9976	- 0.0663
	3	72.0123	- 0.0089	1.0407	- 0.0645	71.5020	- 0.0081	1.0367	- 0.0679
	4	76.4655	- 0.0137	1.4552	- 0.0931	76.0266	- 0.0129	1.4596	- 0.0970
	5	90.3714	- 0.0170	5.4564	- 0.2097				

Table VI

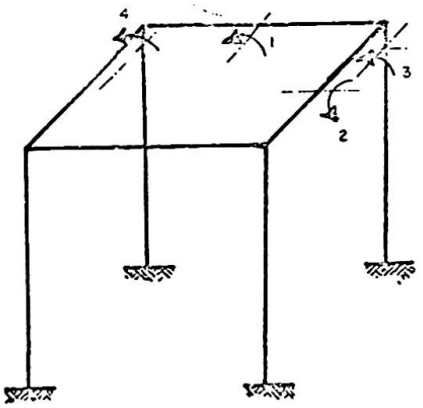

H= .10 W ≠ 0 P=0

NL=0 , NC=0

NL=1 , NC=0

Figure 13

		PLASTIC HINGE ORDER			
		1	2	3	4
NL=0 , NC=0	QP	146.243	171.4713	186.4638	187.3258
	Δ_1	.0.0051	-0.0058	-0.0066	-0.0066
	Δ_2	0.0111	0.0130	0.0140	0.0416
	Δ_3	-0.2569	-0.5581	-0.7379	-0.7792
NL=0 , NC=0	QP	146.2433	171.4620	178.6744	179.2672
	Δ_1	-0.0051	-0.0058	-0.0062	-0.0063
	Δ_2	0.0111	0.0130	0.0135	0.0325
	Δ_3	-0.2569	-0.5580	-0.6444	-0.6727
NL=1 , NC=0	QP	146.243	179.603	180.296	
	Δ_1	-0.0051	+0.0087	+0.0084	
	Δ_2	0.0111	-0.0040	-0.0069	
	Δ_3	-0.2569	-0.7373	-0.7719	

Table VII

		NL = 0		NC = 0	
		Qp	Δ_1	Δ_2	Δ_3
PLASTIC HINGE ORDER	1	67.695	-0.0098	0.9475	-0.0876
	2	71.840	-0.0120	1.0370	-0.0956
	3	72.040	-0.0139	1.0451	-0.0898
	4	76.385	-0.0189	1.3656	-0.1199
	5	88.249	-0.0246	5.4655	-0.2455

Table VIII

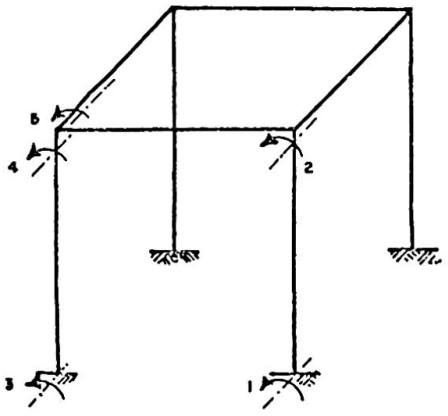

H=1.0 W ≠ 0 P=0

NL=1 NC=0

Figure 14

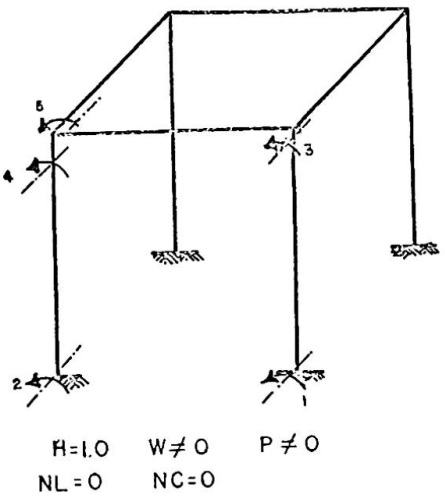

Figure 15

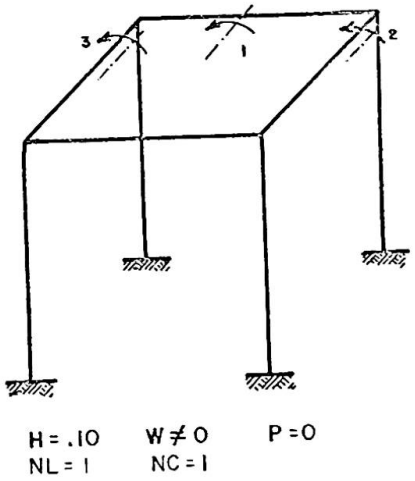

Figure 16

REFERENCES

1. Neal, B. G., "The Plastic Method of Structural Analysis" John Wiley & Sons, 1956.

2. Potts, Richard G. and Brungraber, Robert J., "Inelastic Behavior of Structural Frameworks" ASCE Vol. 93, No. ST3, Proc. Paper 5298, June 1967, pp. 287-313.

3. Hrennikoff,A. P., "Plastic and Elastic Design Compared" Seventh Congress of IABSE, Publications, Rio de Janeiro, August 10-16, 1964, pp. 205-212.

4. Wang, Chu-Kia, "General Computer Program for Limit Analysis" ASCE, Vol. 89, No. ST6, Proc. Paper 3719, December 1963, Part I, pp. 101-117.

5. Harrison, H. B., "Plastic Analysis of Rigid Frames of High-Strength Steel Accounting for Deformation Effects" Preprint Paper No. 2222, presented at the Engineering Conference, March 13-17, 1967, pp. 135-144.

6. Rubenstein, M. F. and Karsgozian, "Building Design Using Linear Programming", ASCE Vol. 92, ST4, Part II, Proc. Paper No. 5012 December 1966.

7. Baker, T. F., Horne, M. R. and Heyman, T., "Steel Skeleton" Cambridge, Cambridge University Press, 1956.

8. "The Commentary on Plastic Design in Steel", WRC-ASCE Joint Committee, ASCE Manual of Engineering Practice No. 41, 1961.

9. Lay,M. G. and Smith, P. D., "Role of Strain Hardening in Plastic Design", ASCE Vol. 91, No. ST3, Part I Proc. Paper No. 4355, June 1965, pp. 25-43.

10. Hrennikoff, A. P., "The Importance of Strain-Hardening in Plastic Design", ASCE Vol. 91, No. ST4, Proc. Paper No. 4424, August 1965, pp. 23-34.

11. Davies, J. M., "Collapse and Shakedown Loads of Plane Frames", ASCE Vol. 93, No. ST3, Proc. Paper No. 5259, June 1967, pp. 35-50.

12. Tezcan, S. S. and Ovunc B., "An Iteration Method for the Non-Linear Buckling of Framed Structures" Space Structures Edited by R. M. Davies, Part IV, No. 45, Blackwell Scientific Publications, Oxford and Edinburg, 1967.

13. Tezcan, S. S., "Computer Analysis of Plane and Space Structures" ASCE Vol. 92, No. ST2, Proc. Paper No. 4780, April 1966.

SUMMARY

In the present paper an attempt has been made to solve the space or plane framework structures accounting for the finite deformation effects, the reduction of plastic moments due to axial member forces, the change in flexural stiffness caused by member axial forces and the influence of shear forces to the deflection. But the effect of strain hardening and the reduction of plastic moment due to member shear forces are neglected. Also the spread of the plastic zone and the residual stresses due to live loads are ignored.

RÉSUMÉ

Cette étude essaie de résoudre les systèmes de portiques plans ou dans l'espace en tenant compte des effets des déformations finies, de la réduction des moments plastiques et de la variation de rigidité à la flexion dues aux efforts axiaux et de l'influence des efforts de cisaillement sur la déformation. On a négligé cependant l'effet du durcissement ainsi que la réduction du moment plastique due aux efforts de cisaillement. De même on ne tient pas compte de l'extension de la zone plastique ni des tensions résiduelles dues à la charge de service.

ZUSAMMENFASSUNG

In diesem Beitrag ist der Versuch unternommen worden, ebene und räumliche Rahmentragwerke mit Berücksichtigung der Wirkung endlicher Verformungen, der Abminderung der plastischen Momente unter Achsiallasten, des Wechsels der Biegesteifigkeit aufgrund der Stabachsialkräfte sowie des Einflusses der Querkräfte auf die Durchbiegungen zu lösen. Hingegen sind die Wirkung der Verfestigung und die Abminderung des plastischen Moments infolge Stabquerkräfte vernachlässigt worden. Ebenso sind die Ausbreitung der plastischen Zone und die Eigenspannungen infolge Verkehrslast unberücksichtigt.

DISCUSSION LIBRE / FREIE DISKUSSION / FREE DISCUSSION

TSUNEYOSHI NAKAMURA
Ph.D. Assistant Professor of Architecture, Kyoto University

In view of the contents of Section 3 of the general report by Professors O. Steinhardt and H. Beer, the two papers (1) and (2) by Ryo Tanabashi and Tsuneyoshi Nakamura should also be referred to as a possible approach to the plastic design of tall multi-story frames. In Ref. (1), the linear minimum weight design of a broad class of tall multi-story frames of practical interest has been established in a simple and explicit analytical form by introducing a new concept of "frame moment". The general solution for comparatively large lateral forces has been obtained due to the particular circumstance in Japan where equivalent static lateral forces due to earthquake disturbances are comparatively larger than those in other countries. The solution may, however, be readily modified for a more general case where the vertical forces are dominant compared to lateral forces in several stories from the top. This design is regarded as the preliminary design.

When a rigid-plastic preliminary design is constructed for a design problem, one may readily find the axial force distribution corresponding to the bending moment distribution at the collapse state of the simple plastic theory. Hence the secondary design may be accomplished by assigning the plastic moment to a column in such a way that the known axial force and bending moment acting upon its end sections would not violate the corresponding bending moment-axial force-interaction yield conditions.

The last step is to modify the above secondary design against the unfavorable effect of the additional moments induced by the sidesway deflections under large axial forces in the last hinge point state. It should be noted that the last hinge point load factor must be equal to or less than the true failure load factor and may be used as the base of the design. The last hinge point state may be constructed iteratively starting from the above secondary design. The crucial point here is that the iterative process is to be carried out not with respect to the moments as an analysis but with respect to the cross-sectional dimensions as a design problem. An example of a 30-story frame treated in Ref. (2) has shown a rapid convergence of the present procedure.

This last hinge point design is regarded as a standard design for the problem with which any actual design may be compared. Since any augmentation in stiffnesses and plastic strengths would not decrease the elastic critical load factor and the rigid-plastic collapse load factor, any actual design may be accomplished in reference to this standard design by appropriate augmentations such that the actual design is guaranteed to possess a greater failure load factor than the last hinge point load factor of the standard design satisfying other various practical requirements.

(1) Ryo Tanabashi and Tsuneyoshi Nakamura, "The Minimum Weight Design of a Class of Tall Multi-story Frames Subjected to Large Lateral Forces", Proc. 15th Japan National Congress for Appl. Mech., pp 72-81, 1965.

(2) Ryo Tanabashi and Tsuneyoshi Nakamura, "An Approach to the Last Hinge Point Design of Tall Multi-story Frames", Proc. Symposium on the External Forces and Structural Design of High-rise and Long-span Structures, pp 169-179, Tokyo, Sept. 1965. (Japan Society for the Promotion of Science)

Elasticity or Plasticity?

Élasticité ou plasticité?

Elastizität oder Plastizität?

W. OLSZAK
Prof.Dr., Dr.h.c.
Poland

A very interesting discussion is going on on elasticity and plasticity. I should like to contribute to it some further remarks.

A reversible (or elastic) deformation, as you all know, is the response of a material in the first stage of the loading process. It may be linear or non-linear. It is not accompanied by energy dissipation. (We confine ourselves to discussing isothermal processes).

Viscous flow is observed when the body is maintained for a long period under the action of external forces. This may be either reversible or irreversible; however, it is always connected with energy dissipation.

A plastic deformation is a kind of defence (self-defence) of the material against overloading. It is always irreversible and is always connected with energy dissipation.

Thus it may be seen that there is not only a quantitative, but, essentially, also a qualitative difference between elastic, plastic, and time-dependent phenomena.

The above remarks hold, as a rule, for any material; they are also true for our engineering materials from which our structures are made.

In consequence, the response of our engineering structures to various kinds of external agents depends (1) on the duration of the application of loads and (2) on their intensity.

The Theory of Elasticity deals with reversible phenomena, and is not interested in and, therefore, cannot account for such effects as the time-dependent deformation processes which are generally called the rheological (or viscous) phenomena as, e.g., creep, relaxation etc.; but it also cannot account for plastic effects.

On the other hand, the designer - a conscientious designer - wants to know what really is going to happen to his structure in the course of its existence, let us say, in a year, or two, or five; and perhaps also, what is going to happen if the structure - by accident or purposely - is overloaded, overloaded in comparison with the originally planned design load.

Thus, there is no contradiction and, of course, no competition between the "elastic" and "inelastic" approaches. Consequently, there is also no competition or clash between the Theory of Elasticity and the Theory of Plasticity: these theories simply cover different questions. Thus, they are complementary.

The Theory of Plasticity is, if I may put it in a somewhat simplified way, a kind of extension of the Theory of Elasticity.

It is to-day quite obvious that the Theory of Elasticity is a well developed and logically built up discipline. It has been worked on for about three centuries since Robert Hooke's famous statement "Ut tensio, sic vis" has been published*). Thus, he formulated one of the basic assumptions of the (physically) linear Theory of Elasticity (law of proportionality between strains and stresses). The other assumption is that the deformations and strains are small (geometrical linearity). With these two fundamental assumptions the elegant and impressive structure of the classical Theory of Elasticity with all the required basic principles, variational theorems, methods of solutions, comprising countless effective applications, has been established.

The Theory of Plasticity is not less important, however quite different, somewhat more complex and, moreover, far younger. The foundations of the mathematical theory of perfectly plastic materials were laid in two splendid papers by Barre de Saint-Venant and Maurice Lévy (C.R. Acad. Sci., Paris 1870). But then, for about 30 or 40 years, nothing happened in this domain. Only in 1904 M.T. Huber, and later independently R.v.Mises (1913) and H. Hencky (1924) established the "energetic" yield criterion for the onset of plastic deformations in three-diemnsional states of stress. So the age of the Theory of Plasticity is to-day not even a hundred years, from which only the last 50 or even 40 years are of importance. It is quite clear that, under such circumstances, some questions are still open, especially for assessing the theoretical treatment of phenomena of work-hardening, finite deformations and some others. Anyhow, constant progress is being made in all basic and applied aspects and it is fair to state that the results achieved so far have already widened our basic knowledge and have well served numerous engineering branches.

In conclusion I should like to remark that man has always been and is very inquisitive creature: we examine everything, starting with ourselves, down to bacteria and virus, we reach out - at the other extreme - to the moons and galaxies. So I think it is quite natural that we cannot prevent people from being curious and having a penetrating mind in connection with the properties, life and reliability of our materials and structures in all the circumstances they have to face and also after they have exceeded the elastic range of response.

I also think that - so far - scientific research seems to constitute the only way of satisfying one's own personal curiosity being at the same time instrumental towards solving numerous social and public problems and needs; it likewise seems it will continue to be so in the field of structural engineering.

---

*) R.Hooke, De potentia restitutiva, London 1678. As a matter of fact, Hooke's principle of his balance spring was first expressed in a Latin anagram "ceiiinosssttuu" (1676), a form which commonly was used in scientific circles of the time to establish priority of discivery without actually disclosing anything that might be of use for possibly jealous collegues.

Plastic Design of Tall Buildings

Dimensionnement plastique de bâtiments élancés

Plastische Bemessung von Hochhäusern

LYNN S. BEEDLE
Professor of Civil Engineering and Director
Fritz Engineering Laboratory
Lehigh University
Bethlehem, Pennsylvania

The conference topic, Plastic Design of Tall Buildings, has been particularly timely in connection with a current project of the American Society of Civil Engineers. An ad hoc committee of ASCE is currently (1968) nearing completion of its work in revising ASCE Manual No. 41, "Plastic Design in Steel". Included in the committee are many members from abroad, and their attendance at this meeting has made possible a number of valuable informal discussions.

Much additional information is now available on the status of plastic design, new research, new applications, and problems requiring further study. The second edition of ASCE Manual No. 41 is being revised on a modest basis to include this information, to incorporate braced multi-story frames, and to encompass modifications to simple plastic theory where necessary to extend its applicability. It will cover steels with yield points up to 65 ksi, and additional attention is given to repeated loading effects. It is hoped that the second edition of the Manual will be available early in 1969.

Discussion by Professor Hrennikoff

With respect to the prior discussion by Professor Hrennikoff, two comments are pertinent. In the first place, so-called elastic design would have the same inadequacies that he attributes to plastic design. If what Professor Hrennikoff says is true, then most of the buildings designed in the last two decades would either be unsafe or would be uneconomical--and that can scarcely be the case. It was in 1945 that the American Institute of Steel Construction first incorporated a provision to allow a 20% increase in stress at points of interior support in continuous beams. This amounted to a direct use, albeit on a somewhat arbitrary basis, of the plastic strength of steel structures. It is a provision that has been used in design ever since. In Europe plastic design has been used for decades in proportioning continuous beams. Thus one cannot in any way understand why Professor Hrennikoff continues to be concerned.

In the second place, as engineers we tend to be interested in stress. But the user and the owner are concerned about safety (that the structure has adequate strength) and with performance (that it doesn't deform too much). These latter are the truly important criteria: strength and deformation. Where stress is a logical basis for design it is only so because it assures that one or the other of these two design requirements will be met.

Therefore, we reject Professor Hrennikoff's thesis.

Contributors to the Plastic Theory of Structures

Earlier in the discussion of this theme, Professor Massonnet mentioned a conference on engineering plasticity at Cambridge University, England. It was the writers privilege to be able to attend this conference which honored Sir John Baker on the occasion of his completing his service to Cambridge. This honor to Sir John (Fig. 1) was particularly appropriate because he put into motion a new era in structural design. As a pioneer into new areas of structural design, he understood the weaknesses of past design techniques and the significant opportunities for improvement. Not only was he able to set forth the new concept, but he made that essential next step: to stimulate in a dramatic way the application of research findings to design. It is indeed fortunate that the engineering profession continues to benefit from his active contributions.

Fig. 1

The Conference on Engineering Plasticity was also important, as are all conferences, because of the people who attended. A special group are the four shown in Fig. 2--individuals who were true pioneers in various aspects of maximum load design*. Commencing from the right, Professor Prager headed a most important team at Brown University; their studies and writings are the major contributions to the mathematical theory of plasticity. It was Professor Baker's genius that made plastic design a practical, useful technique for the structural engineer. Professor Johansen gave the profession the

Fig. 2

---

*Regretably, the photograph does not include M. Massonnet, also present at the Conference, and in Europe a leader in plastic design developments.

yield line theory. Finally, Dr. Stüssi, honorary president of the IABSE, gave us searching and challenging questions; and it is only the fact that it has been possible to answer these questions that plastic design has become the practical and useful tool that it is today.

Not included in the photograph, but active in this current New York IABSE conference (and pictured in Fig. 3) is one who, more than any other, has made possible the rapid advances in all aspects of steel design in the United States: T. R. Higgins, Director of Engineering and Research of the American Institute of Steel Construction. He is an integral member of the pioneering group. His grasp of the essence of new concepts, his untiring participation in the work of research councils, and his leadership in transferring research to practice have contributed significantly to the remarkable advances in design techniques that are available to the practicing engineer in the world today.

Fig. 3

Leere Seite
Blank page
Page vide

Remarques de l'auteur du rapport introductif
Bemerkungen des Verfassers des Einführungsberichtes
Comments by the author of the introductory report

O. STEINHARDT
Deutschland

Das Thema III (Hochhäuser) behandelt Stahlskelettkonstruktionen vorwiegend ohne Innenstützen, ferner mit Verbänden oder auch ohne aussteifende Wand- und Deckenscheiben.

Anhand der zu Thema IIIa bzw. teilweise zu IIIb eingegangenen R e f e r a t e könnte man eine Diskussion nach folgenden Teilfragen gliedern, die jeweils einen Einfluss auf die hier insgesamt in Frage stehende Traglasttheorie nehmen: 1. Von wesentlichem Einfluss ist zunächst die M a t e r i a l f r a g e, die sowohl eine Unterscheidung nach Stählen mit ausgeprägter Fliessgrenze und hochfesten Stählen verlangt, als auch weiterhin (insbesondere für den erstgenannten Fall) eine Berücksichtigung der Höhe der Fliessgrenze, die z.B. beim deutschen Stahl St 37 zwischen 2,2 - 3,0 Mp/cm^2 liegen kann. Durch die Grösse der hierdurch sich ergebenden plastischen Momente wird das Kräftespiel zwischen Trägerlagen und Stützen stark beeinflusst. - 2. Ein multipler S i c h e r h e i t s f a k t o r soll neben den Lastschwankungen auch weitere Einflüsse (z.B. unsichere Materialkennwerte, geometrische Imperfektionen und Eigenspannungen) eventuell auch auf statistischer Grundlage erfassen; dies wird im wesentlichen unter Thema I untersucht. - 3. Zum engeren Thema der B a u f o r m e n wäre eine Unterscheidung nach ebenen und räumlichen Systemen von Bedeutung; im Sinne der Referate scheint dabei der Fall: S t ü t z e n ausschliesslich im "elastischen Bereich", T r ä g e r l a g e n im "plastischen Bereich" heute schon eine weitgehende Aussprache zu erlauben. - 4. Zuletzt wäre dann noch im Hinblick auf das Thema zu unterscheiden zwischen u n v e r s c h i e b l i c h e n (und quasi-unverschieblichen) Stockwerkrahmen einerseits, sowie v e r s c h i e b l i c h e n Stockwerkrahmen andererseits. -

Aus den bisherigen Referaten sowie aus weiteren Veröffentlichungen geht hervor, dass für sehr hohe verschiebliche Rahmenkonstruktionen eine Bemessung nach der Plastizitätstheorie zwar noch wirtschaftliche Vorteile bringen kann, dass jedoch die Materialersparnis (trotz grossem Berechnungs- und Konstruktionsaufwand) auf

höchstens 10% begrenzt sein dürfte. - Bei vorgenommener B e s c h r ä n k u n g auf unverschiebliche bzw. quasi-unverschiebliche Stockwerkrahmen können, insbesondere falls letztere bei horizontaler Belastung höhen-proportionale Knotenverschiebungen erfahren, die Nachweise für die Trägerlagen gemäss der Traglasttheorie, sowie für die Stützen vorzugsweise nach der Elastizitätstheorie mit befriedigender Exaktheit vorgenommen werden. Es wird hier in vielen Sonderfällen möglich sein, Teil-Ersatzsysteme einzuführen.

Die einzelnen Verfasser sagen zu den aufgeführten Leitgedanken i.W. Folgendes: Ein befriedigend exaktes Berechnungsverfahren bei quasi-unverschieblichen Stockwerkrahmen halten sowohl HEYMAN als auch MASSONNET für möglich, wobei erstgenannter nur die bisher aufgeführten Forderungen verwendet, letztgenannter darüber hinaus zusätzliche konstruktive Massnahmen für die Trägerauflagerungen empfiehlt; es können dann die Träger "plastisch" dimensioniert werden, die durchlaufenden Stützen wie zentrisch belastete Knickstäbe! - HRENNIKOFF, der eine orientierende plastische Traglastuntersuchung nicht ausschliesst, warnt vor ihrer allgemeinen Anwendung als Ersatz der Elastizitätstheorie; bei vorerwähnten Einschränkungen dürfte er jedoch ihrer zweckmässigen Anwendung zustimmen. - Die wichtigen Untersuchungen der LEHIGH-University scheinen zu beweisen, dass bei w e n i g e n Stockwerken die "plastische Ausnutzung" der Stützen theoretisch unsicher und wirtschaftlich ungünstig sein kann. - VOGEL's Beitrag bietet eine Berechnungsweise für plastisch-beidachsig beanspruchte Stützen u n v e r s c h i e b l i c h e r Rahmen an.

Die Forschergruppe EDMONTON-Canada befasst sich mit dem Zusammenspiel zwischen Stockwerkrahmen- und Schubwänden, wobei solche praktischen Grenzen für die "Schubwandsteifigkeit" ermittelt werden, die es erlauben, quasi-unverschiebliche Rahmen zugrunde zu legen. Darüber hinaus wird eine auf Computer orientierte Methode für allgemeine Berechnungsansätze geboten.

Die Verwendung h o c h f e s t e r S t ä h l e wird von NEEDHAM, der LEHIGH-University und von OVUNC behandelt. Im Hinblick auf die vorher als zweckmässig erachteten E i n s c h r ä n k u n g e n für eine brauchbare "Plastizitätstheorie" ergäben sich keine zu komplizierten Verhältnisse; auch NEEDHAM möchte - selbst bei räumlichen Rahmen - plastische Gelenke in den Stützen vermeiden.

Es kann zusammenfassend festgestellt werden, dass durch e i n s c h r ä n k e n d e Voraussetzungen hinsichtlich Baustahl, Geometrie und konstruktiver Ausbildung von Stockwerkrahmen (mit begrenzter Höhe) zurzeit eine zuverlässige Handhabung der Plastizitätstheorie denkbar ist, dass dagegen ihre a l l g e m e i n e Anwendung auf grosse Schwierigkeiten stösst, da zuviel fallweise auftretende Einflussfaktoren das Kräftespiel zwischen Trägerlagen und Stützen sowie das Stabilitätsverhalten des gesamten Tragsystems beeinflussen.

III b

Bâtiments de grande hauteur sans poteaux intérieurs, avec ou sans noyau rigide.

Hochhäuser ohne Innenstützen mit und ohne Kern

Column-Free Box-Type Framing with and without Core

Leere Seite
Blank page
Page vide

DISCUSSION PRÉPARÉE / VORBEREITETE DISKUSSION / PREPARED DISCUSSION

Column-Free Box-Type Framing with and without Core

Bâtiments de grande hauteur sans poteaux intérieurs, avec ou sans noyau rigide

Hochhäuser ohne Innenstützen mit und ohne Kern

TAKEO NAKA
Dr., Prof. Emeritus
Dept. of Arch.

BEN KATO
Dr., Assoc. Prof.
Dept. of Arch.

MASAMI NAKAO
Lecturer of Engrg. Research Inst.
University of Tokyo

§ 1 Introduction

To examine the possibility to represent by some parameters the elastic behavior of box-type framing(without core) subjected to lateral force,a numerical analysis is practiced with some amount of digital computation. The method of analysis used is the method mentioned in the APPENDIX in which the shear deformations of panel-zone,column and beam are ignored,that is,HD_K and $SD_{K,i}$ are put to zero,$CAS_{K,i}$ and $BAS_{K,i}$ are put to infinity,moreover,$G_{K,i}$ is omitted from the variables.

HITAC 5020E of the Computer Centre in Univ. of Tokyo is used at the digital computation.

§ 2 Table of symbols

I_c ----- moment inertia of column
I_B ----- moment inertia of beam
$_cA_n$ ----- sectional area of column
K_0 ----- standard rigidity
K_c ----- rigidity ratio of column
K_B ----- rigidity ratio of beam
A ----- a half of replaced sectional area of column
d_c ----- depth of replaced section of column
λ ----- slenderness ratio of column
h ----- height of story
l ----- width of span
r ----- number of story of one block unit frame
n ----- number of bay of one block unit frame
δ_M ----- bending deformation of frame
δ_S ----- shearing deformation of frame
H ----- height of frame
P ----- lateral force at the top of frame
GA_F ----- shearing stiffness of frame
EI_F ----- bending stiffness of frame

§ 3 Assumptions, limitations, idealizations and parameters

1) Numerical analysis is carried out for the frame subjected to a lateral force at its top as shown in FIG 3-1 to know its fundamental behavior. Analyzed frames are of 5 and 10 story frames as one block unit, each have the same members as columns and the another same members as beams.

2) The column member section is replaced with a model as shown in FIG 3-2 so that it has the same moment inertia and the same sectional area with the actual section, as

$$I_c = A \cdot d_c^2/2 \qquad \text{----- (3-1)}$$

$${}_cA_n = 2 \cdot A \qquad \text{----- (3-2)}$$

3) Defining parameter γ as $\gamma = I_c/h^2$, we have

$$I_c = \gamma \cdot h^2 \qquad \text{----- (3-3)}$$

$${}_cA_n = 4 \cdot \gamma / q_c^2 \qquad \text{----- (3-4)}$$

where, q_c is introduced as $q_c = d_c/h$.

Considering that

$$q_c = \frac{2}{h}\sqrt{\frac{I_c}{{}_cA_n}} = \frac{2}{\lambda} \qquad \text{----- (3-5)}$$

and $\lambda = 20 \sim 25$ in recent frame design, the value of q_c is from 0.08 to 0.1. From this fact, 0.1 is adopted as the value of q_c in the analysis.

4) Letting $K_c = 1.0$, we have the value of K_0 as

$$K_0 = I_c/h = \gamma \cdot h \qquad \text{----- (3-6)}$$

Now, defining parameter α as $\alpha = I_B \cdot h/(I_c \cdot l)$, we have $K_B = \alpha$ and

$$I_B = \alpha \cdot \gamma \cdot h \cdot l \qquad \text{----- (3-7)}$$

5) The value of parameter γ is put to 1.0 in the analysis. Viewing Eqs.(3-3),(3-4),(3-6) and (3-7), we can know that this assumption influences only for the result concerning to the stiffness of frame which is to be corrected by being multiplied $1/\gamma$ to the direct result.

6) Parameter β is considered as $\beta = r/n$ to represent the slenderness of frame.

§ 4 Results of numerical analysis

1) To replace the F-frame* to a equivalent single chord member

From the corner column area $A_{eff.}$ equivalent to the F-frame calculated from the numerical ${}_RS$*, efficiency of inner column $r_A = (A_{eff.} - A_{con.})/A_{in.}$ is obtained, using the symbols of FIG 4-1. Efficiency r_A is represented as shown in FIG 4-2 by the parameters α, β and h/l. The numerical results obtained here are not enough to represent r_A by an approximate equation, however, we can know from FIG 4-2 that the value of r_A is influenced mainly by α and h/l.

If we can know the efficiency r_A of a frame, the equivalent corner column area is obtained as

$$A_{eff.} = A_{con.} + r_A \cdot A_{in.}$$

2) Vertical resistant forces between F-frame and W-frame*

Distribution of vertical resistant forces between F-frame and W-frame(this corresponds to the distribution of shearing stress of box-beam at its corner) got from the numerical analysis is shown typically in FIG 4-3. Now, the value of F_{mean}/P is shown in FIG 4-4-a,-b using the parameters α,β and h/l. From these figures, we can know that the value of F_{mean}/P is influenced mainly by β and h/l. F_{mean}/P is shown again using the parameters β and h/l in FIG 4-4-c.

3) Bending deformation of frame

The bending deformation δ_M and the shearing deformation δ_S of a cantilever as shown in FIG 3-1 the section of which is shown in FIG 4-1, are as follows by beam theory.

$$\delta_M = P \cdot H^3 / (3 \cdot EI_F) \quad , \quad \delta_S = P \cdot H / (GA_F) \qquad \text{----- (4-1)}$$

Now the bending deformation and the shearing deformation obtained in the numerical analysis are δ_M' and δ_S' respectively.

a) Efficiency of moment inertia

The actually efficient moment inertia being I_F', the ratio δ_M/δ_M' defines the efficiency of moment inertia $k'=I_F'/I_F$. The value of this efficiency k' is shown in FIG 4-5-a,-b using the parameters α,β and h/l. The value of k' being influenced mainly by β,h/l and r, this is again shown in FIG 4-5-c using β,h/l and r.

b) Ratio of the bending deformation to the shearing deformation

From Eq.(4-1) we have Eq.(4-2).

$$\delta_M/\delta_S/H^2 = (GA_F)/(3 \cdot EI_F) \qquad \text{----- (4-2)}$$

Because the right-side term of Eq.(4-2) is a specific quality of a section having the dimension of L^{-2}, the ratio $\delta_M'/\delta_S'/H^2$ obtained in the numerical analysis represent a dimensional ratio of the bending deformation to the shearing deformation. So the value $\delta_M'/\delta_S'/H^2$ is shown using the parameters α,β and h/l in FIG 4-6-a, -b.

4) Axial strain ratio of column

Axial strain ratios of the columns of the frame at the top of it(shown as "T") and at the base of it(shown as "B") are shown in FIG 4-7 and FIG 4-8 as to the F-frame and the W-frame respectively,using the parameters α,β and h/l and total story number of the frame r. It is to be noticed that the ratio of the W-frame at the base seems to be indifferent to the value of α.

* See APPENDIX.

Acknowledgements --- The writers acknowledge Mr.Igarashi and Mr. Kitamura of Fudo Construction Co. of their help for drawing.

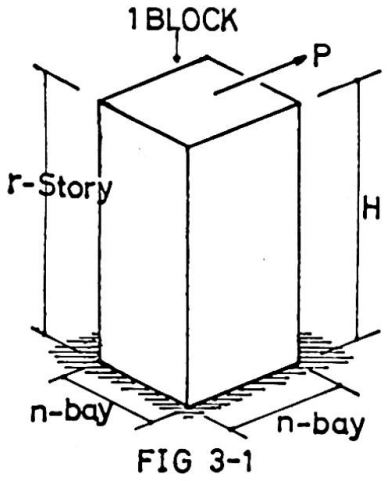

FIG 3-1

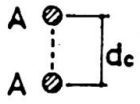

FIG 3-2

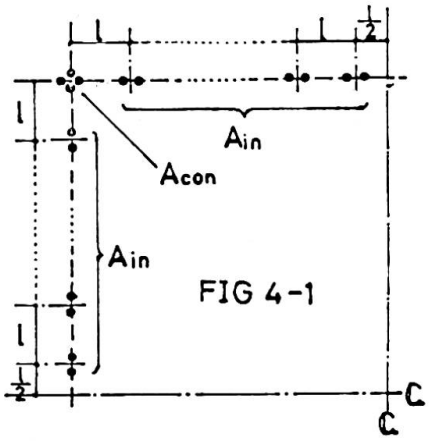

FIG 4-1

FIG 4-2 EFFICIENCY OF INNER COLUMN

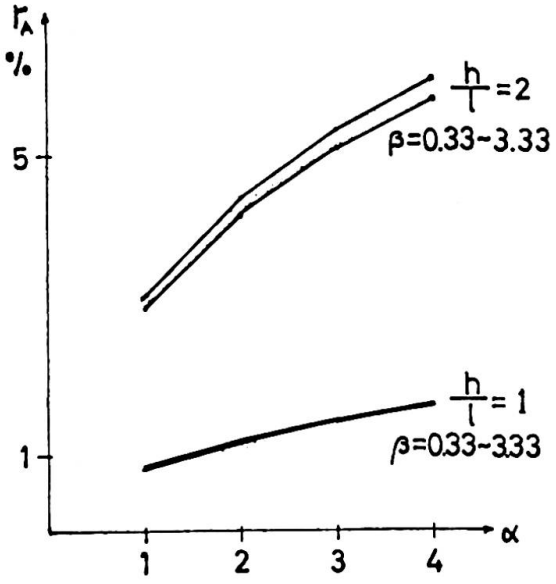

FIG 4-3

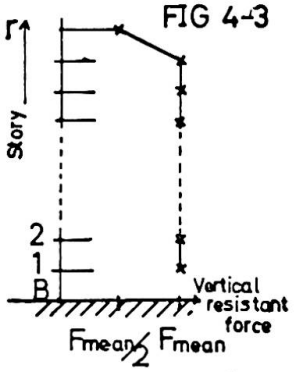

FIG 4-4-a

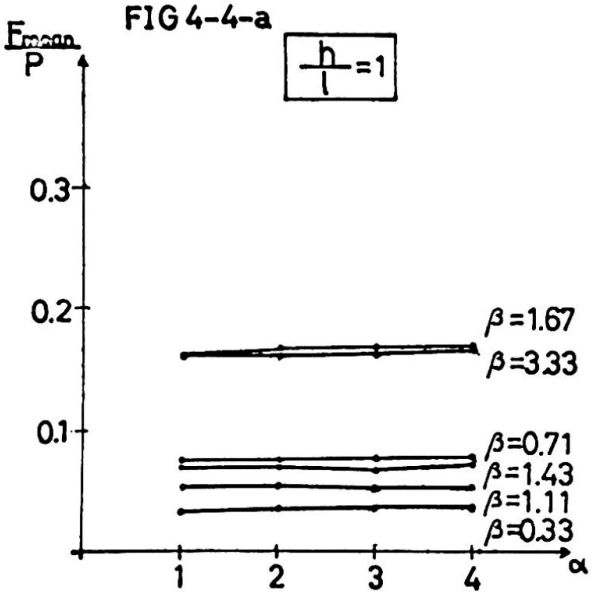

FIG 4-4-b

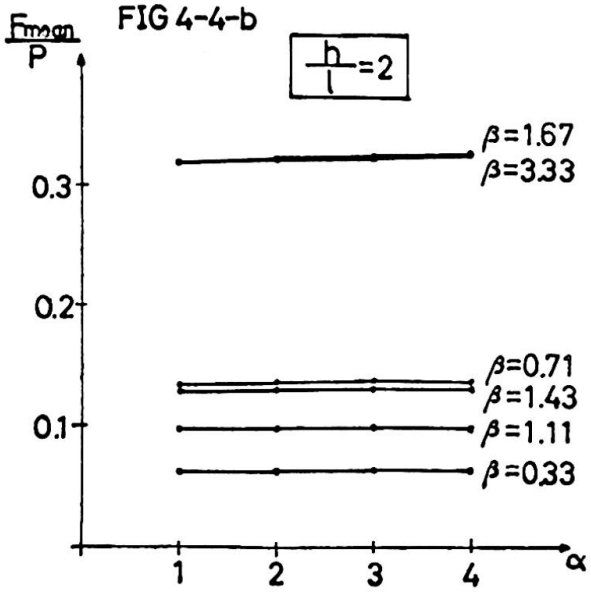

FIG 4-4-c

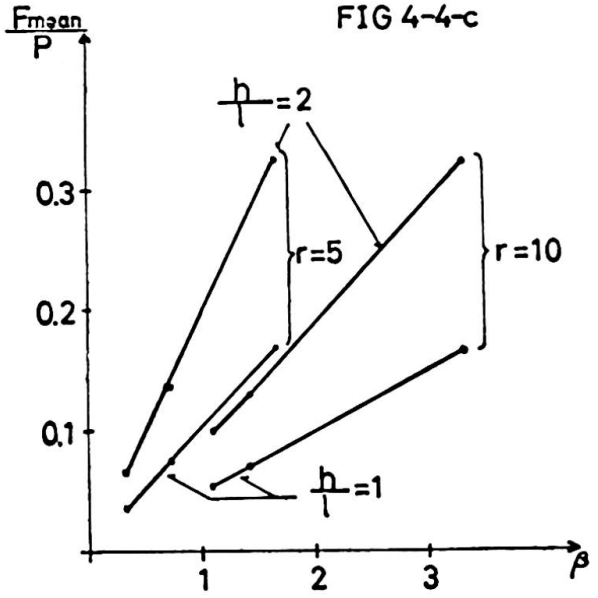

FIG 4-5-c

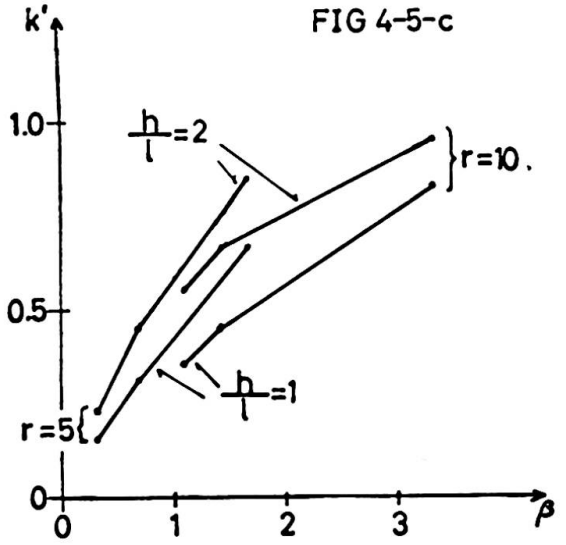

FIG 4-5-a

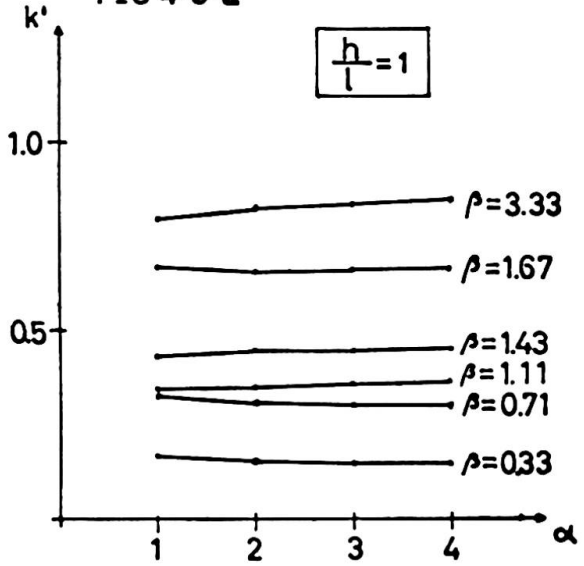

FIG 4-5-b

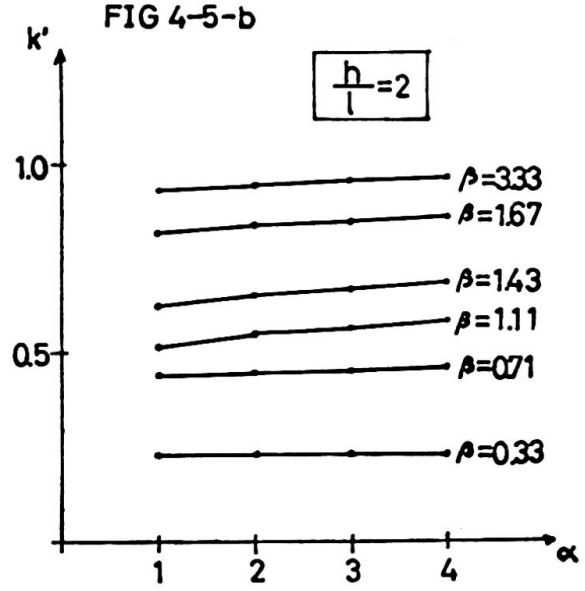

FIG 4-6-a

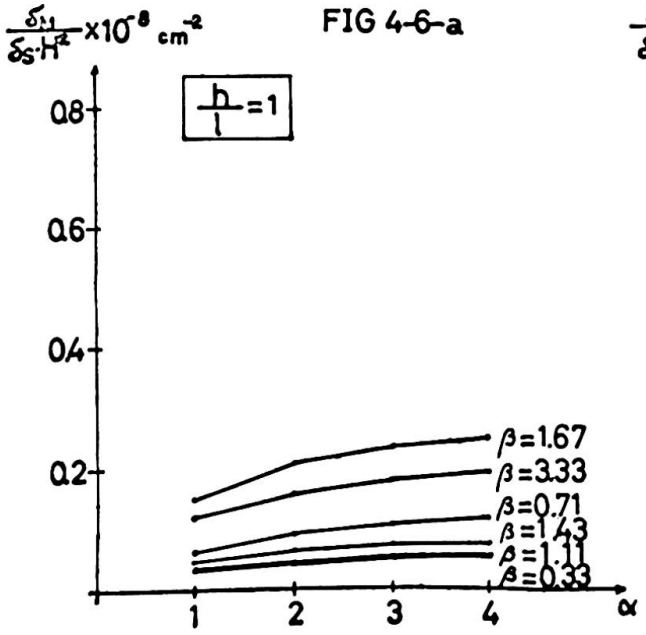

FIG 4-6-b

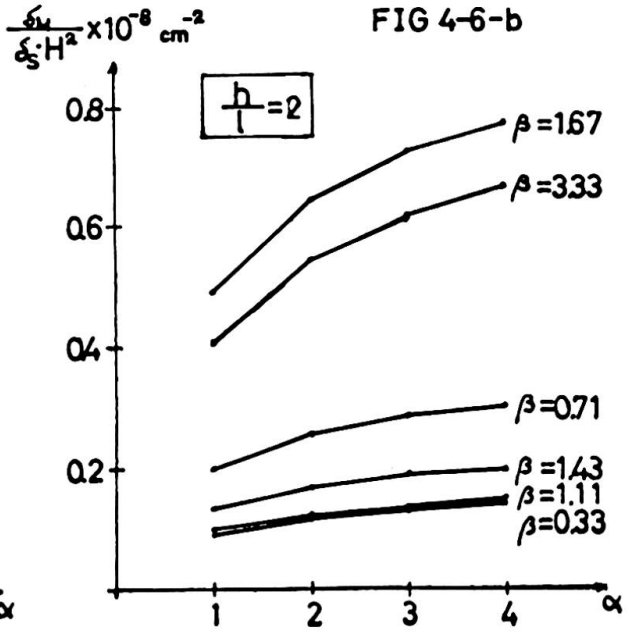

FIG 4-7 COLUMN AXIAL STRAIN RATIO OF W-FRAME

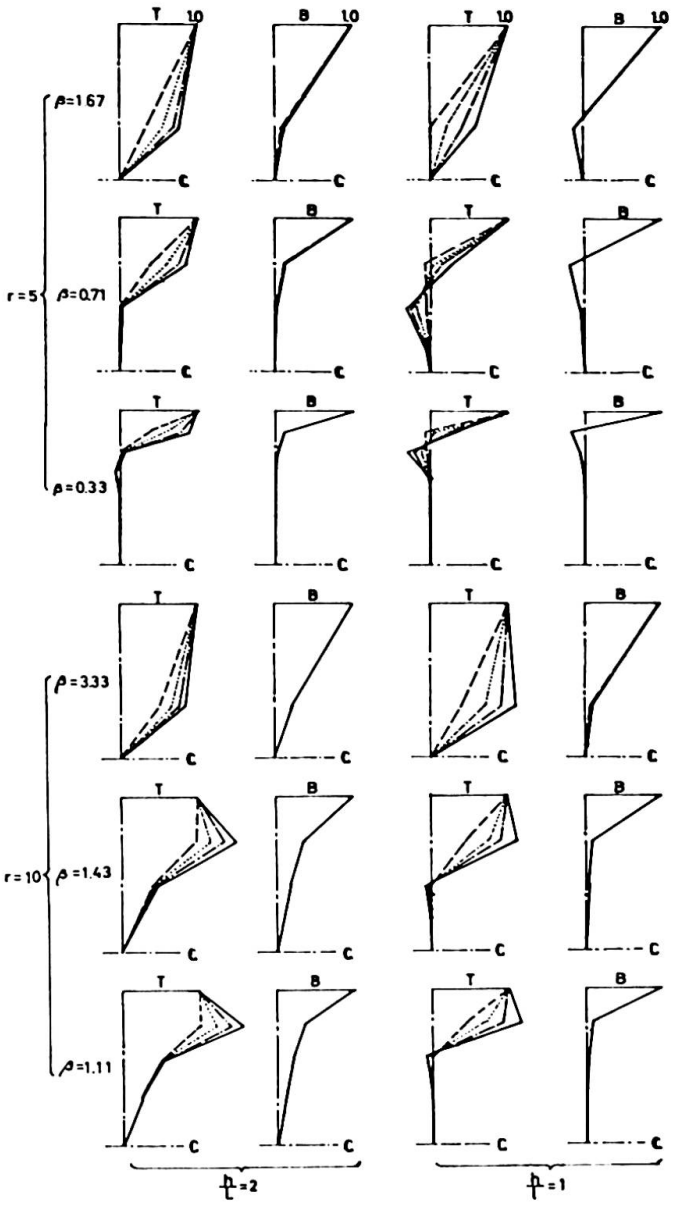

FIG 4-8 COLUMN AXIAL STRAIN RATIO OF F-FRAME

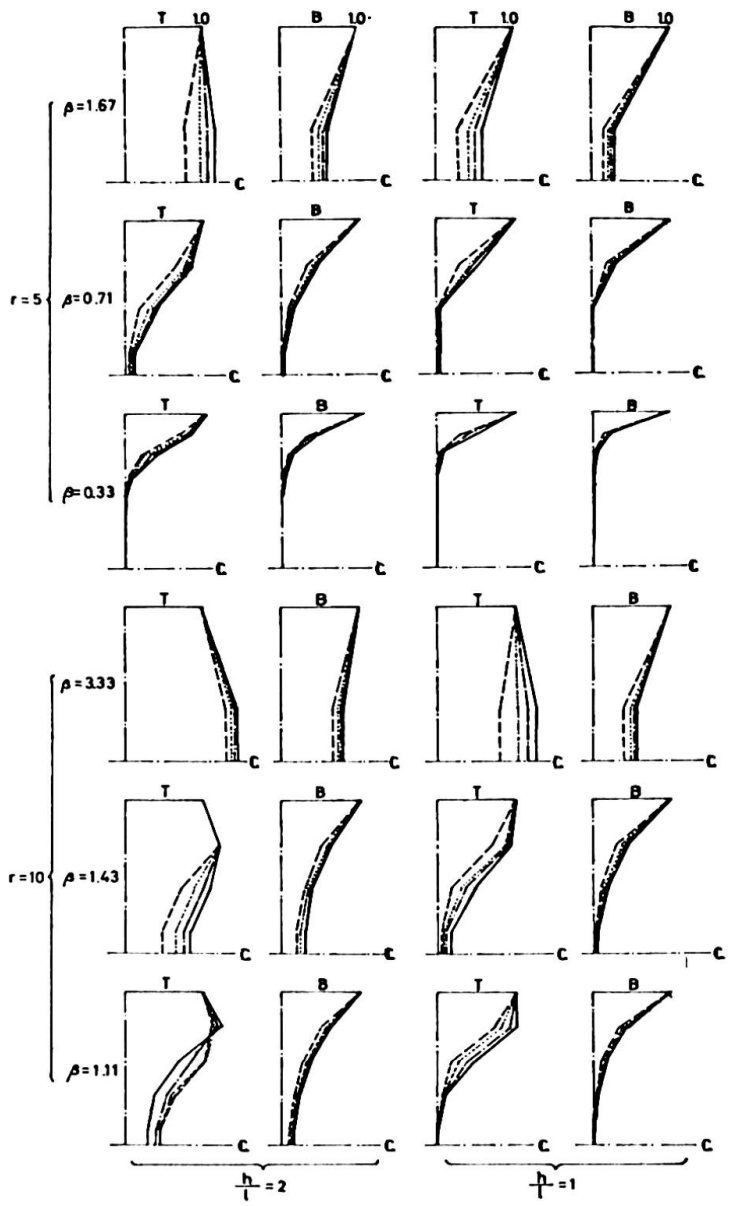

APPENDIX --- Method of Analysis ---

A-1 Introduction

The method of analysis mentioned hereafter is to analyze a box-type framing subjected to lateral force as shown in FIG A-1 that has its load carring members for lateral load at its outside only.

Assumptions are as follows.

(1) Consider the axial deformation of column and do not consider the axial deformation of beam.
(2) Do not consider the out-of-plane rigidity of the frame placed perpendicular to the lateral force(called "F-frame" hereafter).
(3) F-frame is to act upon the frame parallel to the lateral force(called "W-frame" hereafter) as a vertical spring complex connected to the W-frame at each story node.

Figures or equations are shown for the case that the F-frame and the W-frame either has a vertical line of symmetry for simplicity,however,the same method can be used with a slight change in the application of equations when no such line is exist.

A-2 Analysis of F-frame

F-frame is as shown in FIG A-2. The method to analyze the F-frame subjected to vertical force as shown in the same figure is explained in this section.

(a) Expression of end-moments

Using subscripts "k" and "i" to represent story-level and column-row respectively,dimensions around the k-story i-column node(called "node (k,i)" hereafter) are shown in FIG A-4. End-moments named as shown in FIG A-5 are expressed by the Eq.(A-1) using the simplifications of Eq.(A-2),where the sign of $G_{K,i}$ is fixed as shown in FIG A-6.

(b) Equation of moment equilibrium

Considering the equilibrium of moment around the center of (k,i) panel-zone,Eq.(A-3) is obtained.

(c) Equation of equilibrium of vertical force

Considering the equilibrium of vertical force at node (k,i), Eq.(A-4) is obtained.

(d) Deformation equation of panel-zone

From the condition of deformation of (k,i) panel-zone,next equation is derived.

$$\left\{\frac{1}{\alpha_{K,I}}\cdot\frac{E}{2(1+\nu)}\cdot TP_{K,i}\cdot HD_K\cdot SD_{K,I}\right\}\cdot G_{K,i}=M1_{K,i}+M3_{K,i}+RS2_{K,i}\cdot(M2_{K,I}+M4_{K,i-1})+RS1_{K,i+1}\cdot(M2_{K,i+1}+M4_{K,i})$$

where, $\alpha_{K,i}$ is a constant about the deformation of panel-zone and is put to unity when the beams and the columns around it have H-section.

Using Eqs.(A-3),(A-4) and (A-5),F-frame can be sufficiently analyzed.

To replace F-frame with a vertical spring complex,following two steps are taken.

1) Calculate the flexibility matrix ${}_R\mathbf{F}$ about the vertical force and displacement at the edge of F-frame,as

$${}^T\{D_1, D_2, \ldots\ldots, D_r\} = {}_R\mathbf{F}\cdot{}^T\{F_1, F_2, \ldots\ldots, F_r\}$$

2) Then,calculate the stiffness matrix ${}_R\mathbf{S}$ that represent the vertical spring complex,by inverting ${}_R\mathbf{F}$,as

$${}_R\mathbf{S}=({}_R\mathbf{F})^{-1}$$

A-3 Analysis of total frame

The method to analyze the total frame as the W-frame subjected to the lateral force and resisted by the vertical spring complex as shown in FIG A-3 is explained in this section.

Using the matrix ${}_R\mathbf{S}$, vertical resistant force F_k is represented by Eq.(A-6).

$$F_k = \sum_{j=1}^{r} {}_R S_{k,j} \cdot D_j \qquad \text{----- (A-6)}$$

(a) Expression of end-moments

Eq.(A-1) is used.

(b) Equation of moment equilibrium

Eq.(A-3) is used.

(c) Equation of equilibrium of vertical force

Eq.(A-4) is used generally. For i=1, Eq.(A-7) is used in place of Eq.(A-4), considering Eq.(A-6).

$$(-3 \cdot BK_{k,i+1} \cdot h_0 / S_{i+1}) \cdot T_{k,i} + (-3 \cdot BK_{k,i+1} \cdot h_0 / S_{i+1}) \cdot T_{k,i+1} + \{6 \cdot BK_{k,i+1} \cdot (h_0 / S_{i+1})^2 + 0.5 \cdot h_0^2 \cdot {}_R S_{k,k} / E / K_0\} \cdot Y_{k,i} - 6 \cdot BK_{k,i+1} \cdot (h_0 / S_{i+1})^2 \cdot Y_{k,i+1} + \sum_{j \neq k} (0.5 \cdot h_0^2 \cdot {}_R S_{k,j} / E / K_0) \cdot Y_{j,i} = 0 \qquad \text{----- (A-7)}$$

(d) Deformation equation of panel-zone

Eq.(A-5) is used.

(e) Equation of equilibrium of lateral force

Considering the equilibrium of lateral force at story k, Eq.(A-8) is obtained.

Using Eqs.(A-3),(A-4),(A-5),(A-7) and (A-8), total frame can be fully analyzed.

****

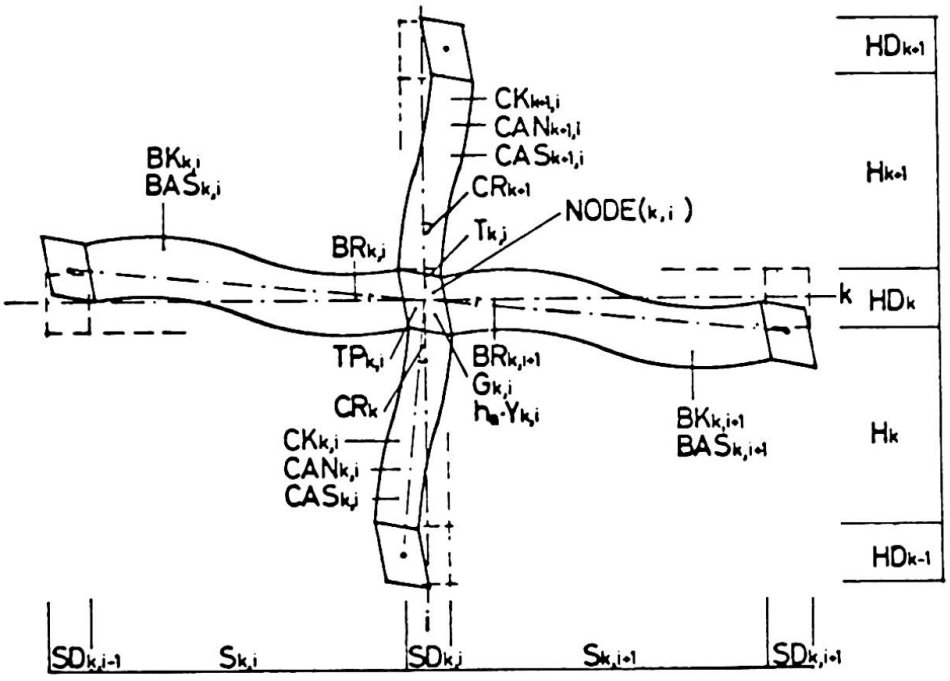

FIG A-4

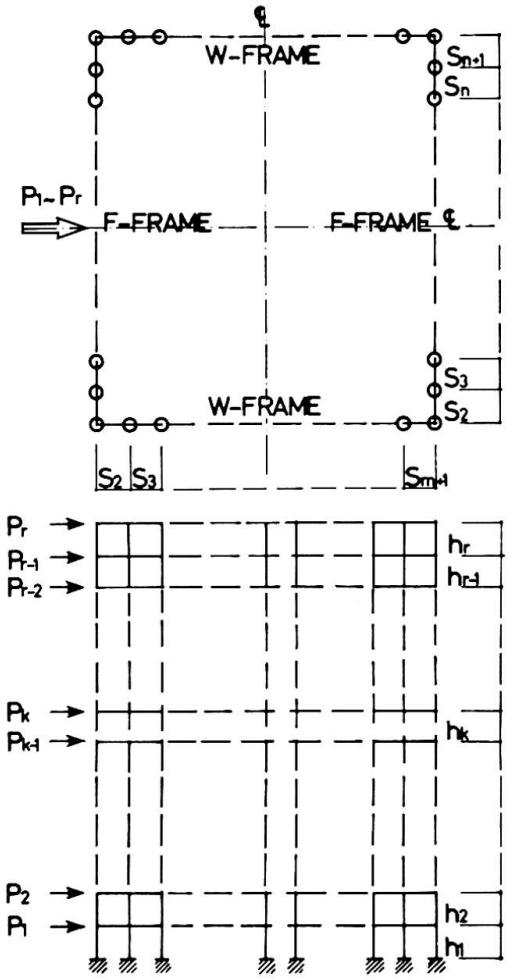

FIG.A-1

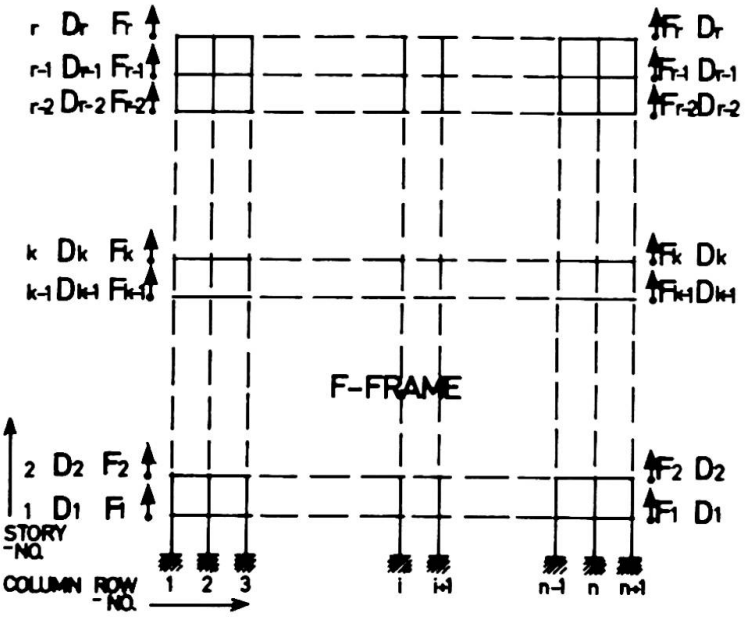

FIG.A-2

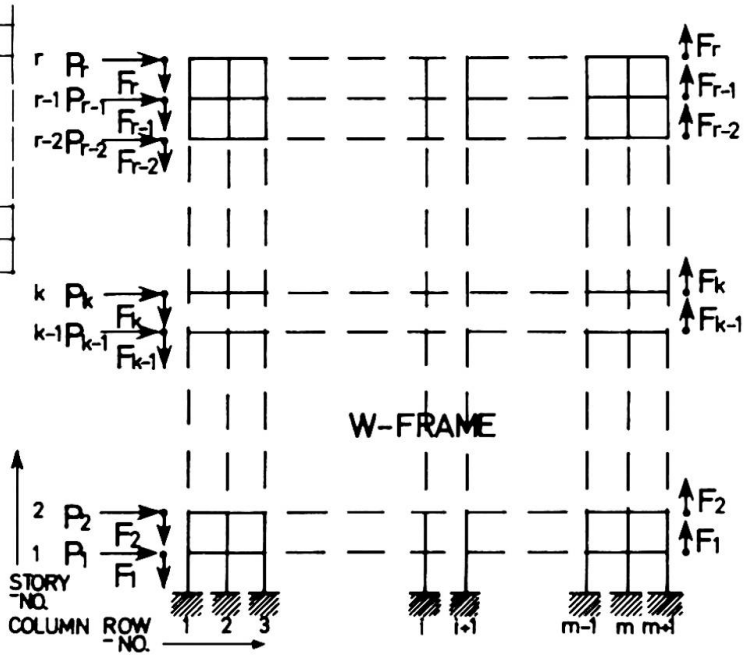

FIG.A-3

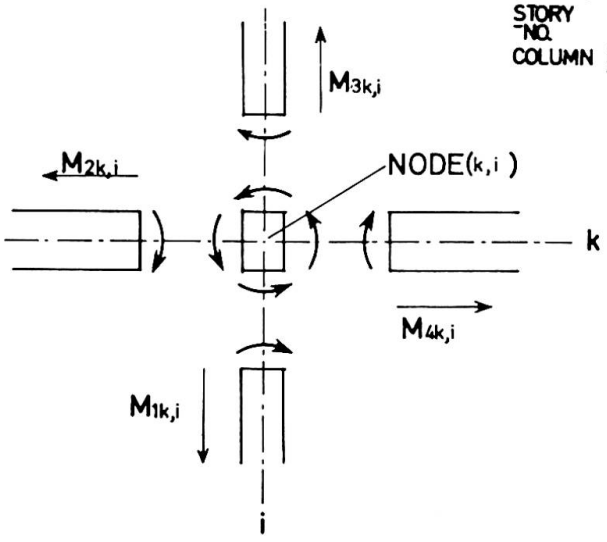

FIG.A-5

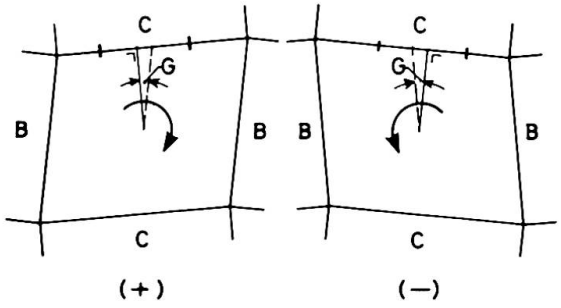

FIG.A-6

$$T\left[\frac{M1_{k,i}}{CK_{k,i}}\;\middle|\;\frac{M2_{k,i}}{BK_{k,i}}\;\middle|\;\frac{M3_{k,i}}{CK_{k+1,i}}\;\middle|\;\frac{M4_{k,i}}{BK_{k,i+1}}\right]$$

$$= 2\cdot E\cdot K_0 \cdot \left[\begin{array}{ccccccccccccccc}
CA_{k,i} & CB_{k,i} & & & & CC_{k,i} & CC_{k,i} & & & & & & & -CC_{k,i} & 0 \\
+CC_{k,i} & +CC_{k,i} & 0 & 0 & 0 & \times RH2_k & \times RH1_k & 0 & 0 & 0 & 0 & 0 & 0 & \times(1+RH1_k+RH2_k) & \\
\times RH2_k & \times RH1_k & & & & & & & & & & & & & \\
\hline
BA_{k,i} & & BB_{k,i} & & & & & & & & & & & & \\
+BC_{k,i} & 0 & +BC_{k,i} & 0 & 0 & BA_{k,i} & 0 & BB_{k,i} & 0 & 0 & BC_{k,i} & -BC_{k,i} & 0 & 0 & 0 \\
\times RS2_{k,i} & & \times RS1_{k,i} & & & & & & & & \times h_0/S_{k,i} & \times h_0/S_{k,i} & & & \\
\hline
CA_{k+1,i} & & & CB_{k+1,i} & & CC_{k+1,i} & & & CC_{k+1,i} & & & & & & -CC_{k+1,i} \\
+CC_{k+1,i} & 0 & 0 & +CC_{k+1,i} & 0 & & 0 & 0 & & 0 & 0 & 0 & 0 & 0 & \\
\times RH1_{k+1} & & & \times RH2_{k+1} & & \times RH1_{k+1} & & & \times RH2_{k+1} & & & & & \times(1+RH1_{k+1}+RH2_{k+1}) & \\
\hline
BA_{k,i+1} & & & & BB_{k,i+1} & & & & & & -BC_{k,i+1} & & BC_{k,i+1} & & \\
+BC_{k,i+1} & 0 & 0 & 0 & +BC_{k,i+1} & BA_{k,i+1} & 0 & 0 & 0 & BB_{k,i+1} & & 0 & & 0 & 0 \\
\times RS1_{k,i+1} & & & & \times RS2_{k,i+1} & & & & & & \times h_0/S_{k,i+1} & & \times h_0/S_{k,i+1} & &
\end{array}\right]$$

$$\times\; T\left[\begin{array}{ccccc|ccccc|ccccc}
T_{k,i} & T_{k-1,i} & T_{k,i-1} & T_{k+1,i} & T_{k,i+1} & G_{k,i} & G_{k-1,i} & G_{k,i-1} & G_{k+1,i} & G_{k,i+1} & Y_{k,i} & Y_{k,i-1} & Y_{k,i+1} & CR_k & CR_{k+1}
\end{array}\right] \qquad \text{-------(A-1)}$$

$$\left.\begin{array}{llll}
RH1_k = \dfrac{HD_{k-1}}{2\cdot H_k} & CA_{k,i} = CY_{k,i} + 0.5 & BA_{k,i} = BY_{k,i} + 0.5 \\
RH2_k = \dfrac{HD_k}{2\cdot H_k} & CB_{k,i} = CY_{k,i} - 0.5 & BB_{k,i} = BY_{k,i} - 0.5 \\
RS1_{k,i} = \dfrac{SD_{k,i-1}}{2\cdot S_{k,i}} & CC_{k,i} = 2\cdot CY_{k,i} & BC_{k,i} = 2\cdot BY_{k,i} \\
RS2_{k,i} = \dfrac{SD_{k,i}}{2\cdot S_{k,i}} & CY_{k,i} = \dfrac{1.5}{1+\frac{24(1+\nu)\cdot K_0\cdot CK_{k,i}}{CAS_{k,i}\cdot H_k}} & BY_{k,i} = \dfrac{1.5}{1+\frac{24(1+\nu)\cdot K_0\cdot BK_{k,i}}{BAS_{k,i}\cdot S_{k,i}}}
\end{array}\right\} \text{---(A-2)}$$

EQUILIBRIUM OF MOMENT AT NODE (k, i)

V.	C.
$T_{k,i}$	$0.5\cdot CK_{k,i}\cdot\{1+(1+2\cdot RH2_k)^2\cdot CC_{k,i}\} + 0.5\cdot CK_{k+1,i}\cdot\{1+(1+2\cdot RH1_{k+1})^2\cdot CC_{k+1,i}\}$ $+0.5\cdot BK_{k,i}\cdot\{1+(1+2\cdot RS2_{k,i})^2\cdot BC_{k,i}\} + 0.5\cdot BK_{k,i+1}\cdot\{1+(1+2\cdot RS1_{k,i+1})^2\cdot BC_{k,i+1}\}$
$T_{k-1,i}$	$0.5\cdot CK_{k,i}\cdot\{(1+2\cdot RH2_k)\cdot(1+2\cdot RH1_k)\cdot CC_{k,i}-1\}$
$T_{k,i-1}$	$0.5\cdot BK_{k,i}\cdot\{(1+2\cdot RS2_{k,i})\cdot(1+2\cdot RS1_{k,i})\cdot BC_{k,i}-1\}$
$T_{k+1,i}$	$0.5\cdot CK_{k+1,i}\cdot\{(1+2\cdot RH1_{k+1})\cdot(1+2\cdot RH2_{k+1})\cdot CC_{k+1,i}-1\}$
$T_{k,i+1}$	$0.5\cdot BK_{k,i+1}\cdot\{(1+2\cdot RS1_{k,i+1})\cdot(1+2\cdot RS2_{k,i+1})\cdot BC_{k,i+1}-1\}$
$G_{k,i}$	$CK_{k,i}\cdot(1+2\cdot RH2_k)\cdot RH2_k\cdot CC_{k,i} + CK_{k+1,i}\cdot(1+2\cdot RH1_{k+1})\cdot RH1_{k+1}\cdot CC_{k+1,i}$ $+0.5\cdot BK_{k,i}\cdot\{(1+2\cdot RS2_{k,i})\cdot BC_{k,i}+1\} + 0.5\cdot BK_{k,i+1}\cdot\{(1+2\cdot RS1_{k,i+1})\cdot BC_{k,i+1}+1\}$
$G_{k-1,i}$	$CK_{k,i}\cdot(1+2\cdot RH2_k)\cdot RH1_k\cdot CC_{k,i}$
$G_{k,i-1}$	$0.5\cdot BK_{k,i}\cdot\{(1+2\cdot RS2_{k,i})\cdot BC_{k,i}-1\}$
$G_{k+1,i}$	$CK_{k+1,i}\cdot(1+2\cdot RH1_{k+1})\cdot RH2_{k+1}\cdot CC_{k+1,i}$
$G_{k,i+1}$	$0.5\cdot BK_{k,i+1}\cdot\{(1+2\cdot RS1_{k,i+1})\cdot BC_{k,i+1}-1\}$
$Y_{k,i}$	$BK_{k,i}\cdot(1+2\cdot RS2_{k,i})\cdot BC_{k,i}\cdot h_0/S_{k,i} - BK_{k,i+1}\cdot(1+2\cdot RS1_{k,i+1})\cdot BC_{k,i+1}\cdot h_0/S_{k,i+1}$
$Y_{k,i-1}$	$-BK_{k,i}\cdot(1+2\cdot RS2_{k,i})\cdot BC_{k,i}\cdot h_0/S_{k,i}$
$Y_{k,i+1}$	$BK_{k,i+1}\cdot(1+2\cdot RS1_{k,i+1})\cdot BC_{k,i+1}\cdot h_0/S_{k,i+1}$
CR_k	$-CK_{k,i}\cdot(1+2\cdot RH2_k)(1+RH1_k+RH2_k)\cdot CC_{k,i}$
CR_{k+1}	$-CK_{k+1,i}\cdot(1+2\cdot RH1_{k+1})(1+RH1_{k+1}+RH2_{k+1})\cdot CC_{k+1,i}$

$$\Sigma(V.)\times(C.)=0 \qquad (A\text{-}3)$$

EQUILIBRIUM OF VERTICAL FORCE AT NODE(k,i)

V.	C.
$T_{k,i}$	$BK_{k,i}\cdot(1+2\cdot RS2_{k,i})\cdot BC_{k,i}\cdot h_0/S_{k,i} - BK_{k,i+1}\cdot(1+2\cdot RS1_{k,i+1})\cdot BC_{k,i+1}\cdot h_0/S_{k,i+1}$
$T_{k,i-1}$	$BK_{k,i}\cdot(1+2\cdot RS1_{k,i})\cdot BC_{k,i}\cdot h_0/S_{k,i}$
$T_{k,i+1}$	$-BK_{k,i+1}\cdot(1+2\cdot RS2_{k,i+1})\cdot BC_{k,i+1}\cdot h_0/S_{k,i+1}$
$G_{k,i}$	$BK_{k,i}\cdot BC_{k,i}\cdot h_0/S_{k,i} - BK_{k,i+1}\cdot BC_{k,i+1}\cdot h_0/S_{k,i+1}$
$G_{k,i-1}$	$BK_{k,i}\cdot BC_{k,i}\cdot h_0/S_{k,i}$
$G_{k,i+1}$	$-BK_{k,i+1}\cdot BC_{k,i+1}\cdot h_0/S_{k,i+1}$
$Y_{k,i}$	$0.5\cdot CAN_{k,i}\cdot h_0^2/K_0/HC_k + 0.5\cdot CAN_{k+1,i}\cdot h_0^2/K_0/HC_{k+1}$ $+2\cdot BK_{k,i}\cdot BC_{k,i}\cdot(h_0/S_{k,i})^2 + 2\cdot BK_{k,i+1}\cdot BC_{k,i+1}\cdot(h_0/S_{k,i+1})^2$
$Y_{k-1,i}$	$-0.5\cdot CAN_{k,i}\cdot h_0^2/K_0/HC_k$
$Y_{k,i-1}$	$-2\cdot BK_{k,i}\cdot BC_{k,i}\cdot(h_0/S_{k,i})^2$
$Y_{k+1,i}$	$-0.5\cdot CAN_{k+1,i}\cdot h_0^2/K_0/HC_{k+1}$
$Y_{k,i+1}$	$-2\cdot BK_{k,i+1}\cdot BC_{k,i+1}\cdot(h_0/S_{k,i+1})^2$

$* \; HC_k = 0.5\cdot(HD_k + HD_{k-1}) + H_k \; *$

$$\sum (V.)\times(C.) = \frac{h_0}{2\cdot E\cdot K_0} F_{k,i} \qquad \text{---------(A-4)}$$

DEFORMATION EQUATION OF PANEL ZONE

V.	C.
$T_{k,i}$	$0.5\cdot CK_{k,i}\cdot\{(1+2\cdot RH2_k)\cdot CC_{k,i}+1\} + 0.5\cdot CK_{k+1,i}\cdot\{(1+2\cdot RH1_{k+1})\cdot CC_{k+1,i}+1\}$ $+BK_{k,i}\cdot(1+2\cdot RS2_{k,i})\cdot RS2_{k,i}\cdot BC_{k,i} + BK_{k,i+1}\cdot(1+2\cdot RS1_{k,i+1})\cdot RS1_{k,i+1}\cdot BC_{k,i+1}$
$T_{k-1,i}$	$0.5\cdot CK_{k,i}\cdot\{(1+2\cdot RH1_k)\cdot CC_{k,i}-1\}$
$T_{k,i-1}$	$BK_{k,i}\cdot(1+2\cdot RS1_{k,i})\cdot RS2_{k,i}\cdot BC_{k,i}$
$T_{k+1,i}$	$0.5\cdot CK_{k+1,i}\cdot\{(1+2\cdot RH2_{k+1})\cdot CC_{k+1,i}-1\}$
$T_{k,i+1}$	$BK_{k,i+1}\cdot(1+2\cdot RS2_{k,i+1})\cdot RS1_{k,i+1}\cdot BC_{k,i+1}$
$G_{k,i}$	$CK_{k,i}\cdot RH2_k\cdot CC_{k,i} + CK_{k+1,i}\cdot RH1_{k+1}\cdot CC_{k+1,i}$ $+BK_{k,i}\cdot RS2_{k,i}\cdot BC_{k,i} + BK_{k,i+1}\cdot RS1_{k,i+1}\cdot BC_{k,i+1} - 0.25\cdot TP_{k,i}\cdot HD_k\cdot SD_{k,i}/(1+\nu)/K_0/\alpha_{k,i}$
$G_{k-1,i}$	$CK_{k,i}\cdot RH1_k\cdot CC_{k,i}$
$G_{k,i-1}$	$BK_{k,i}\cdot RS2_{k,i}\cdot BC_{k,i}$
$G_{k+1,i}$	$CK_{k+1,i}\cdot RH2_{k+1}\cdot CC_{k+1,i}$
$G_{k,i+1}$	$BK_{k,i+1}\cdot RS1_{k,i+1}\cdot BC_{k,i+1}$
$Y_{k,i}$	$2\cdot BK_{k,i}\cdot RS2_{k,i}\cdot BC_{k,i}\cdot h_0/S_{k,i} - 2\cdot BK_{k,i+1}\cdot RS1_{k,i+1}\cdot BC_{k,i+1}\cdot h_0/S_{k,i+1}$
$Y_{k,i-1}$	$-2\cdot BK_{k,i}\cdot RS2_{k,i}\cdot BC_{k,i}\cdot h_0/S_{k,i}$
$Y_{k,i+1}$	$2\cdot BK_{k,i+1}\cdot RS1_{k,i+1}\cdot BC_{k,i+1}\cdot h_0/S_{k,i+1}$
CR_k	$-CK_{k,i}\cdot(1+RH1_k+RH2_k)\cdot CC_{k,i}$
CR_{k+1}	$-CK_{k+1,i}\cdot(1+RH1_{k+1}+RH2_{k+1})\cdot CC_{k+1,i}$

$$\sum (V.)\times(C.) = 0 \qquad \text{---------} \quad (A\text{-}5)$$

*** TABLE OF SYMBOLS ***

P_K ----- lateral force
F_K ----- vertical force at the edge of F,W-frame
D_K ----- vertical displacement at the edge of F,W-frame
$M1_{K,i}$ ----- end-moment of column
$M2_{K,i}$ ----- end-moment of beam
$M3_{K,i}$ ----- end-moment of column
$M4_{K,i}$ ----- end-moment of beam
H_K ----- length of column
HD_K ----- depth of beam
HC_K ----- height of story
$S_{K,i}$ ----- length of beam
$SD_{K,i}$ ----- depth of column
$CK_{K,i}$ ----- rigidity ratio of column
$BK_{K,i}$ ----- rigidity ratio of beam
$CAS_{K,i}$ ----- area efficient for shear deformation of column
$BAS_{K,i}$ ----- area efficient for shear deformation of beam
$CAN_{K,i}$ ----- sectional area of column
$TP_{K,i}$ ----- thickness of panel-zone
$T_{K,i}$ ----- rotation of panel-zone at column side
$G_{K,i}$ ----- shear strain of panel-zone
$Y_{K,i}$ ----- ratio of vertical displacement of node to h_0
CR_K ----- chord rotation of story
$BR_{K,i}$ ----- chord rotation of beam
h_0 ----- standard height of story
K_0 ----- standard rigidity
E ----- modulus of elasticity
ν ----- Poisson's ratio
$\alpha_{K,i}$ ----- shear deformation constant of panel-zone

****

EQUILIBRIUM OF LATERAL FORCE AT STORY k

V.	C
$T_{k,i}$	$CK_{k,i}\cdot(1+2\cdot RH2_k)\cdot CC_{k,i}$
$T_{k-1,i}$	$CK_{k,i}\cdot(1+2\cdot RH2_k)\cdot CC_{k,i}$
$G_{k,i}$	$2\cdot CK_{k,i}\cdot RH2_k\cdot CC_{k,i}$
$G_{k-1,i}$	$2\cdot CK_{k,i}\cdot RH1_k\cdot CC_{k,i}$
R_k	$-2\cdot(1+RH1_k+RH2_k)\cdot\sum_i CK_{k,i}\cdot CC_{k,i}$

$$\sum(V.)\times(C.) = -\frac{H_k}{2EK_0}\sum_k' P_k \quad \text{-----(A-8)}$$

SUMMARY

The possibility to represent by some parameters the elastic behavior of box-type framing subjected to lateral force is investigated. As parameters of this purpose, α, β, γ, h/l and r seem to be sufficient from the result of § 4.

The number and variety of sample frames taken in the numerical analysis are not sufficient to represent the elastic behavior by some approximate equations using these parameters, however, the orientation to do so is now clear and some criteria for preliminary design can be found in the figures of §4.

RÉSUMÉ

On a étudié la possibilité de représenter par quelques paramètres le comportement élastique de portiques en caisson soumis à des forces latérales. Comme le montre § 4, les paramètres α, β, γ, h/l et r sont suffisants pour ce propos.

Le nombre et la diversité restraints des exemples de portiques considérés dans l'analyse numérique ne permettent pas de représenter le comportement élastique par quelques équations approximatives entre ces paramètres, cependant on voit clairement le chemin à suivre pour ce faire, en outre les figures de § 4 faciliteront un dimensionnement préliminaire.

ZUSAMMENFASSUNG

Es wird die Möglichkeit untersucht, das elastische Verhalten kastenförmiger Rahmentragwerke mit einigen Beiwerten zu beschreiben, falls dieses seitlichen Kräften unterworfen ist. Es scheint, dass für dieses Unterfangen die Parameter α, β, γ, h/l und r den Ergebnissen von § 4 genügen. Die Zahl und die Veränderlichkeit der durch die numerische Rechnung geprüften Rahmen sind für die Darstellung des elastischen Verhaltens durch angenäherte, obige Beiwerte verwendende Gleichungen ungenügend; trotzdem ist die zu verfolgende Richtung bekannt und für die Vorbemessung können einige Charakteristiken aus den Figuren des § 4 entnommen werden.

Leere Seite
Blank page
Page vide

III c

Résistance aux actions dynamiques du vent et des séismes

Dynamisches Verhalten bei Wind und Erdbeben

Dynamic Effects of Wind and Earthquake

Leere Seite
Blank page
Page vide

DISCUSSION PRÉPARÉE / VORBEREITETE DISKUSSION / PREPARED DISCUSSION

Specifications on Multi-Story Buildings and in Particular on Steel Structures in Seismic

Recommandations pour le calcul des bâtiments à plusieurs étages en zone sismique avec référence spéciale aux constructions en acier

Empfehlungen für mehrstöckige Gebäude, insbesondere für Stahltragwerke in Erdbebengebieten

ELIO GIANGRECO
Italy

The Convention of European Constructional Steelwork Associations has appointed a special Commission for compiling the "Recommenda - tions" for the design of steel structures in seismic area.Such Commission, known as Commission XIII, has begun his works in 1965 and in a first stage has accurately studied all international standards on the argument by making comparison and analysing those parts that the different recommendations have in cpmmon.

On the basic of the aquired knowledges and taking into account the most recent standards, the Commission has outlined a text of recommendations with comments where the general principles of the standards have been explained and some particular cases have been treated. Numerical coefficients have also been given. The Commission has decided that buildings in seismic area can be designed only if the equivalent static forces proportional to the masses in motion through a suitable seismic coefficient are introduced.Such coefficient has been fixed on the basis of the most recent studies of seismic engineering based on the spectral analysis of earthquakes and has been considered as the product of four elementary factors: the intensity seismic factor, the foundation factor, the response factor and the masses distribution factor.

The influence of each factor has been pointed out both from a qualitative and a quantitative point of view by introducing suitable schemes and simplified formulations.

In the text have also been treated the problems of torsional actions due to seismic motions as well as the stresses due to vertical actions.

Studies for preparing a further chapter on the efficiency of connections between members both of the up structure and of the foundation structure are going on. In examining the factors which define the seismic factor the Commission has paid a particular at

tention to the evaluation of the response coefficient of the structures. As it is known this coefficient depends on the natural period of vibration of the structure as it is shown by the spectral analysis of the earthquakes.

In the following it has been reported on some researches carried out for the evaluation of the natural period of vibration of buildings.

- Period of vibration of framed structures

Because of the difficulties of evaluating the natural period of vibration, simplified formulations have been suggested by some Authors which relate the period T to the number of floors of a building, and sometimes to its geometric and elastic characteristics.

Among the most widely used formulae, the following ones may be listed:

$$T = 0,1\ n,$$

and:

$$T = \frac{0,05}{\sqrt{D}}\ H$$

which are respectively used by S.E.A.O.C. standards for framed structures and structures with stiffening walls.

In the formulae above, n represents the number of floors, and H and D respectively the height and the transversal dimension of the building in feet.

It is worth writing also the formula suggested by Ifrim for plane frames:

$$T = \frac{2\pi}{\xi}\sqrt{\frac{M_o\ l_o^3}{E\ J_o}} \qquad (1)$$

where M_o, l_o and J_o are spectively the base mass lenght and moment of inertia, E the elastic modulus of the material and ξ a parameter which depends on the number of floors and columns as well as on the masses and stiffnesses distribution on the height.

In order to check the validity of the proposed formulations some studies on the argument have been carried out in the "Istituto di Tecnica delle Costruzioni" of the University of Naples.

Firstly plane structures with or without windbracing have been considered; secondly a dynamic analysis of three dimensional frames has been undertaken.

1) - Plane structures

For plane structures a sistematic theoretic study has been carried out by releasing all simplifying hypothesis formulated in the papers dealing with the argument. In fact either the possibility of joints to rotate and the inertial forces acting on each beam have been taken into account. The latter circumstance requires an iterative process if the elastic characteristics vary with the period of vibration.

If a value of the lowest frequency is fixed (in particular it has been assumed the value corresponding to infinitely rigid beams and weightless columns hypothesis) it is possible to calculate the functions rectifying the elastic characteristics of all rods. Next

a unit displacement is given to all the joints of the structure, one per time, and the structure is solved each time. Then the matrix of the reactions of fictitious supports is obtained.

As it is known the n eigenvalues are proportional to the n squares of natural vibration of the structure. Comparing the lowest of the eigen values with the one fixed, a new iteration process can be carried out assuming the new frequency as starting value.

The investigation has been extended to frames with a number of floors ranging from 2 and 24, and with a number of spans m between 1 and 14.

In a first stage frames with fixed joints and without windbracing have been considered; then the analysis for braced structures has been formulated. With regard to common frames the fundamental period of vibration depends obviously on the number of floors and spans as well as on the variation law of moments of inertia on the height of the frame, on the inertia of beams and on the mass of all rods. The analysis of design characteristics of several steel buildings has suggested some variation laws of the cross section of columns with the height and consequently of their masses. With regard to beams the variation of their moment of inertia with the height does not seem to seriously influence the value of the period of vibration.

Using the Computer it has been possible to calculate the frequencies of vibration of a large number of frames whose geometric characteristics range as stated before. Besides it has been tried to find a variation law of the unknown parameter as function of the data.

With regard to unbraced frames the following expression has been obtained for the period of vibration:

$$T = 2\pi l_o^2 \sqrt{\frac{\mu_o}{E\ J_n}}\ T' \qquad (2)$$

where l_0 is average height of columns, J_n the moment of inertia of the columns of the last floor, μ_o the distributed mass of the beam.

The quantity T' given by graphs on fig. 1 and 2 for 1 and 14 spanned frames respectively, can be expressed by:

$$T' = 0{,}31 + f(\alpha)\ n - \frac{1{,}3\ m^3}{10^m}$$

where n is the number of floors, m the number of spans and $f(\alpha)$ is related to the variation law of moments of inertia of columns with the height of the frame through the expression:

$$\frac{J_i}{J_n} = \alpha\ (n-i) + 1 \qquad (3)$$

Obviously if the behaviour of the J_i/J_n is not linear a suitable value for α has to be chosen which is able to better approximate the exact curve. Function $f(\alpha)$ is shown in fig.3.

With regard to the variation laws of moments of inertia 3 and 4 in fig. 1 and 2 some comparison have been made with the formula sug

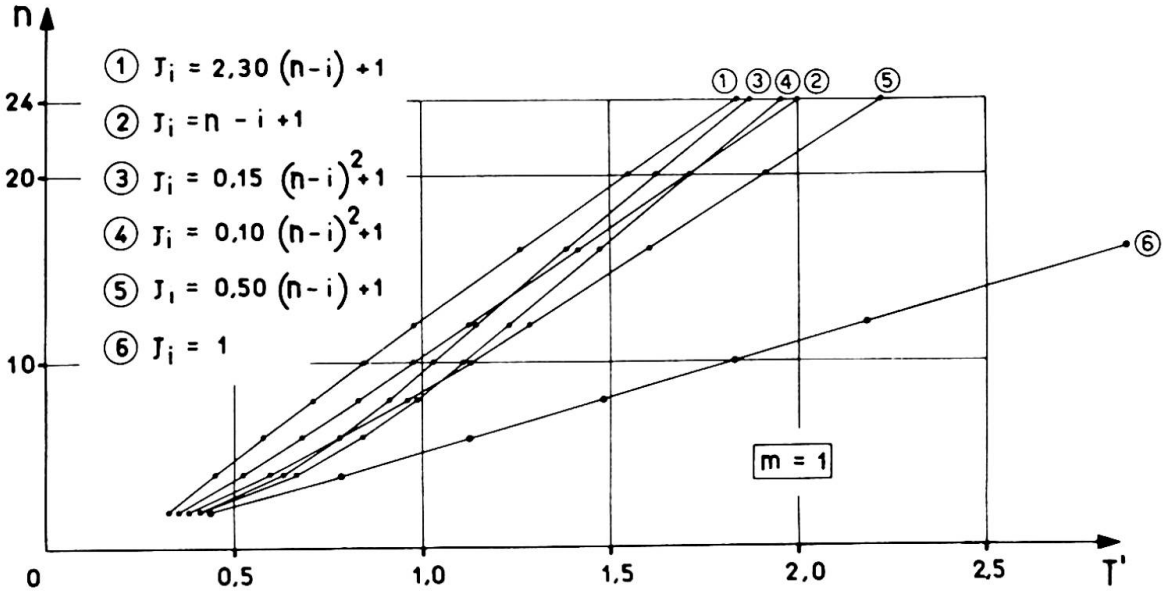
n
24
20
10
0
0,5
1,0
1,5
2,0
2,5
T'
① $T_i = 2,30\,(n-i) + 1$
② $T_i = n - i + 1$
③ $T_i = 0,15\,(n-i)^2 + 1$
④ $T_i = 0,10\,(n-i)^2 + 1$
⑤ $T_i = 0,50\,(n-i) + 1$
⑥ $T_i = 1$
m = 1

Fig. 1

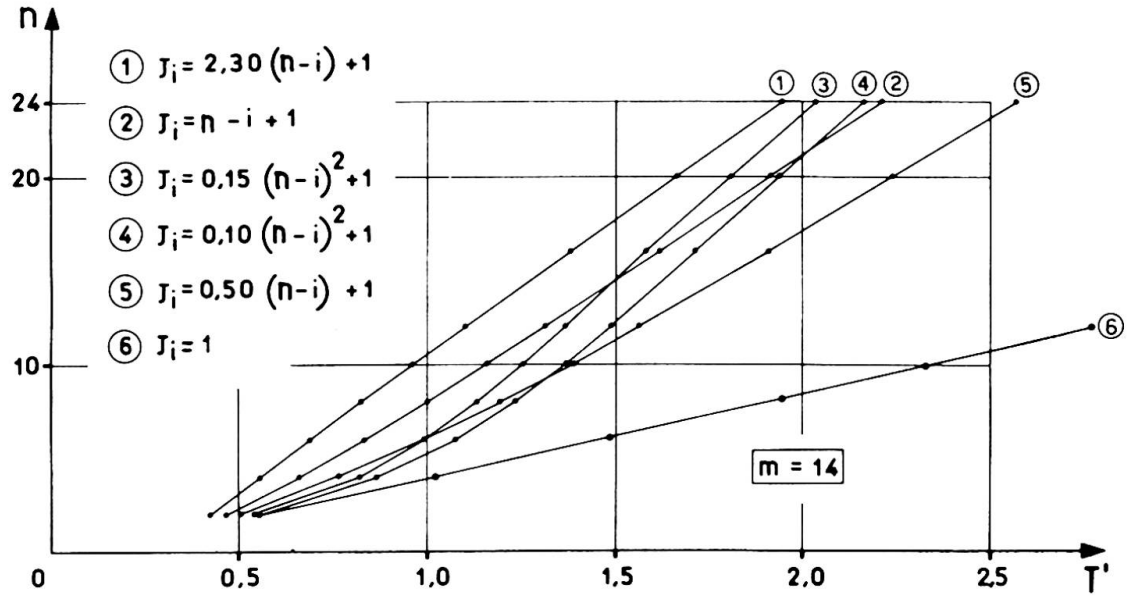
n
24
20
10
0
0,5
1,0
1,5
2,0
2,5
T'
① $T_i = 2,30\,(n-i) + 1$
② $T_i = n - i + 1$
③ $T_i = 0,15\,(n-i)^2 + 1$
④ $T_i = 0,10\,(n-i)^2 + 1$
⑤ $T_i = 0,50\,(n-i) + 1$
⑥ $T_i = 1$
m = 14

Fig. 2

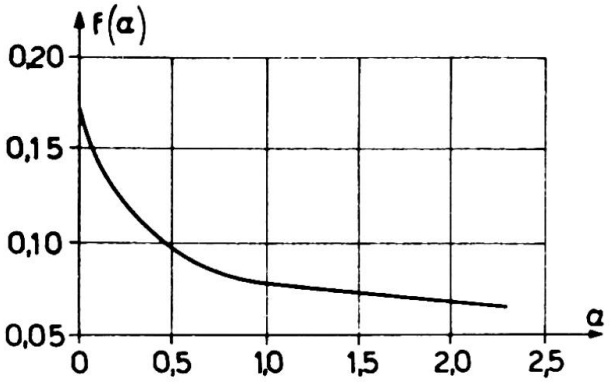

Fig. 3

gested by Housner and Brady:

$$T = 1{,}08\sqrt{n} - 0{,}86$$

and with that one by Ifrim (1) previously mentioned (fig.4 and 5).

In the same graphs concerning 1 and 14 spanned frames, both tha values obtained through calculations and those derived by using (2) are shown. Finally a qualitative graph shows what one might obtain if beams were infinitely rigid.

Later the investigation has been extended to braced frames with beams arranged according to "St. Andrew's Cross". It is assumed that beams are weightless and so slender that cannot absorb any thrust.

The procedure which has been followed is practically the same of that for ordinary frames. The difference consists in the fact that the matrix of stiffnesses of which are sought the eigenvalues is obtained as summation of two distinct matrices: the first one concerning the rods of structures and derived as before; the second one regarding the rods of bracing. The latter is tridiagonal because is independent on the rotation of joints and is invariant during calculations iterations. Such matrix can be immediately calculated and depends on the cross section area of rods as well as on the geometric dimensions of the mesh.

Introducing the equivalent moment of inertia:

$$J_e = \frac{A\, l^2 \sin^3 \phi}{12}$$

where:

A is the area of cross section of bracing rod;
l the width of the mesh;
ϕ the slope of bracing rods with respect to the horizontal, one has that the second stiffnesses matrix looks formally the same than that relative to frames with infinitely rigid beams.

Also in this stage several numerical examples have been carried out. Investigations have been performed on 1 to 14 spanned frames and with number of floors ranging from 2 to 24. Besides different variation laws of the moment of inertia on the height of the building and different stiffness ratios have been considered.

From the analysis of the results it seems still possible to apply the (2) if J_n is replaced by the fictitious moment of inertia

$$\bar{J}_n = J_n + \frac{\Sigma J_{e,n}}{m+1}$$

$\Sigma J_{e,n}$ is relative to the equivalent moments of inertia of all bracing rods of the last floor.

Similarly the parameter α will be still defined through the (3) where J_i and J_n must be replaced by $\bar{J}_i$ and $\bar{J}_n$. In such a way the equivalent moment of inertia of bracing rods has been "distributed" to all the columns at each floor, making still valid the (2).

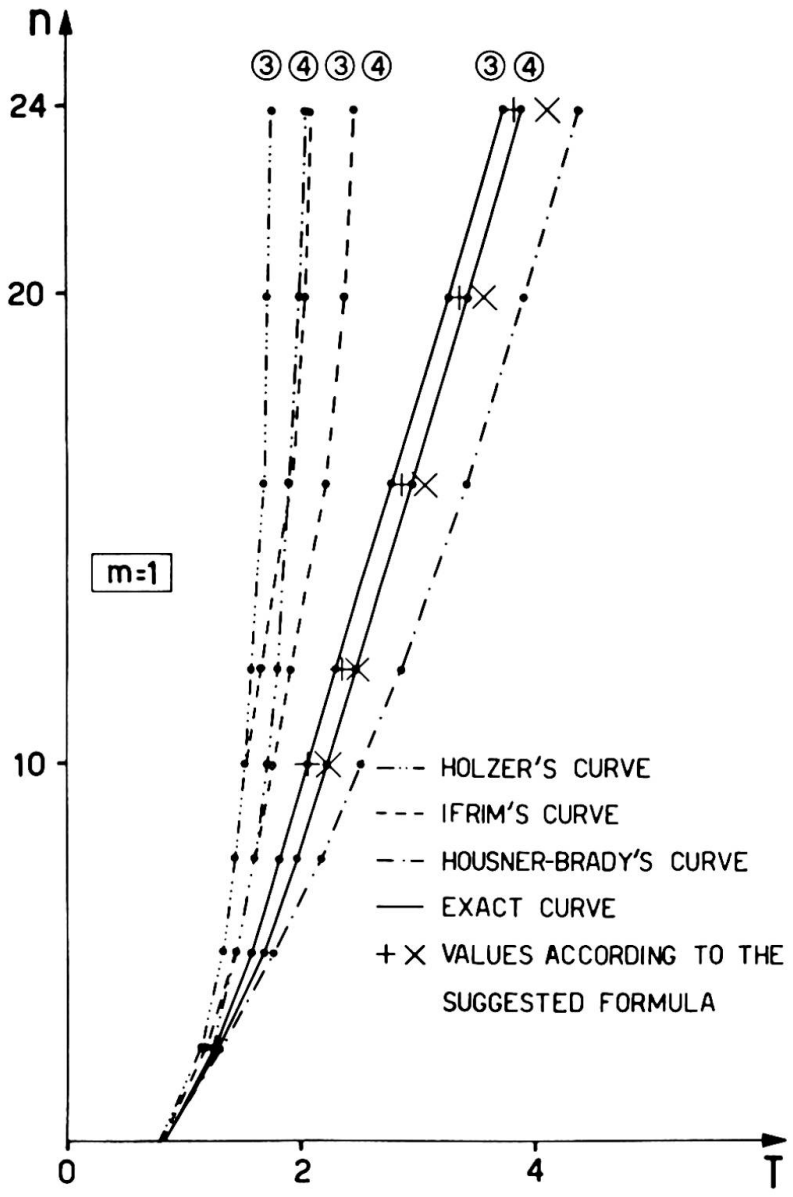
n
24
20
10
0
2
4
T
③④③④
③④
m=1
HOLZER'S CURVE
IFRIM'S CURVE
HOUSNER-BRADY'S CURVE
EXACT CURVE
+ × VALUES ACCORDING TO THE SUGGESTED FORMULA

Fig. 4

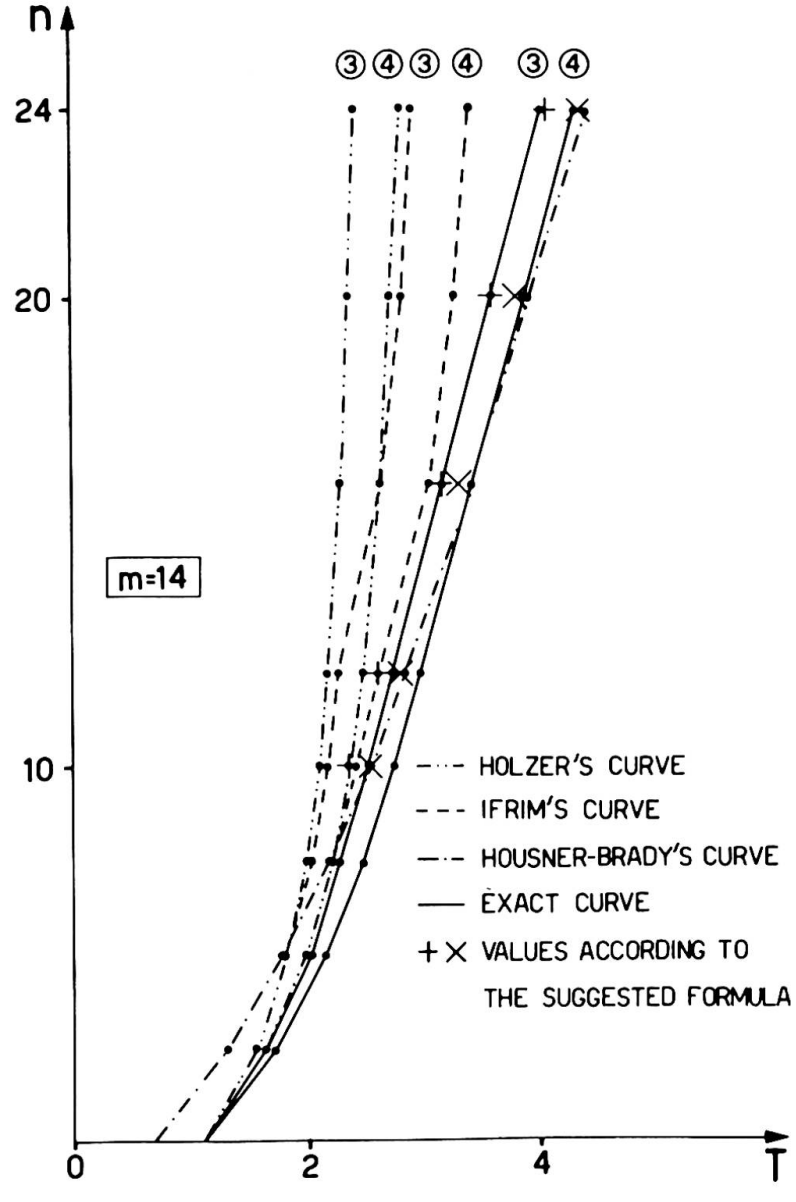
n
24
20
10
0
2
4
T
③④③④
③④
m=14
HOLZER'S CURVE
IFRIM'S CURVE
HOUSNER-BRADY'S CURVE
EXACT CURVE
+ × VALUES ACCORDING TO THE SUGGESTED FORMULA

Fig. 5

Doing in this way it has been implicitely assumed that stiffners stiffness may change with joints rotation. Since this does not correspond to the real phenomenon it seems reasonable to introduce a reduction factor k. On the other hand since the ratio beams stiffness over columns stiffness increases with the number of spans, one may conclude that vibrations modes for multi-spanned frames usually exhibit smaller joints rotations. Therefore it can be predicted that factor k increases with the number of spans. Numerical results confirm this assumption giving values of k ranging from 0,65 and 1,00 for a number of spans between 1 and 14. The error is smaller than 20% also in limit cases.

In conclusion the following expression for the period of braced frames can be proposed:

$$T = 2\pi l_o^2 \sqrt{\frac{\mu_o}{E J_n}} \sqrt{\frac{m+1}{\frac{\sum J}{J_n} + \frac{e,n}{J_n}}} \kappa T'$$

2) - Space Structures

The problem of dynamics of space frames has been set up and analyzed in a second stage of studies.

The following fundamental hypotheses have been assumed:

a - linear elasticity of all members of structure;
b - infinite rigidity of each horizontal structure with regard to the deformations in the plane;
c - negligible torsional stiffness of resisting members of the structure.

Under these hypotheses for the generic space frame with in horizontal structures (such as the one shown in fig. 6) the dynamic deformed configuration is determined if the components:

$$u_i, \quad v_i, \quad \phi_i \qquad (i = 1,2 \ldots\ldots n)$$

for eabh horizontal structure are known. The u_i, v_i, ϕ_i correspond respectively to a rigid translation in the x direction, in the y direction and to a rigid rotation around the origin 0 of the i-th horizontal structure coinciding with its centroid.

The elastic response of the structure to a generic system of displacements and rotations given to each horizontal member can be represented therefore in the following form:

$$\begin{aligned}
X_j &= \sum_{i=1}^{n} A_{xx,ij}\, u_i + \sum_{i=1}^{n} A_{xy,ij}\, v_i + \sum_{i=1}^{n} A_{x\phi,ij}\, \phi_i \\
Y_j &= \sum_{i=1}^{n} A_{yx,ij}\, u_i + \sum_{i=1}^{n} A_{yy,ij}\, v_i + \sum_{i=1}^{n} A_{y\phi,ij}\, \phi_i \qquad (4) \\
M_j &= \sum_{i=1}^{n} A_{\phi x,ij}\, u_i + \sum_{i=1}^{n} A_{\phi y,ij}\, v_i + \sum_{i=1}^{n} A_{\phi\phi,ij}\, \phi_i
\end{aligned}$$

where X_j, Y_j, M_j are respectively the elastic reactions in the x and y direction and the torsional reaction around O arising at the level of the j-th horizontal structure. The coefficients A_{ij} represent the influence coefficients of the structure, i.e the elastic reactions at the j-th level due to displacements u_i, v_i, ϕ_i of the i-th level. They can be easily deduced if for each plane frame belonging to the space structure the reactions r_{ij} are known. Such reactions are due to the unit displacement of the generic i-th beam for all other beams prevented from translation.

In dynamics, if σ is the generic frequency of the structure in free vibrations, the displacements of the generic horizontal member turn out to be:

$$u_i = \bar{u}_i \sin \sigma t$$
$$v_i = \bar{v}_i \sin \sigma t$$
$$\phi_i = \bar{\phi}_i \sin \sigma t$$

Assumed that at each horizontal structure the mass is uniformely distributed, the inertial reactions in the x and y direction and the torsional reaction around O will be:

$$\bar{X}_j = - m_j \frac{d^2 u_j}{dt^2} = m_j \sigma^2 \bar{u}_j \sin \sigma t$$

$$\bar{Y}_j = - m_j \frac{d^2 v_j}{dt^2} = m_j \sigma^2 \bar{v}_j \sin \sigma t \qquad (5)$$

$$\bar{M}_j = - m_j \rho_j^2 \frac{d^2 \phi_j}{dt^2} = m_j \rho_j^2 \sigma^2 \bar{\phi}_j \sin \sigma t$$

where m_j is the total mass of the horizontal structure and ρ_j is the polar radius of giration of its area around O.

If columns masses are neglected, the equations of dynamic equilibrium are immediately obtained by equating (4) to (5). Setting the determinant of the coefficients of the system equal to zero one gets the algebraic equation of 3n degree in σ^2 whose roots σ_1^2, ... σ_n^2 allow the evaluation of the 3n free frequencies of the multi-story space structure.

It is obvious on the other hand that an iterative process is necessary if one wants to improve the values obtained by taking into account the mass of members. One should in fact recalculate the coefficients A_{ij} starting from the σ_i computed in the first cycle and taking into account the inertial forces of the beams and columns. Then the solution of the system of equations of dynamic equilibrium will lead to new values σ_i. The iteration process should be carried out as long as two consecutive solutions give almost the same value for the frequencies.

It should be born in mind, however, that in almost all cases the masses of horizontal structures are much larger that those ones of the columns. Consequently the values of σ_i given by the first iterative process are practically exact.

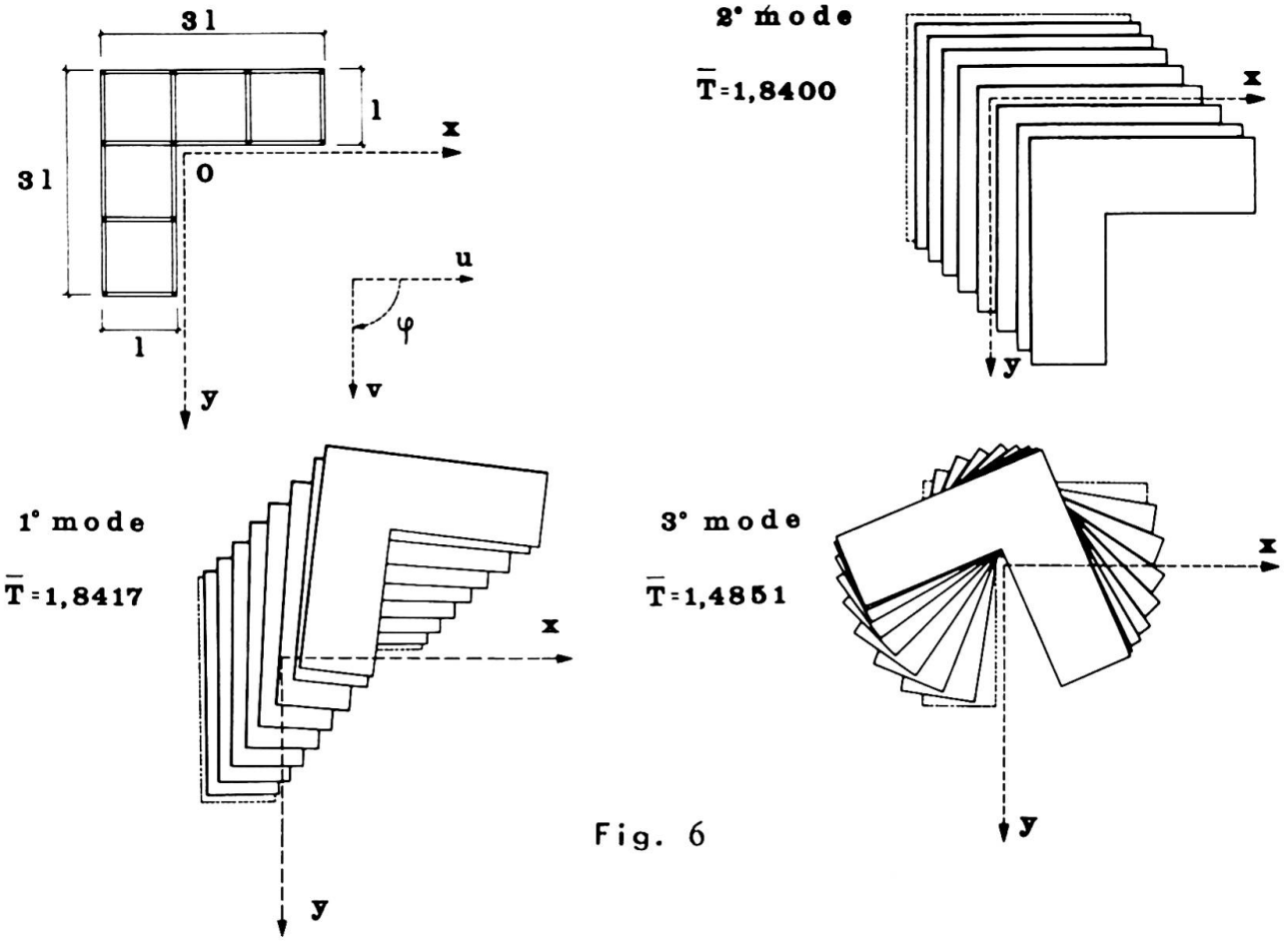
3l
l
x
0
3l
u
φ
l
y
v
2° mode
T̄=1,8400
x
y
1° mode
T̄=1,8417
x
y
3° mode
T̄=1,4851
x
y

Fig. 6

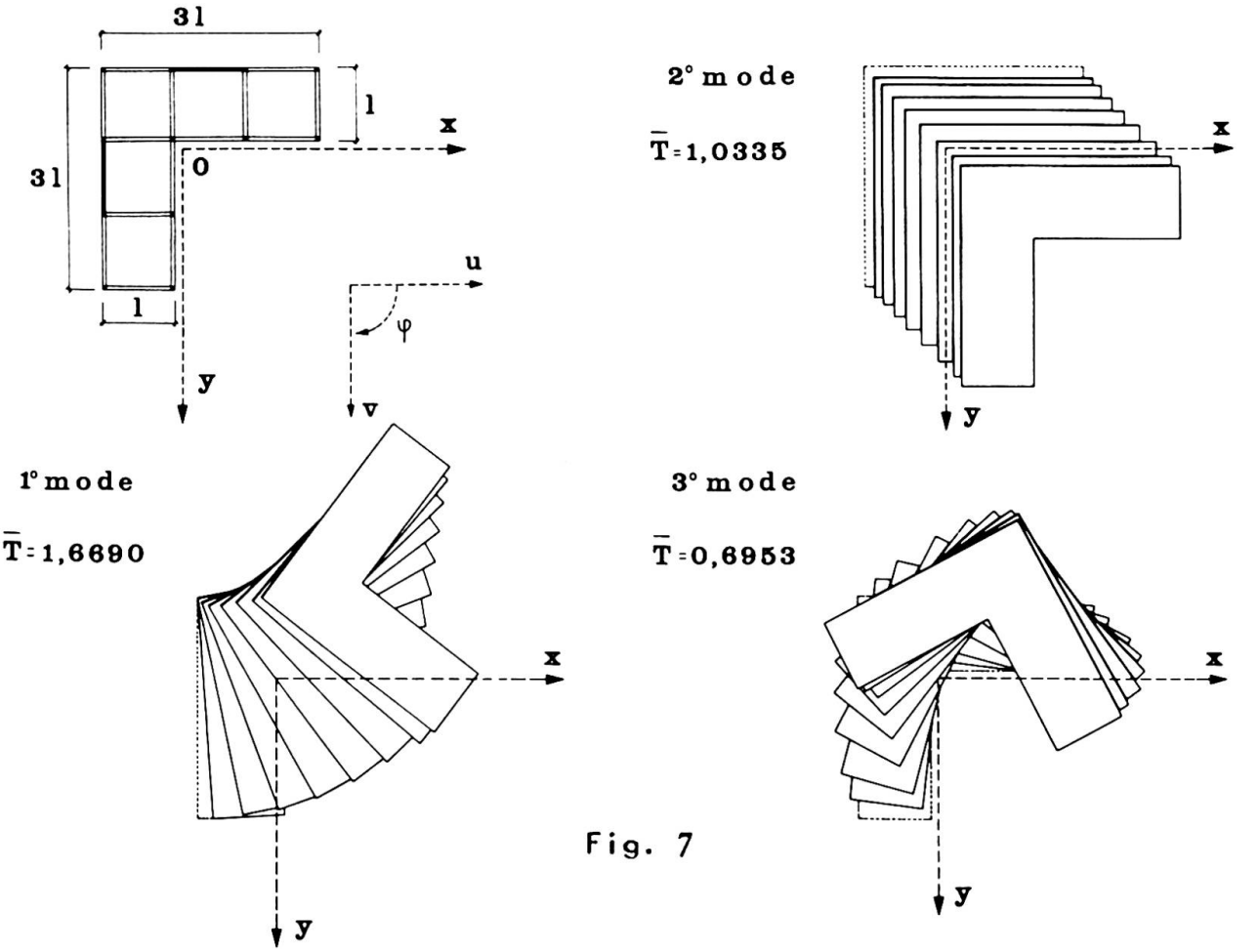
3l
l
x
0
3l
u
φ
l
y
v
2° mode
T̄=1,0335
x
y
1° mode
T̄=1,6690
x
y
3° mode
T̄=0,6953
x
y

Fig. 7

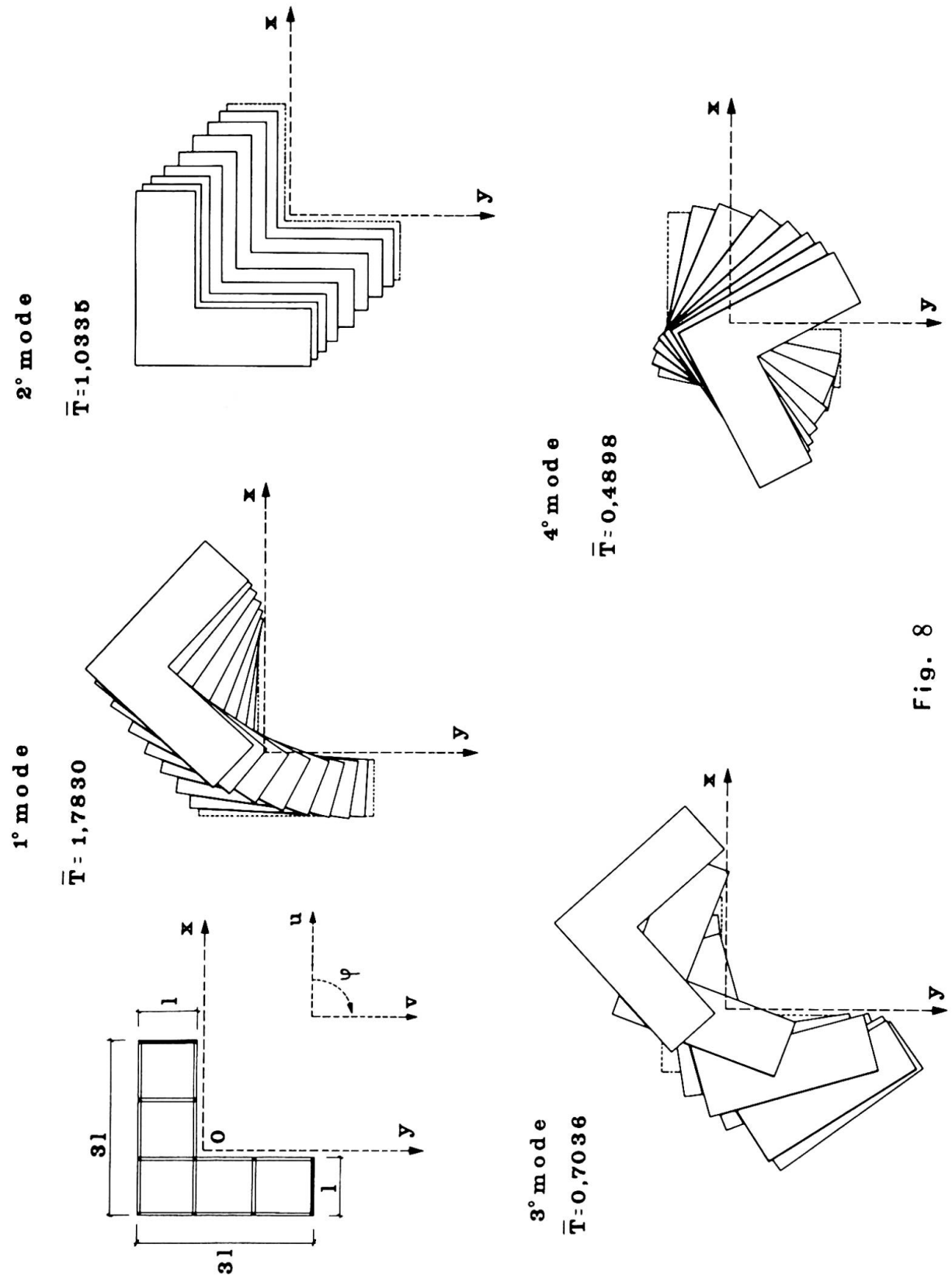
2° mode
T̄=1,0335
1° mode
T̄= 1,7830
4° mode
T̄= 0,4898
3° mode
T̄=0,7036
x
y
u
v
φ
O
l
3l

Fig. 8

The foregoing procedure has been applied to a steel building with L plan and eight horizontal structures and with two orders of mutually orthogonal frames.

Three structural schemes of the building have been considered: the first one without windbracing (fig.6) and the other two with windbracing arranged as shown in figs. 7 and 8.

The dynamic analysis of the three space schemes has been carried out with the computer.

In the graphs previously mentioned have been represented the modes of vibration of $\overline{T}$ related to the period T by:

$$\overline{T} = \frac{T}{\sqrt{\frac{M_o \, l_o^3}{E \, J_n}}}$$

A comparison has been made between the results obtained in this way and the other ones given by decomposing the space structure in plane frames.

It can be concluded that the period of vibration obtained in the hypotheses of plane behaviour is usually smaller than the real value.

SUMMARY

It is briefly reported on the works of the Commission XIII of the Convention of European Constructional Steelwork Associations concerning the recommendations for designing steel structures in seismic area. The results of a study on the dynamic behaviour of plane and space framed structures are also shown. Finally some simplified formulae obtained through a large numerical investigation are suggested.

RÉSUMÉ

L'article résume très brièvement les travaux de la Commission de la Convention Européenne des Associations de la Construction Métallique, concernant les recommandations pour le calcul des bâtiment dans les zones seismiques. On expose aussi les résultats d'une étude sur le comportement dynamique de structures en portique dans l'espace. On donne l'expression de formules simplifiés pour le calcul de la période de vibration.

ZUSAMMENFASSUNG

Es wird ein kurzer Abriss von der Arbeit der Kommission XIII der Europäischen Konvention der Stahlbauverbände gegeben bezüglich der Empfehlungen zur Bemessung von Stahlbauten in Erdbebengebieten. Ebenso wird eine Studie über das dynamische Verhalten ebener und räumlicher Rahmentragwerke aufgezeigt. Schliesslich werden einige vereinfachte, durch erweiterte numerische Nachforschungen erzielte Formeln für die Schwingungsdauer angegeben.

Leere Seite
Blank page
Page vide

Factors affecting Response of Buildings to Wind and their Experimental Determination

Eléments ayant une influence sur la réponse d'édifices aux vents et leur détermination expérimentale

Faktoren, die die Reaktion von Gebäuden auf Windbelastungen beeinflussen und ihre experimentelle Bestimmung

SEAN MACKEY
Taikoo Professor of Engineering
University of Hong Kong

Wind action on buildings and structures has both static and dynamic effects. The static effects are primarily concerned with steady displacements obtained from steady forces and pressures resulting from time-averaged wind velocities. By custom, buildings have been designed to resist these effects. Dynamic effects, on the other hand are concerned with the tendency to set the structure oscillating. Increasing use of tall slender buildings with lightweight cladding and large column-free floor areas has forced engineers to pay much more attention to dynamic wind effects. Structural damping is a major factor which should be taken into account in this respect, since to decrease the resonant amplitudes of oscillation the dissipation of energy through structural damping must exceed the relevant energy inputs from the wind.

By applying the statistical theories used for communications technology the analysis of atmospheric turbulence is effected and its characteristics are represented by its energy spectra, its lateral correlation functions, and its probability distribution. Studies made to date, indicate that for heights up to that where the gradient winds prevail, variation in mean wind speed generally follows a power law profile, the exponent of which varies with ground roughness from about 0.15 for open unobstructed country to around 0.43 for heavily built-up urban centres, according to DAVENPORT [1] .

Investigations made by DAVENPORT [1] and SHIOTANI [2] show that the spectral density varies with the surface drag coefficient, which is a

function of the ground roughness. Except for some slight falling-off of energy with height, spectra obtained at different locations are more or less similar in shape and this has led DAVENPORT to suggest a universal type of formula:

$$\frac{n\ S(n)}{K\ \bar{V}^2} = C\ \frac{x^2}{(1+x^2)^{4/3}}$$

where n is the frequency; $\bar{V}$ is the mean wind speed; K is the drag coefficient; x is directly proportional to $\frac{n}{\bar{V}}$ and C is a constant.

Spatial correlation studies by the same investigators yield a spatial correlation coefficient, (i.e. $\sqrt{\text{coherence}}$), approximated by the exponential function:

$$R \propto e^{-\frac{\Delta S}{L}}$$

where Δs is the spatial separation and L is the scale of turbulence proposed by TAYLOR [3] . But in this respect, SINGER,[4] investigating radio masts, found the spatial correlation coefficient of similar wind components measured at different heights to be a function of the height ratio. Moreover, he found that within his range of interest cross spectra were essentially zero.

Apart from considerations of stability against time-averaged wind forces, the designer of tall buildings must also concern himself with the direct consequences to his structures of the fluctuating dynamic character of the wind. These include, inter alia, collapse of the structure due to peak load or fatigue; minor damage to the fabric, lift shafts, or partitions arising either from excessive deflexion or high local loading; and discomfort to the occupants caused by high sway accelerations.

Preferably, design factors should be simple and easy to apply. In this respect DAVENPORT'S simplified dynamic approach, using a gust factor G which takes into account the dynamic characteristics of the structure, has much to commend it. He suggests on expression for the wind pressure, p , at a point on the structure given by:

$$p = G\,\bar{p} = \left(1 + g\ r\ \sqrt{B + \frac{SF}{Y}}\right)\bar{p}$$

where:-

h = structure height

n_o = fundamental natural frequency of structure

T = time interval used for finding averages;
$\bar{V}$ = design velocity;
g = peak factor depending on n_o , and T ;
r = roughness factor depending on ground conditions and h ;
B = excitation from background turbulence, depending on h
S = scale factor depending on height/width ratio of structure n_o & $\bar{V}$
F = wave number at resonance = $n_o/\bar{V}$
γ = critical damping ratio;
$\frac{SF}{\gamma}$ = excitation due to resonant turbulence.

Essentially, these formulae predict the static equivalent load corresponding to the maximum deflexion. In applying them to natural gust loading, investigators have made several assumptions, including the following:

(i) wind is a stationary random process
(ii) variation of wind velocity with height follows a power law
(iii) velocity distribution is Gaussian in character
(iv) pressure coefficients are independent of frequency.

In order to assess correctly the effects of wind on a building it is necessary to know the spectrum of the wind; its spatial correlation, and the dynamic characterestics of the building. The dynamic characteristics include a knowledge of the natural frequency of the building and its damping. These are given by the following equations:

$$\frac{1}{\omega_r^2}[K]\{X^{(r)}\} = [M]\{X^{(r)}\}$$

$$\frac{1}{2\beta_r\omega_r}[C]\{X^{(r)}\} = [M]\{X^{(r)}\}$$

where the matrices $[K]$; $\{X^{(r)}\}$; $[M]$ and $[C]$ refer to the stiffness; the column mode shape; the mass and the damping, respectively. The results derived from application of these equations depends on the accuracy of determining the elements in $[K]$ and $[C]$. The elements in $[K]$ depend on the type of the structure and the properties of the materials used. Such factors as column and beam deformation; rotation of joints; floor and wall deformation; soil distortion and rigidity of foundations must be considered. Because of difficulties in obtaining experimentally the necessary information from full-scale buildings considerable reliance has had to be placed on mathematical models in order to evolve the methods of analysis now

available.

Correlation of model tests with the behaviour of full-scale buildings has been attempted by several investigators using three different types of approach. One of these, known as the resonance method, involves excitation of the building by means of a vibrator; the second makes use of run-down tests by pulling the building laterally and letting it go; the third relies on wind as the means of excitation, and a somewhat similar method developed by TANAKA [5] , involves measurement of minute vibrations excited by irregular forces such as microtremors and others

NIELSEN [6] has shown that decay tests can lead to overestimation of structural damping by several hundred percent, and he has succeeded in obtaining vibration characteristics of a 9-storey steel-framed building by steady-state tests. From the natural frequencies, damping and mode shapes obtained for several modes in this test he found the stiffness matrix giving the "best fit" to the modal properties determined experimentally. But NIELSEN'S experiment showed that any increase in the force level applied produced a corresponding increase in percentage damping and a slight decrease in resonance frequency. He also found for his building an additional mode of vibration, further to the normal modes, generated by the floor slabs vibrating laterally in phase as deep horizontal beams.

Similar investigations have been carried out by ENGLEKIRK & MATTHIESEN [7] on an 8-storey reinforced concrete building combining rectangular frames with shear walls, and by CRAWFORD & WARD [8] , using random wind excitation on a steel-framed building with a central concrete core. In the latter instance the natural periods were computed both for frame action only and for frame and core combined. The experimental results lie somewhere between the two values calculated and the ratios of the first three modes of vibration are not in agreement with the observed ratios. The investigators considered that this discrepancy resulted either from the fact that the window sections were not considered in calculating the shear stiffness and/or possible beam flexure and non-interaction of the core and structure. No measurements were taken simultaneously on the central core and on the framed structure to confirm this hypothesis.

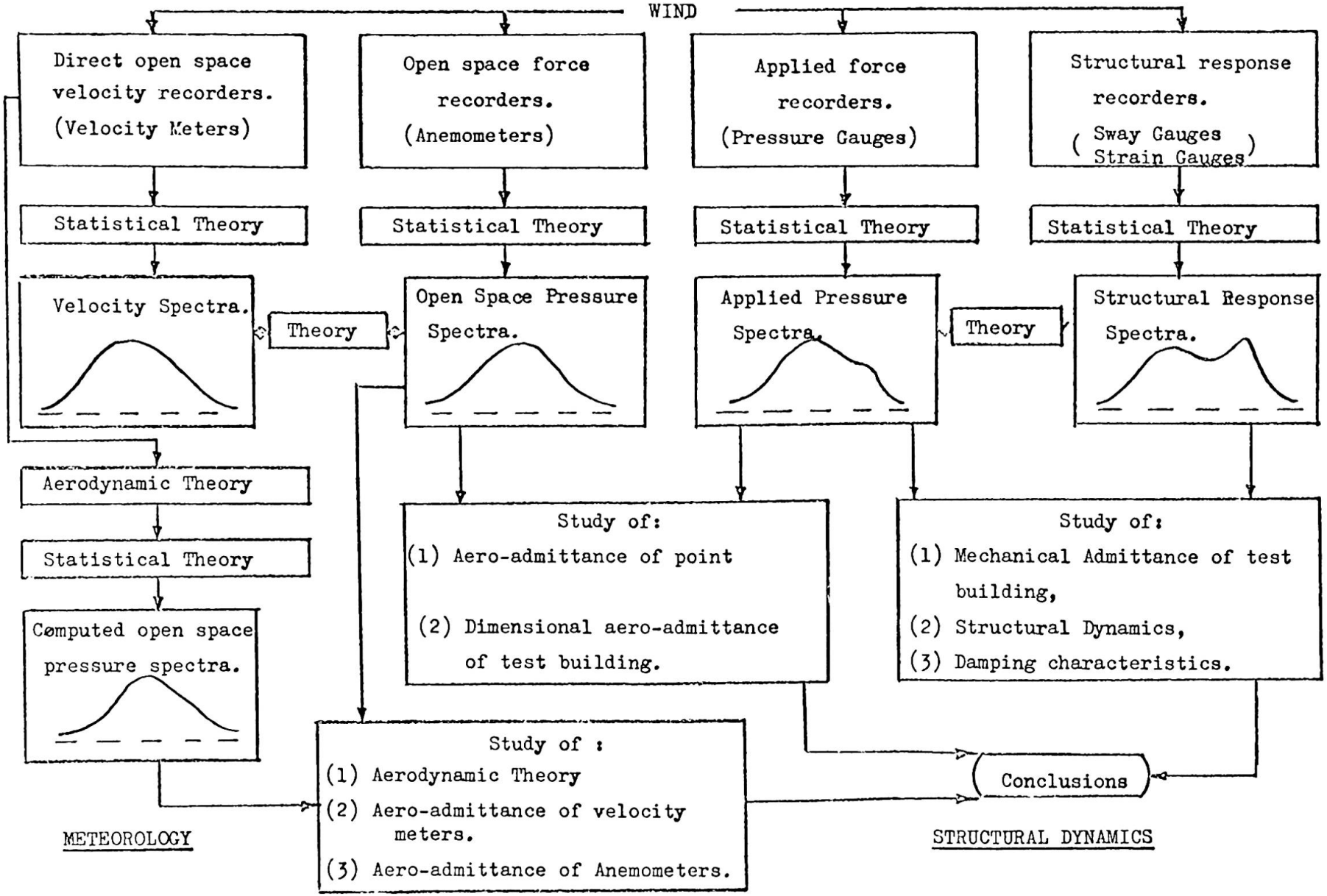

FIG. 1 - IDEALISED FLOW DIAGRAM FOR STUDY OF WIND EFFECTS ON STRUCTURES

The inadequacy of our present knowledge of these matters and the urgent need for comprehensive studies of natural winds and the response behaviour of full-scale structures under excitation from this cause are clearly demonstrated in the papers by BORGES [9] and by NEWMARK & HALL [10]. Such experiments are costly to execute and there is need for international collaboration in their planning to ensure that the results obtained from them are of real value, and cover both normal seasonal winds and those of typhoon magnitude.

An investigation, currently being undertaken at the University of Hong Kong is planned with this objective in mind. The nature of the investigation is diagrammatically set out in Fig. 1. but its scope must necessarily be limited initially, because of inadequacy of instruments for recording absolute wind velocities. In considering this figure it should be noted that a stationary statistical ergodic state is assumed and that the spectra referred to are vertically, horizontally and time-wise correlated.

It is anticipated that considerable difficulties will be experienced in determination of the aerodynamic admittance of the experimental building. Difficulties are also anticipated in determining, with sufficient accuracy, the actual patterns of wind-flow over the experimental site due to the limited funds available for instrumentation and site levelling.

In brief, the Hong Kong research involves construction of an experimental building on a low-lying exposed land area on the south-east coast of Hong Kong Island. The building is of fully-welded steel-framed construction with reinforced-concrete floors and glass curtain-wall cladding, so arranged that any part of the cladding may be disconnected temporarily from the structural frame. The building measures 60 ft. x 30 ft. in plan and ten-storeys or 100 ft. tall. It is so designed that it can be divided vertically into four sections, as shown in Fig. 2., each capable of acting independently of the others. Under high velocity winds the separate sections will be coupled together with shear connectors at every floor-level

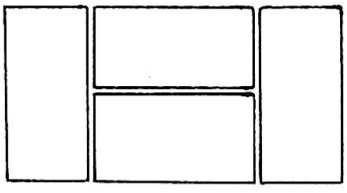

Fig. 2.

so that the whole building can act as a single monolithic unit. Uncoupled, the sections will be tested for sway under seasonal winds of moderate velocity. Dynamometers, installed across the vertical joints at various floor levels will record the drag effects of wind between the uncoupled sections.

Ahead and on one side of the building, approximately 200 ft. away from the nearest face two lines of free-standing latticed-steel masts, approximately 175 ft. tall, are being erected. Quick-response gust anemometers, designed by the Electrical Research Association of Great Britain, are attached to the masts in pairs at fixed height intervals. Collectively these anemometers, 60 in number, are being used to determine the wind spectra and the spatial correlation.

The pressure distribution over the faces of the building is being measured by 72 pressure gauges developed by the Building Research Station at Watford. The sway response of the building is to be recorded by Physitech Inc. electro-optical tracking instruments, which track the paths of targets attached to various points of the building.

The Benson-Lehner data logger installed accepts up to 240 channels of low-level analogue inputs in the range $\pm$ 10 mV to $\pm$ 500 mV full-scale deflexion, time multiplexes the data, makes an analogue-to-digital conversion, and records the binary or binary coded decimal equivalent on one-half inch wide, 9-track, magnetic tape. Operation of the system is illustrated in Fig. 3.

The analogue signals are sampled sequentially at the rate of 10 samples/second/channel by a reed relay multiplexer followed by a solid state submultiplexer which also performs the function of amplifying the low-level signals to $\pm$10 volts f.s.d. for maximum A-D converter resolution. No arithmetic is performed within the system, therefore all data indicated or recorded will be a function of the analogue signal level and amplifier gain. Identification data is included in the information recorded on the magnetic tape to provide the means of knowing which groups of channels have been selected for the scan sequence. This identification data also serves to identify the gain setting of the amplifier, as an individual amplifier gain is permanently associated with a particular channel group.

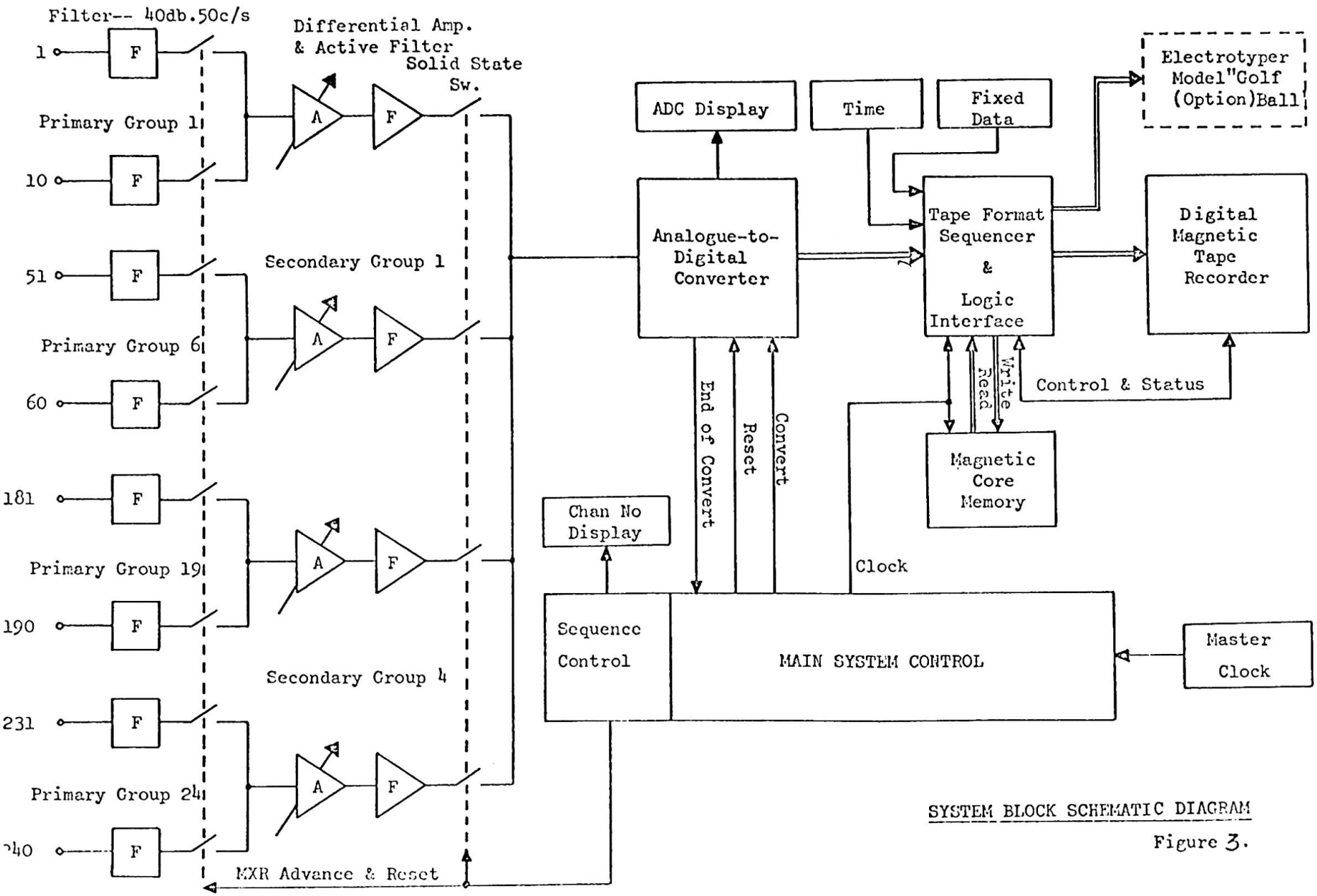

SYSTEM BLOCK SCHEMATIC DIAGRAM

Figure 3.

Analogue data is converted into a 9-bit binary two's complement digital format by the conventional method of successive approximation, each bit conversion occupying a time of 1.5 microseconds. The system accepts a continuous stream of data during the entire data acquisition and recording process, i.e. the scanning of the input channels is a continuous operation. Whilst interlock gaps are being generated on the magnetic tape, in accordance with IBM System/360 format requirements, digital data is stored in a buffer core store. The store is an AMPEX RF-2 of size 4096 words x 12 bits and, in operation, is made to resemble two independent stores of 2048 x 12. As one half of the store is being filled with digital data, the other half is unloaded at a transfer rate of 28,800 characters per second, via the tape format sequencer, to the digital magnetic tape unit.

The whole project is now nearing completion and recording is expected to commence in September of this year.

References

1. DAVENPORT, A.G. "The Relationship of Wind Structure to Wind Loading" Proc. Int. Conf. N.P.L. Lond. (1963)

2. SHIOTANI, M. "Lateral Structures of Gusts in High Winds" Phy. Sc. Lab. Nihon Univ. (1967)

3. TAYLOR, G.I. "Statistical Theory of Turbulence" Proc. Roy. Soc. A151 (1935): 156(1936)

4. SINGER, I.A. "Wind Gust Spectra" Ann. New York Acad. Sc. 116. Art.1. (1964)

5. TANAKA, T. "An Instrument for Brief Measurement of the Natural Period of a Building" Bull. Earthq. Res. Inst. 40 (1962)

6. NIELSEN, N.N. "Vibration Tests of a Nine-Storey Steel Frame Building" J. Engr. Mech. Div. ASCE. EMI. Proc. No.4660(1966)

7. ENGLEKIRK, R.E. & MATTHIESEN, R.B. "Forced Vibration of an Eight-Storey Reinforced Concrete Building" Bull. Seism. Soc. of Am. 57. (1967)

8. CRAWFORD, R. & WARD, H.S. "Determination of the Natural Periods of Buildings" Bull. Seism. Soc. of Am. 54 (1964)

9. BORGES, J.F. "Dynamic Loads"
Prel. Publ. I.A.B.S.E. 8th Congr. (1968)

10. NEWMARK, N.M. & HALL, W.J. "Dynamic Behaviour of Reinforced and Prestressed Concrete Buildings under Horizontal Forces and the Design of Joints"
Prel. Publ. I.A.B.S.E. 8th Congr. (1968)

SUMMARY

The response of a building to winds is governed by the meteorological data, the interaction of the wind and the building and the dynamic characteristics of the building. The available data is reviewed.

The author describes a project which will allow correlation of results from an experimental, 10-storey building with model results and existing code requirements. Wind velocities, pressure distributions over the building and the deflexion responses of the building will be measured.

RÉSUMÉ

La résistance au vent d'un bâtiment dépend des données météorologiques, de l'interaction du vent et de la construction, ainsi que de ses caractéristiques dynamiques. Les données connues sont revues ici. En plus, l'auteur décrit un projet qui permet de comparer les exigences des normes existantes avec les résultats d'un bâtiment d'essai de dix étages ainsi qu'avec les valeurs mesurées sur modèles réduits.

ZUSAMMENFASSUNG

Der Windwiderstand eines Gebäudes richtet sich nach den meteorologischen Gegebenheiten, nach der Wechselwirkung von Wind und Gebäude und nach den dynamischen Charakteristiken der Bauten. Diese Gegebenheiten werden berücksichtigt. Der Verfasser beschreibt ein Projekt, welches die Beziehung von Resultaten eines zehnstöckigen Gebäudes mit Modelergebnissen und bestehenden Norm-Anforderungen erlaubt. Gemessen werden die Windgeschwindigkeiten, Druckverteilungen über das Gebäude sowie die Ausbiegungen.

Behavior of Steel Frames Subjected to Repeated and Reversed Loads

Comportement des portiques multi-étagées en acier sous l'effet de charges répétitives et alternatives

Das Verhalten von Stahlrahmentragwerken unter Einfluß periodisch veränderlicher Wechsellasten

LAUREN D. CARPENTER
Instructor in Civil Engineering
Lehigh University
Bethlehem, Pennsylvania

LE-WU LU
Associate Professor of Civil Engineering
Lehigh University
Bethlehem, Pennsylvania

1) Introduction

Recent work in earthquake engineering has centered around full scale dynamic testing of multi-story buildings (Refs. 1 and 2) and computer studies of the behavior of simple systems under recorded earthquake motions or models thereof (Refs. 3, 4 and 5). Some tests have been performed to study the behavior of steel and concrete beams and frames under simulated wind, earthquake or impact loads. In recent tests at the University of California at Berkeley cantilever beams were tested under cyclic loads to study the behavior of these beams near the connecting zone (Refs. 6 and 7). In addition, as adjuncts to recent tests of multi-story frames at Lehigh University to study the static behavior under a monotonic load application, four frames were tested under a reversed loading after large inelastic deformations had occurred (Refs. 8 and 9). Currently available methods of analysis were found to adequately describe the static behavior of these test frames under the combined effect of gravity and monotonically increasing lateral loads. However, these methods were found to be inadequate to describe the static behavior of the frames under reversed loading even for relatively simple structures.

A research program has been initiated at Lehigh University in order to extend plastic design concepts to the design and analysis of structures subjected to seismic loadings. In the experimental portion of this program, two series of tests on single and multi-story frames were planned. This discussion gives a brief account of the first series of tests which has been completed recently.

2) Design of Test Frames

The test frames involved in the first series were designed to be typical of current aseismic design practice. The prototype frame was

an eight-story, single-bay structure. A bay width of 15 feet, story height of 10 feet and bent spacing of 18 feet were selected for the prototype frame shown in Fig. 1.

A three-story assemblage was designed to represent levels 5, 6 and 7 from the top of the building from which a single story frame representing level 7 was selected for the initial test. Half-story columns above level 5 and below level 7 were used to locate the point of inflection in the double curvature columns. The two frames in the first series are shown in Fig. 1 in their relative position with respect to the prototype frame.

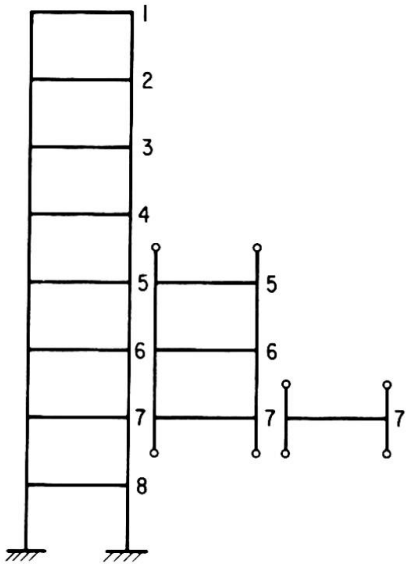

Fig. 1 Prototype Frame and Test Frames

The design and therefore the testing of the frame utilized a single horizontal load applied to the top of the assemblage. The frame was designed for constant story shear because for an eight-story frame the variation in the total aseismic design shear (Ref. 10) in the lower stories is usually small (Ref. 11). In addition, the envelope of maximum dynamic shear obtained from several modes of a shear type building has small variations in the lower portions of such a building (Ref. 12).

The gravity loadings used in the design were 80 psf full live load and 80 psf dead load on all the floors. An average live load reduction of 40% was used for both beams and columns. The working horizontal load was the summation of the design shears from the top of the structure down to and including the component at level 5. The working shear was equal to about 3½ percent of the sum of the dead loads through level 7.

The design also incorporated a ratio of column stiffness to beam stiffness which was selected to be representative of buildings designed using current aseismic design practice in California.

The plastic design method which was used to determine the members initially assumes no P-Δ effect and a likely-to-occur mechanism (Ref. 13). A plastic moment balancing analysis then was used to check that all moments are less than or equal to their fully plastic values. From the resulting moment diagram and sections required, the Δ's were calculated and the P-Δ moments were found. Redesign then included this P-Δ effect

and the sections required initially were altered when necessary.

Once the above set of members were selected, the frame was analyzed using the computer program (Ref. 14) described in the next section. By using this program repeatedly the members were selected such that they satisfied the requirements of aseismic design practice.

In summary, the three-story frame was designed and analyzed plastically and then checked by the allowable-stress method. The single-story frame was selected as a duplicate of the lower floor of this frame. The resulting member sizes selected were an 8WF40 section for the columns and a 10WF29 section for the beams. The member sizes and frame geometry for both frames are shown in Fig. 2.

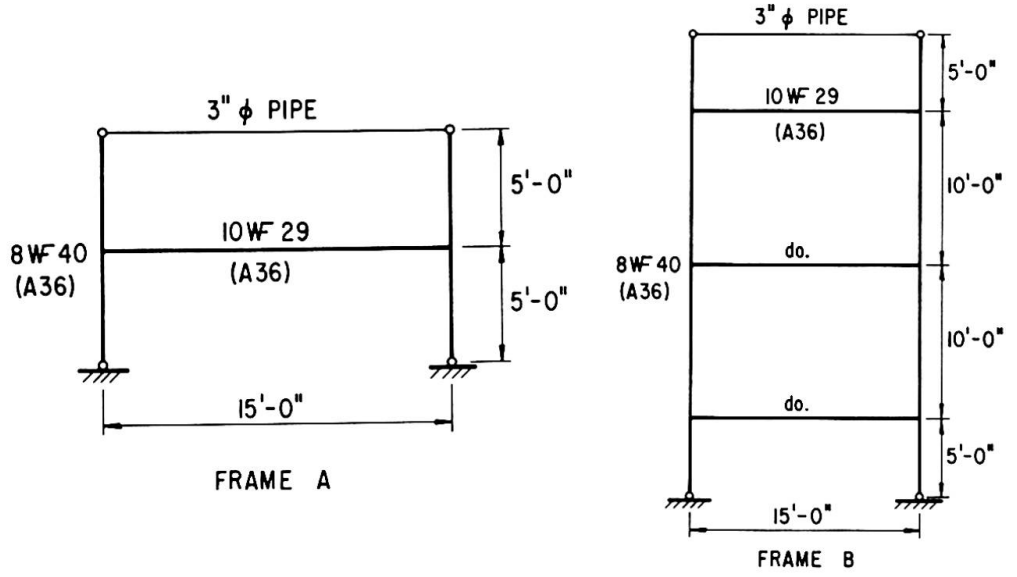

Fig. 2 Geometry and Member Sizes for Test Frames

3) Analyses of Test Frames

When the frames were analyzed under the combined earthquake and gravity loads, the change in member stiffness due to axial force, the overturning effects of the lateral load and the P-Δ moment were included.

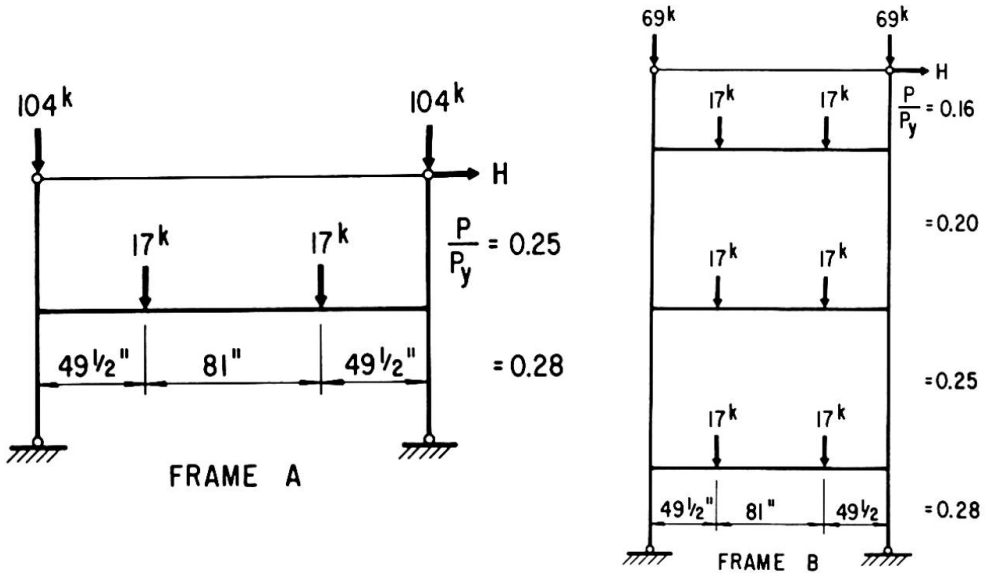

Fig. 3 Loads and Axial Load Ratios for Test Frames

At the working level of the monotonically applied horizontal load and the gravity loads shown in Fig. 3 the results of this second-order analysis were used to check the adequacy of the beams and columns with the AISC interaction formulas and satisfactory results were obtained. (In addition, the members of both frames were checked under the working level of gravity load only).

The analysis of each frame was then continued into the inelastic range past the point of frame instability. The load-deflection curves for both frames were essentially the same as shown in Figs. 4a and 4b.

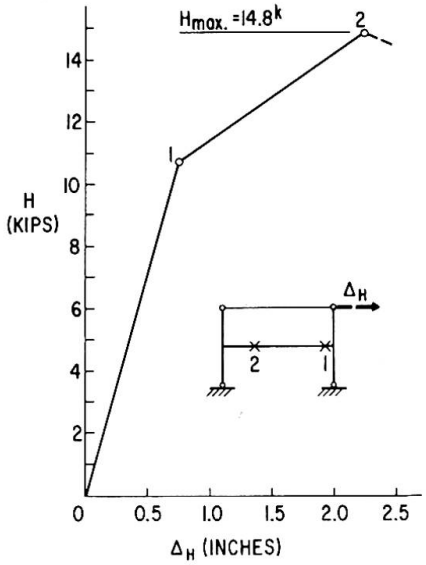

Fig. 4a Load-Deflection Curve for Frame A

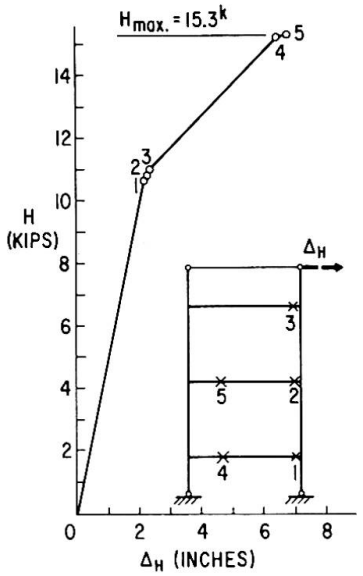

Fig. 4b Load Deflection Curve for Frame B

For the single-story frame the frame instability load and mechanism load coincide at a lateral load of 14.8 kips and at a deflection of 2.26 inches at the point of load application. However, the three-story frame became unstable at a load of 15.3 kips and a corresponding deflection of 6.83 inches before formation of a failure mechanism.

The single-story frame had a combined mechanism at its maximum load with the first hinge forming at the leeward end of the beam and the second hinge at the windward load point on the beam. The three-story frame had a similar pattern of hinge formation with the first hinge forming at a load of 10.7 kips in comparion to the working value of 5.2 kips. Since the ratio of maximum load to the working load is 2.9, a considerable savings could have been realized by utilizing more of the inelastic strength of the frame in design while keeping within acceptable drift limitations. In fact, a 13% lighter frame using 8W35 columns and 10W25 beams was analyzed under factored gravity plus lateral loads (L.F. = 1.30) (Ref. 13). The maximum load in this case was 8 kips which is considerably higher than the factored lateral load of 6.75 kips. However, for the former three-story frame which was designed for a lateral load of 3½ percent of total dead load, the ultimate value of lateral load is about 10 percent of the working dead load.

The above analyses were based on handbook values for cross-sectional properties and on the nominal static yield stress of 36 ksi specified for ASTM A-36 steel. The analyses were repeated after the cross-sectional shapes of the actual members used in the frames were measured and after the static yield stress levels were determined by testing tension specimens cut from adjacent pieces of the same length of steel. All material used was gag straightened by the producer.

4) Test Setup and Loading Program

The two frames were tested under constant (working) gravity loads and a program of statically applied cyclic horizontal displacements of the top of the frames similar to those used by E. P. Popov on the cantilever beams (Refs. 6 and 7).

Two unique devices were used to load and to brace the frames without offering any restraint to in-plane movements. Gravity-load simulators were used to apply the constant vertical loads to the quarter points of the beams through a spreader beam and to the column tops, and bracing linkages were used to prevent out-of-plane movements of the members of the frames (Ref. 15). The horizontal displacement was produced by mechanically displacing the top of the frame. Overall views of the test setups for the two frames are shown in Fig. 5.

Zero-moment end conditions were imposed on the ends of the columns at the assumed points of inflection above and below the main portions of each frame. Pinned-bases utilizing roller bearings were used at the lower end of each of the lower half-story columns. A pinned-end tie beam between the two ends of the top half-story columns was used. to distribute the horizontal force.

Displacements and rotations of various points throughout the frame were measured mechanically and electrically. Strain gages were used extensively throughout the structure. Computations from the strain gage readings and the measured deflections of the gaged points reduce the frames to determinate components.

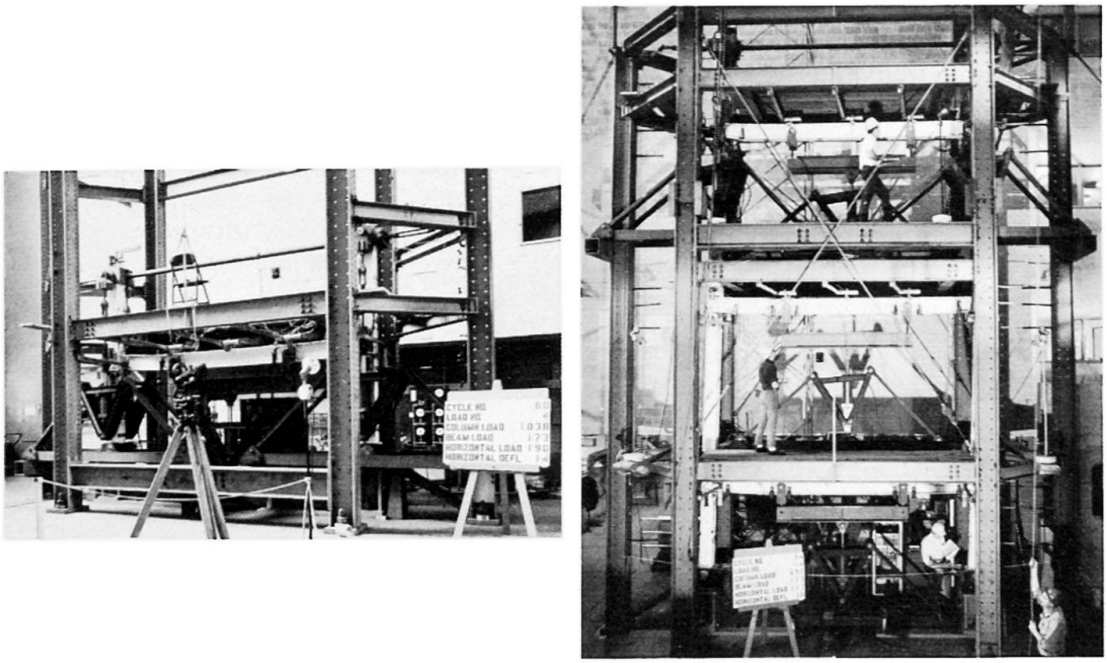

Fig. 5 Test Arrangements for Frame A and Frame B

Initially the gravity loads were applied to the frames and then sets of lateral displacements of increasing amplitudes were applied to the frames in a cyclic manner. In each case, the amplitudes to be cycled were selected to bracket the plastic hinge occurrences and other intermediate points on the respective load-deflection curves. For displacements in the elastic range three cycles were used at each amplitude and for inelastic range displacements five cycles were used. The number of replications at each amplitude was set to observe the stability of the hysteresis loops at the various amplitudes of deflection and inelastic conditions of the frames. The amplitudes selected for Frame A are superimposed on the load-deflection curve as shown in Fig. 6. The resulting displacements program is also given.

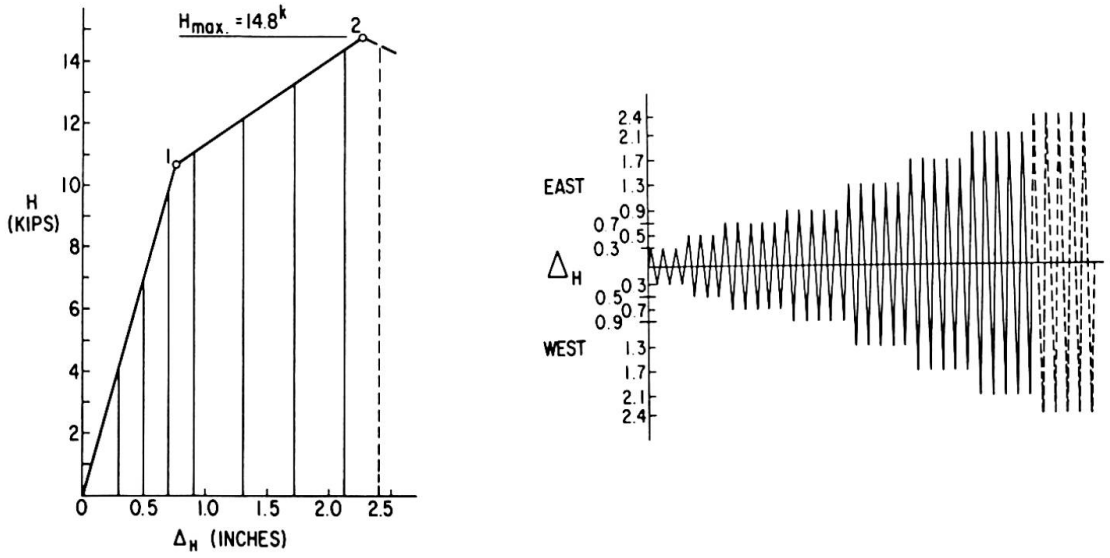

Fig. 6 Cycling Amplitudes and Horizontal Displacement Programs for Fram

During the tests, complete sets of static readings were taken at suitable intervals to permit construction of the hysteresis loops.

5) Test Results

Sixty cycles of horizontal displacement with increasing amplitudes were applied to the single-story frame with a maximum displacement of 5.2 inches which is 14 times the deflection at working load and 2.3 times the deflection at the maximum horizontal load. The three-story frame had 54 cycles at various amplitudes of displacement applied to it with a maximum cycled displacement of 10 inches. (At the end of the test 13.5 inches were applied in one direction). The displacement is 9 times the working load displacement and 1.5 times the deflection at the maximum predicted load. The ratios given above indicate the toughness and ductility of these steel frames. Cycles at selected amplitudes are shown in Fig. 7 for Frame B.

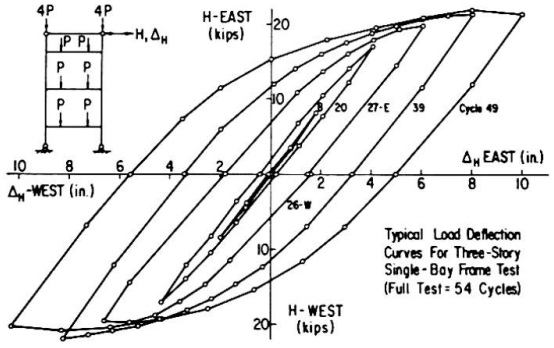

Fig. 7 Selected Load-Deflection Curves for Frame B

For the single-story frame the deflection at which the maximum load was reached was predicted closely by the monotonic analysis. But, for the three-story frame the maximum load occurred at a somewhat higher deflection (about 8 inches compared to the 6.8 inches predicted).

In addition, the replications of cycles at all amplitudes, even those beyond the frame instability deflection, showed stable results. This stability of the loops is indicated in Fig. 8 for the largest cycled amplitudes during the test of Frame A.

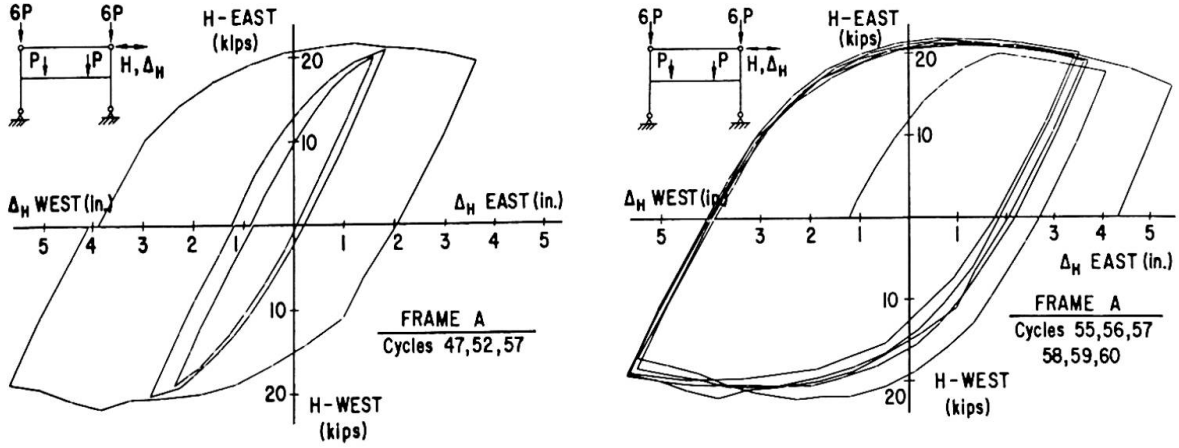

Fig. 8 Selected Load-Deflection Curves and Stability of Load-Deflection Curves for Frame A

Both tests showed a considerable reserve capacity for steel frames when subjected to cyclic lateral displacements. In each case, the maximum load the frame could withstand was about 40 percent greater than that predicted by the second-order elastic-plastic analysis of the frames under monotonically increasing lateral loads. (This percentage was computed after the analysis was redone with the actual experimental plastic moment values.)

One significant factor which tends to increase the lateral load over that predicted previously is the actual location of the plastic hinges in the beams. The analysis assumes no finite size for the beam-to-column connection whereas the yielding for the initial hinges was centered about one-half the depth of the beam from the column flange. Simple plastic analysis of Frame A shows a 17.5 percent increase in shear carrying capacity when the location of the first hinge is shifted as described above. (A preliminary estimate of the increase for a second-order analysis is 13 to 14 percent.)

The load-deflection behavior under reversed loading shows a higher maximum load than given by the monotonic analysis. However, this monotonic analysis agrees with the experimental results of the previous frame tests when the actual locations of the plastic hinges are considered. Therefore, this significant increase in maximum load is mainly due to the residual P-Δ moments existing in the frame when the reversed loading begins.

In addition, on each of the large cycles once the deflection at the maximum load had been exceeded the load carrying capacity dropped off much slower than the monotonic analysis indicated. For the monotonic analysis this downward slope is about 3 kips/inch, whereas the experimental curve showed a slope of about 1 kip/inch. This latter effect is mainly due to strain-hardening of the steel in the plastic hinge locations.

6) Conclusions

The following tentative conclusions may be drawn from the preliminary results presented in this paper:

1. The hysteresis loops are very stable even for deformations greater than those corresponding to the maximum lateral load.
2. A considerable increase in lateral load carrying capacity over that expected from a monotonic analysis is possible.
3. Strain-hardening plays an important role in the behavior of the frames for displacements greater than those at the maximum load.
4. The presence of the residual P-Δ moments has significant effects on frame behavior and must be included in developing a rational method of analysis for repeatedly loaded frames.

References

1. Nielson, N. N.
Vibration Tests of a Nine-Story Steel Frame Building, Journal of the Engineering Mechanics Division, ASCE, Vol. 92, No. EM1, Proc. Paper 4660, Feb., 1966, pp. 81-110.

2. Bouwkamp, J. G. and Clough, R. W.
Dynamic Properties of a Steel Frame Building, Steel Research for Construction, AISI, February, 1966.

3. Velestsos, A. S. and Newmark, N. M.
Effect of Inelastic Behavior on the Response of Simple Systems to Earthquake Motions, Proceedings of the Second World Conference on Earthquake Engineering, Vol. II, 1960, Japan, pp 895-912.

4. Berg, G. V.
A Study of the Earthquake Response of Inelastic Systems, Steel Research for Construction, AISI, February, 1966.

5. Goel, S. C.
Inelastic Behavior of Multi-Story Building Frames Subjected to Earthquake Motion, Ph.D Dissertation, University of Michigan, 1967.

6. Popov, E. P. and Franklin, H. A.
Steel Beam-to-Column Connections Subjected to Cyclically Reversed Loading, Steel Research for Construction, AISI, February, 1966.

7. Popov, E. P. amd Pinkney, R. B.
Behavior of Steel Building Connections Subjected to Repeated Inelastic Strain Reversal - Experimental Data - Report No. 67-31, University of California at Berkeley, December 1967.

8. Yarimci, E.
Incremental Inelastic Analysis of Framed Structures and Some Experimental Verifications, Ph.D. Dissertation, Lehigh University, 1966.

9. Arnold, P., Adams, P. F., and Lu, Le-Wu
The Effect of Instability on the Cyclic Behavior of a Frame, Fritz Laboratory Report No. 297.24, September, 1966.

10. Seismology Committee
Recommended Lateral Force Requirements
Structural Engineers Association of California, 1967.

11. Anderson, A. W , et al
Lateral Forces of Earthquake and Wind, Transactions, ASCE, Vol. 117, 1952, pp. 716-780.

12. Degenkolb, H. J.
Earthquake Forces on Tall Structures, Booklet 2028, Bethlehem Steel Corporation.

13. Driscoll, G. C., Jr., et al
Plastic Design of Multi-Story Frames, Fritz Laboratory Report No. 273.20, Summer, 1965

14. McNamee, B. M.
The General Behavior and Strength of Unbraced Multi-Story Frames Under Gravity Loading, Ph.D. Dissertation, Lehigh University, June 1967.

15. Yarimci, E., Yura, J. A., and Lu, Le-Wu
Techniques for Testing Structures Permitted to Sway, Experimental Mechanics, Society for Experimental Stress Analysis, Vol. 7, No. 8, Aug., 1967, pp. 76-84

Acknowledgments

The experimental study presented in this discussion forms part of a general investigation on "Behavior of Steel Frames Subjected to Repeated Loading" being carried out at Fritz Engineering Laboratory, Lehigh University, under the sponsorship of the American Iron and Steel Institute. Technical guidance is provided by a special Task Force organized by the Institute whose membership includes: I. M. Viest (chairman), G. V. Berg, H. J. Degenkolb, G. C. Driscoll, Jr., T. V. Galambos, C. W. Pinkham, E. P. Popov and J. L. Stratta. The authors would like to acknowledge the support given by the Institute and the advice received from the members of the Task Force.

SUMMARY

The experimental behavior of two steel (A36) frames, a single-story, single-bay frame and a three-story, single-bay frame, recently tested under constant gravity loads and a program of gradually increasing amplitudes of cyclic lateral displacement is summarized. The design and the second-order elastic-plastic analyses of the test frames under monotonically applied horizontal load are outlined and comparisons with experimental results are made.

RÉSUMÉ

Le comportement expérimental de deux portiques multi-étagés en acier A36 (Equivalent à Adx charpente), portique à un niveau et à une travée, et portique à trois niveaux et une travée, récemment testés pour des charges normales constantes et pour des déplacements cycliques latéraux dont les amplitudes ont été incrémentées graduellement, est resumé. Le calcul et les analyses du second ordre dans le domaine élasto-plastique des portiques sous charge horizontales unidirectionnelles, sont présentés, ainsi que le rapprochement avec les résultats expérimentaux.

ZUSAMMENFASSUNG

Das Verhalten eines einfachen Ein-Stockwerkrahmens und eines Drei-Stockwerkrahmens, beide mit der Stahlsorte A36 auseführt, wurde kuerzlich experimentell untersucht. Die Beanspruchung des Tragwerkes setzt sich zusammen aus vertikalen Kräften von konstanter Grösse (Graditationskräfte), und Kräften welche aus den veränderlichen, horizontalen Knotenverschiebungen resultieren. Die Konzeption der Versuchsanordnung sowie die elasto-plastischen Berechnungen zweiter Ordnung sind beschrieben und Vergleiche mit den experimentellen Resultaten wurden aufgestellt.

Performance of Steel Beams and Their Connections to Columns During Severe Cyclic Loading

Comportement de poutres en acier et de leur assemblage sur colonnes sous d'importantes charges périodiques

Das Verhalten von Stahlträgern und ihren Anschlüssen an Stützen unter schweren zyklischen Belastungen

E.P. POPOV
Professor of Civil Engineering
University of California, Berkeley

Introduction

In the Preliminary Publication for the 1968 IABSE Eighth Congress, D. Sfintesco makes reference to some of the earlier work at the University of California on steel beam-to-column connections subjected to repeated and reversed loading (1, 2). It is the purpose of this discussion to call attention to further published results (3, 4) and to provide the readers with a summary on the new work which should shortly become generally available in print (5, 6). It is gratifying that the earlier analyses as well as the penetrating opinions and observations by D. Sfintesco expressed in the Preliminary Publication are in essential agreement with the later findings.

Conventional stationary structures such as buildings, bridges and towers are not immune to dynamic loadings. As pointed out by J. Ferry Borges in the Preliminary Publication, such loadings are associated with wind and earthquake, as well as machinery, traffic, and blast loads. The general effect on stationary structures due to such loads is essentially analogous. However, the loading of buildings caused by strong earthquakes is particularly severe.

During an earthquake the soil on which a building is situated becomes subjected to a rapid back-and-forth motion in horizontal and vertical directions. The horizontal motion usually causes the more damaging effect. A representative accelerogram for a horizontal movement for an earthquake (7) is shown in Fig. 1. The typical rapidly varying inputs at the ground level reflect themselves in relatively slow swaying motions of buildings. This is due to the fortunate lack of resonance between the frequency of the ground motion input and the natural period of vibration of typical high-rise buildings.

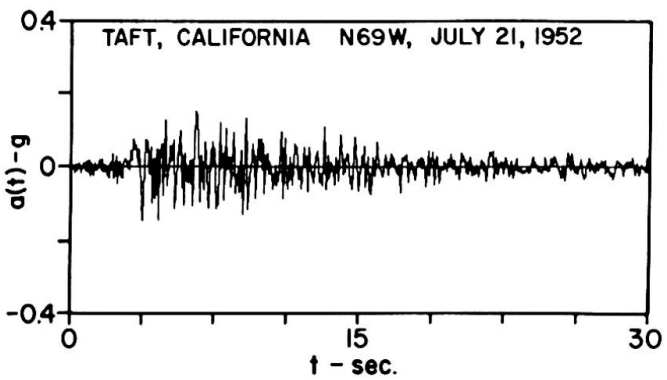

Fig. 1

The swaying motion of a severely strained building is shown schematically in Figs. 2(a) and (b), where it is assumed that the columns are relatively inflexible. This is in conformity with the current design practice which permits essentially only elastic action in the column, but allows substantial inelastic deformation in the beams and their connections to the columns.

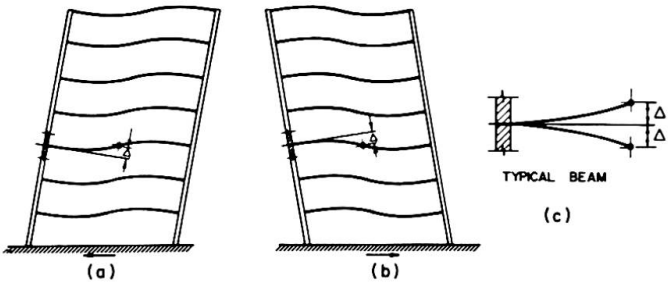

BEHAVIOR OF A FRAME IN AN EARTHQUAKE

Fig. 2

On the above basis all specimens for the first series of the California experiments were so designed that yielding occurred in the beams and their connections and not in the columns. Such yielding of the members provides damping of the structure and assures dissipation of the energy input due to an external cause such as an earthquake.

In the specimens designed for this series of experiments no attempt was made to simulate gravity loading. The question of simulating more accurately the loading on actual beams, as well as of permitting columns to exhibit some controlled yielding, is the subject of a current investigation (8).

Details of Specimens

The specimens selected in the first series of the California tests resembled the isolated element of a building frame shown in Fig. 2(c). The details of the specimens are shown in Figs. 3, 4, 5, and 6. In the specimens of the F1 type, Fig. 3, the beam was directly welded to the column stub. In the specimen of the F2 type, Fig. 4, welded connecting plates were used. In the specimen of the F3 type, Fig. 5, the attachment of the beam to the column stub through the connecting plates was achieved using high-strength bolts. The welded detail W1 for connecting a beam to the web of the column is shown in Fig. 6. All of these details represent the types widely used in the construction of steel buildings.

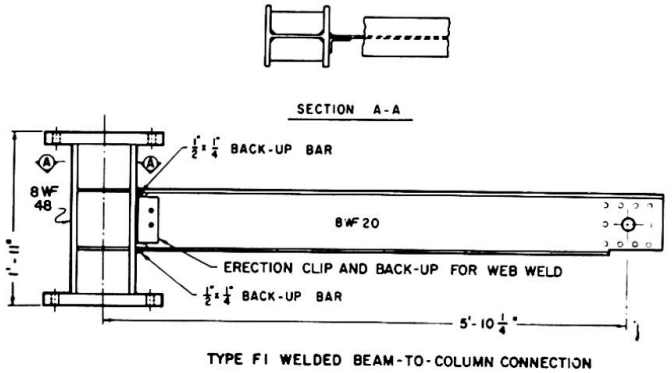

TYPE F1 WELDED BEAM-TO-COLUMN CONNECTION

Fig. 3

In several of the specimens of the F2 and the F3 types the thickness of the connecting plates was varied. For two web connected specimens, designated as W2, the connecting plates were tapered or shaped to provide a more gradual change in the cross-section of the beam flange. A total of twenty specimens using A-36 steel were fabricated according to above details. Four additional specimens, two of the F1 type and two of the F2 type, using A-441 steel formed a part of the same series of experiments (4, 5). The specimens made of a higher strength steel are identified by letters HS and referred to as F1HS and F2HS.

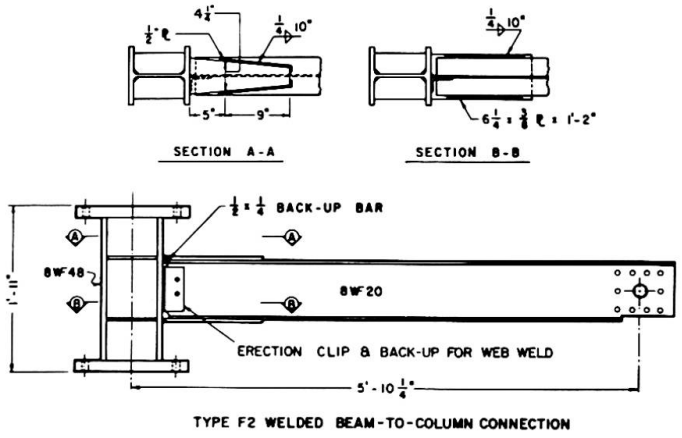

TYPE F2 WELDED BEAM-TO-COLUMN CONNECTION

Fig. 4

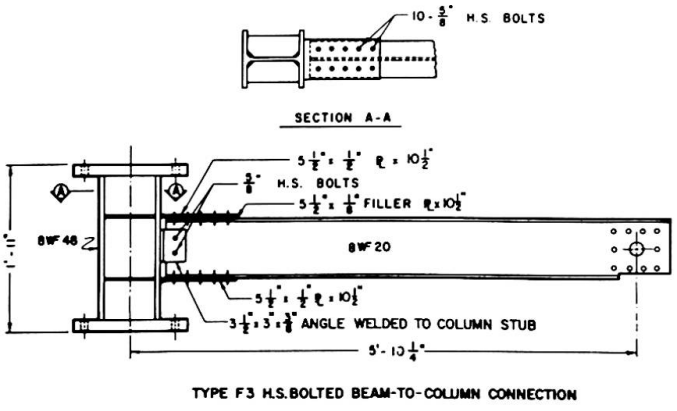

TYPE F3 H.S.BOLTED BEAM-TO-COLUMN CONNECTION

Fig. 5

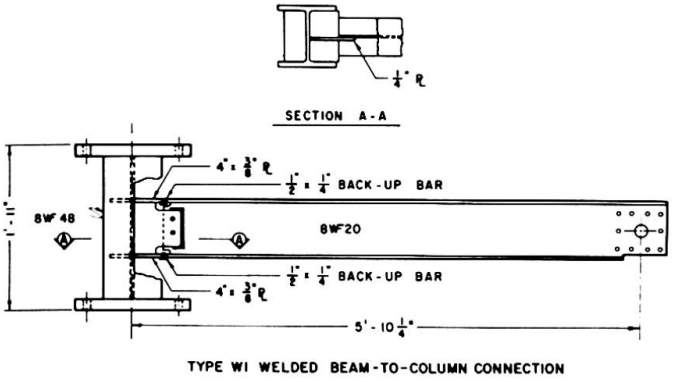

TYPE WI WELDED BEAM-TO-COLUMN CONNECTION

Fig. 6

Experimental Procedure

The basic experimental set-up is shown in the photograph of Fig. 7. A double acting hydraulic cylinder provided the desired load input at the tip of the cantilever. Experiments were controlled either by a strain gage near the built-in end of the cantilever, or by a selected tip deflection. Some typical loading programs are shown in Fig. 8. A considerable variety of such programs was used in the experiments.

In Fig. 8(a) the step-ladder type of sequence for the tip deflection is shown. Here the displacement amplitudes are arbitarily increased gradually. An experiment with a few strong initial displacements followed by the step-ladder sequence of the tip deflection is shown in Fig. 8(b).

Numerous measurements were recorded during the experiments (4, 5). Among these the load-deflection characteristics of the beam are particularly important.

Principal Experimental Results

Applying repeated and reversed loading of the type shown in Fig. 8 causes considerable yielding in the specimens during each cycle of loading application. Therefore, as is to be expected, after a number of cycles the specimens fail. The manner of failure is strongly dependent on the type of specimen, whereas the number of cycles to failure depends on the amplitudes of the tip deflection. These results are summarized in Table 1. For a more complete description of the experiments and the results, the reader is referred to References 4 and 5.

TABLE I

Specimen	Cycles to Failure	Type of Cycling Number of Cycles at Given Tip Deflection*	Total Energy Absorption kip - in.
F1-C1	28	5 at ± 1 in.; 5 at ± 2 in.; 10 at ± 3 in.; 8 at ± 4 in.	-------
F1-C2	22 1/2	22½ at ± 3 in.	2,411
F1-C3	120	100 at ± 1 in.; 20 at ± 3 in.	3,734
F1-C4	39 1/2	20 at ± 2 in.; 19 1/2 at ± 3 in.	2,837
F1-C6	32	5 at ± 3/4 in.; 5 at ± 1 1/2 in.; 10 at ± 1 1/2 in. to ± 4 in.; 12 at ± 4 in.	2,574
F2-C1	18	5 at ± 1 in.; 5 at ± 1 1/2 in.; 8 at ± 3 in.	-------
F2-C4	44	42 at ± 1 1/2 in.; 2 at ± 2 in.	2,495
F2A-C7	38 1/2	15 at ± 3/4 in.; 15 at 1 1/4 in.; 8 1/2 at ± 1 3/4 in.	1,054
F2B-C8	32 1/2	15 at ± 3/4 in.; 15 at ± 1 1/4 in.; 2 1/2 at ± 1 3/4 in.	533
F3-C1	9 1/2	5 at ± 2 1/2 in.; 4 1/2 at ± 4 in.	-------
F3-C5	30	30 at approximately ± 2 1/2 in.	1,533
F3A-C7	65 1/2	15 at ± 3/4 in.; 15 at ± 1 1/4 in.; 15 at ± 1 3/4 in.; 15 at ± 2 1/4 in.; 5 1/2 at ± 3 in.	2,488
F3B-C7	33 1/2	15 at ± 3/4 in.; 15 at ± 1 1/4 in.; 3 1/2 at ± 1 3/4 in.	704
W1-C7 **	37	15 at ± 3/4 in.; 15 at ± 1 1/4 in.; 7 at ± 2 in.	926
W1-C9	51 1/2	2 at ± 1 3/4 in.; 15 at ± 3/4 in.; 15 at ± 1 1/4 in.; 15 at ± 1 3/4 in.; 4 1/2 at ± 2 1/4 in.	1,500
W2A-C7	46 1/2	15 at ± 3/4 in.; 15 at ± 1 1/4 in.; 15 at ± 1 3/4 in.; 1 1/2 at ± 2 1/4 in.	1,189
W2B-C10	30	5 at ± 1 3/4 in.; 15 at ± 3/4 in.; 10 at ± 1 1/4 in.	651
F1HS-C7	74	15 at ± 3/4 in.; 15 at ± 1 1/4 in.; 15 at ± 1 3/4 in.; 15 at ± 2 1/4 in.; 14 at ± 2 3/4 in.	3,597
F1HS-C11	73	5 at ± 2 1/4 in.; 15 at ± 3/4 in.; 15 at ± 1 1/4 in.; 15 at ± 1 3/4 in.; 15 at ± 2 1/4 in.; 8 at ± 2 3/4 in.	3,539
F2HS-C7	35 1/2	15 at ± 3/4 in.; 15 at ± 1 1/4 in.; 5 1/2 at ± 1 3/4 in.	897
F2HS-C9	54 1/2	2 at ± 1 3/4 in.; 15 at ± 3/4 in.; 15 at ± 1 1/4 in.; 15 at ± 1 3/4 in.; 7 1/2 at ± 2 1/4 in.	2,149

* Tip deflections are approximate, and are measured from mean position.
** Results from two defectively fabricated W1 specimens are not included.

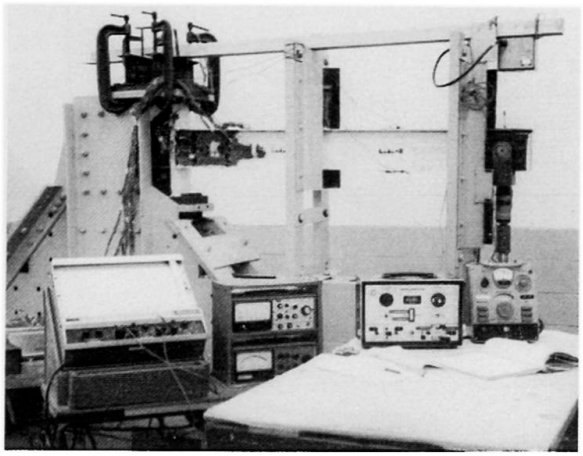

Fig. 7

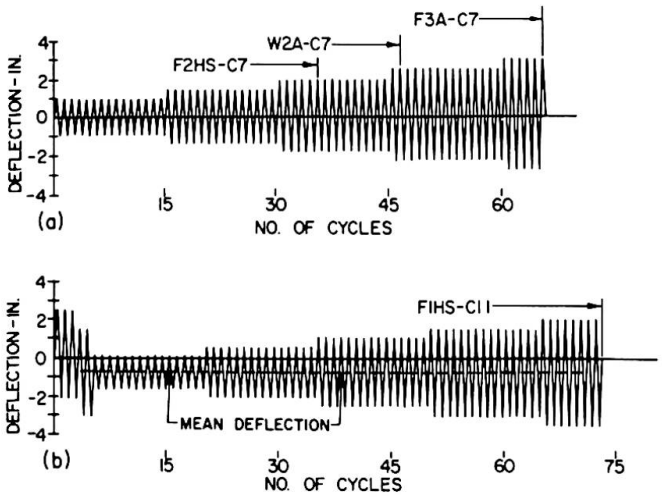

Fig. 8

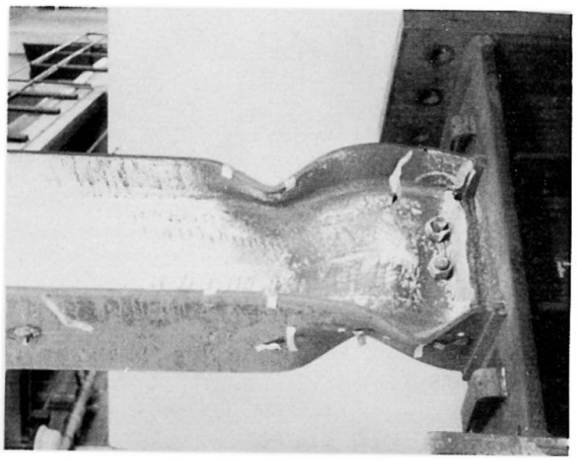

Fig. 9

A few photographs showing the manner of the ultimate failure of specimens are reproduced in Fig. 9, 10 and 11. Although such information is significant, one does not design for this condition to occur, and it is more important to answer the following two questions:

1. Can steel beams and their connections to columns withstand a sufficient number of cycles of large amplitude, i.e. of load reversals causing severe plastic strains, without breaking during a major earthquake?

2. How dependable is the energy absorption capacity per cycle during severe straining of steel?

An examination of Table 1, bearing in mind the exceptional severity of the imposed strains in the reported experiments, provides an affirmative answer to the first question. With the exception of two defectively fabricated specimens, for each specimen the number of cycles before failure occured was quite large in relation to what might be anticipated during a severe earthquake.

An examination of the hysteresis loops is necessary to answer the second question. Three sequences of hysteretic loops from one of the experiments are shown in Fig. 12. Their remarkable repetitivness and reproductibility during a number of consecutive identical cycles is noteworthy. Experimental evidence also clearly demonstrates that the onset of flange buckling does not cause the capacity of the beam to deteriorate significantly. The gradual work-softening which may be noted from Fig. 12 appears to be of no importance in seismic design as it occurs only after an excessively large number of load reversals.

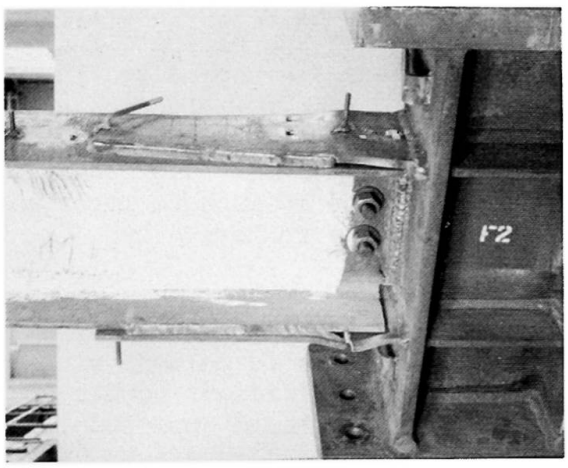

Fig. 10

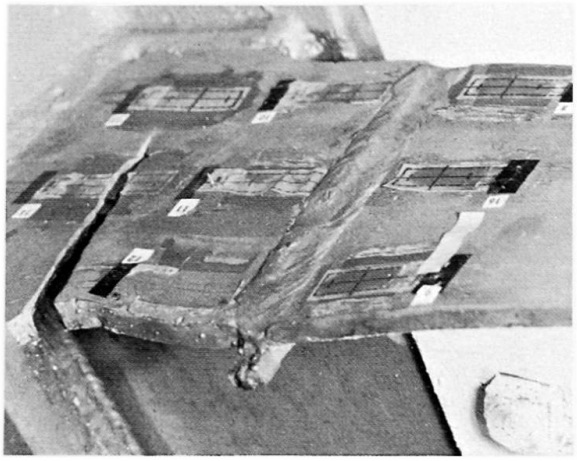

Fig. 11

The completed experiments further provided good evidence on the increase in the size of the hysteresis loops with increasing deflections. This is illustrated in Fig. 13. An approximate linear relationship between the area enclosed by the hysteresis loops with the increasing plasticity ratio has been proposed (4, 5). Therefore, on the basis of the experimental evidence, it appears that the reliability of the energy absorption capacity of properly designed and fabricated structural steel beams and their connection, is assured.

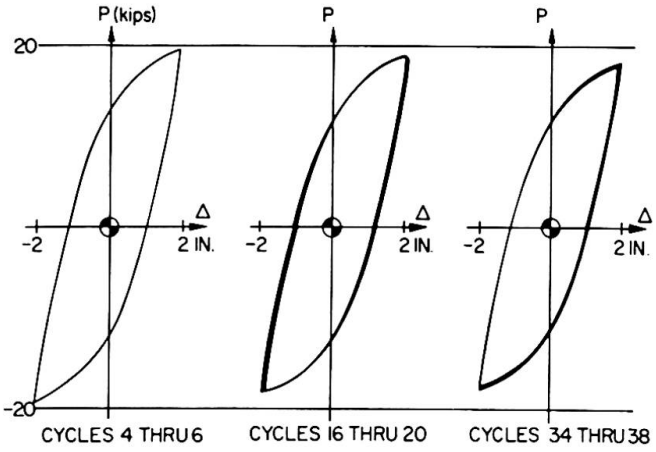

Fig. 12 Specimen F2-C4

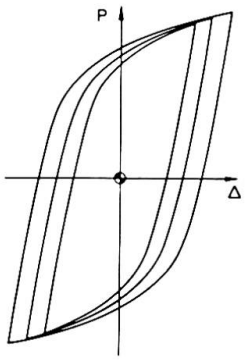

Fig. 13

Application of Experimental Results

Once one is satisfied that the hysteresis loops are reproducible during consecutive identical cycles of load application, and that the increase of the loops with increasing deflections is reasonably well established, this information can be put in mathematical form suitable for the analysis of structures. The well-known Ramberg-Osgood representation of non-linear load-displacement relationships together with Masing's hypothesis provide suitable mathematical formulations (5, 9).

Precisely this type of idealization has been applied by Berg (10) to some of the hysteresis loops generated in these experiments. By using such a formulation he studied the response of the assumed structure to a very severe ground motion are shown in Fig. 14(a), (b) and (c). The same results superposed on the same graph are shown in Fig. 15. The lateral displacements for the assumed structure having one degree of freedom are shown in Fig. 16 for a longer period of time. From this figure it is seen that often the displacements are not as severe as shown in Fig. 15 and are essentially elastic in their character.

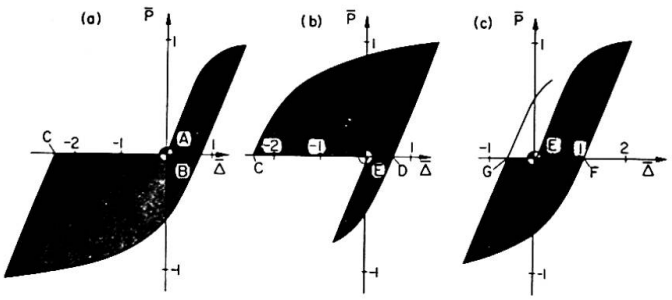

Fig. 14

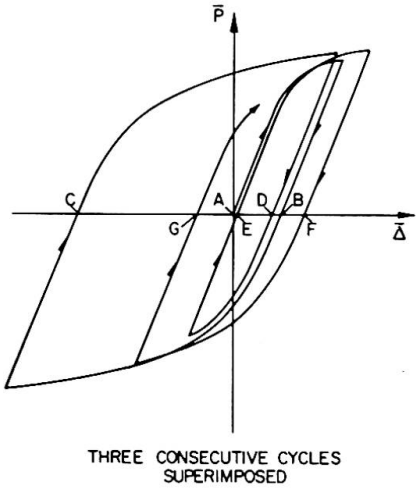

Fig. 15

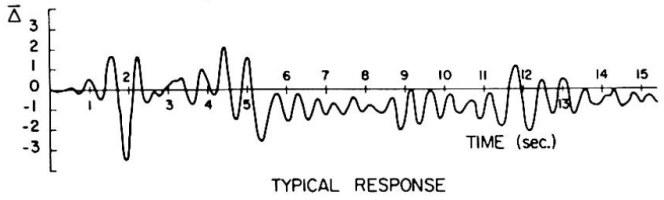

Fig. 16

Studies such as made by Berg for the above simple problem are the kind that are needed for real structures. From such studies the behavior of any one connection can be determined for an assumed earthquake. The amount of energy to be dissipated (shaded areas in Fig. 14) could be found and an assessment of the adequacy of the joint be made. Such a procedure would place the aseismic design of buildings on a more rational basis.

Acknowledgements

The work reported in this discussion was sponsored by the American Iron and Steel Institute. Among the number of people who have participated in this program, the writer is particularly indebted to R. B. Pinkney, a graduate student at the University of California, who participated in all phases of this investigation.

References

1. Bertero, V. V., and Popov, E. P., "Effect of Large Alternating Strains on Steel Beams", J. of Struct. Division ASCE, Vol. 91, ST1, Feb. 1965, pp. 1-12.

2. Popov, E. P., and Franklin, H. A., "Steel Beam-to-Column Connections Subjected to Cyclically Reversed Loading", Proceedings 34th Annual Convention, Struct. Eng. Assoc. of California, October 1965, pp. 79-86.

3. Popov, E. P., "Low-Cycle Fatigue of Steel Beam-to-Column Connections", Internat. Symposium on The Effects of Repeated Loading of Materials and Structural Elements, Mexico City, 1966, Vol VI.

4. Popov, E. P., and Pinkney, R. B., "Behavior of Steel Building Connections Subjected to Repeated Inelastic Strain Reversal-Experimental Data", University of California, Berkeley, SESM 67-31, December 1967.

5. Popov, E. P., and Pinkney, R. B., "Alternating Inelastic Strains in Steel Connections", J. of Struct. Division ASCE, (in preparation).

6. Popov, E. P., "Reliability of Steel Beam-to-Column Connections under Cyclic Loading", Fourth World Conference on Earthquake Engineering, Santiago, Chile, January 1969, (in preparation).

7. Courtesy of Professor Joseph Penzien.

8. Current AISI Project 145 under the supervision of V. V. Bertero and E. P. Popov.

9. Jennings, P. C., "Periodic Response of a General Yielding Structures", J. of Eng. Mech. Division ASCE, Vol. 90, EM2, April 1964, pp. 131-166.

10. Berg, G., "A Study of the Earthquake Response of Inelastic Systems", Preliminary Reports - Steel Research for Construction, February 1966, AISI.

SUMMARY

In this discussion attention is called to the availability of some of the new experimental results on the inelastic behavior of steel cantilever beams and their connections to column stubs during repeated and reversed cyclic loading. The described experiments attempt to simulate the conditions which develop in structural steel frames during an earthquake.

RÉSUMÉ

Cette contribution signale l'existence de nouveaux résultats expérimentaux concernant le comportement inélastique de poutres consoles en acier et leur liaison à des colonnes courtes soumises à des charges périodiques répétées et alternées. Le but des expériences décrites est de simuler les conditions qui se développent dans des ossatures en acier pendant un tremblement de terre.

ZUSAMMENFASSUNG

In diesem Beitrag soll auf einige der neueren experimentellen Ergebnisse über das inelastische Verhalten von Kragträgern aus Stahl aufmerksam gemacht werden, sowie ihren Anschlüssen an Stützenabschnitte, wenn die Träger wiederholten, zyklischen Wechselbelastungen ausgesetzt sind. Anhand der angeführten Versuche wird versucht, die Bedingungen nachzuahmen, die während eines Erdbebens in Rahmenkonstruktionen aus Stahl auftreten.

Leere Seite
Blank page
Page vide

Inelastic Behavior of the Steel Framed Structure Subjected to the Seismic Force

Comportement inélastique de structures en câdres d'acier soumises à des forces sismiques

Unelastisches Verhalten des Stahlrahmentragwerkes unter Erdbebenkraft

BEN KATO
Associate Professor

HIROSHI AKIYAMA
Research Associate

The University of Tokyo
Japan

Introduction

To clear the safety of the structure against earthquake, it is necessary to know the inelastic behavior of beams, columns and entire frames until their collapse state under alternating loading as the author states. This discussion concerns to evaluation of the inelastic behavior of steel structural members.

It is known that the conventional simple plastic theory cannot predict the actual inelastic behavior of the steel structures even in monotonous loading, and it can be said that this mainly comes from the fact that the strain hardening property of the material is not taken into account in that analysis, and the effect of the applied axial load is not evaluated reasonably.

We suggest the solution for the beam-column subjected to axial compression and bending moment which makes allowance for the strain hardening and the effect of the axial compression. The load deflection diagram under alternating loading is shown to be obtained from the load deflection diagram under monotonous loading by the simple definite procedure.

Furthermore, the response analysis of the one mass vibration model of the steel structure is done using the clarified inelastic characteristics, and the difference of the response is shown to be attributed to the difference of evaluation of the effect of the strain hardening upon the structure.

Inelastic Behavior of Steel Members

Monoaxial bending only is treated here, and the effect of shear stress is ignored. Lateral buckling is also out of the matter. Breaking-off and local buckling of the section element of the member are considered to be the most effective origins of the collapse of the member and these origins can be predicted by some material tests.

General feature of the stress strain relation of steel may be expressed by the diagram as shown in Fig.(1).

As the bending deformation is obtained by integration of the

curvature along member axis, to determine the moment curvature relation is the essential procedure.

Moment Curvature Relation--- Case I when the bending moment is applied in monotonous way: The bending moment is to be applied about x-x axis in Fig.(2), and the section of the member is assumed to be symmetric about the axis perpendicular to the bending axis. Axial compression is kept in constant, and the moment increases gradually.

Let the solid line of Fig.(3) be the strain distribution at the arbitrary inelastic state under moment M, and the broken line be that of after infinitecimal increase of the curvature due to the increase of moment. Then the following relation are derived from the equilibrium condition of stress.

$$dH_1=-\frac{d\phi}{\phi}H_1\ ,\quad dH_1'=-\frac{d\phi}{\phi}H_1'\ ,\quad dH_2=-\frac{d\phi}{\phi}H_2\ ,\quad dH_2'=-\frac{d\phi}{\phi}H_2'$$

$$dS_e=(dH_1B_1+dH_2B_2)e_1+(dH_1'B_1'+dH_2'B_2')e_2$$

$$dI_e=(dH_1B_1H_1^2+dH_2B_2H_2^2)e_1+(dH_1'B_1'H_1'^2+dH_2'B_2'H_2'^2)e_2$$

$$dO=\left\{-(dH_1B_1H_1-dH_2B_2H_2)e_1-(dH_1'B_1'H_1'-dH_2'B_2'H_2')e_2\right\}/S_e$$

where ϕ: curvature $d\phi$: increment of ϕ

ε_y: strain at yield point

ε_{st}: strain at strain hardening point

e_1: $(E_1-E_2)/E_1$ e_2: $(E_2-E_3)/E_1$

H_1: distance from the transient neutral axis to the compression fibre where the strain is equal to ε_y.

H_2: distance from the transient neutral axis to the tension fibre where the strain is equal to-ε_y.

H_1': distance from the transient neutral axis to the compression fibre where the strain is equal to ε_{st}.

H_2': distance from the transient neutral axis to the tension fibre where the strain is equal to-ε_{st}.

S_e: effective area, which means the sectional area of the ficticious elastic bar which has the equivalent axial rigidity to the actual bar in the specified inelastic state.

I_e: effective moment of inertia, which means the moment of inertia of the ficticious elastic bar which has the equivalent flexural rigidity to the actual bar in the specified inelastic state.

dO: movement of the transient neutral axis

B_i, B_i' : width of the section at H_i, H_i' respectively.

After the increase of the curvature $d\phi$, these quantities will change as follows.

$$H_1\rightarrow H_1+dH_1+dO\ ,\quad H_2\rightarrow H_2+dH_2-dO$$

$$H_1'\rightarrow H_1'+dH_1'+dO\ ,\quad H_2'\rightarrow H_2'+dH_2'-dO$$

$$S_e\rightarrow S_e+dS_e\ ,\quad I_e\rightarrow I_e+dI_e\ ,\quad \phi\rightarrow\phi+d\phi\ ,\quad M\rightarrow M+E_1I_e\,d\phi$$

M-ϕ relation may be pursued successively using the above relaion throughout the whole strain range. Numerical calculation is performed easily by the aid of the electronic digital computer.

Case II when the bending moment is applied alternatingly: It is very complicated to describe the exact M-ϕ relation under alternating bending. So by the aid of the simplified model given below, an outline of the relation is sought after.

1. Member section is sandwitch type as shown in Fig(4).
2. Stress strain relation of steel under alternating loading is as shown in Fig.(5b). To be more precise, with regard to the stress in definite sign the stress strain relation has the same configuration as that under monotonous loading as shown in Fig.(5a).

On such a model it is easily understood that the M-ϕ relation under alternating loading is obtained as shown in Fig.(6b). Fig.(6a) shows the M-ϕ relation under monotonous bending. Comparing Fig.(6a) and Fig.(6b), it can be seen that in Fig.(6b) with regard to the bending moment in one direction the M-ϕ relation has the same configuration as that shown in Fig.(6a).

The actual shape of section differs from that provided by the condition 1. Hence when the bending moment is removed, the residual stress is introduced over the section. In this paper, however, the effect of such a residual stress is assumed to be negligible, so the M-ϕ relation obtained above becomes applicable to any section.

Load Deflection Curve of Steel Members--- Deflection of the member is readily obtained by integration of the curvature corresponding to the bending moment produced by the external loads. For the exact solution numerical integration technique is effective, but in some cases approximate solution provides facility for engineering purposes. Especially the solution under alternating loading is uselessly troublesome. Hence for this case some devices in approximation are needed.

When the bending stress is determined uniquely by the external loads, the correlation between the load deflection curve under alternating loading and that under monotonous loading is similar to the correlation as exists in M-ϕ relation. As is shown in Fig.(7), the load deflection diagram under alternating loading is readily obtained from that under monotonous loading. With regard to a definite direction of loading, the load deflection curve in Fig.(7b) has the same configuration as that in Fig.(7a).

But in general, geometry change of the member affects upon the bending moment distribution. In Fig.(8) two cantilever columns are shown for example. When the end load is applied alternatingly under constant axial load P, lateral deflection produces secondary bending. When the end load is removed after some extent of the inelastic deformation in one direction, deflection remains and to remove the residual moment at the fixed end, end loads of $-P\delta/\ell$ in the case of Fig.(8a) and $-P\delta$ in the case of Fig.(8b) are required respectively. In such a state residual stress still remains along the member axis as shown in Fig.(9). Here, we assume that the residual stress shown in Fig.(9) has no effect upon the load deflection relation under further application of the end load in the opposite direction. Based on the assumption, we can depict the load deflection curve as shown in Fig.(10), that is, the load deflection curve under alternating loading is obtained from that under monotonous loading in the same manner as is shown in Fig.(7). In Fig.(7) the abscissa is the basal line whereas in Fig.(10) the broken line which shows the tentative unloaded state of the member is the basal line, and with regard to the load deflection relation in one side of this line, the curve under alternating loading has the same configuration as that under monotonous loading. From this figure it can be seen that the summation of the plastic deformation in one direction until collapse does not exceed the plastic deformation capacity under monotonous loading.

Comparison with Test Result--- Load deflection curves were obtained using the test specimens as shown in Fig.(11). In specimen(A) the column is subjected to axial thrust and the transverse shear force increasing proportionally according to

the following condition.

$$P=V\cos\psi \ , \quad Q=V\sin\psi$$

Where V is the applied load.

In specimen(B) the column is subjected to constant axial load and alternating end moment conducted through beams.

Stress strain relation of the material was obtained from the stub column test, and is shown in Fig.(12). The maximum stress was reached by occurence of the local buckling of flanges.

M-ϕ relation obtained from the procedure mentioned above is shown in Fig.(13). Load deflection curve of the specimen(A) is shown in Fig.(14), and the curve of the specimen(B) is shown in Fig.(15) in which the theoretical curve under monotonous bending is shown by the curve ABC.

Collapse of the member was assumed to occur when the stress at the point where the maximum moment grows reachs σ_B over entire section. M_B corresponds to such a stress distribution. In Fig. (14) and (15) theoretical curves after collapse are drawn on the assumption that the maximum moment of the specimen is kept to be M_B.

In these figures the test results agree with the theoretical prediction fairly well, and the effect of the strain hardening upon the inelastic behavior is very remarkable.

Response Analysis of the Framed Structure

Restoring Force Characteristics--- The cantilever column shown in Fig.(16) represents the fundamental element of the framed structure subjected to seismic force. To see the general feature of resistance of the framed structure to seismic force, a simple outline of the inelastic behavior of the cantilever column is sought after through the approximate approach.

The M-ϕ relation under the constant thrust obtained above may be approximated by two linear segments ignoring the elastic part of it. The first segment is parallel to the abscissa at M_{PC}.

At first the deflection of the member is evaluated ignoring the effect of the secondary bending caused by the geometry change. In Fig.(17) the part of the column ab is in inelastic range under the given loads P and Q, the the distribution of the curvature along the member is expressed as shown in Fig.(17b). This is reduced to the simplified model as shown in Fig.(17c) in which the curvature of the inelastic part ab is approximated by the mean value of the curvatures at the both ends of ab, then the mean value ϕ_o may be written as follows.

$$\phi_o = \frac{\phi_{st}+\phi_f}{2} = \frac{M_f - M_{PC}}{2D_{st}} + \phi_{st} \qquad (1)$$

Where ϕ_{st}: the curvature at the starting point of the strain hardening.

D_{st}: the flexural rigidity in strain hardening range. Namely the slope of the second segment.

M_{PC}: the fully plastic moment under axial force.

M_f: the fixed end moment

The lateral deflection δ_b and the slope θ_b at point b are given as follow.

$$\delta_b = (\phi_o l_1^2)/2 \ , \quad \theta_b = \phi_o l_1$$

Then the lateral deflection at the top of the member may be given as follows.

$$\delta = \phi_o l_1 l_2 + (\phi_o l_1^2)/2 \qquad (2)$$

Where l_1: the length of the inelastic part of the member.

l_2: the length of the elastic part of the member.

As the bending effect of the thrust P is ignored, the follwing

relation will hold for any shear force Q'.

$Q'l_2 = M_{pc}$, $Q'l = Q'(l_1 + l_2) = M_f$

These are translated as:

$l_1/l = (\alpha-1)/\alpha$, $l_2/l = 1/\alpha$, $\alpha = M_f/M_{pc}$

From equation(1) and (2), introducing the expression $M_{pc} = D\phi_y$, and $\beta = \phi_{st}/\phi_y$, the lateral deflection is written as follows.

$$\delta = \left(\frac{\alpha-1}{2} \times \frac{D}{D_{st}} + \beta\right)\left(\frac{\alpha^2-1}{2\alpha^2}\right) l^2 \phi_y \qquad (3)$$

Where D: flexural rigidity in the elastic range

As the second step, the effect of the secondary bending must be taken into account. This effect is illustrated in Fig. (18) where the curve ac shows the deflected configuration of the member. Horne*had approximated this configuration by the straight line connecting the both ends of the members as shown in Fig. (18a). Then the equivalent lateral force Q which provide the same bending moment at the fixed end is given as follows.

$$Q = (M_f - P\delta)/l = (\alpha M_{pc} - P\delta)/l \qquad (4)$$

Equation (3)and (4) give the Q-δ relation.

This approximation, however, underestimates the secondary bending and the another approximation as shown in Fig.(18b) is proposed, where the point* shows the coordinate $(\delta, (\alpha-1)l/2\alpha)$. $(\alpha-1)l/2\alpha$ denotes the midheight of the inelastic portion, and the deflected shape of the member is approximated by the straight line also. This choice seems to be rather arbitrary, but it will be shown later that this gives the better approximation to the exact solution. In this approximation the equivalent horizontal shear force is given as follows.

$$Q = \left\{\alpha M_{pc} - \left(\frac{2\alpha}{\alpha+1}\right)P\delta\right\} / l \qquad (5)$$

Comparison with the exact solution is made in Fig.(19) with regard to the Q-δ relation using the same section member as shown in Fig.(11), and the same stress strain relation as shown in Fig.(12).

In the case of no axial thrust these two methods coincide, however when the axial force becomes larger, it can be seen that the later method gives better approximation than the former one. In Fig.(20) Q-δ diagram for the same member derived from the conventional theory ignoring the strain hardening is given. Comparing these two figures, it can be seen that the effect of the strain hardening is very significant.

Besides, from Fig.(19) it can be seen that the inelastic deflection curve may be approximated by the linear relation without substantial error. Hence the fundamental feature of the restoring force characteristics of the framed structure may be suggested to be the relation as shown in Fig.(10).

Response Analysis of the 1 Mass System--- Using the restorig force characteristics given in Fig.(21) the response analysis was done . For an example, one mass viburation system as shown in Fig.(21) is chosen.

The ground motion is of N-S component of El Centro 1940, May(the peak value of acceleration is 330 gals)

Governing equation of the sytem is as follows.

$$m(\ddot{y}+\ddot{y}_o)+f(y)=0$$

Where y: deflection , y_o: ground motion

f(y): restoring force characteristics

Result of the analysis is given in Fig.(22). Fig.(22a) shows the residual plastic deflection after the ground motion is faded away. Fig.(22b) shows the maximum deflection during the

earthquake and Fig.(22c) shows the summation of the plastic deflection in one direction.

The ordinate of these diagram expresses the yield force coefficient which is given as follows.

$f=F_y/mg$

Where g: acceleration of gravity

The abscissa expresses the plastic deflection divided by the initial elastic limit deflection which corresponds to the initial elastic limit stress F_y.

In these figures, the parameter K denotes the strain hardening effect. When the strain hardening does not exist, the value is equal to the slope of the basal line ff' in Fig.(21) which denotes the effect of the secondary bending by the weight of the mass.

From these figure it can be seen that the plastic deflection is considerably affected by the strain hardening effect and especially development of the residual deflection is moderated by the strain hardening.

Conclusion

The more precise aspect of the inelastic behavior of the steel members has been pursued by the experiment and the analysis which makes allowance for the strain hardening property of steel.

The effect of the strain hardening property upon the deflection response of the steel framed structure to an earthquake was evaluated, and that was shown to be very remarkable.

Reference

* Horne M.R. , Medland I.C. : Collapse Loads of Steel Frameworkes Allowing for the Effect of Strain Hardening.
Proc. Institution of Civil Engineers 1966, May

Fig.(1) Stress Strain Relation

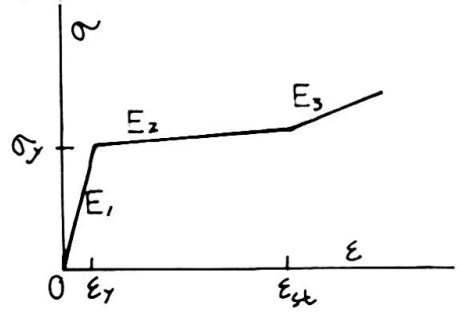

Fig.(2) Section Shape

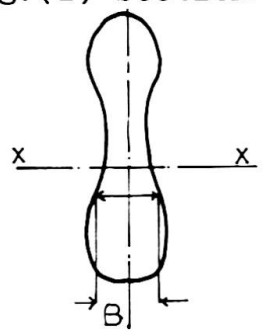

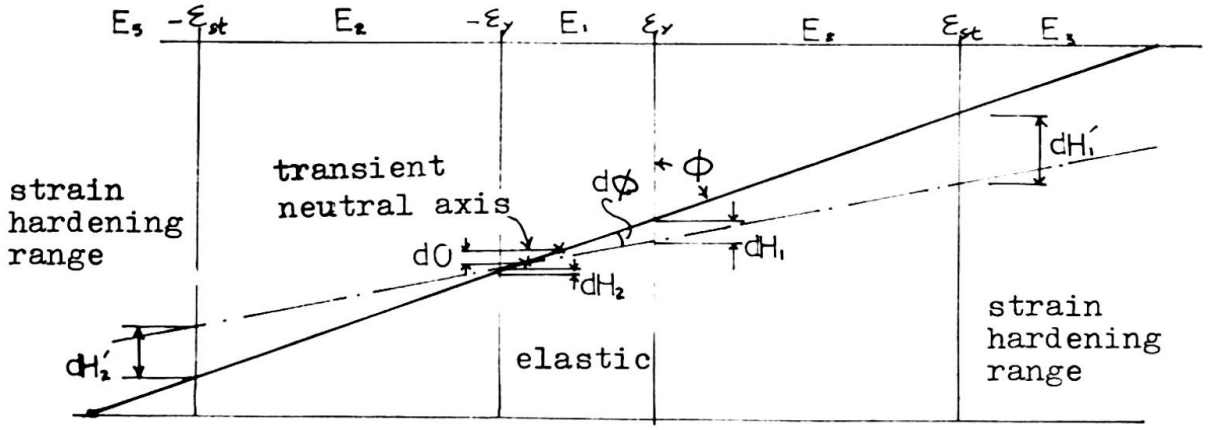

Fig.(3) Strain Distribution over the Section

Fig.(4) Simplified Section

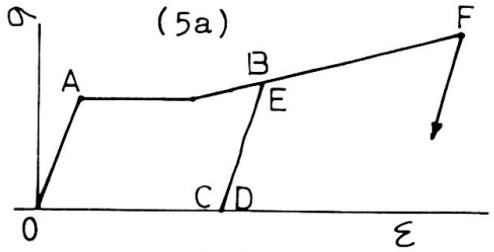

Fig.(5) Stress Strain Relation

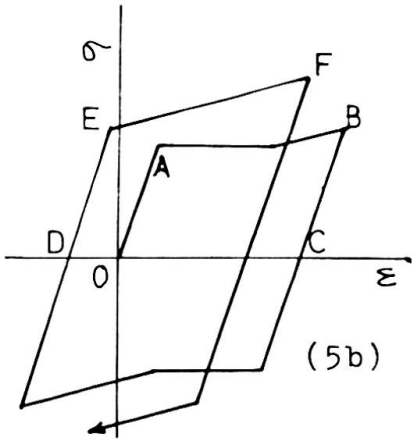

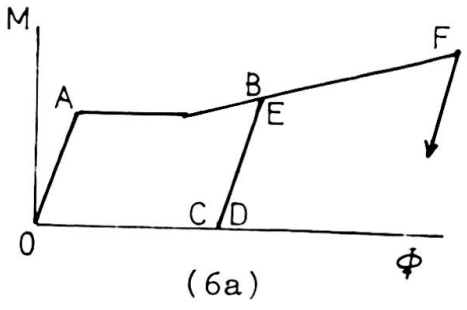

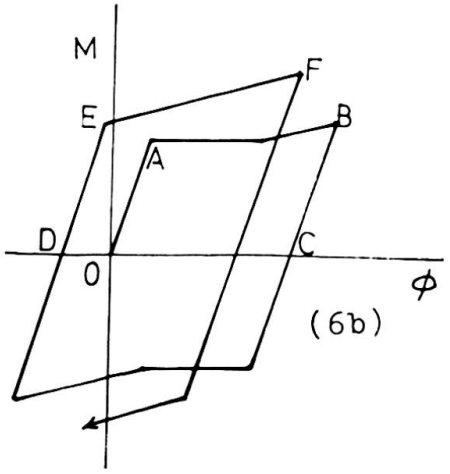

Fig.(6) M-φRelation

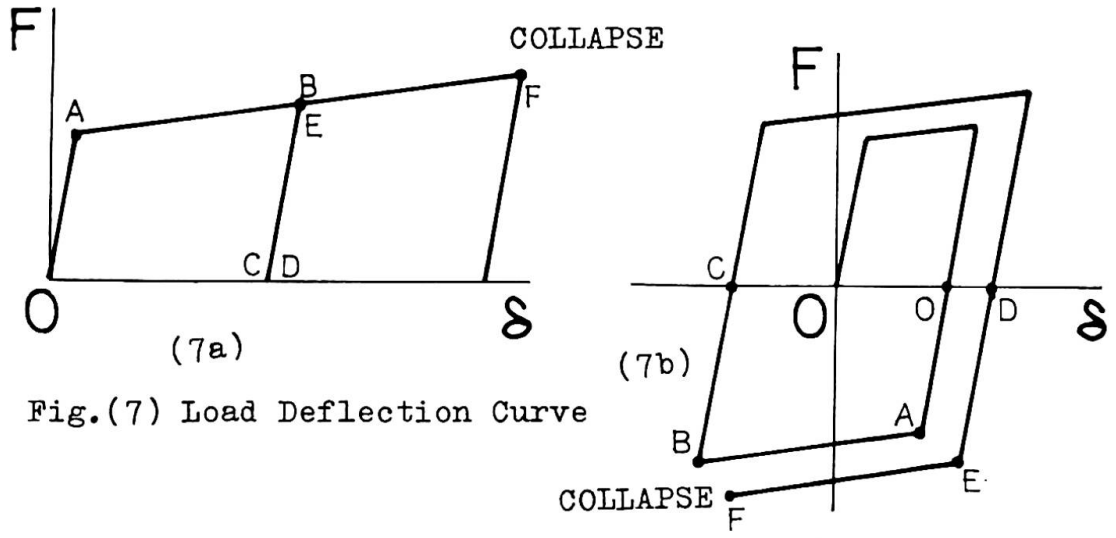

Fig.(7) Load Deflection Curve

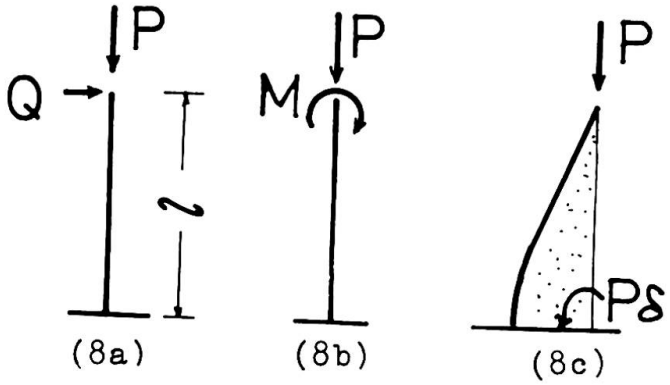

Fig.(8) Cantilever Column

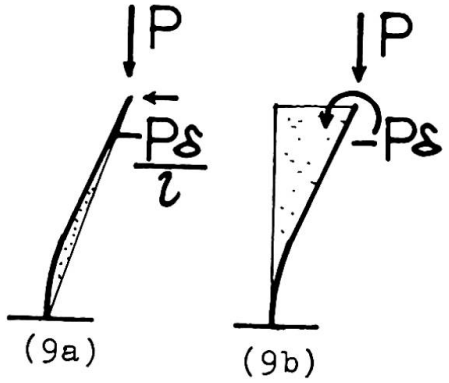

Fig.(9) Residual Stress

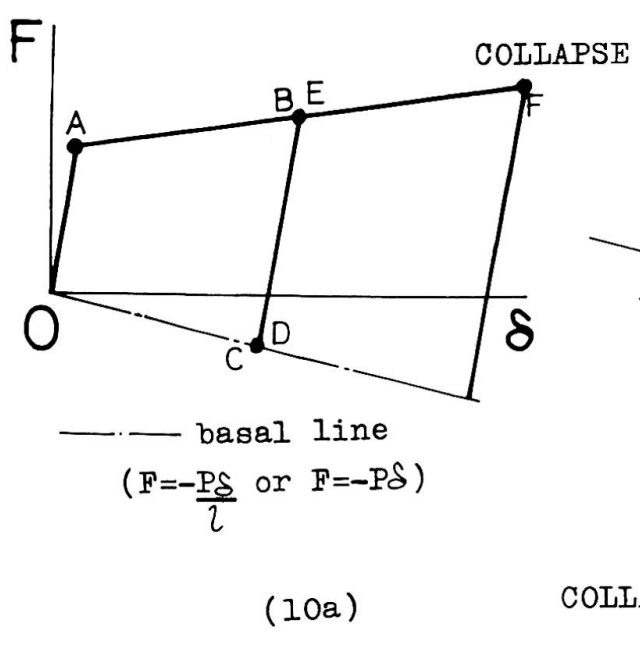

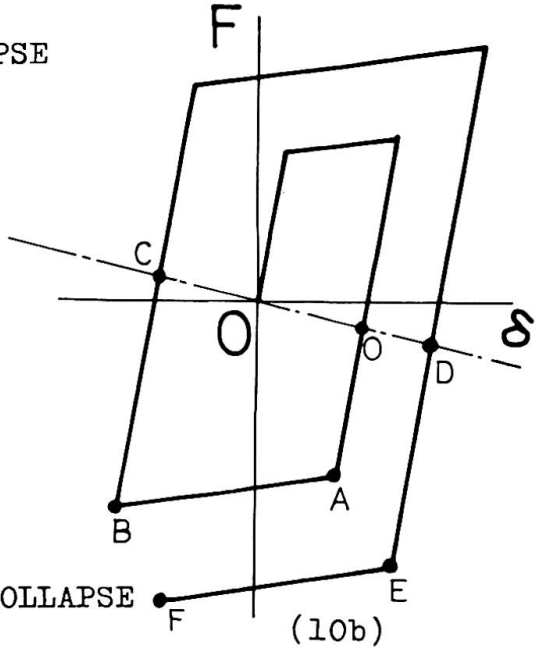

Fig.(10) Load Deflection Curve under Alternating Loading

Fig.(11) Tect Specimens

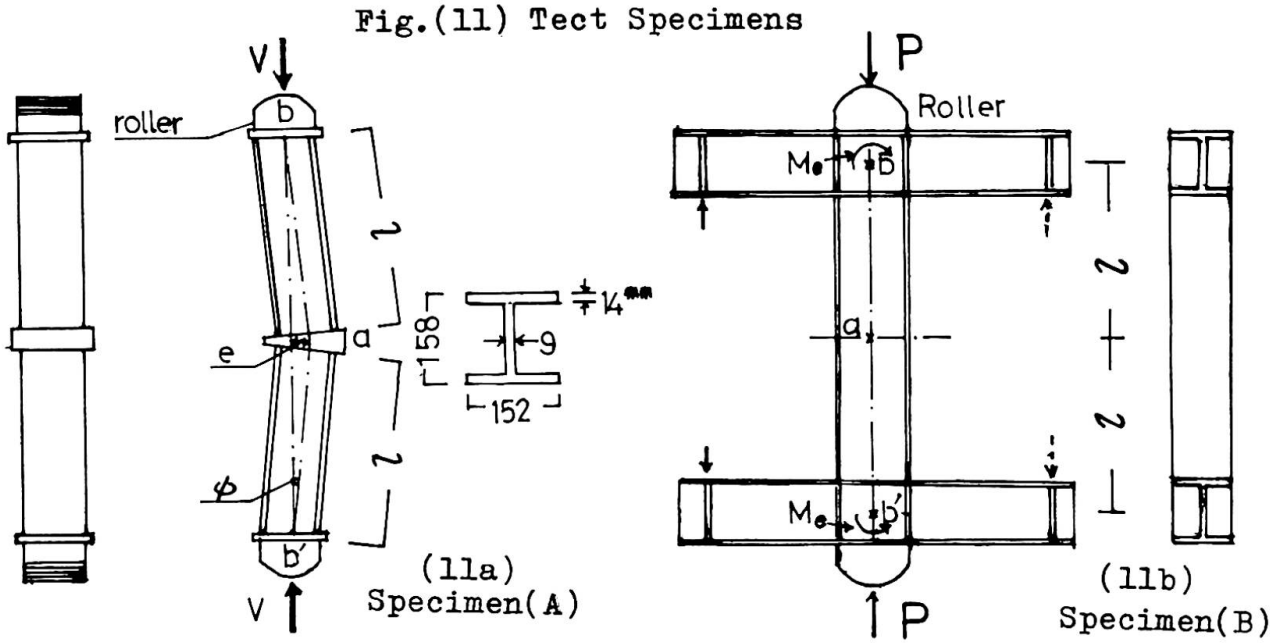

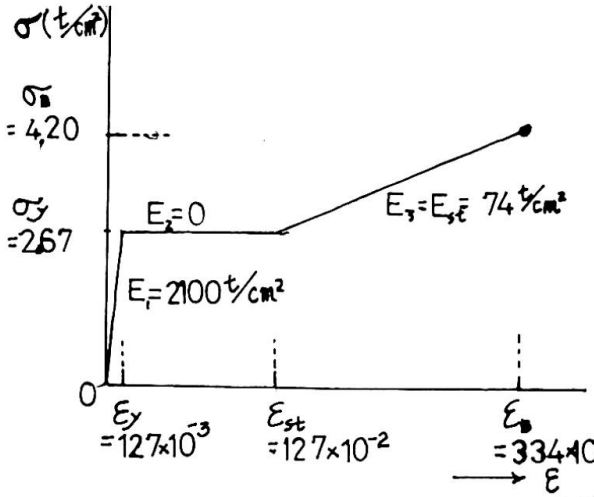

Fig.(12) Stress Strain Relation

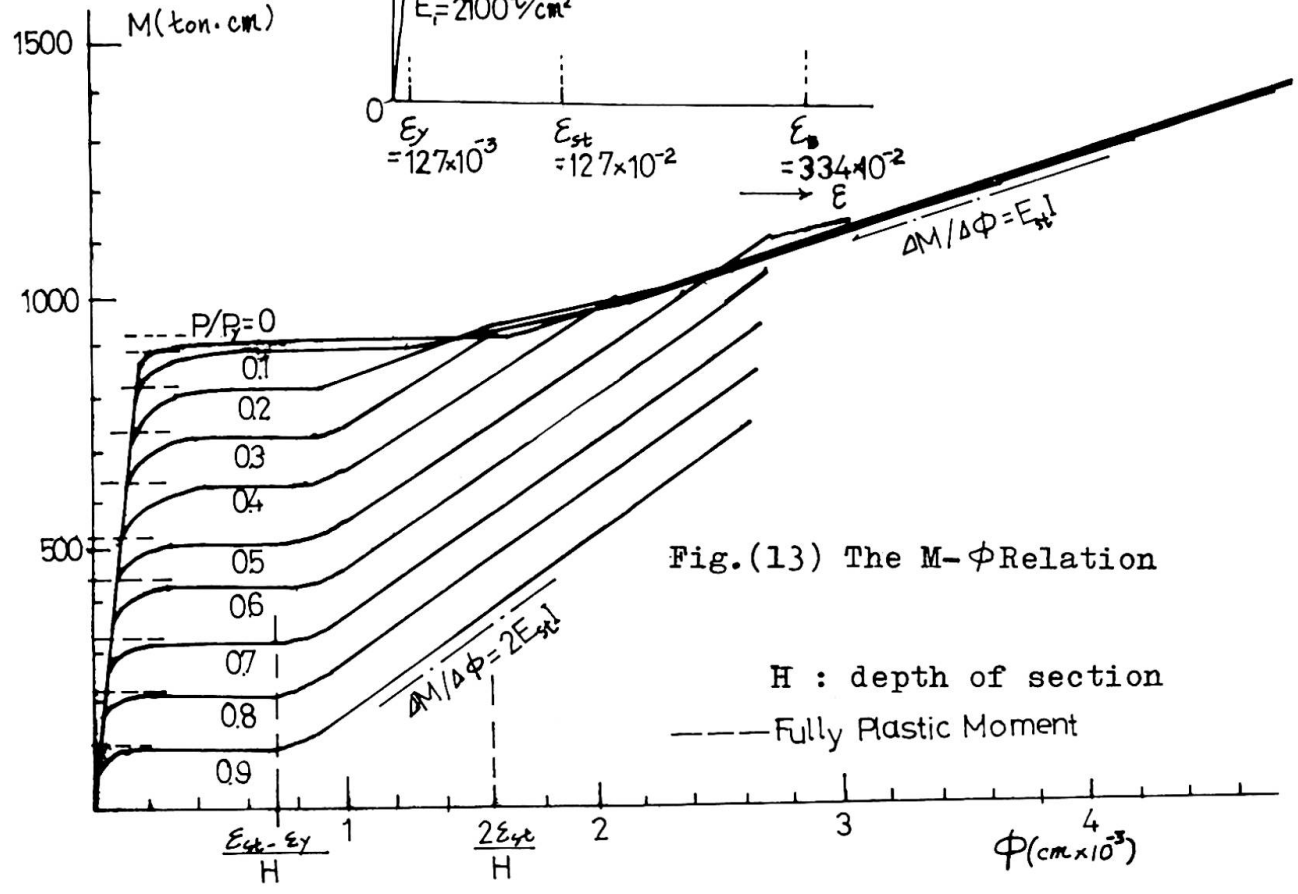

Fig.(13) The M-φ Relation

H : depth of section

———Fully Plastic Moment

Fig.(14) Load Deflection Curve of (A)

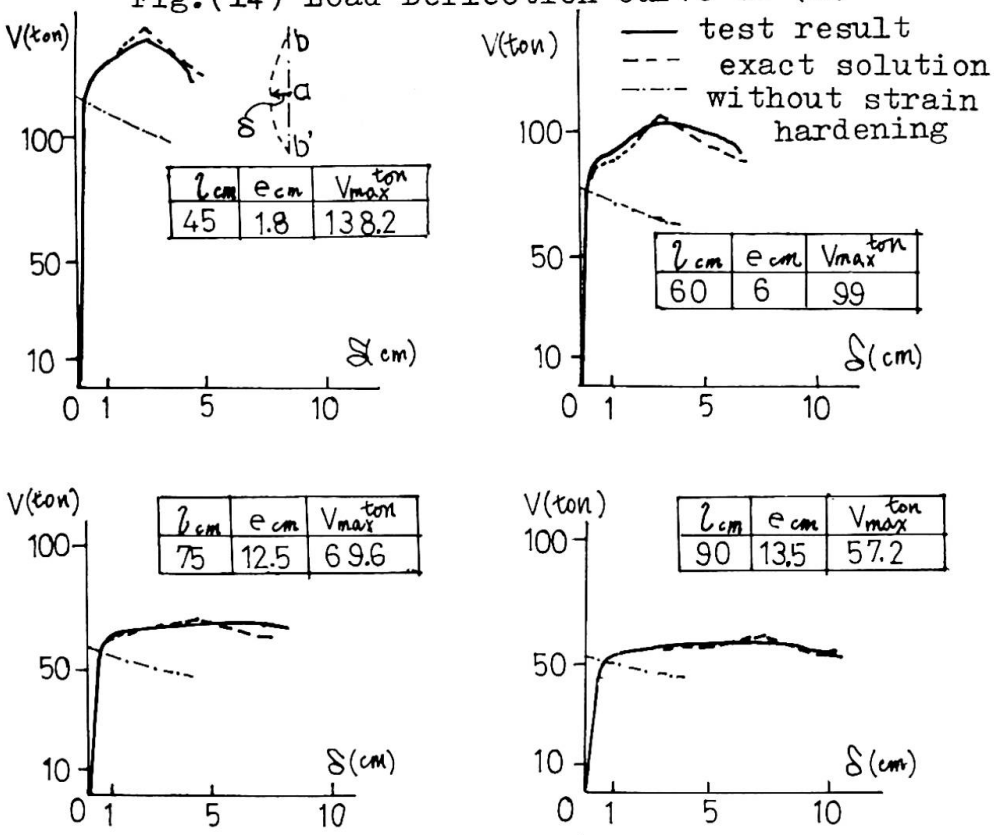

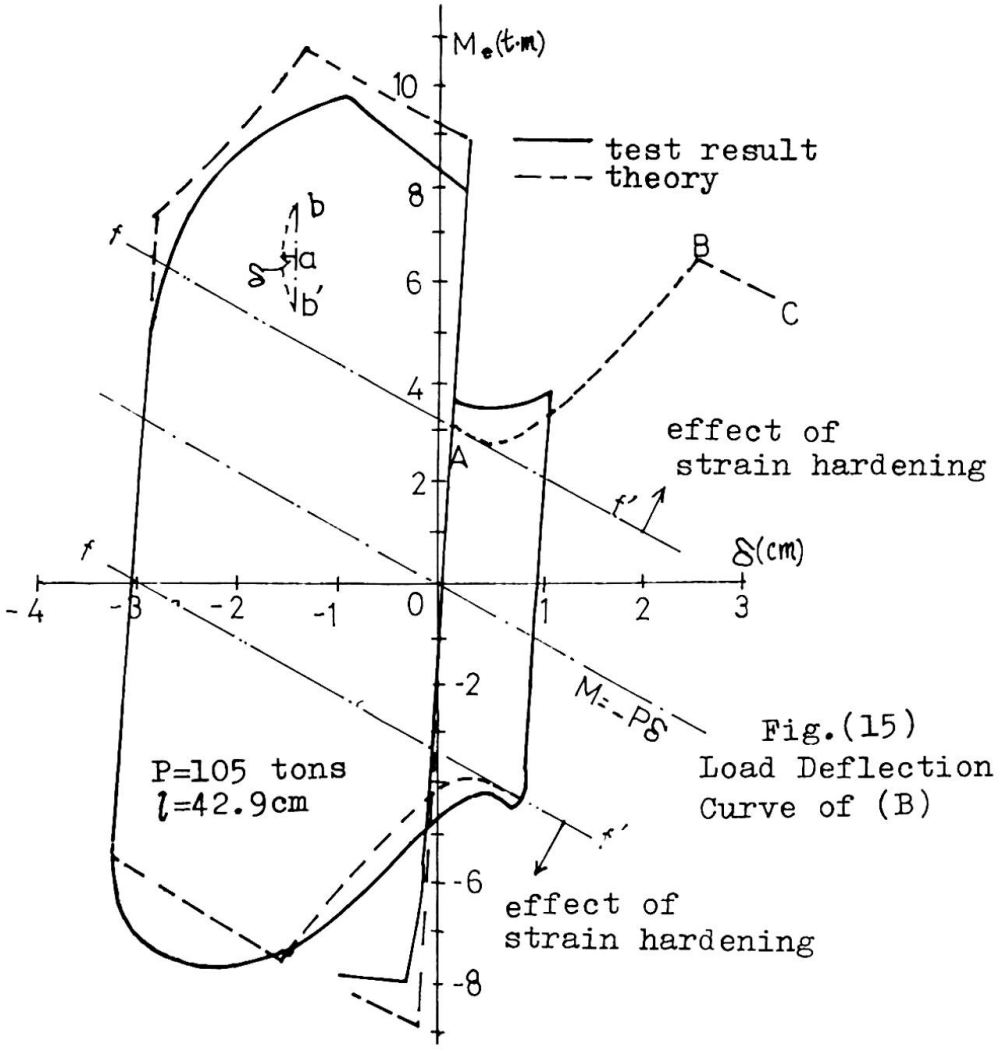

Fig.(15) Load Deflection Curve of (B)

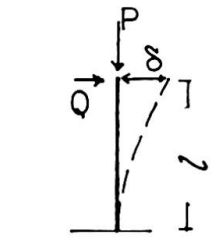

Fig.(16)

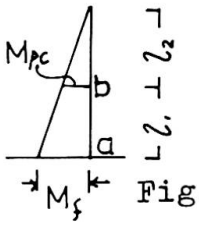

Fig.(17a)

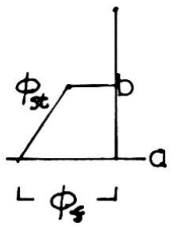

Fig.(17b)

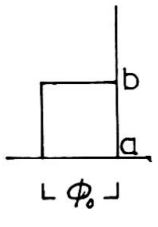

Fig.(17c)

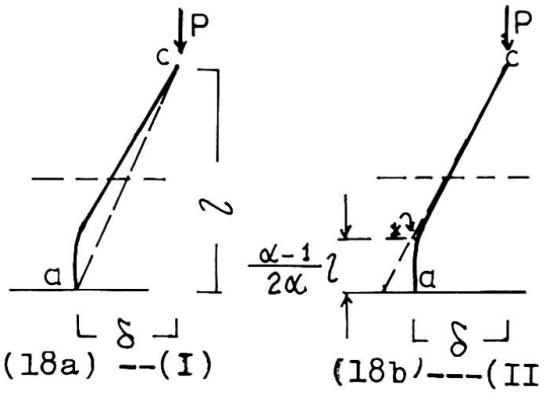

Fig.(18) Approximated Deflection

Fig.(19) Load Deflection Curve

——— Exact Solution • Collapse State

– – – Approximation I —·—·— Approximation II

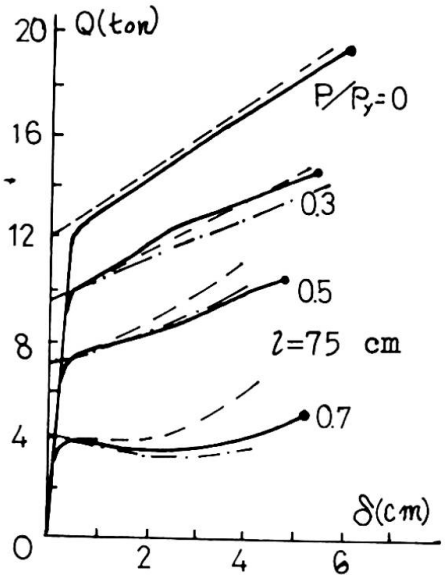

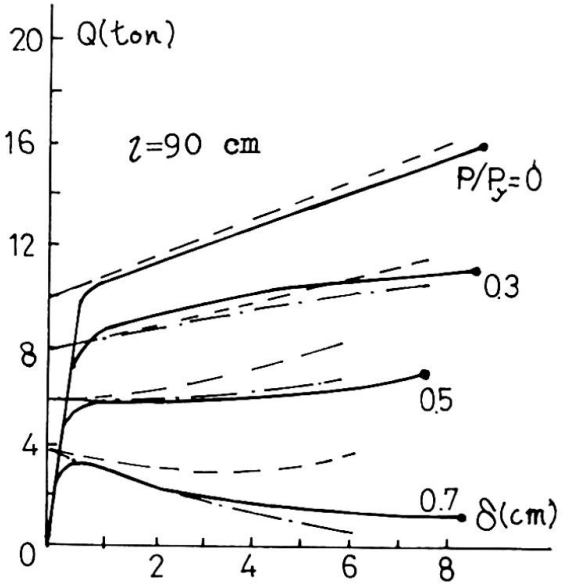

Fig.(20) Load Deflection Curve P_y: yield axial force

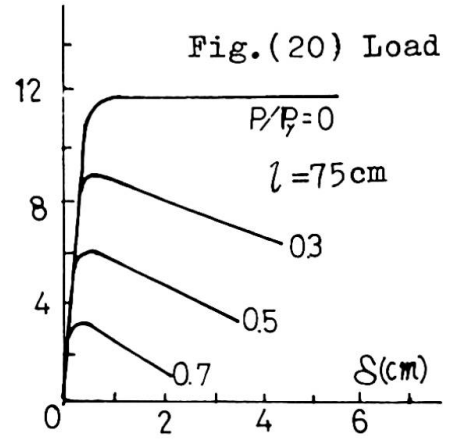

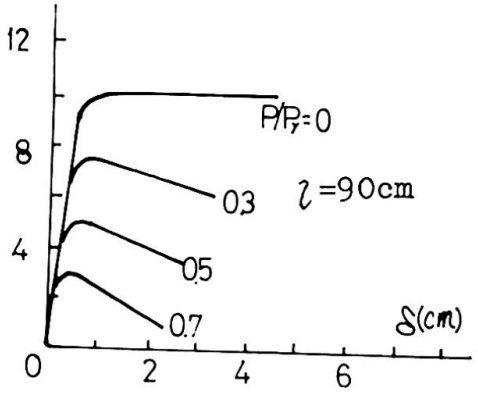

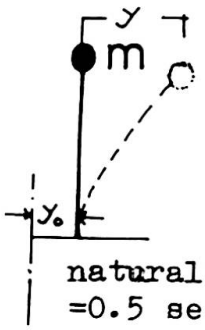

natural period
=0.5 sec.

(21a) One Mass System

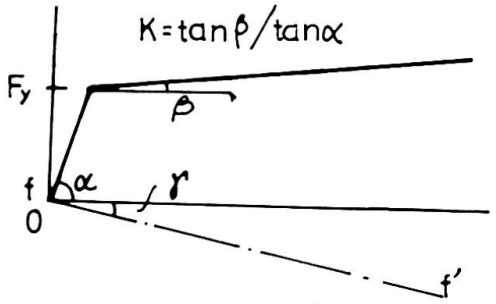

$\tan\gamma/\tan\alpha = -0.05$

Restoring Force
Characteristics

(21b)

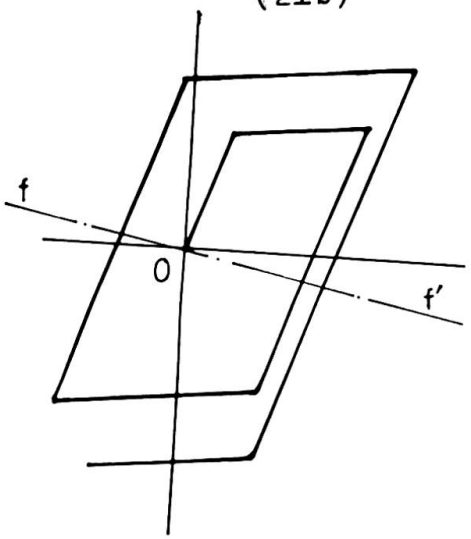

Fig.(21)

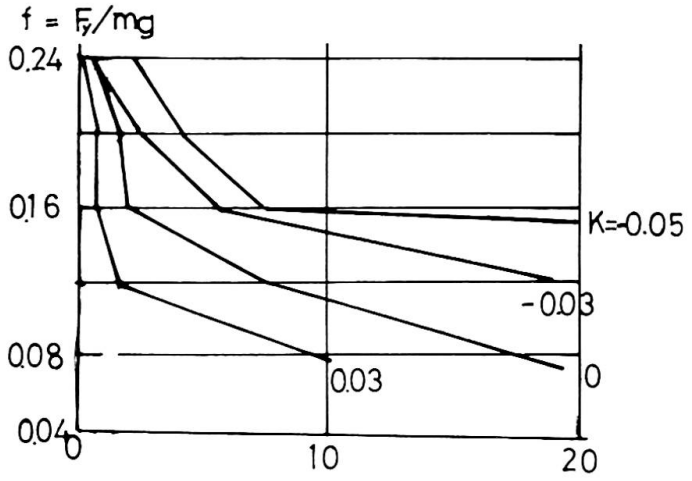

(22a)

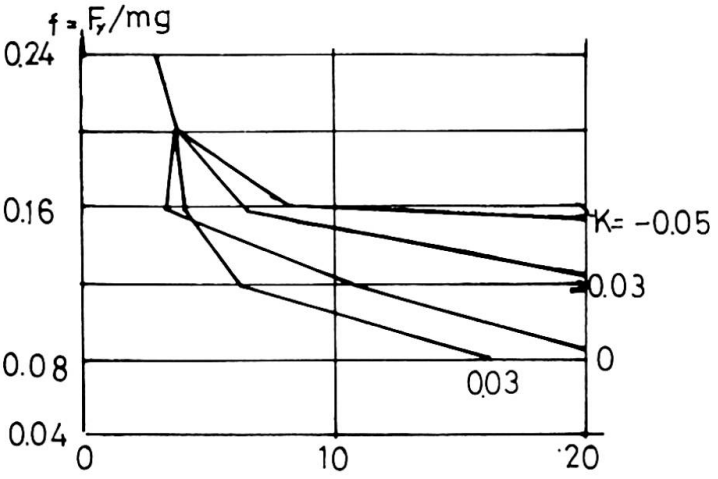

(22b)

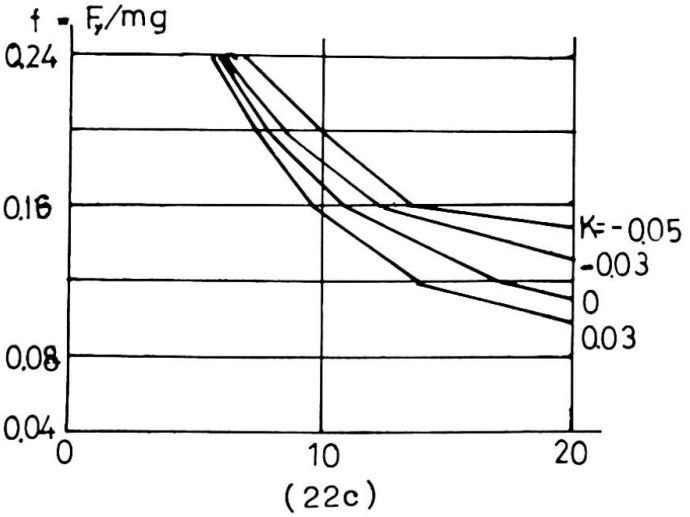

(22c)

Fig.(22) Deflection Response

SUMMARY

The more precise aspect of the inelastic behaviour of the steel member has been pursued by the analytical method which makes allowance for the strain hardening property of steel.

And the effect of the strain hardening property upon the deflection response of the steel framed structure to an earthquake was evaluated.

RÉSUMÉ

Des connaissances plus précises du comportement plastique de membres en acier ont été obtenues par la méthode analytique, ce qui permet de tenir compte du durcissement de l'acier. Cet effet du durcissement sur la déformation du portique d'acier due à un tremblement de terre a été évalué.

ZUSAMMENFASSUNG

Genaue Kenntnisse des plastischen Verhaltens von Stahlbauteilen wurden mit analytischen Berechnungen angestrebt, wodurch die Verhärtung des Stahls berücksichtigt werden konnte. Die Wirkung der Verhärtung auf die Verformung des Stahlrahmens wurde abgeschätzt.

Leere Seite
Blank page
Page vide

The Design of Multi-Story Buildings against Wind

Dimensionnement de bâtiments élancés par rapport aux efforts du vent

Bemessung von Hochhäusern auf Wind

A.G. DAVENPORT
Professor
Director, Boundary Layer Wind Tunnel Laboratory
the University of Western Ontario
Faculty of Engineering Science
London, Ontario, Canada

Submitted as a discussion of the paper "Dynamic Effects of Wind and Earthquake", by D. Sfintesco.

The author's paper reminds us of the similarities and differences in the approach to the wind and earthquake design of tall buildings. Taken together with the papers by Ferry Borges and also by Newmark and Hall, a fairly comprehensive survey of the subject is presented.

The historical allusion made by Sfintesco to the notable work by Gustav Eiffel and Sir Benjamin Baker reminds us of their insight into the action of the wind on structures. Their recognition of the influence of the size of the structure on the response and its dynamic response to wind, in many senses is clearer than several contemporary viewpoints.

In this discussion, the writer draws attention to two approaches to designing tall buildings against wind which perhaps answer some of these questions posed by Eiffel and Baker regarding both the size effect and the resonant response. These approaches are:

a) a Gust Factor approach; and
b) the use of wind tunnel modelling.

A design approach embodying gust factors has been described in several papers. It is already in use in the Danish Standards and is currently under consideration for incorporation in the National Building Code of Canada.

DESIGN CRITERIA FOR WIND LOADING

Sfintesco refers to most of the significant wind effects on tall buildings; namely, collapse, damage to masonry and finishes, damage to windows and cladding, fatigue damage, and comfort of occupants.

Some tentative design criteria for these effects are as follows:

1) Collapse: Current design conceives of the structure withstanding a wind having a recurrence interval of about 30 years, with a safety factor on the minimum stress of roughly 2.0. In fact, this may be the least critical requirement in most tall buildings. It might be more logical to use a far more improbable wind speed and a lower safety factor; for example, a once-in-500-year wind speed and a safety factor of 1.1 might give a more rational evaluation of risk.

2) Damage to masonry and finishes: Masonry and plaster appears to become sensitive to cracking under racking loads when the story deflection is in the range 1/8" - 1/2". This corresponds to an average building drift limitation of the order of 1/250 to 1/1000. If the average interval for redecorating is 3 years and if a 10% risk that damage would be done within this period was acceptable, an average recurrence interval of 30 years would be appropriate. The actual deflection criterion should properly be related to the kind of partition and masonry or other elements used.

3) Windows and cladding: Cladding and window lights today represent a very large proportion of the total cost of tall buildings. An acceptable breakage rate of 1 light per building every ten years might be acceptable: unacceptable deflections on the windows should probably not be permitted to occur more often than once every 5 years.

4) Fatigue: This is the most common cause of failure of structures damaged by wind. It can probably best be evaluated by use of cumulative damage laws. Procedures for its evaluation have been described by Davenport. It is likely to arise whenever dynamic stress amplitudes are high. These circumstances indicate the desirability of wind tunnel tests.

5) Comfort of occupants: It appears that the threshold of perception

of human beings to horizontal vibration occurs when the maximum acceleration is roughly in the range 0.5 - 1.5% of gravity: 1.5 - 5.0% of gravity may be annoying.

Of course, all of the above must be regarded as opinions rather than inflexible yardsticks: the subject matter concerned is essentially statistical, and the decision making cannot be made without some uncertainty. The suggested criteria are summarized in Table 1.

TABLE 1

TYPICAL CRITERIA FOR DESIGN OF TALL BUILDINGS AGAINST WIND

Unserviceability Symptom	Acceptance Criteria	Recurrence Interval: Years
1) Collapse	Safety factor = 1.1	500
2) Cracking of masonry & finishes	Max. def'n. $< \frac{1}{250} \rightarrow \frac{1}{1000}$ of height	30
3) Windows and cladding:		
a) perceptible deflections;	a) dependent on size of light, colour and type of glass	a) 5
b) breakage	b) <1 breakage per building	b) 10
4) Fatigue	Cumulative damage <100%	500
5) Comfort of occupants	Max. acc'n. <.5 → 1.5%g	10

DESIGN APPROACH #1 -- GUST LOADING FACTOR

This approach consists of the following phases:

1) The prediction of extreme average wind speeds from long term meteorological records such as those indicated in Fig. 1.

2) The adjustment of these wind speeds obtained at the meteorological observation station to the terrain conditions and height of the structure by means of profiles such as those shown in Fig. 2.

3) The determination of mean pressures using pressure coefficients appropriate to the particular flow conditions and structural shape as illustrated in Fig. 3.

4) The determination of the gust amplification factor using the gust pressure factor G defined below and in Fig. 4.

The gust pressure factor is intended to take account of the superimposed dynamic effect of gusts. It is used in conjunction with the mean load so that the total wind loading at any point on the building is,

$$p(Z)_{max} = G\,\bar{p}(Z)$$

where $\bar{p}(Z)$ refers to the mean pressure at height Z and given by such pressure coefficients as those in Fig. 3.

The factor G is the gust factor given by,

$$G = 1 + gr\sqrt{B+R}$$

in which g = peak factor, r = roughness factor, B = excitation by background turbulence, and R = excitation by turbulence resonant with structure.

The quantity,

$$R = \frac{S\,F}{\beta}$$

in which F = gust energy ratio, s = size reduction factor, and β = damping factor.

An explanation of these factors follows. In all cases, the mean velocity $\bar{V}$ is the velocity at the roof level. Graphs of g, r, B, F and s are shown in Fig. 4.

1) The peak factor g is the ratio of the peak dynamic response to the RMS response of the structure. It is a function of the average fluctuation rate of the response and the averaging period of the mean T. T should be between 5 min. and 1 hour. An expression for ν is

$$\nu = n_o \sqrt{\frac{R}{B+R}}$$

where R and B are defined below. For a peaked response, the

value of $\frac{R}{R+B}$ is near to unity and $\nu \simeq n_o$, n_o being the natural frequency.

2) The expression $r\sqrt{B+R}$ is in fact the RMS response of the structure to gusts. r is a roughness factor dependent on the terrain. r^2B is the contribution to the variance (mean square) response due to "background excitation", while r^2R is the contribution to the variance from the resonant response of the structure at its natural frequency.

3) The significant effect of size of the structure in reducing the dynamic load is seen both in B and the size reduction factor s.

4) The gust energy ratio F reflects the distribution of energy with frequency in the wind and hence the energy available to excite resonance.

5) The critical damping ratio β should include contributions to the damping from both mechanical and aerodynamic origin. For tall buildings, however, neglect of the aerodynamic damping is generally not significant. Suggested values of the mechanical damping are as follows:

Concrete	$\beta = .010 - .020$
Steel	$\beta = .005 - .010$

If the deflected shape of the structure both in the fundamental mode of vibration and under the action of steady wind is approximately rectilinear, as usually is the case with tall prismoidal buildings, an approximate expression for the maximum deflection and acceleration amplitudes can be derived. To do so, it is necessary to define an effective stiffness K which is the base bending moment per radian of rectilinear rotation of the structure. Knowing the base bending moment M under either inertia loading (dynamic) or the static wind loading either deflections or acceleration amplitudes may be found. Expressed in radians, the amplitude will then be simply M_o/K.

It is convenient to express the base bending moment in terms of the aerodynamic coefficient C_M so that,

$$C_M = \frac{1}{bh^2} \int_A Z\, C_p\, dA$$

where dA is an element of the projected frontal area, C_p is the local pressure coefficient on the front or rear surfaces at position Z and the integral is taken over front and rear surfaces.

The maximum deflection as a fraction of height is then computed from the expression

$$\frac{deflection}{h} = G\, \tfrac{1}{2}\rho V_o^2\, C_M\, bh^2/K$$

The maximum acceleration amplitudes invariably occur at the natural frequency and an approximate expression for the peak acceleration in the wind direction is,

$$maximum\ sway\ acceleration = 4\pi^2 n_o^2\, gr\sqrt{R}\, C_M\, \tfrac{1}{2}\rho V_o^2\, bh^3/K$$

$$= gr\sqrt{R}\, C_M\, \tfrac{1}{2}\rho V_o^2\, bh^3/I_o$$

where I_o is the moment of inertia of the building about the base, ie. $I_o = \sum m(Z)\, Z^2$, where $m(Z)$ is the mass in dynamic units at height Z.

Experience in the use of this approach generally indicates the following results:

1) Loading is on average in accordance with standard loadings used but the differentiation in loading between structures and between urban and rural terrains in significantly broader than standard approaches imply.

2) Tall slender structures with light damping incur relatively large dynamic gust factors (up to 3 times the mean load). Broad faced structures of relatively stiff construction incur relatively little dynamic amplification, perhaps only 30% greater than the mean load.

3) Structures in urban areas are affected more by turbulence than in rural area, but the mean loading is substantially lower.

4) Use of the correct velocity profile, wind tunnel testing conditions and dynamic gust factor are all highly significant and serious discrepancies can arise if this is not done.

DESIGN METHOD #2 -- BOUNDARY LAYER WIND TUNNEL MODELLING

Recently, strong and well justified criticism has been directed toward the use of aeronautical-type wind tunnels for investigation of pressures on models of structures. In some cases, the results of such tests can be highly misleading.

Seemingly a more promising development is the use of the boundary layer wind tunnel large enough to accommodate structural model testing. At present, only two or three such tunnels probably exist. That at the Boundary Layer Wind Tunnel Laboratory at The University of Western Ontario is of this type.

The application of this type of study is worthwhile in the investigation of large, important, structures exposed to the wind.

An outline of the possible phases of a wind tunnel study for the design of a tall building is given below in Table 2. The design procedure is illustrated diagrammatically in Figs. 10 and 11.

Perhaps the principal virtue of this approach is the understanding that evolves of the real way in which a structure is likely to behave in service; this understanding cannot really be duplicated by artificial formulation of wind loading parameters. While significant economy can be achieved by better tailoring the material in a structure to meet its actual behaviour, the greatest economy is achieved by recognition of problems at the design stage rather than after the structure is in service. The approach allows a number of problems which so far have been left unsettled to be studied; in particular, these problems include the question of maximum deflections, maximum acceleration, and the susceptibility of the structure to fatigue.

BIBLIOGRAPHY

A. G. Davenport "New approaches to the design of structures against wind action". Proceedings of Canadian Structural Engineering Conference, Toronto 1968. Published by Canadian Institute of Steel Construction.

A. G. Davenport "Gust loading factors". Jnl. of Str. Div., Proc. of Am. Soc. Civ. Eng., Vol. 93, pp 12-34, June 1967.

L. E. Robertson "On tall buildings" in "Tall Buildings". Ed. A. Coull, B. Stafford-Smith, Pergamon Press, 1967.

A. G. Davenport "The estimation of load repetitions on structures with application to wind induced fatigue and overload". Paper presented at the RILEM Symposium on the "Effects of Repeated Loading of Materials and Structures", Vol. 1, Mexico City, Sept. 15-17, 1966.

"Vejledning for fastsaettelse of vindbelastninger". Dansk ingeniorforenings standards for building construction, Teknisk Forlag, Kobenhavn, Denmark 1966.

M. Jensen, and N. Franck "Model scale tests in the natural wind, Part II", Danish Technical Press, Copenhagen, 1965.

International Conference on "Wind Effects on Buildings and Structures". NPL Teddington, England 1963, Pub. H.M.S.O., 1965.

International Seminar on "Wind Effects on Buildings and Structures". N.R.C., Ottawa, Canada, 1967, Proc. to be published by Univ. of Toronto Press.

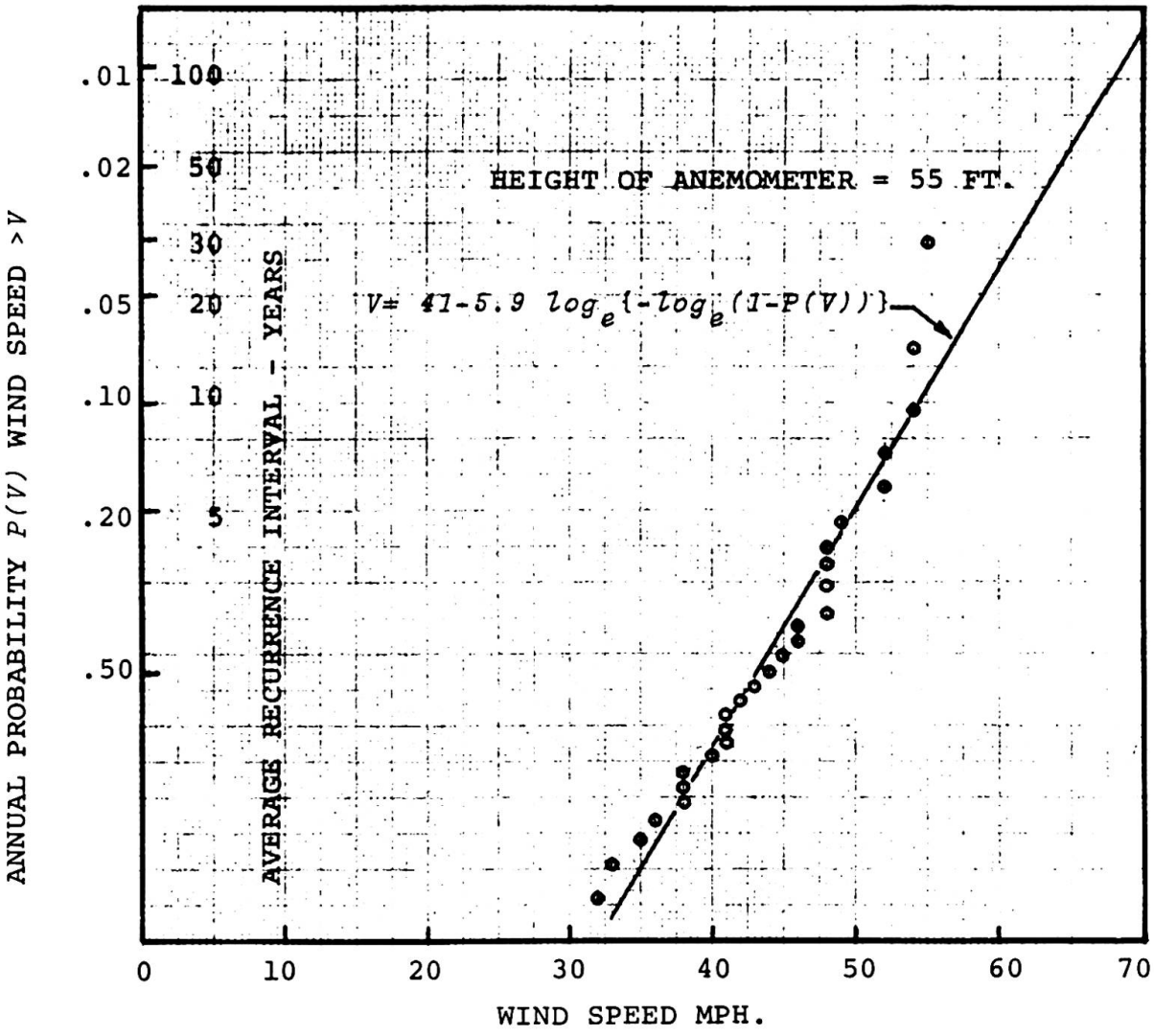

FIG. 1. EXTREME ANNUAL HOURLY AVERAGE WIND SPEEDS AT TORONTO MALTON AIRPORT (1939-1965).

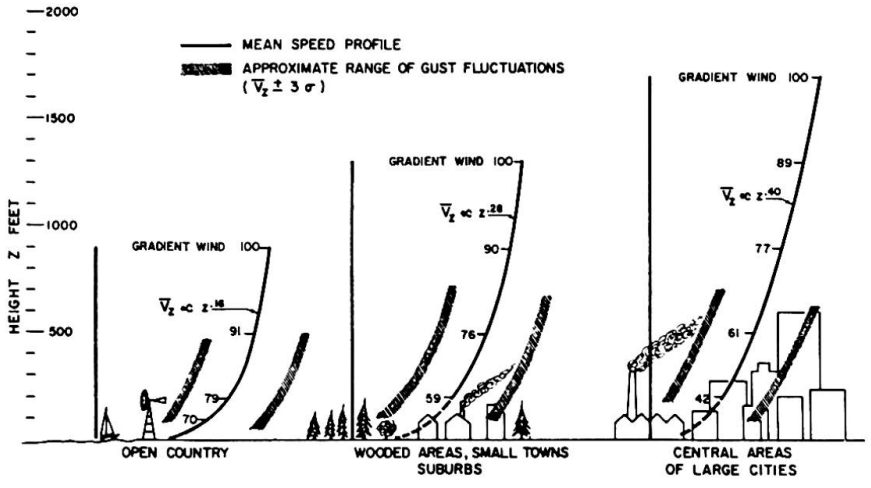

FIG. 2 MEAN WIND VELOCITY OVER LEVEL TERRAINS OF DIFFERING ROUGHNESS.

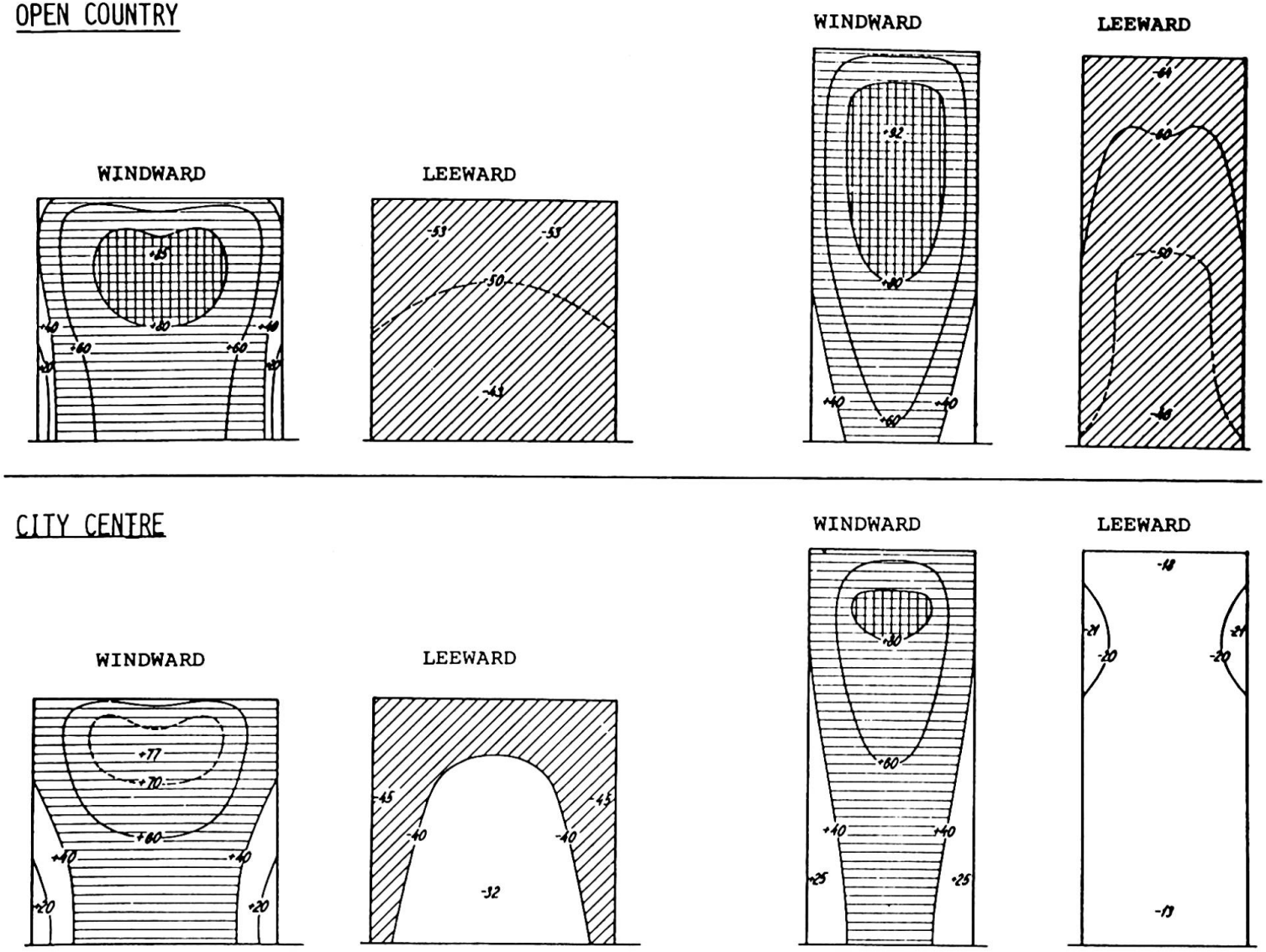

FIG. 3 TYPICAL AERODYNAMIC PRESSURE COEFFICIENTS (AFTER JENSEN-1965)(WIND NORMAL TO FACE: COEFFICIENTS REFERENCED TO VELOCITY PRESSURE AT ROOF LEVEL)

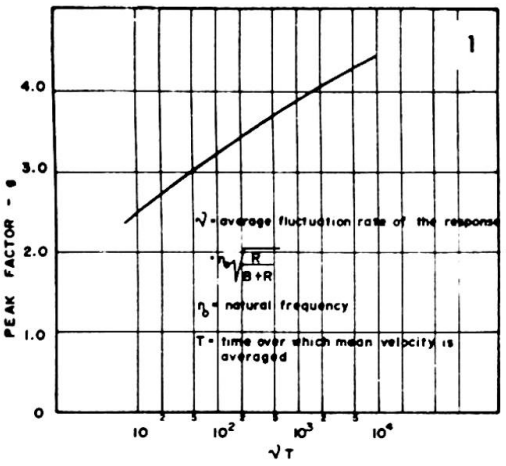

PEAK FACTOR

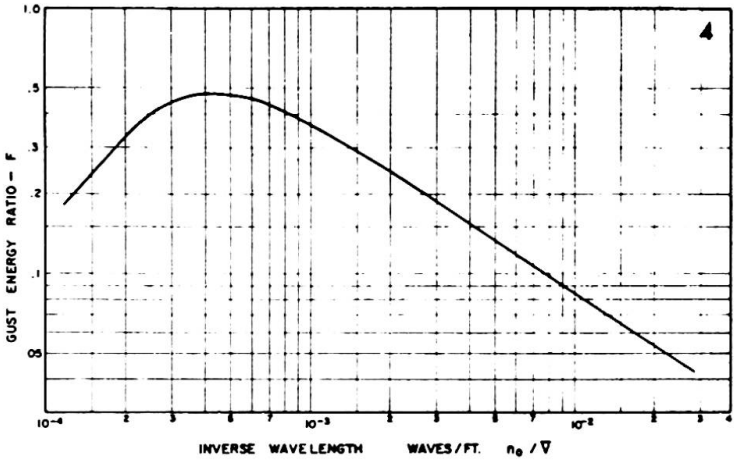

GUST ENERGY RATIO

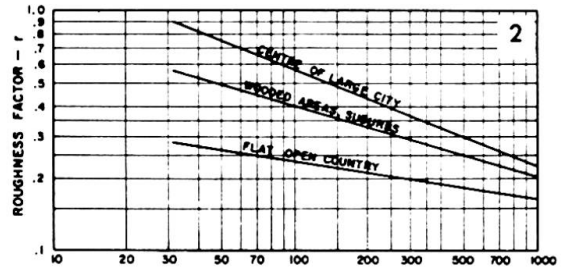

ROUGHNESS FACTOR

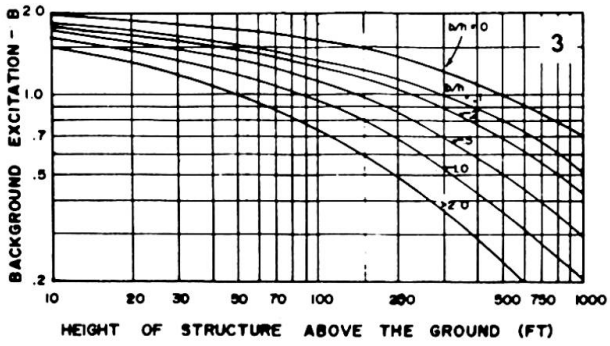

EXCITATION CAUSED BY BACKGROUND TURBULENCE

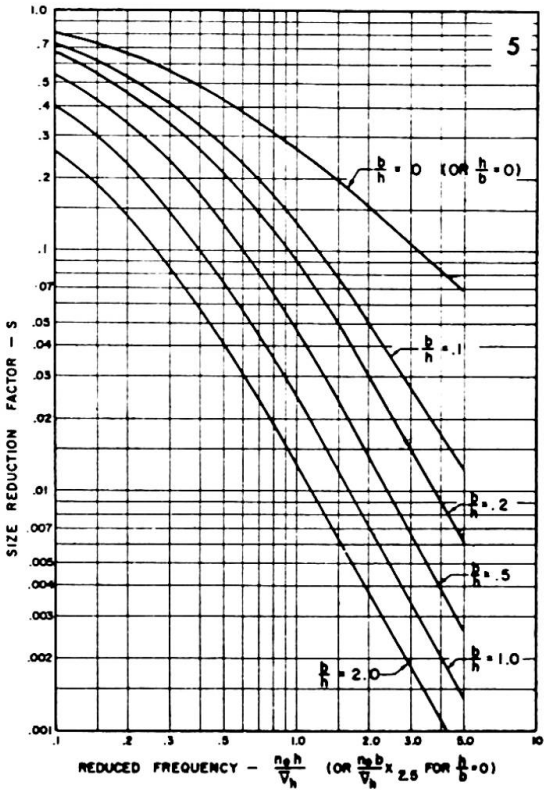

SIZE REDUCTION FACTOR

GUST FACTOR: $G = 1 + gr\sqrt{B+R}$ $\qquad R = \frac{SF}{\beta}$

FIG. 4

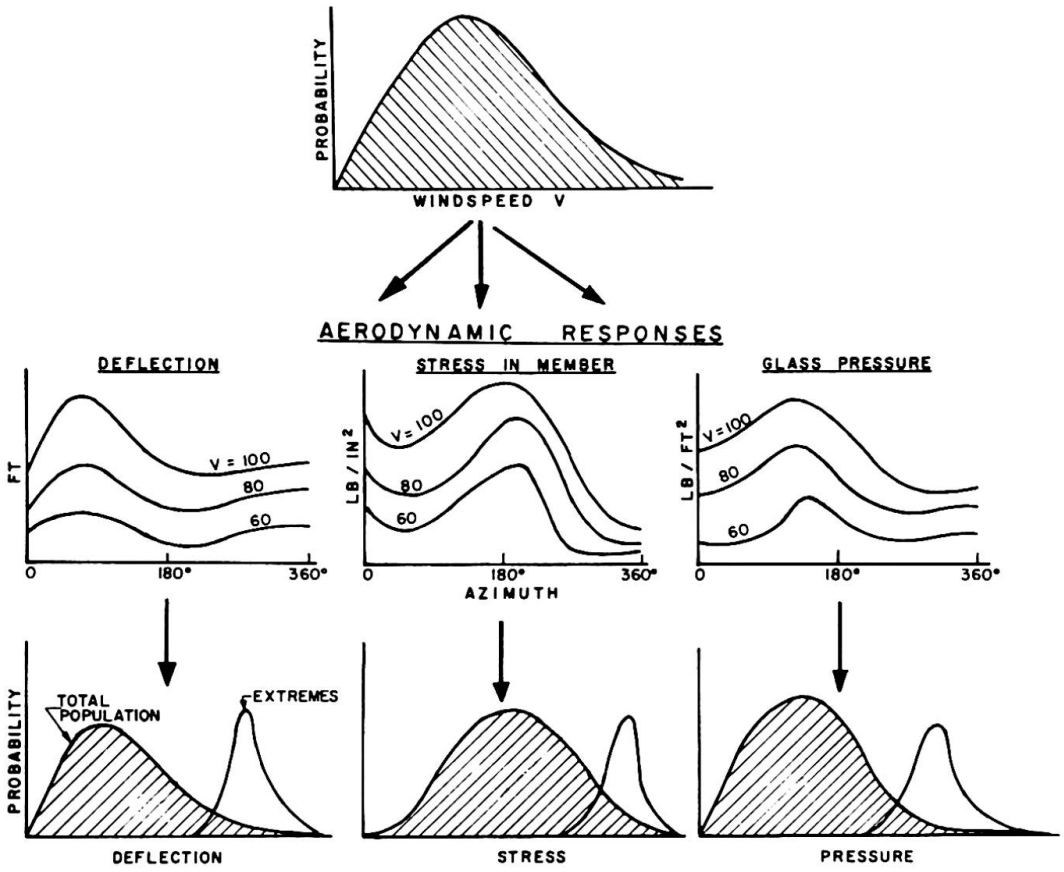

FIG. 5 DETERMINATION OF PROBABILITY DISTRIBUTIONS OF STRUCTURAL RESPONSE

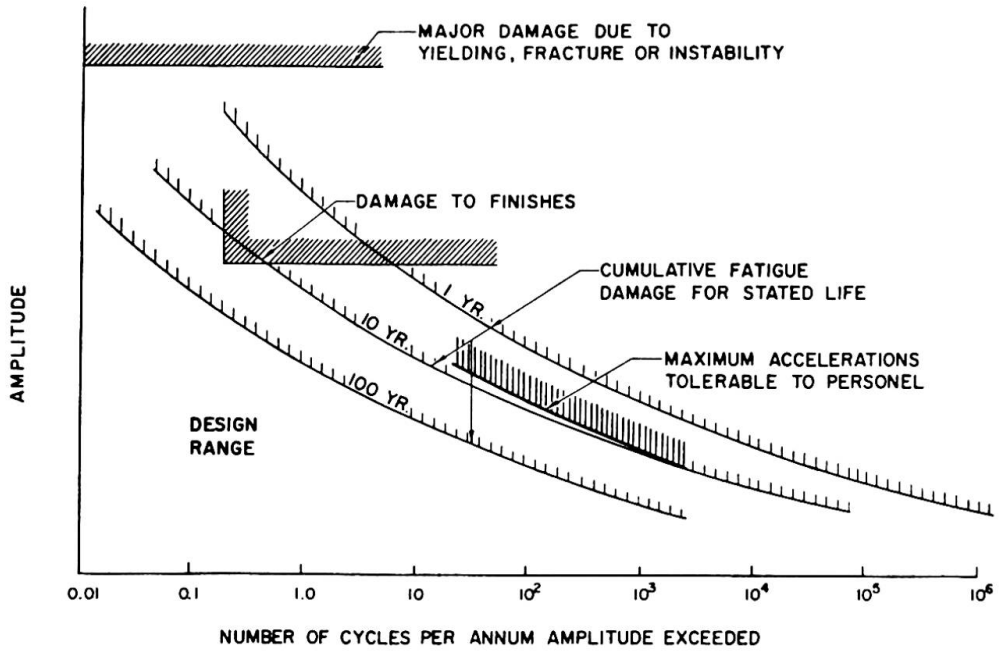

FIG. 6 ENVELOPE OF DESIGN LIMITATIONS

DISCUSSION LIBRE / FREIE DISKUSSION / FREE DISCUSSION

M. YAMADA
Prof. Dr.-Ing., Univ. Kobe, Japan

In der Schlussfolgerung des Diskussionsbeitrages der Herren Carpenter und Le-Wu Lu, Lehigh University, über " Das Verhalten von Stahlrahmentragwerken unter Einfluss periodisch veränderlicher Wechsellasten ", wurde die Vergrösserung der horizontalen Widerstände durch Wechselbelastung als die wichtigste experimentelle Tatsache gezeigt.

Hier möchte der Verfasser diese experimentelle Tatsache und ihre Ursache durch seine analytischen Untersuchungsergebnisse erklären, da es darüber noch keine analytische Behandlungen in diesem Fachgebiet gibt.

Fig. 1 zeigt die Beziehung zwischen wechselseitig wiederholten Biegemoment-Krümmungen des I-Querschnittes mit der Berücksichtigung des Verfestigungsvorganges.
Darin

- k : zeigt das Verhältnis der Querschnittsflächen zwischen einseitigem Flansch und Steg.
- n : zeigt das Verhältnis der Achsialdruckkraft zur Fliesslast.
- μ_{st}: zeigt die Neigung der Spannungs-Dehnungslinie im plastischen Bereich, hier etwa 0,01 E.

Dieses Bild zeigt den Fall unter einer verhältnismässig niedrigeren Achsialdruckkraft, d.i. 1/6 der achsialen Fliesslast.

Fig. 2 zeigt den Fall unter einer mittleren Achsialdruckkraft d.i. 1/3 der achsialen Fliesslast.

Fig. 3 zeigt den Fall unter einer verhältnismässig hohen Achsialdruckkraft, d.i. 1/2 der achsialen Fliesslast.

Aus diesen analytischen Untersuchungen kann man folgende Ergebnisse feststellen.

1. Unter einer kleineren Krümmungsamplitude bleibt der Querschnitt ganz elastisch.

2. Unter einer bestimmten mittleren Krümmunsamplitude (d.i. zwischen Fliessbeginn des Stabes und Kreuzpunkt der elastischen Linie mit der Asymptote zur völlig plastifizierten Linie) wird die Hysteresisschleife allmählich schmal und die Widerstände werden grösser als der anfängliche Fliesswert. Zum Schluss schwindet diese Hysteresisschleife und wird ganz elastisch mit einer Vergrösserung der horizontalen Widerstände.

3. Unter einer grösseren Krümmungsamplitude wird die Hysteresisschleife von Anfang an ein Parallelogramm mit einer bestimmten Vergrösserung der Widerstände.

Durch diese analytische Untersuchungem wird die Vergrösserung der horizontalen Widerstände der mehrstöckigen Stahlrahmen bei der wiederholten plastischen Belastung ganz klar.

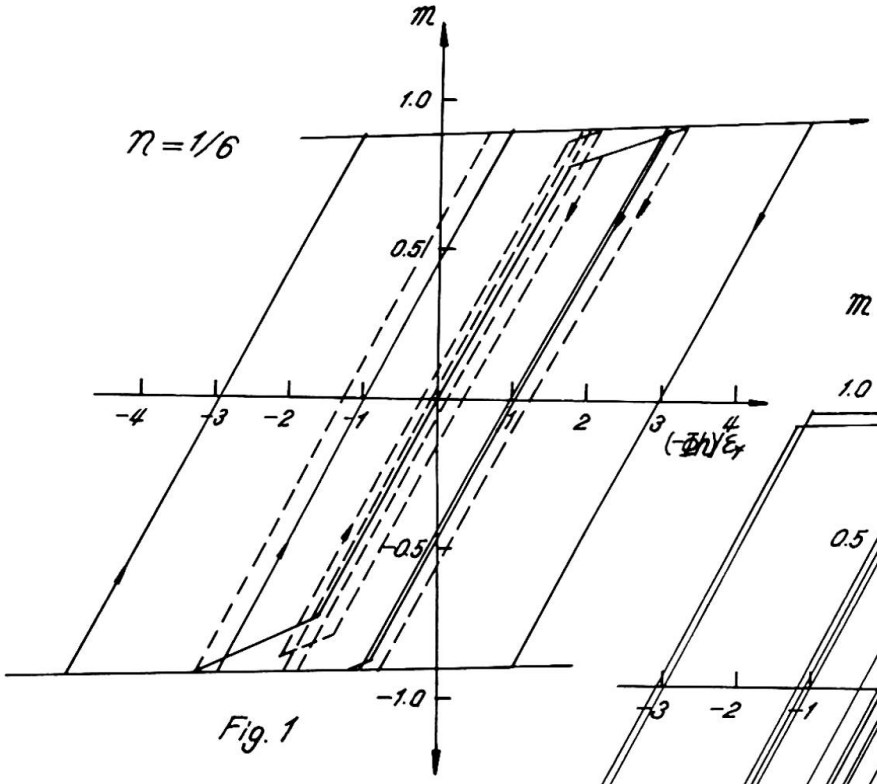

Fig. 1

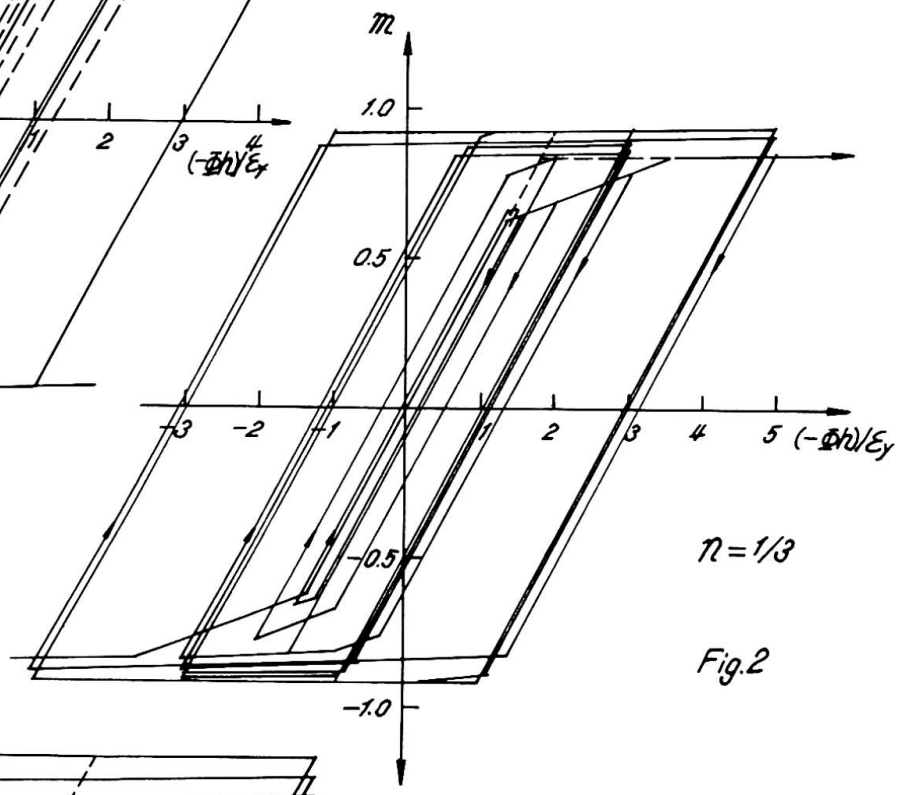

Fig.2

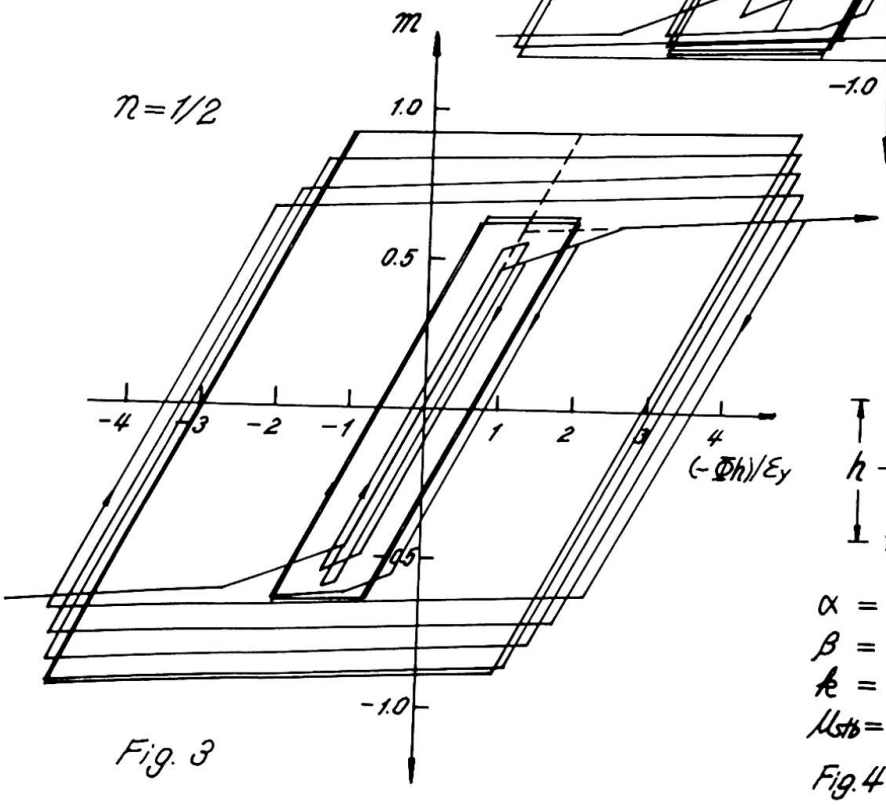

Fig. 3

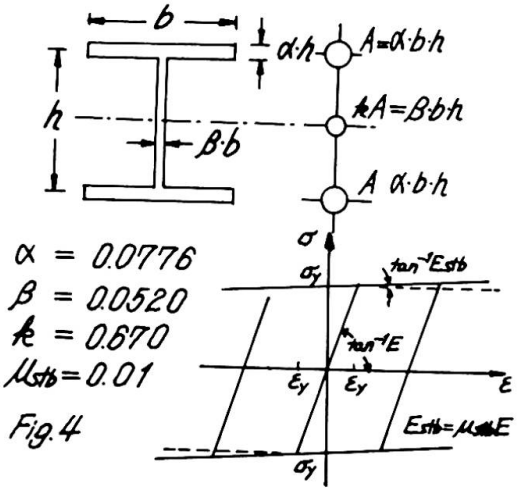

Fig.4

Leere Seite
Blank page
Page vide

FREE DISCUSSION

Discussion libre

Freie Diskussion

E. INGERSLEV
Partner, Ingerslev & Partners, London

A previous speaker had regretted the difficulty in obtaining co-operation with a certain international society. This difficulty should not be experienced with the International Association for Shell Structures, many of whose members are present at this conference including the President, I would particularly like to bring to the notice of this conference the existance of the Working Group for Tower Structures which has recently been formed under the IASS to deal with special structural problems arising in Tower Structures such as Radio Towers, Cooling Towers, Chimneys and Tall Multi Storey buildings. And foremost amongst the problems is that of wind loading, not only the the static but even more the dynamic loading from gusts and the eddying effect.

The collaps of 3 Cooling Towers in 1965 at Ferrybridge were discussed in great detail at a conference at the Institution of Civil Engineers in 1967 and amongst many other things this brought to light the dangerous effect not only of the eddying effect on the Tower itself but even more from a row of Towers in front. The eddies from two neighbouring Towers in the front row were shown to have opposite rotation at any one given time, thus magnifying the effect in the gap between them with disastrous effect on a Tower in the next line if it happens to be in line with the thus produced concentrated pulsating gusts.

I would also like to draw the attention of the Conference to a recent article in the June 68 issue of the Journal of the American Institution of Civil Engineers by Vellozzi & Cohen on Gust Responsive Factors.

Finally I would suggest that some of the lessons learnt in the building of very large chimneys could with profit be used in the design of very tall Multi-storey buildings. I have particularly in mind certain elastic joints and shock absorbers at one or more levels so as to change the natural frequency of the Tower structure out of the danger zone and absorbe the energy induced.

Leere Seite
Blank page
Page vide

Remarques de l'auteur du rapport introductif
Bemerkungen des Verfassers des Einführungsberichtes
Comments by the author of the introductory report

D. SFINTESCO
France

Dans le rapport préliminaire, j'avais souhaité voir entreprendre l'étude expérimentale de cadres à étages, sous sollicitations alternées en zone non linéaire, afin notamment de déterminer les effets des déformations plastiques successives et du raffermissement du métal.

Une telle étude vient d'être entreprise à Lehigh par Carpenter et Lu, avec un soin extrême de refléter la réalité, tant dans les proportions constructives que dans le mode de sollicitation. Les résultats obtenus à ce jour ont apporté la preuve que ces effets bénéfiques dépassent notablement les prévisions théoriques, ce qui se trouve d'ailleurs confirmé, quant à l'effet du raffermissement, par l'analyse et l'expérimentation de Kato et Akiyama.

La remarquable stabilité des courbes d'hystérésis pour des sollicitations alternées importantes, l'effet favorable des moments P - Δ résiduels et l'augmentation de capacité portante qui en résulte sont autant de facteurs dont la prise en compte dans le calcul s'impose déjà. Il est intéressant de noter à ce propos que la prochaine édition du Manuel américain "Commentary on Plastic Design" comportera un chapitre consacré aux fortes sollicitations répétées en zone non linéaire.

Par contre, l'étude expérimentale de la contribution des divers types de remplissages à l'absorption d'énergie - également suggérée dans mon rapport - ne semble pas encore avoir eu lieu. Elle pourrait être d'importance pour permettre d'avoir une notion plus précise et plus sûre du taux d'amortissement qui leur est dû. Cela se réfère d'ailleurs aussi bien aux sollicitations sismiques qu'à celles dues au vent

En ce qui concerne les assemblages des ossatures métalliques sujettes aux actions sismiques, le chercheur est un peu déçu - à première vue - de ne presque rien trouver dans la littérature, tout comme le praticien pourrait être un peu perplexe devant l'absence de toute règle ou recommandation spéciale, sauf celle d'exercer convenablement son métier, c'est-à-dire de concevoir et de calculer correctement les assemblages et de les faire réaliser avec soin.

Les expériences simples et claires de Popov justifient cependant de façon très nette cette situation et démontrent l'inutilité de tout recours à des dispositions spéciales.

Tout cela est de nature à renforcer, s'il en était besoin, la confiance dans le métal en tant que matériau idéal pour les ossatures dans les zones sismiques. De plus, cette évidence acquise par l'expérience offre des bases réalistes aux études sur modèle mathématique, comme le prouvent déjà quelques publications américaines récentes qui représentent un pas en avant dans l'étude rationnelle des ossatures métalliques en zones sismiques.

Il est évident que rien ne peut fournir d'informations plus sûres sur un bâtiment qu'un bâtiment. Les études sur bâtiments réels, menées par Bouwkamp à Berkeley, aussi bien d'ailleurs que par Jennings, par Matthiesen et par plusieurs chercheurs japonais, complètent de façon plus synthétique nos informations sur la tenue d'ensemble des bâtiments et représentent le lien entre la théorie, les essais en laboratoire et la réalité.

Il n'est évidemment pas possible d'avoir des séismes sur commande pour les besoins de la recherche et il faudrait beaucoup de chance pour avoir un appareillage complet de mesures installé sur un bâtiment au lieu même et au moment même d'un séisme naturel. Il semble par conséquent intéressant de noter que Penzien, à Berkeley, vient de lancer l'idée saisissante d'une plateforme expérimentale de 30 m au carré, susceptible de supporter un bâtiment réel et de le soumettre à un mouvement sismique programmé à volonté. Si cette idée avait pu sembler utopique, elle ne l'est plus guère depuis que Penzien en a étudié le projet. Elle serait financièrement réalisable et bien d'autres recherches avec, en renonçant par exemple à l'une de ces expériences spectaculaires qui inquiètent le monde. Voilà un choix à faire si l'on veut servir l'humanité.

Et maintenant quelques mots sur le vent.

L'étude de ce que j'appellerais "la première moitié du problème", l'action du vent, a été entreprise de façon très approfondie tant par des études théoriques que par des essais en soufflerie et par des mesures sur bâtiments réels.

Par contre, les chercheurs semblent avoir toujours reculé jusqu'à présent devant la complexité de l'étude expérimentale de la "seconde moitié" - celle qui importe en fin de compte - c'est-à-dire la réponse réelle du bâtiment dans son ensemble. Cette réponse, c'est-à-dire les contraintes et les déplacements réels, risque cependant d'être très différente de ce qu'admet le mode actuel de calcul, qui reflète plutôt mal la réalité physique.

Le projet en cours de réalisation par Mackey représente sans nul doute la recherche la plus importante et la plus réaliste jamais entreprise dans ce domaine. Elle pourrait fournir des vues plus claires, dans un domaine pratiquement inexploré, sauf sur le papier et à l'aide d'hypothèses qui semblent négliger des circonstances évidentes.

Une action concertée sur le plan international serait tout à fait indiquée. Il existe d'ailleurs un "Groupe d'étude international" qui a organisé, il y a un an, un très intéressant symposium à Ottawa, mais les propositions que j'avais alors formulées de créer une liaison avec les organismes d'ingénieurs tels que l'A.I.P.C. sont restées sans suite à ce jour.

Il est cependant nécessaire d'apporter des informations valables sur ce problème en entreprenant, dans un cadre plus large et de façon systématique, des observations sur le comportement des bâtiments réels à ossature métallique, sous l'action d'ensemble du vent, afin d'obtenir la combinaison optimale de la sécurité et de l'économie dans le calcul des ossatures métalliques de bâtiments à étages.

III

CONCLUSIONS / SCHLUSSFOLGERUNGEN / CONCLUSIONS

H. BEER
Prof.Dr.techn.
Chairman of the Working Commission II

1. The load-factor on which plastic design is based can't be considered as a real safety factor because overloading is only one reason for producing collapse of the structure. A realistic safety-consideration must comprise all kinds of imperfections as in mechanical properties of materials, design, fabrication, assembling and maintenance. Statistical dates are needed to develop semi-stochastic safety calculations of structures.
2. It is recommended to design unbraced tall multi-storey frames such as to exclude previous plastification of the stanchions. In this case it is possible to apply plastic design to the beams and elastic design to the stanchions.

   The tridimensional static action of multi-storey buildings of the tower type has to be considered not only for every structural component (stanchions, beams) but also for the whole structure.
3. Shear resistant walls or cores reduce very much the lateral sway of the structure and permit introduction of subassemblages to make more easy the application of plastic design theory. The investigations about the interaction between shear-walls and frames show clearly that the rigidity relation in the elastic-plastic range is an important factor in economic design. It is recommended to change the shear wall rigidity along the height of the building to obtain an optimum design of the frames.

   Simplified methods for calculating multi-storey buildings

with and without shear walls are in good agreement with more exact theories and tests, but special attention has to be given to the most unfavorable position of the service load. Otherwise designs can result which are less safe than those intended by the designer (see J.Heyman).

4. In very high tall multi-storey buildings the width of the core walls may not be sufficient to obtain the needed stiffness against lateral sway. Therefore in the USA a new type has been developed, bracing the four walls over the whole width with crossed diagonals. Walls and braced floor slabs form a multicellular box with very great resistance against wind forces. Therefore the local frame action can be calculated considering only subassemblages.
5. An attempt is made to extend plastic design theory such as to check continuously the rotation of the plastic hinge and to lock it if a contra-rotation takes place during loading. Furthermore strength hardening is considered calculating the ultimate load of a frame. This is particular important using high tensile steel.
6. Tests proved that shake down takes place due to alternated wind load and earth-quake but special attention must be given to the dynamic response of the building due to forced vibration. It is shown that the hysteresis taken from the loading cycles is very stable.

Important results of the interaction between frames and bracings had been presented. Though some attemps have been made to get an idea of the amount of damping due to non directly load carrying elements (cladding,walling etc.) a closer investigation should be performed considering particularly its influence on earthquake and wind-load.

7. An important research project for the investigation of the dynamic response of a specially built multi-storey framed building in Hongkong has been presented. It is intended to perform a large test program considering static and dynamic loading measuring the distribution and the dynamic effect of the wind forces. Than theoretical investigations and model tests are not sufficient to get a real idea of the behavior of the building under wind forces and earthquake the Hongkong tests will call the attention of the scientists and engineers.

8. The European Convention of Constructional Steelwork Associations has elaborated a first draft of Recommendations for the design of buildings in earthquake regions. The chairman of the corresponding Commission Prof. Giangreco has presented a simplified method to calculate the natural frequency of bi- and tridimensional frames considering different modes of vibrations.

The Working Commission II is convinced that further research work as well as tests should be carried out at an international level to clarify the behavior of multi-storey buildings taking into account static and dynamic loading.

Leere Seite
Blank page
Page vide